2012

DISCOVERY OF GZ-793A, A NOVEL VMAT2 INHIBITOR AND POTENTIAL PHARMACOTHERAPY FOR METHAMPHETAMINE ABUSE

David B. Horton
University of Kentucky, davidhorton114@gmail.com

STUDENT AGREEMENT:

I represent that my thesis or dissertation and abstract are my original work. Proper attribution has been given to all outside sources. I understand that I am solely responsible for obtaining any needed copyright permissions. I have obtained and attached hereto needed written permission statements(s) from the owner(s) of each third-party copyrighted matter to be included in my work, allowing electronic distribution (if such use is not permitted by the fair use doctrine).

I hereby grant to The University of Kentucky and its agents the non-exclusive license to archive and make accessible my work in whole or in part in all forms of media, now or hereafter known. I agree that the document mentioned above may be made available immediately for worldwide access unless a preapproved embargo applies.

I retain all other ownership rights to the copyright of my work. I also retain the right to use in future works (such as articles or books) all or part of my work. I understand that I am free to register the copyright to my work.

REVIEW, APPROVAL AND ACCEPTANCE

The document mentioned above has been reviewed and accepted by the student's advisor, on behalf of the advisory committee, and by the Director of Graduate Studies (DGS), on behalf of the program; we verify that this is the final, approved version of the student's dissertation including all changes required by the advisory committee. The undersigned agree to abide by the statements above.

David B. Horton, Student

Dr. Linda Dwoskin, Major Professor

Dr. Jim Pauly, Director of Graduate Studies

DISCOVERY OF GZ-793A, A NOVEL VMAT2 INHIBITOR AND POTENTIAL PHARMACOTHERAPY FOR METHAMPHETAMINE ABUSE

DISSERTATION

A dissertation submitted in partial fulfillment of the requirements for the degree of Doctor of Philosophy in the College of Pharmacy at the University of Kentucky

By

David B. Horton

Lexington, Kentucky

Director: Dr. Linda Dwoskin, Professor of Pharmaceutical Sciences
Lexington, Kentucky

2012

ABSTRACT OF DISSERTATION

DISCOVERY OF GZ-793A, A NOVEL VMAT2 INHIBITOR AND POTENTIAL PHARMACOTHERAPY FOR METHAMPHETAMINE ABUSE

Methamphetamine abuse is a serious public health concern affecting millions of people worldwide, and there are currently no viable pharmacotherapies to treat methamphetamine abuse. Methamphetamine increases extracellular dopamine (DA) concentrations through an interaction with the DA transporter (DAT) and the vesicular monoamine transporter-2 (VMAT2), leading to reward and abuse. While numerous studies have focused on DAT as a target for the discovery of pharmacotherapies to treat psychostimulant abuse, these efforts have been met with limited success. Taking into account the fact that methamphetamine interacts with VMAT2 to increase DA extracellular concentrations; the focus of the current work was to develop novel compounds that interact with VMAT2 to inhibit the effects of methamphetamine. Lobeline, the principal alkaloid found in *Lobelia inflata,* inhibits VMAT2 binding and function. Inhibition of VMAT2 was hypothesized to be responsible for the observed lobeline-induced inhibition of methamphetamine-evoked DA release in striatal slices and decrease in methamphetamine self-administration in rats. Lobeline has recently completed Phase Ib clinical trials demonstrating safety in methamphetamine abusers. Lobeline is also a potent inhibitor of nicotinic acetylcholine receptors (nAChRs), limiting selectivity for VMAT2. Chemical defunctionalization of the lobeline molecule afforded analogs, *meso*-transdiene (MTD) and lobelane, which exhibited decreased affinity for nAChRs. MTD, an

unsaturated analog of lobeline, exhibited similar affinity for VMAT2 and increased affinity for DAT compared to lobeline. Conformationally-restricted MTD analogs exhibited decreased affinity for DAT compared to MTD, while retaining affinity at VMAT2. One analog, UKMH-106 exhibited high affinity and selectivity for VMAT2 and inhibited METH-evoked DA release from striatal slices. Unfortunately, the MTD analogs exhibited poor water solubility which limited further investigation of these promising analogs. Importantly lobelane, a saturated analog of lobeline, exhibited increased affinity and selectivity for VMAT2 compared to lobeline. To improve water solubility, a N-1,2-dihydroxypropyl (diol) moiety was incorporated into the lobelane molecule. GZ-793A, an N-1,2-diol analog, potently and competitively inhibited VMAT2 function, exhibiting over 50-fold selectivity for VMAT2 over DAT, serotonin transporters and nAChRs. GZ-793A released DA from preloaded synaptic vesicles, fitting a two-site model with the high-affinity site inhibited by tetrabenazine and reserpine (classical VMAT2 inhibitors), suggesting a VMAT2-mediated mechanism of release. Further, low concentrations of GZ-793A that selectively interact with high-affinity sites on VMAT2 to evoke DA release, inhibit methamphetamine-evoked DA release from synaptic vesicles. Results showed that increasing concentrations of GZ-793A produced a rightward shift in the METH concentration response; however, the Schild regression revealed a slope different from unity, consistent with surmountable allosteric inhibition. In addition, GZ-793A specifically inhibited methamphetamine-evoked DA release in striatal slices and methamphetamine self-administration in rats. To examine the possibility that GZ-

793A produced DA depletion, the effect of a behaviorally active dose of GZ-793A on DA content in striatal tissue and striatal vesicles was determined. GZ-793A administration did not alter DA content in striatal tissue or vesicles and pretreatment with GZ-793A prior to methamphetamine administration did not exacerbate the DA depleting effects of methamphetamine. Importantly, GZ-793A was shown to protect against methamphetamine-induced striatal DA depletions. Thus, GZ-793A represents an exciting new lead in the development of pharmacotherapies to treat methamphetamine abuse.

KEYWORDS: Lobeline, Methamphetamine, Vesicular Monoamine Tranporter-2, Drug Discovery, GZ-793A

David B. Horton
Student's Signature

March 27, 2012
Date

DISCOVERY OF GZ-793A, A NOVEL VMAT2 INHIBITOR AND POTENTIAL PHARMACOTHERAPY FOR METHAMPHETAMINE ABUSE

By

David B. Horton

Dr. Linda Dwoskin
Director of Dissertation

Dr. Jim Pauly
Director of Graduate Students

March 27, 2012

ACKNOWLEDGEMENTS

Througout my life I have been blessed with a wonderful opportunity to continually pursue my dreams. This has been made possible by an outpouring of support from numerous individuals that have played an important role in my success. First and foremost, I would like to thank God for giving me the strength and perserverance to complete this thesis and opportunity to impact the world through science.

I want to thank my parents, Charles and Linda Horton for always pushing me to be the best that I can be. This Ph.D. is dedicated to the both of you. I am who I am because of your love, support and kindness. You are the greatest parents a son could ever ask for and I am eternally grateful for that.

I want to also thank the rest of my family and friends, as you always provided a much needed outlet to my scientific career. To Brandon (my brother), G, Corbin, Hunter, Boyle, Lucas, Taylor, Buff, Rose, and Ken, thank you. The times that I shared with you during this experience helped me tremendously and I could not have accomplished what I did without your support.

I would like to thank my advisor, Dr. Linda Dwoskin for her patience, support and guidance. She pushed me to be a great scientist and to ask the right questions, which are not always the easy questions. Further, I would like to thank my committee, Dr. Peter Crooks, Dr. Michael Bardo, Dr. Gregory Graf, Dr. Peter Wedlund and Dr. Wayne Cass for their time, consideration and insightful comments that greatly improved my thesis and scientific career. I would like to thank Catina Rossoll and Charolette Garland as they provided much needed support throughout this long and ardous process.

Finally, I would like to offer a tremendous thanks to my wife, Ashley. Your patience, support, encouragement and love is on every page of this thesis and I can not begin to tell you how much you have helped me throughout this process. From staying up late to proof-read to listening to my rants and complaints, you have always been there for me. You are my rock and without you, this would not have been possible. I love you and can’t thank you enough.

TABLE OF CONTENTS

LIST OF TABLES

LIST OF FIGURES

CHAPTER ONE

Introduction

I. Methamphetamine Background

Methamphetamine (METH; N-methyl-1-phenylpropan-2-amine; Fig.1) is a highly addictive psychostimulant and N-methyl derivative of amphetamine (AMPH; Fig 1). Structurally METH is characterized by a phenyl ring connected to a secondary amine by an ethyl side chain with a methyl group on the α-carbon. METH exists in two stereoisomers with the S(+)-enantiomer being more biologically active than the D(+)-enantiomer (Cruickshank and Dyer, 2009).

METH was first synthesized from ephedrine in 1893 by Japanese chemist, Nagai Nagayoshi (Anglin et al., 2000). In 1919, Akira Ogata first synthesized the crystalline form through a reduction of ephedrine with red phosphorus and iodine (Anglin et al., 2000). METH use became widespread beginning with soldiers in World War II for its ability to increase energy, alertness, and appetite suppression (Gonzales et al., 2009). In the years following World War II, METH and related stimulant use increased in young adults, particularly students and blue collar workers for the performance-enhancing benefit (Anglin et al., 2000). The U.S. Food and Drug Administration approved METH under the trade name “desoxyn” in 1944 for the treatment of narcolepsy, depression, alcoholism and hay fever (Berman, et al., 2009; Steinkellner et al., 2011). METH and related stimulants were available over-the-counter until the late 1950’s, significantly contributing to its use and abuse (Anglin et al., 2000). The use of prescribed METH increased

rapidly, reaching a peak with over 31 million prescriptions in 1967 (Anglin et al. 2000). The medicinal uses of METH were more tightly regulated with the passage of the Comprehensive Drug Abuse Prevention and Control Act of 1970, which limited the indications for which METH can be prescribed (Gonzales et al., 2009). The U.S. government classifies METH as a schedule II controlled substance with strict regulations governing its use. METH is recognized as a highly addictive substance which is only available through a prescription that cannot be refilled. Currently METH is only approved for clinical use in the treatment of attention-deficit hyperactivity disorder (ADHD), nacrolepsy and obesity (Sulzer et al., 2005).

As a result of the restricted prescribed use and production of METH, illicit METH production began in the early 1960's in clandestine laboratories in the Western U.S. (Anglin et al., 2000). In the 1970's and 1980's, METH use continued to grow with increased popularity amongst motorcycle gangs with an influx of crystallized METH ("ice") into Hawaii and California from Southeast Asia (Gonzales et al., 2009). METH was easily synthesized with common household products and precursors found in over-the-counter cold and allergy medicine (Derlet and Heischober, 1990; Barr et al., 2006). Due to the relative ease of production of METH and the availability of METH precursors, illicit production increased rapidly in the 1990's. Both small clandestine labs and larger "super labs" began to arise in locations across the U.S., Mexico and Canada (Barr et al., 2006). In 2000, the U.S. Federal Drug Enforcement Agency seized over 6,300 illegal METH labs in the U.S. and the number of lab seizures increased 25%

between 2001 to 2005, with the peak number of reported METH lab seizures occurring in 2004 (Sulzer et al., 2005; United Nations Office on Drugs and Crime, 2007). Not surprisingly, METH is the most commonly synthesized illegal drug in the U.S., with an estimated world-wide synthesis of over 2.9 billion doses of METH (100 mg) in 2005 (United Nations Office on Drugs and Crime, 2007). More recent figures show that the number of METH lab seizures increased 26% from 2008 to 2009 (United Nations Office on Drugs and Crime, 2011).

As a result of the rise in METH production, the U.S. government passed numerous laws and regulations, such as the Combat Methamphetamine Epidemic Act in 2005. This act limited the consumer availability of precursors such as pseudoephedrine, which are used in the illicit production of METH (Gonzales et al., 2009). Despite these efforts to control and limit supplies needed for METH production, METH use continues to rise in the U.S.. While METH use was traditionally popular among blue collar adult males, METH abuse has increased in popularity among women, students and young professionals (Gettig et al., 2006). Further, METH use has increased in homosexual and bisexual males, as METH is known to increase sexual performance (Gettig et al., 2006). METH use is often involved with risky sexual behavior and is highly prevalent in people with human immunodeficiency virus (HIV; Yamamoto et al., 2010). Thus, a significant health risk persists in these individuals. According to a 2008 Drug and Alcohol Services Information System report, AMPHs were the primary cause of over 170,000 substance abuse emergency room admissions, with over 80% of these cases involving METH (DASIS, 2008). In 2009, the

number of people illicitly using METH in the past month increased 59% compared to 2008 (NSDUH, 2009).

Currently, METH is the second most abused illicit drug in the world, after marijuana, with an estimated global usage at 15-16 million users (Krasnova and Cadet, 2009; Cruickshank and Dyer, 2009). Over half of the world's METH use occurs in Asia, while use is increasing in other regions of the world such as Africa and South America (United Nations Office on Drugs and Crime, 2011). Thus, METH abuse represents a world-wide health concern.

II. Clinical Pharmacology of METH

METH is a highly addictive psychostimulant with deleterious health risks associated with its use. METH is commonly referred to as "meth", "glass", "go", "speed", "crystal", or "ice", and is available in many different forms including tablet, powder, free base, and crystallized form (Derlet and Heischober, 1990; Anglin et al, 2000). METH can be taken orally, smoked, snorted (insufflation) or injected to obtain its stimulatory and euphoric effects (Karila et al., 2010). The onset of the effects of METH is dependent on the method of administration. The effects of METH are almost immediate following intravenous injection or smoking, while effects are seen within 5 and 20 minutes following snorting or oral ingestion, respectively (Anglin et al., 2000).

METH acts as a central nervous system (CNS) stimulant, producing increased alertness, energy, self-esteem, respiration, hyperthermia, sexuality and euphoria, as well as decreased appetite (Derlet and Heischober, 1990; Gonzales et al., 2009). While METH elicits similar effects to that of cocaine, the half-life of METH is much longer than other stimulants with a range from 8 to 12 hours (Gonzales et al., 2009; Karila et al., 2010).

Acute physical side effects of METH include increased blood pressure, tachycardia and hyperthermia, while psychological effects include increased agitation, aggression, anxiety, insomnia, hallucinations and paranoia (Barr et al., 2006; Cruickshank and Dyer, 2009). Consumption of high doses of METH can lead to renal and liver failure, cardiac arrhythmias, heart attacks, strokes, psychosis, delirium, seizures and death (Krasnova and Cadet, 2009). Chronic METH use leads to serious health risks from impaired cardiovascular function, e.g., hypertension, coronary heart disease, stroke and sudden cardiac death (Hanson, 2002; McGee et al., 2004; Kaye et al., 2007). In addition to these cardiovascular events, chronic use of METH has been associated with neurological symptoms such as anxiety, depression, social isolation, and reductions in attention, memory and cognition (Simon et al., 2000; Sekine et al., 2001; Freese et al., 2002; Salo et al., 2007; Darke et al., 2008; Krasnova and Cadet, 2009). Disruption of METH use in those abusing the drug repeatedly leads to METH- related withdrawal symptoms such as depression, anxiety, disturbed sleep, reduced energy, hyperphagia, and increased METH craving

(Gossop et al., 1982; Srisurapanont et al., 1999; Zweben et al., 2004; Homer et al., 2008; McGregor et al., 2008).

III. Dopamine and Reward

a. Dopamine Pathways

Psychostimulants such as METH, cocaine and nicotine elicit their stimulant and rewarding effects through activation and modulation of the mesolimbic, mesocortical and nigrostriatal dopamine (DA) pathways (Di Chiara et al., 2004; Wise, 2009). The mesolimbic DA pathway is characterized by neurons originating in the ventral tegmental area and innervating the nucleus accumbens (NAc), ventral palladium and amygdala (Fig 2). The mesocortical DA pathway originates in the ventral tegmental area (VTA) and projects to the prefrontal cortex (Fig 2). The mesolimbic and mesocortical DA pathways are involved in motivation, reward, emotion and cognition (Wise, 1978; Simon et al., 1980; Di Chiara and Imperato, 1988; Pierce and Kumaresan, 2006). Modulation of DA neurotransmission in the NAc and medial prefrontal cortex is important in primary reward, learning and cue-associated reinforcement (Everitt and Robbins, 2005; Chen et al., 2010). The nigrostriatal DA pathway originates in the substantia nigra and innervates the striatum (Fig 2). This pathway is involved in movement, motor control and conditioning (Robertson and Robertson, 1989; Everitt and Robbins, 2005). While these pathways were originally referenced as being anatomically and functionally distinct, they actually overlap and often share functionalities (Bjorklund and Dunnett, 2007; Wise, 2009). Thus, DA

neurotransmission in the mesolimbic, mesocortical and nigrostriatal pathways play important roles in the rewarding properties of abused psychostimulant drugs (Everitt and Robbins, 2005; Wise, 2009).

b. DA

DA (Fig. 1) is a catecholamine neurotransmitter involved in reward, emotion and movement. The biosynthesis of DA is shown in Fig 3. DA biosynthesis begins with the hydroxylation of the amino acid L-tyrosine by tyrosine hydroxylase (TH) to form L-dihydroxylphenylalanine (L-DOPA) in the axon terminals of DA neurons. TH requires the cofactors, Fe^{2+}, O_2 and tetrahydropteridine and the hydroxylation of L-tyrosine is the rate-limiting step in the biosynthesis of DA (Cooper et al., 2003). L-DOPA is then decarboxylated by DOPA-decarboxylase to form DA. The action of DOPA-decarboxylase requires pyridoxal phosphate (vitamin B6) as a cofactor and also occurs in the cytoplasm of the axon terminals (Cooper et al., 2003). Following synthesis, DA is stored in synaptic vesicles in the presynaptic axon terminal until ready to be used. DA can be stored in large dense core vesicles (LDCV) or small synaptic vesicles (SSV). LDCVs are located away from the synaptic cleft, while SSVs are located near the synapse or “active zone” (Ludwig and Leng, 2006). As such, LDCVs are sometimes referred to as the non-readily releasable pool of vesicles, while SSVs are referred to as the readily releasable pools. When a DA neuron is stimulated, an action potential travels into the axon terminal opening voltage gated Ca^{2+} ion channels, leading to the influx of Ca^{2+} into the terminal (Cooper et

al., 2003). Sensors on SSVs are activated by increases in Ca^{2+} ion concentrations, leading to exocytosis (Ludwig and Leng, 2006). In exocytosis, vesicles fuse with the synaptic plasmalemma membrane and release the contents (DA) of the vesicles into the synaptic cleft. Exocytosis is a rapid process, occuring within milliseconds of vesicle fusion (Almers et al., 1991). Exocytosis is followed by endocytosis where the empty vesicle is internalized and refilled with DA (Sudhof, 2004). Once in the cytosol, DA can bind to pre and postsynaptic receptors, undergo metabolism, or be taken back up into the presynaptic terminal by the DA transporter (DAT).

c. DA Receptors

Following DA release into the synaptic cleft, DA can bind to pre and postsynaptic DA receptors (Fig 3). There are two types of DA receptors in the brain, D1- like and D2-like receptors. Both types of DA receptors are metabotropic G-protein coupled receptors, consisting of 7 transmembrane domains (TMDs). Activation of D1-like receptors increases production of cyclic adenosine monophosphate (cAMP) by stimulating adenylate cyclase while activation of D2-like receptors inhibits adenylate cyclase decreasing cAMP production. D1-like receptors consist of D1 and D5 receptors, while D2-like receptors consist of D2, D3 and D4 receptors. D1 and D2 receptors are more abundant in the brain, being present 10-100 times more than D3, D4, and D5 receptors (Hurley and Jenner, 2006). D1 receptors are located primarily in the striatum and cortex (more abundant in the striatum than the cortex), while D5

receptors are located primarily in the hippocampus, thalamus and hypothalamus. D2 receptors are located in the striatum and cortex, while D3 receptors are located primarily in the island of Calleja, nucleus accumbens and olfactory tubercle, and D4 receptors are in cortex (Hurley and Jenner, 2006). Both D3 and D4 receptors have decreased expression in the striatum. In addition to postsynaptic localization of D2 receptors, D2 receptors are located on the presynaptic membrane where they act as autoreceptors modulating DA neurotransmission through a negative-feedback mechanism. Activation of D2 autoreceptors on midbrain neurons increases K^+ conductance through activation of coupled K^+ channels, hyperpolarizing DA neurons and reducing DA neurotransmission (Lacey et al., 1987; Cass and Zahniser, 1991). Activation of D2 autoreceptors on presynaptic terminals decreases DA synthesis through an inhibition of adenylate cyclase activity, subsequently decreasing cAMP-induced activation of TH (Onali and Olianas, 1989; Onali et al., 1992).

d. DA metabolism

DA is inactivated by undergoing metabolism in both the synaptic cleft and presynaptic terminal. DA is metabolized by two main enzymes, catechol-O-methyl transferase (COMT) and monoamine oxidase (MAO). DA is metabolized into 3-methoxy-4-hydroxyphenylacetaldehyde by COMT in the synaptic cleft. 3-methoxy-4-hydroxyphenylacetaldehyde can then be further metabolized into homovanillic acid by MAO. An alternate metabolic pathway is the metabolism of DA into dihydroxyphenylacetic acid (DOPAC) by MAO in the presynaptic terminal

(Fig 3). Additionally, DOPAC can then be metabolized into homovanillic acid by COMT.

e. DA Transporter

In addition to metabolism, DA is inactivated by being transported back into the presynaptic terminal through DAT (Fig 3). As such, DAT regulates DA neurotransmission by determining DA concentrations in the synaptic cleft available for postsynaptic receptor stimulation. While DAT exhibits affinity for DA, DAT also transports other substrates into DA nerve terminals such as AMPH, METH, methylenedioxymethamphetamine, tyramine, 5-HT, norepinephrine, and 1-methyl-4-phenylpyridinium (MPP+). Numerous DAT inhibitors have been synthesized including cocaine, methylphenidate, GBR-12909, GBR-12935, WIN 35,428, nomifensine, buproprion, and mazindol (Cooper et al., 2003; Torres et al., 2003).

DAT consists of 620 amino acid residues arranged in 12 hydrophobic TMDs spanning the plasma membrane (Torres et al., 2003). The N and C termini of DAT are both located in the cytoplasm on the interior side of the plasma membrane. Additionally, a large extracellular loop exists between TMDs 3 and 4, possessing multiple glycosolation sites available for post-translational modification (Torres et al., 2003). The structural regions involved in substrate translocation are controversial. Using chimeric constructs of DAT and the norepinephrine transporter (NET), Giros and colleagues discovered that the first five TMDs were involved in substrate translocation (Giros et al., 1994). Using

similar techniques, Amara and colleagues concluded that TMD4 through TMD8 were important for substrate translocation (Buck and Amara, 1995). Studies using chimeras made from human and bovine DAT found that TMD3 was involved in determining DA affinity (Lee et al., 1998). Specifically, site-directed mutagenesis studies showed that the phenylalanine residue in TMD3 is crucial for the binding of DA (Chen et al., 2001). Recently, utilizing the crystal structure of the leucine transporter, a related sodium dependent transporter, a 3-D model of DAT was constructed as a structural template (Indarte et al., 2008). Using this model and performing docking studies, Indarte and colleagues determined that TMDs 1 and 6 combine with TMDs 3 and 8 to form the binding pocket for DA (Indarte et al., 2008). DAT inhibitors and substrates are proposed to bind to different regions of DAT protein. Cocaine and related phenyltropane analogs inhibit DA uptake through a proposed interaction with TMDs 5-8, while GBR inhibitors (GBR-12909 and 12935) are proposed to interact with TMDs 1 and 2 (Giros, et al., 1994; Vaughan and Kuhar, 1996; Vaughan et al., 1999).

DAT is localized on DA neurons, at the cell bodies, on axonal membranes and perisynaptically at nerve terminals (Pickel et al., 1996; Hersch et al., 1997; Torres et al., 2003; Mengual and Pickel, 2004). In the brain, DAT is found in striatum, nucleus accumbens, olfactory tubercle, cingulated cortex, frontal cortex, lateral habenula and on cell bodies in the VTA and substantia nigra (Ciliax et al., 1995; Torres et al., 2003). In regions where DAT is present in low levels such as the prefrontal cortex, DA is transported out of the synapse through the NET (Moron et al., 2002). DAT is also found outside the brain in the body periphery.

DAT has been found in the stomach, pancreas and kidney, and in these locations, DAT inactivates peripheral DA involved in paracrine and autocrine signaling (Eisenhofer, 2001).

DAT is a member of the SLC6 family of Na^+/Cl^- dependent transporters, which also includes NET and serotonin transporter (SERT). Transport of DA through DAT is driven by the Na^+ gradient from the Na^+/K^+ transporting ATPase and accompanied by the co-transport of Na^+ and Cl^- ions (Cooper et al., 2003; Torres et al., 2003). The stoichiometry of substrate transport is the co-transport of two Na^+ ions and one Cl^- ion for each DA molecule (Krueger, 1990). Traditionally, DA transport was thought to occur through an "alternating access model" of transport (Jardetzky, 1966). In this model, DA and co-substrates (ions) bound to the outward facing binding site of the transporter. Then, the transporter underwent a conformational change in which the binding site with the bound DA and ions face the cytosol, where DA and ions were released into the cytosol. Transport of DA generates an electrochemical current which can be measured using voltage clamp and can be blocked by transporter inhibitors (Sonders et al., 1997; Torres et al., 2003). The existence of transport-mediated currents and the reliance on electrochemical gradients provides evidence for a transporter-mediated channel-like mechanism of substrate and ion transport (Sonders and Amara, 1996). In this model of transport, DAT undergoes a conformational change in which DAT protein acts as a single channel opening, allowing the passage of DA and ions through the plasma membrane. The probability of these openings is increased by the presence of substrates and ions (Sonders and

Amara, 1996). Additionally, DAT transporter currents may play a role in membrane depolarization and regulation of DA release. Utilizing patch clamp recordings, DA transport through DAT was shown to be accompanied by an inward current (mediated by Cl^- ion flow) that elicited an excitatory response, leading to an increase in DA neuron firing rate (Ingram et al., 2002). Thus, the ion channel-like current flow through DAT protein modulates membrane potential and DA release from DA neurons.

Numerous studies utilizing DAT knock-out (KO) mice have been performed demonstrating the importance of DAT in DA neurotransmission and the mechanism of action of psychostimulants (Gainetdinov, 2008). DAT KO mice exhibit decreased weight gain and long term survival rates compared to wild-type (WT) mice, due to the decreased food intake in DAT deficient mice (Giros, et al., 1996). As expected, the lack of DA clearance by DAT in DAT KO mice resulted in an increased extracellular DA. In DAT KO mice, DA persists in the extracellular compartment 100-300 times longer compared to WT mice (Giros, et al., 1996; Jones et al., 1998a). Further, DAT KO mice exhibited a 5-fold increase in extracellular DA levels and 20-fold decrease in tissue DA concentrations due to the disruption of the DA reuptake and recycling (Gainetdinov et al., 1998; Jones et al., 1998a). As expected, DAT KO mice exhibit increased locomotor activity compared to WT mice, presumably due to the increased concentration and action of extracellular DA (Giros et al., 1996). In addition to disrupting DA clearance, DA synthesis rates were doubled in DAT KO mice compared to WT mice (Jones et al., 1998a). Interestingly, TH levels were 90% lower in DAT KO

mice compared to WT, suggesting an increase in efficiency to synthesize DA in DAT KO mice (Jones et al., 1998a). Consistent with these results, D2 receptor expression was decreased by 45% in DAT KO mice compared to WT mice, which could further explain the increase in DA synthesis as D2 autoreceptors inhibit DA synthesis by decreasing TH activity (Giros et al., 1996; Jones et al., 1999). DAT KO also altered DA metabolism by COMT which was increased by 400% in DAT KO mice compared to WT mice (Jones et al., 1998a).

Studies utilizing DAT KO mice have contributed also to the understanding of the mechanism of action of psychostimulants. Unlike in WT mice, AMPH or cocaine treatment did not increase locomotor activity in DAT KO mice, suggesting a role for DAT in the mechanism of action of these drugs (Giros et al., 1996). Consistent with these results, AMPH or cocaine treatment did not increase extracellular DA in the striatum of DAT KO mice, and behavioral studies demonstrated that DAT KO mice exhibit decreased cocaine self-administration rates compared to WT mice (Jones et al., 1998b; Gainetdinov, 2008; Thomsen et al., 2009). In contrast, microdialysis experiments show that AMPH and cocaine increase extracellular DA in the NAc in DAT KO mice (Carboni et al., 2001). Further, DAT KO mice self-administer cocaine and exhibit conditioned place preference for AMPH, despite lacking the presumed pharmacological target of cocaine and AMPH (Rocha et al., 1998, Budygin et al., 2004). Thus, even though DAT is one of the pharmacological targets of AMPH and cocaine, evidence exists for the role of other neurotransmitter transporters such as SERT, NET and the

vesicular monoamine transporter (VMAT) in the rewarding effects of these drugs (Budygin et al., 2004; Gainetdinov, 2008).

DAT function is regulated by multiple post-translational modifications and protein-protein interactions. Analysis of the amino acid sequence of DAT reveals multiple sites of phosphorylation and other post-translational modifications such as glycosylation and ubiquitination (Torres et al., 2003; Jayanthi et al., 2007). Phosphorylation by kinases such as protein kinase C (PKC), cAMP-dependent protein kinases, mitogen-activated protein kinases, and tyrosine kinases modulate DAT activity. Studies utilizing phorbol 12-myristate 13-acetate, which activates PKC, have demonstrated that phosphorylation by PKC reduces DAT transport activity by altering DA surface levels (Vaughan et al., 1997; Zhang et al., 1997; Zhu et al., 1997). PKC-dependent endocytosis of DAT is also mediated by ubiquitination of DAT on the amino terminus of DAT (Miranda et al., 2007; Miranda and Sorkin, 2007). Further, PKC-mediated DAT trafficking is characterized by internalization through a clathrin-associated endocytosis mechanism that is dynamin dependent (Daniels and Amara, 1999). Constitutive internalization and recycling of DAT, which is important for membrane homeostasis, is also mediated by a clathrin-dependent mechanism (Sorkina et al., 2005). Furthermore, recent research illustrates that residues 60-65 on the N-terminal domain are important for the prevention of clathrin-dependent constitutive internalization of DAT (Sorkina et al., 2009). In addition, other kinases such as protein kinase A (PKA), Ca^{2+}/calmodulin-dependent kinases and tyrosine kinases have been shown to upregulate DAT surface expression

(Zahniser and Doolen, 2001). Substrates such as DA, AMPH and METH, as well as reactive oxygen species and nitric oxide have been shown to decrease DAT surface expression through a PKC-mediated mechanism; while D2 receptor agonists and DAT inhibitors, such as cocaine, increase DAT cell-surface expression (Zahniser and Doolen, 2001; Cervinski et al., 2005). Further, DAT has been shown to interact with other proteins such as the D2 receptor, syntaxin 1A, synaptogyrin-3, and α-synuclein, which can further modulate DAT trafficking and function (Lee et al., 2001, 2004, 2007; Egana et al., 2009, Eriksen et al., 2010).

f. Vesicular Monoamine Transporter

Once transported back into the presynaptic nerve terminal, DA is metabolized into DOPAC by MAO. However, DA that is not metabolized by MAO is repackaged into synaptic vesicles by the vesicular monoamine transporter (VMAT; Fig 3). VMAT belongs to the major facilitator and solute carrier superfamily of transporters (Pao et al., 1998; Eiden et al., 2004). VMAT exists in humans in two isoforms, VMAT1 and VMAT2, encoded by separate genes SLC18A1 and SLC18A2, respectively (Eiden and Weihe, 2011). VMAT1 is located primarily in endocrine cells found in adrenal medulla chromaffin cells and absent in adult neuronal cells. Conversely, VMAT2 is located in neuronal cells of the CNS as well as in sympathetic adrenal chromaffin cells and neurons in the intestine and stomach (Peter et al., 1995). VMAT2 is expressed in all monoamine neurons primarily localized to cell bodies and axon terminals, and is responsible for packaging DA, serotonin (5-HT), norepinephrine (NE),

epinephrine (E) and histamine into small synaptic vesicles. Thus, VMAT2 represents a vital protein in regulating neuronal monoamine transmission.

VMAT2 KO mice have been generated to elucidate the importance of VMAT2 function in neurotransmission. Homozygous VMAT2 KO mice were born without complication, suggesting that VMAT2 was not important in gestation and birth (Takahashi et al., 1997). However, most of the homozygous KO mice died on the first day due to a lack of feeding, with 100% mortality by postnatal day 14 (Takahashi et al., 1997; Fon et al., 1997). Heterzygous VMAT2 KO mice survived, exhibiting ~50% less VMAT2 binding compared to WT mice (Takahashi et al., 1997). Monoamine levels in VMAT2 KO mice were significantly decreased compared to WT mice, while no differences in brain structure and DA neuronal projections were found (Fon et al., 1997). Interestingly, DA synthesis was increased in VMAT2 KO mice; however DA metabolite levels were similar to those found in WT mice, demonstrating the importance of VMAT2 in sequestering newly synthesized DA into vesicles to prevent degradation (Fon et al., 1997; Wang et al., 1997).

VMAT2 transports monoamines from the cytosol into vesicles against a high concentration gradient (>10^5; Wimasalena, 2010). To accomplish this, VMAT2-mediated transport utilizes electrochemical and transmembrane pH gradients (~1.5 units) generated by a V-type ATPase (Kirschner, 1962; Schuldiner, 1994). ATPases, found in virtually all eukaryotic cells and organelles, utilize the hydrolysis of ATP to drive the transport of protons across a

membrane (Nelson et al., 2000). In VMAT2, the ATPase generates a H^+ electrochemical gradient, acidifying the interior lumen of the synaptic vesicle (Yelin and Schuldiner, 2000). VMAT2, utilizing an antiport transport mechanism, couples the efflux of two protons out of the vesicle to the transport of one substrate molecule into the vesicular lumen (Knoth et al., 1981; Schuldiner, 1994; Schuldiner et al., 1995; Parsons, 2000). Specifically, the efflux of the first proton from the vesicular lumen elicits a conformational change in the transporter, which exhibits high affinity monoamine binding sites on the cytosolic face. Following monoamine binding, the efflux of the second proton generates a conformational change in the transporter, in which the monoamine-bound face of the transporter is toward the vesicular lumen. In this orientation, monoamine-binding affinity is now reduced, allowing the release of the monoamine into the vesicle. In addition to the proton gradient, VMAT2-mediated transport in synaptic vesicles is also dependent upon cytosolic amine concentrations, extra vesicular media and the number of transporters in the vesicular membrane (Wimalasena, 2011).

Studies examining VMAT2 kinetic uptake parameters determined that the order of substrate uptake efficiency was 5-HT>DA>E>NE (Wimalasena, 2011). Similar to DAT, VMAT2 transports MPP+, sequestering MPP+ from the cytosol into synaptic vesicles which protects the neuron from MPP+-induced toxicity (Liu et al., 1992). In addition, AMPH and related compounds are also transported by VMAT, which plays a critical role in their mechanism of action (Sulzer et al., 2005). Numerous studies have focused on the ability of two well known inhibitors of VMAT2, reserpine and tetrabenazine (TBZ). Reserpine (Fig. 1) is an indole

alkaloid historically used to treat high blood pressure. Reserpine inhibits monoamine uptake at VMAT2 with high affinity and can be surmounted by increasing concentrations of substrate, indicative of competitive inhibition (Schuldiner et al., 1995). Further, reserpine binding is modulated by the transmembrane pH gradient (Yelin and Schuldiner, 2000; Wimalasena, 2011). Reserpine binds to the high affinity substrate binding site inhibiting the efflux of H^+ thereby preventing the conformational change necessary to transport the ligand into the vesicular lumen. Reserpine becomes trapped in the active site and is not readily dissociated. With reserpine in the active site, VMAT2 cannot efflux another proton to return the transporter to its active, high affinity state (Schuldiner et al., 1995). Therefore, reserpine has been classified as an irreversible inhibitor of VMAT function.

TBZ (Fig. 1) is a benzoquinolizine derivative, marketed as Xenazine, and currently FDA approved to treat Huntington's chorea. TBZ inhibits monoamine uptake with high affinity, however unlike reserpine, TBZ is proposed to interact with a site distinct from the substrate site (Pletscher, 1977; Scherman and Henry, 1984; Schuldiner, 1994). This conclusion is based upon studies showing that TBZ binding is 1) not dependent on the pH gradient, 2) not inhibited by reserpine binding at reserpine concentrations that inhibit substrate transport and 3) substrates (5-HT, DA, NE) displace TBZ only at concentrations 100-fold higher than their affinity for the substrate site (Scherman and Henry, 1984). Unlike reserpine, TBZ is relatively short acting with respect to inhibition of VMAT2 function. Radiolabeled TBZ and its derivative dihydrotetrabenazine (DTBZ) have

been used extensively to study VMAT2 binding, regulation, distribution and expression (Yelin and Schuldiner, 2000).

In addition to exhibiting different tissue distribution, VMAT1 and VMAT2 also display different affinities for substrates and inhibitors. VMAT2 has been shown in cell expression systems to exhibit 4-5-fold higher affinity for DA, 5-HT, NE, and E compared to VMAT1 (Peter et al., 1994). Despite the difference in affinities for monoamines between the two isoforms of VMAT, the rank order of affinities is similar for both transporters (Yelin and Schuldiner, 2000). Interestingly, both isoforms exhibit affinity not different from one another for MPP+ and AMPH, but VMAT2 exhibits over two orders of magnitude higher affinity for histamine compared to VMAT1 (Peter et al., 1994). In regards to inhibitors, both VMAT1 and VMAT2 exhibit similar affinity for reserpine (K_i = 0.034 and 0.012 µM, respectively). Conversely, VMAT2 exhibits high affinity for TBZ; Ki = 0.097 µM), while VMAT1 exhibits low affinity for TBZ (Ki = > 20 µM; Wimalasena, 2011).

Similar to DAT, VMAT2 consists of 12 TMDs. Despite this similarity and the fact that both proteins transport common substrates, VMAT2 and DAT share little structural homology (Hoffman et al., 1998). VMAT is a 70 kDa glycoprotein located within the membrane of synaptic vesicles. While both VMAT1 and VMAT2 are derived from different genes, they exhibit high structural homology (~60%; Adam et al., 2008; Wimalasena, 2011). Sequence analysis of VMAT2 reveals a 521 amino acid protein, with both the N and C termini facing outward

towards the cytoplasm (Liu et al., 1992; Yelin and Schuldiner, 2000). A large hydrophilic loop occurs between TMDs 1 and 2 facing the interior lumen of the vesicle, which is presumed to be involved in post-translational modification and regulation, as this loop contains multiple sites for glycosylation (Yelin and Schuldiner, 2000). Further, four aspartic residues in TMDs 1, 6, 10 and 11 (Asp 34, Asp 267, Asp 404, and Asp 431), as well as a lysine residue in TMD 2 (Lys 139), are important in transporter function and substrate and reserpine binding (Yelin and Schuldiner, 2000). His419 (between TMD 10 and 11) has also been shown to play an important role in monoamine transport, possibly through H+ translocation and energy coupling required for transport (Wimasalena, 2010). Studies using chimeras have shown that regions encompassing TMDs 5-8 and TMDs 9-12 are important for the high affinity interaction with monoamines and TBZ (Peter et al., 1996).

Similar to DAT, VMAT2 can undergo post-translational modifications regulating VMAT2 function, expression and localization. Studies utilizing pheochromocytoma cells of the rat adrenal medulla (PC12) showed that treatment with cAMP down regulated vesicular monoamine transport, suggesting a role of phosphorylation in the modulation of VMAT activity (Nakanishi et al. 1995). In Chinese hamster ovary, PC12 and COS cells, casein kinase I and II phosphorylated the carboxyl-terminus of VMAT2, but not VMAT1, suggesting a difference in the regulation of the two isoforms (Krantz et al., 1997). Further phosphorylation in VMAT2 affected the subcellular localization and membrane trafficking of VMAT (Krantz et al., 1997). Using PC12 cells, Hersh and

colleagues found that in the presence of PKA, VMAT2 is preferentially sorted to LDCVs and not to SSVs (Yao et al., 2004). Interestingly, the effect of PKA on VMAT2 sorting is not due to phosphorylation of the protein, but rather glycosylation of the C terminus (Yao et al., 2004). In addition to action by kinases, G-proteins have been shown to regulate VMAT2 activity. Guanosine-triphosphate-bound G-proteins inhibited both monoamine uptake and reserpine binding in PC12 cells (Ahnert-Hilger et al., 1998; Holtje et al., 2000). This inhibition of uptake is attenuated by increasing monoamine concentrations, suggesting that G-protein mediated inhibition is through an effect on monoamine affinity for the transporter (Ahnert-Hilger et al., 2000). Similar to results seen in the phosphorylation studies, VMAT2 was more susceptible to regulation by G-proteins compared to VMAT1 (Holtje et al., 2000). More recent studies utilizing site-directed mutagenesis have shown that the first intracellular loop is responsible for G-protein-mediated regulation of VMAT activity (Brunk et al., 2006). Collectively, these studies demonstrate that intravesicular monoamine concentration can modulate VMAT activity, regulating vesicular filling and subsequently affecting neurotransmission.

IV. METH mechanism of action

As discussed previously, METH is an N-methyl derivative of AMPH. METH and AMPH exhibit similar rewarding effects, pharmacokinetic properties, and mechanism of action to release DA in brain (Sulzer et al., 2005). Many initial studies concerning the rewarding effects and mechanism of action of AMPH-like

stimulants utilized AMPH, while studies examining DA neurotoxicity were performed using METH (Sulzer et al., 2005). In the subsequent discussion of the mechanism of action of METH, early mechanistic studies using AMPH will be discussed, in addition to studies using METH, as both drugs employ the same mechanism of action to increase extracellular DA and elicit reward.

a. METH action at plasma membrane transporters

Experiments utilizing DAT KO mice provide evidence for a role of other monoamine transporters such as SERT and NET in addition to DAT in the mechanism of action of AMPH and METH (Budygin et al., 2004; Gainetdinov, 2008). Similar to DAT, SERT is a plasma membrane transporter belonging to the Na^+/Cl^- dependent transporter SLC6 family (Rothman et al., 2003). Unlike DA transport through DAT, one molecule of 5-HT is transported with only one Na^+ ion and one Cl^- ion (Gu et al., 1998). Structurally, SERT is composed of 630 amino acid residues arranged into 12 hydrophobic TMDs, with both N and C termini located in the cytoplasm and characterized by a large extracellular loop between TMDs 3 and 4 (Rudnick, 2006). Substrate binding and translocation is believed to occur through an interaction with TMDs 1, 3, 6 and 8, while inhibitors are proposed to interact with same domains (Rudnick, 2006). SERT is located primarily on serotoninergic neurons, as well as peripheral locations such as the lung, placenta and platelets (Jayanthi et al., 2007). In the brain, SERT is located on 5-HT nerve cell bodies originating primarily from the dorsal and medial raphe nucleus, SN, VTA and hypothalamus (Hoffman et al., 1998). 5-HT and DA

containing neurons co-innervate many brain regions. Thus SERT is found in striatum, cortex and hippocampus (Hoffman et al., 1998). In brain, SERT functions to terminate the action of 5-HT through the transport of 5-HT from the extracellular space into the presynaptic terminal, where it is metabolized or repackaged into vesicles by VMAT2. 5-HT functions in the CNS as a regulator of mood, sleep, memory, appetite, thyroid function, gastrointestinal function, and sexual drive (Jacobs and Azmitia, 1992). Dysfunction of 5-HT signaling is linked to numerous psychiatric disorders such as depression, suicide, alcoholism, and violence (Jayanthi et al., 2007). Numerous inhibitors of SERT function have been used in the treatment of depression and mood stabilization, such as fluoxetine, paroxetine, sertraline, and citalopram (Rudnick, 2006).

Similar to DAT and SERT, NET is a plasma membrane transporter belonging to the SLC6 family of Na^+/Cl^- dependent transporters. The stoichiometry of NE transport is similar to SERT in that one Na^+ ion and one Cl^- ion is co-transported with one molecule of NE (Gu et al., 1998). NET is structurally homologous to DAT and SERT, and is composed of 617 amino acid residues arranged into 12 TMDs (Torres et al., 2003). Similar to DAT and SERT, the N and C termini of NET are located in the cytoplasm and a large extracellular loop exists between TMDs 3 and 4 (Torres et al., 2003). Studies utilizing chimeric DAT and NET proteins showed that TMDs 1-5 and 9-12 are important for substrate translocation, and TMDs 6-8 are important for interaction with uptake inhibitors such as cocaine, desipramine and nortryptiline (Giros et al., 1994). NET is located on cell bodies and axon terminals of noradrenergic

neurons originating from the locus coeruleus and innervating the hippocampus and cortex (Torres et al., 2003). NET also has been found in peripheral locations, such as placenta, lung, adrenal glands and vas deferens (Torres et al., 2003; Jayanthi et al., 2007). NET functions primarily to terminate the action of NE through the transport of NE from the extracellular space into presynaptic terminals. NE acts as a regulator of attention, arousal, learning, memory, and mood as well as being involved in depression, aggression, thermal regulation and autonomic functioning (Jayanthi et al., 2007). Thus, modulation of NET plays an important role in many diseases and pharmacotherapies. NET inhibitors such as atomoxetine, reboxetine, desipramine, and mazindol have been used in the treatment of depression, attention-deficit hyperactivity disorder, drug abuse and other mental illnesses (Zhou, 2004).

The rewarding effects of AMPH-like compounds are a result of the ability of these compounds to increase extracellular monoamine levels. The first evidence that AMPH elicits its effects through a release of catecholamines from the presynaptic terminal was introduced by Burn and Rand in 1958. These studies demonstrated that AMPH increased blood pressure in animals, but this effect was blocked by the treatment of reserpine, a catecholamine-depleting agent, suggesting that AMPH acts by increasing catecholamine concentrations (Burn and Rand, 1958). Additional results from this study demonstrated that cocaine blocked AMPH-induced release of catecholamines, providing the first evidence that AMPH-induced monoamine release involves plasma membrane transporters (Burn and Rand, 1958). Early studies demonstrated that AMPH

inhibited [^{3}H]monoamine uptake into rat synaptosomes and slices, further demonstrating an interaction of AMPH with plasma membrane transporters (Ross and Renyi, 1964, 1966; Coyle and Snyder, 1969). Initial evidence that AMPH is a substrate for monoamine transporters in the brain was found in studies utilizing PC12 rat chromaffin cells. Using radiolabled AMPH, Bonisch demonstrated that AMPH was transported in a manner similar to that of NE, dependent upon Na^+ and Cl^- gradient and blocked by plasma membrane transporter inhibitors cocaine and desipramine (Bonisch, 1984). Follow-up studies using rat striatal synaptosomes demonstrated that AMPH uptake was saturable with a K_m of 97 nM and a V_{max} of 3.0 fmol/mg/min (Zaczek et al., 1991). Therefore, one mechanism by which AMPH increases monoamine concentrations is by inhibiting uptake of monoamines into presynaptic terminals by acting as a substrate. These early studies examining AMPH uptake through monoamine transporters were complicated by the physiochemical properties of AMPH (Sulzer et al., 2005). Due to the lipophilicity of AMPH, AMPH and related compounds also enter presynaptic terminals through passive diffusion (Fig 4; Fischer and Cho, 1979; Sieden et al., 1993).

In addition to inhibiting monoamine uptake through plasma membrane transporters as a substrate, AMPH also elicits a non-exocytotic release of monoamines from monoaminergic neurons (Fig 4). Early studies using radiolabeled monoamines demonstrated that AMPH released monoamines in rat brain tissue (Glowinski and Axelrod, 1966; Brodie et al., 1969). The ability of AMPH to release DA from neurons is dependent on both a plasmalemmal and

vesicular component. Pifl and colleagues performed [^{3}H]DA release studies utilizing cell lines that expressed DAT only, VMAT2 only and both DAT and VMAT2 (Pifl et al., 1995). Results from this study showed that DAT expression was essential for DA release, as the cell expressing VMAT2 alone did not release DA and the extent of DA release was larger in the cell expressing both DAT and VMAT2. Further evidence for the importance of DAT in the mechanism of action of AMPH was provided by Jones and colleagues in 1998. Using DAT KO mice and fast scan cyclic voltammetry, it was shown that AMPH-mediated DA release was DAT dependent, as AMPH-mediated DA release was not seen in DAT KO mice (Jones et al., 1998). Thus, DAT plays an important role in the effects of AMPH.

AMPH-induced release of DA via DAT has been hypothesized to follow a facilitated exchange diffusion mechanism (Paton, 1973; Arnold et al., 1977; Fischer and Cho, 1979). Based upon a glucose-mediated transport mechanism, AMPH is translocated into the cytosol from the extracellular space as a substrate for DAT (Stein, 1968). As AMPH is released in the cytosol, high affinity DA binding sites on DAT are exposed, enabling the high concentrations of cytosolic DA to bind. One molecule of DA is expected to bind and be released in the extracellular space when the transporter returns to the external face. Reverse transport by this mechanism is dependent upon Na^+ concentrations and follows a one-to-one AMPH molecule to DA molecule ratio. While support for this mechanism is widely found in the literature, results from some studies cannot be explained by this hypothesis. Sulzer and colleagues found that AMPH directly

injected into neurons of the pond snail, *Planorbis corneus*, induced reverse transport of DA into the extracellular space (Sulzer et al., 1995). In this experiment, AMPH was not transported into the neuron through DAT, but DA was still released in a non-exocytotic, reverse transport mechanism. Additionally, increasing cytosolic Na^+ concentrations reversed transport of DA through DAT in the absence of AMPH (Khoshboeui et al., 2003). Further, why DA preferentially binds to the cytosolic face of the transporter and not AMPH, is not explained, as AMPH is not reverse transported out of the neuron, despite interacting with the same site on DAT. Thus, evidence exists for an alternative mechanism of AMPH-induced DA release through DAT.

Recent studies have provided evidence for AMPH-evoked DA release through DAT by a channel-like mechanism. Utilizing patch clamp recordings of *Xenopus* oocytes expressing DAT, it was demonstrated that DAT exhibits transport and leak-associated currents derived from the conductance of monoamine transport (Sonders et al., 1997). Other monoamine transporters, such as NET and SERT have been shown to exhibit similar ion conductance with associated monoamine transport (Galli et al., 1998). Channel-like DA release in the presence of AMPH was demonstrated by Galli and colleagues in 2005 (Kahlig et al., 2005). In this study, AMPH-induced ionic currents were measured using patch clamp and amperometric recordings from human embryonic kidney cell lines expressing DAT. Results from this study showed that AMPH releases DA from neurons through DAT in two ways, a slow, exchange mediated mechanism and a fast, channel-like mechanism. Release of DA through the

channel-like mechanism is characterized by fast bursts of DA efflux containing a large number of DA molecules in each channel-like event. Interestingly, unlike AMPH, the endogenous substrate DA, could not evoke these channel-like events. Thus, AMPH could be evoking DA release through DAT in a facilitated exchange diffusion or channel-like mechanism to increase extracellular DA concentrations.

In addition to evoking DA release through DAT, AMPH and METH also modulate DAT uptake and expression. Synaptosomal DA uptake in striatum was significantly reduced 1 hr following an acute high dose of METH (15 mg/kg; Fleckenstein et al., 1997). This reduction in DAT function is characterized by a decrease in maximal uptake (V_{max}), with no effect on affinity for DA (K_m). However, total DAT binding was not altered, suggesting that METH altered cell surface localization of DAT through a trafficking mediated mechanism. Others have shown that METH-induced DAT internalization is PKC-dependent and similar to substrate-mediated internalization through clathrin-coated vesicles (Saunders et al., 2000; Cervinski et al., 2005; Schmitt and Reith, 2010). Interestingly, the effect of METH to internalize DAT was not seen in the synaptosomes prepared from the nucleus accumbens, suggesting regional modulation of DAT expression and potentially activity (Kokoshka et al., 1998). In addition to the differential regional regulation, the observed changes are also dependent on time following METH treatment. Results from the Gnegy and colleagues showed that exposure to 3 µM AMPH increased DAT cell surface expression levels 70% within 30 sec of exposure and expression remained

elevated for 1 min (Johnson et al., 2005). Thus, AMPH and METH rapidly increase DAT activity immediately following exposure, but decrease DAT expression after 20 min, suggesting that AMPH and METH regulate DAT activity in a complex manner dependent upon time and brain region.

Utilizing fluorescence resonance energy transfer microscopy, DAT was shown to oligomerize in the endoplasmic reticulum and remain oligomerized while trafficking to the plasma membrane (Sorkina et al., 2003). Interestingly, substrates such as AMPH and METH dissociate the DAT oligomers suggesting a possible role in AMPH-mediated DAT trafficking (Chen and Reith, 2008). Results from this study suggest that DAT in the plasma membrane is present in oligomer and monomer forms, and AMPH promotes the formation of monomers resulting in increased DAT internalization.

In summary, DAT plays an important role in the stimulant effects of abused drugs, specifically METH. Through the reversal of DAT function, METH releases DA into the extracellular space leading to its abuse. Furthermore, METH can modulate DAT activity through various mechanisms, such as phosphorylation or altered formation of DAT oligomers. The extensive research on METH and DAT has provided a greater understanding of the mechanism of action of METH and will hopefully contribute to the development of a successful pharmacotherapy for METH abuse.

b. METH at VMAT2

In addition to the effect of METH on DAT, METH interacts with VMAT2 to increase extracellular DA levels (Fig 4). As discussed previously, results from Pifl and colleagues showed that while DAT was necessary for AMPH-induced DA release, cells expressing both DAT and VMAT2 exhibited greater and more sustained release compared to cell expressing just DAT (Pifl et al., 1995). Using neuronal cultures from VMAT2 KO mice, neurons lacking VMAT2 exhibited significantly decreased AMPH-evoked DA release compared to WT neurons (Fon et al., 1997). Thus, the effect of AMPH on vesicular DA stores is critical in the mechanism of AMPH-induced DA release.

AMPH acts to redistribute DA from presynaptic vesicular stores to the cytosol, where it can be reverse transported into the extracellular space through DAT (Sulzer et al., 2005). Low concentrations of AMPH (doses less than 1 mg/kg) are hypothesized to release DA available in the cytosol, while higher concentrations of AMPH (doses greater than 5 mg/kg) are hypothesized to interact with vesicular pools and VMAT2 to redistribute DA to cytosolic pools to then be released into the extracellular space (Seiden et al., 1993). Evidence for a redistribution of DA from vesicles to the cytosol was provided by Sulzer and colleagues in 1995. Direct injection of AMPH into DA neurons of *Planorbis corneus* increased cytosolic DA and decreased vesicular DA concentrations (Sulzer et al., 1995). Further, quantal DA release following injection of AMPH was reduced by >50%, supporting AMPH-induced decreases in vesicular DA storage. Elevated cytosolic DA induces reverse transport leading to DA release into the extracellular space,

One mechanism of AMPH-induced increases in cytosolic DA is the inhibitory effect of AMPH on DA uptake into vesicles. AMPH inhibits the uptake of monoamines into synaptic vesicles (Knepper et al., 1988). AMPH is a substrate for VMAT2, competing with reserpine for the VMAT2 substrate uptake site (Peter et al., 1994; Erickson et al., 1996). In addition to displacing reserpine binding, AMPH also displaces TBZ binding to VMAT2, providing a mechanism for AMPH-induced inhibition of vesicular monoamine uptake (Gonzalez et al., 1994). Thus, one mechanism by which AMPH increases cytosolic DA concentrations is through an inhibition of DA uptake at VMAT2.

In addition to inhibiting DA uptake at VMAT2, AMPH evokes DA release from vesicular stores to increase cytosolic DA concentrations (Sulzer et al., 2005). As a substrate for VMAT2, AMPH acts to release DA from vesicles through an interaction with VMAT2. Similar to the facilitated exchange diffusion model hypothesized for AMPH-induced DA release through DAT, AMPH evokes DA efflux through VMAT2 and may do so via a similar mechanism. Under this proposed mechanism, transport of AMPH into vesicles would increase accessibility to DA binding sites on the inner-facing surface of the transporter. Subsequently, the bound DA will then be reverse transported out of the vesicle and into the cytosol (Sulzer et al., 2005). Several studies have shown that vesicles “leak” monoamines into the cytosol (Floor et al., 1995). Further, this efflux of DA from synaptic vesicles is independent of uptake blockade, as TBZ did not inhibit this DA efflux (Floor et al., 1995). In addition, low concentrations of AMPH evoke DA release from synaptic vesicles that is not dependent on the

electrochemical H+ gradient (Floor and Meng, 1996). Thus, in addition to inhibiting DA uptake through VMAT2, AMPH simultaneously evokes the efflux of DA from vesicles, increasing cytosolic DA.

In addition to a VMAT2-mediated mechanism, AMPH is also proposed to release DA from vesicles through a "weak base" effect (Sulzer et al., 2005). As discussed previously, uptake of monoamines through VMAT2 is coupled to a H^+ electrochemical gradient. Intravesicular monoamine concentration is estimated to be around 500 mM, while cytosolic concentrations are only 25 µM (Johnson, 1988). Thus, VMAT2 uses an H^+ gradient to transport monoamines against a 140,000 to 1 concentration gradient. The H^+ gradient is produced and maintained by the activity of the ATPase proton pump. Consequently, the interior lumen of synaptic vesicles is acidic with an interior pH around 5.5 (Johnson, 1988; Fleckenstein et al., 2007). AMPH is a lipophilic weak base, exhibiting a pKA of 9.88 (Mack and Bonisch, 1979). In addition to active transport through VMAT2, AMPH also diffuses across the synaptic membrane due to its lipophilicity (Peter et al., 1995; Sulzer et al., 2005). In the vesicular lumen, AMPH becomes protonated, causing the vesicular lumen to become more alkaline, which disrupts the pH gradient needed to provide the energy for monoamine transport. The first evidence for this mechanism was provided using the fluorescent weak base quinacrine in real-time estimation of internal pH of isolated chromaffin vesicles. In this study, AMPH was shown to alkalinize vesicular pH, leading to decreased DA uptake and increased DA release from vesicles (Sulzer and Rayport, 1990). Further evidence for the weak base effect was seen with other weak bases, such

as ammonium chloride, chloroquine, and bafilomycin, which are known to disrupt pH gradients in neuronal cells. Incubation with these compounds increased vesicular DA release and decreased vesicular DA content as a result of the alkanization of the vesicular lumen and disruption in the pH gradient (Sulzer et al., 1993; Mundorf et al., 1999; Sulzer and Pothos, 2000).

Despite considerable evidence for the weak base effect of AMPH to release vesicular DA, several arguments to this proposed mechanism exist. Lower concentrations of AMPH have been shown to release DA from synaptic vesicles, independently of the electrochemical pH gradient (Floor and Meng, 1996). Specifically, synaptic vesicles loaded with [^{3}H]DA exposed to 3 µM AMPH rapidly released over 70% of DA, while the pH gradient was only decreased by 12% (Floor and Meng, 1996). Further evidence arises from the fact that bafilomycin A_1, an ATPase inhibitor, decreased the pH gradient 2-fold more than AMPH, but only released DA half as fast as AMPH (Floor and Meng, 1996). Another important caveat to the weak base mechanism is that the *S*(+) stereoisomer of AMPH is more effective in promoting DA release than the *R*(-) stereoisomer, despite having the same effect on vesicular pH (Peter et al., 1994). Interestingly, the *S*(+) isomer of AMPH binds with higher affinity to VMAT2 which could account for the ability of the *S*(+) isomer to preferentially release DA, further supporting a VMAT2-mediated mechanism of vesicular DA release (Erickson et al., 1996; Sulzer et al., 2005). Taken together, these results suggest that the alkalization of vesicles alone cannot fully explain AMPH-induced DA release from synaptic vesicles.

Similar to the effect on DAT, AMPH and METH treatment can modulate VMAT2 activity. Multiple high doses of METH (10 mg/kg, s.c. x 4) significantly decreased DA uptake at VMAT2 at both 1 hr or 24 hrs following treatment (Brown et al., 2000; Hogan et al., 2000). Further, DTBZ binding to VMAT2 was also reduced in striatal vesicles, but not in total striatal homogenates, suggesting a redistribution of VMAT2 protein within the presynaptic terminal (Hogan et al., 2000; Fleckenstein et al., 2007). Western blot analysis revealed that multiple high doses of METH (10 mg/kg x 4) decreased by 80%VMAT2 immunoreactivity in cytoplasmic striatal vesicles (Riddle et al., 2002). Further, redistribution of VMAT2 was not retained in the synaptosomal fraction, suggesting that METH decreases VMAT2 function by trafficking VMAT2 containing vesicles out of presynaptic terminal. METH-induced decreases in VMAT2 immunoreactivity in the striatum were also found by Yamamoto and colleagues further supporting METH-induced VMAT2 redistribution (Eyerman and Yamamoto, 2005). Thus, METH modulates VMAT2 function by altering the subcellular distribution of VMAT2 protein in the presynaptic terminal.

c. METH at MAO

Under physiological conditions, cytosolic DA is rapidly metabolized into DOPAC by MAO. In addition to the redistribution of DA into the cytosol from vesicular stores, AMPH inhibits the enzymatic activity of MAO in the cytosol (Fig 4; Mantle et al., 1976). AMPH is a competitive and reversible low affinity inhibitor of MAO (Sulzer et al., 2005). Thus, in the presence of AMPH, DA is not

metabolized into DOPAC in the cytosol. The increased DA in the cytosol is available for reverse transport through DAT. AMPH itself is not a substrate for MAO oxidation (Sulzer et al., 2005).

d. METH on DA synthesis

In addition to the ability of AMPH to increase cytosolic DA concentrations by redistributing DA from vesicles and inhibiting MAO, AMPH also increases synaptosomal DA synthesis (Sulzer et al., 2005). Using radiolabeled tyrosine, AMPH was demonstrated to exacerbate TH enzymatic activity to increase DA biosynthesis (Kuczenski, 1975). Interestingly, the AMPH-induced increase in DA biosynthesis was found in striatum, but not in the nucleus accumbens or olfactory tubercle, suggesting regional specific modulation of TH activity (Demarest et al., 1983). In addition to inhibiting DA uptake into vesicles, releasing DA from vesicles and inhibiting DA metabolism by MAO, AMPH increases DA synthesis to increase cytosolic DA concentrations available for reverse transport, which can lead to AMPH-induced neurotoxicity.

V. METH-induced neurotoxicity

Acute and repeated METH use is characterized by a decrease in behavioral and cognitive functions, as well as deficits in attention, memory and decision making (Krasnova and Cadet, 2009). These neurological changes are thought to be mediated in part through the neurotoxic effect of METH on monoamine signaling.

Utilizing neuroimaging techniques as well as other assays, the neurotoxic effects of METH have been shown in numerous animal models (monkeys, rats, and mice) and in humans studies. Both acute and high doses of METH have been shown to decrease DA, 5-HT and NE levels in the striatum, cortex, nucleus accumbens, and hippocampus in monkeys and rodents (Seiden et al., 1976, Kogan et al., 1976; Ricaurte et al., 1980; Bakhit et al., 1981; Fumagalli et al., 1998; Graham et al., 2008). A similar decrease in monoamine levels was observed in autopsied brains of human METH users (Wilson et al., 1996; Moxzczynska et al., 2004). Decreases in DAT and SERT levels following METH administration were also observed in both animal models and humans (Wagner et al., 1980; Fumagalli et al., 1999; Melega et al., 2000; Armstrong and Noguchi, 2004; Volkow et al., 2001; Sekine et al., 2003). In addition to changes in plasma membrane transporters, decreases in VMAT2 function and immunoreactivity were observed following METH administration (Riddle et al., 2002; Guilarte et al., 2003; Segal et al., 2005; Eyerman and Yamamoto 2005, 2007). METH also decreases DA and 5-HT synthesis, as evidenced by decreases in TH and tryptophan hydroxylase activity in rodents and humans (Seiden et al., 1976; Hotchkiss et al., 1979; Wilson et al., 1996). Thus, METH mediates numerous changes in monoamine neuron function, significantly altering neuronal signaling.

DA and oxidative stress plays an important role in METH-induced neurotoxicity (Cadet and Krasnova, 2009). The importance of DA in METH-induced neurotoxicity is demonstrated by experimental results showing that α-methyl-p-tyrosine (AMPT), which decreases DA synthesis, protects against

METH-neurotoxicity (Krasnova and Cadet, 2009). Further, heterozygous VMAT2 KO mice exhibit exacerbated METH-induced neurotoxicity compared to WT mice, as evidenced by prolific DA neurodegeneration and significant decreases in DA, DOPAC, and DAT levels in the brain (Fumagalli et al., 1999; Guillot et al., 2008). These studies provide support for the importance of DA in METH-induced neurotoxicity and the important role VMAT2 plays to prevent the neurotoxic effects of METH by sequestering DA into vesicles.

METH acts to increase cytosolic and extracellular DA concentrations, as previously discussed above. Cytosolic DA is rapidly auto-oxidized to form DA quinones, leading to the production of superoxide radicals and hydrogen peroxides (Krasnova and Cadet, 2009). Further, DA metabolism into DOPAC by MAO also produces hydrogen peroxides which can lead to the generation of reactive oxygen species (ROS) causing oxidative stress in the neuron. Due to the lack of free electrons, hydrogen peroxide does not have an oxygen radical, but readily interacts with metal ions such as iron, leading to the production of highly toxic hydroxyl radicals (Cadet and Brannock, 1998). Hydroxyl radicals are very reactive and can cause damage to nucleic acids, amino acids in proteins and phospholipids, damaging lipid membranes (Cadet and Brannock, 1998). Moreover, METH has been shown to decrease levels of antioxidants and free radical scavengers in DA neurons, limiting the ability of DA neurons to decrease oxidative stress (Yamamoto et al., 2010).

In addition to oxidative stress, METH has also been shown to induce neuronal damage through an excitotoxic mechanism. METH administration increases glutamate release in the striatum (Nash and Yamamoto, 1992). Increased glutamate signaling increases intracellular calcium, which stimulates the activity of calcium-dependent enzymes to produce free radicals and nitric oxide (Yamamoto et al, 2010). Nitric oxide reacts with superoxide radicals to form peroxynitrite, which damages DNA and proteins (Krasnova and Cadet, 2009). Nitric oxide and peroxynitrite have also been shown to activate apoptotic pathways leading to neuronal death and impairment of mitochondrial and endoplasmic reticulum function (Yamamoto et al., 2010).

An important aspect of METH-induced neurotoxicity is the effect of METH on body and brain temperature. High doses of METH induce hyperthermia and this increase in temperature is associated with an increase in striatal DA content depletion (Bowyer et al., 1994). Support for the role of hyperthermia is provided by results showing that high doses of METH administered in a cold environment did not decrease striatal DA levels, while METH treatment at normal room temperatures significantly decreased DA levels (Ali et al., 1994). Hyperthermia is proposed to increase ROS formation and glutamate neurotransmission, both leading to oxidative stress and neuronal damage (Yamamoto et al., 2010). Drugs such as AMPT, MK-801, and 2-deoxyglucose attenuate the neurotoxic effects of METH through the ability to attenuate METH-induced hyperthermia (McCann and Ricaurte, 2004). Further, hyperthermia plays a role in METH-induced increases in blood-brain barrier (BBB) damage (Bowyer and Ali, 2006).

METH-induced BBB damage then can lead to neuronal damage and degeneration as well as enhanced vulnerability to environmental toxins and infections (Krasnova and Cadet, 2009; Cadet and Krasnova, 2009; Yamamoto et al., 2010)

VI. Treatment Options for METH abuse

a. Cognitive and Behavioral Therapy

Currently there are no approved medications to treat METH abuse. Thus, cognitive and behavioral therapy is vital for the treatment of METH abuse. Cognitive and behavioral therapy (CBT) employs learning and conditioning in aiding METH abstinence (Lee and Rawson, 2008). While different forms of CBT exists, CBT employs self- and group-help that integrate several intervention techniques such as providing information and assistance on use cessation as well as withdrawal and depression symptoms in an effort to prevent relapse (Rawson et al., 2002; Baker et al., 2005; Lee and Rawson, 2008). Contingency management (CM) is a behavioral therapy aimed at reducing METH use by providing positive reinforcement in exchange for drug abstinence (Prendergast et al., 2006; Roll et al., 2006). This behavioral technique is similar to operant conditioning in that performance of a behavioral task (drug abstinence in this situation) results in the delivery of a reward. Positive reinforcement is usually in the form of a monetary reward. CM has exhibited moderate effectiveness in reducing METH use (Shoptaw et al., 2006; Roll, 2007). In addition to METH, CM therapies have been used in promoting abstinence from multiple drugs such as

cocaine, nicotine, alcohol, opiates and marijuana (Prendergast et al., 2006). Despite the limited success of CBT and CM, behavioral therapies are not efficacious universally (Vocci and Appel, 2007). Thus, the development of pharmacological treatment strategies would be highly beneficial in the treatment of METH abuse.

b. Plasma Membrane Transporters as a Therapeutic Target

METH elicits its rewarding effects, in part, through an interaction with DAT, as previously discussed above. As such, numerous studies have focused on monoamine transporters in the development of pharmacotherapies to treat METH abuse. The antidepressant, buproprion inhibits DA and NE uptake through DAT and NET, and represents an effective therapy in nicotine cessation (Richmond and Zwar, 2003). By increasing monoamine levels, buproprion is hypothesized to alleviate withdrawal symptoms associated with METH abstinence (Karila et al., 2010). Initial clinical studies showed that buproprion attenuates cue-induced cravings for METH (Newton et al., 2006). Despite this decrease in METH cravings, buproprion was not effective in reducing METH use following a 12-week treatment program (Shoptaw et al., 2008; Karila et al., 2010).

In a manner similar to buproprion, methylphenidate (MPD) was hypothesized to be efficacious in treating METH abuse. MPD is a “gold-standard” treatment for childhood attention deficit hyperactivity disorder (ADHD; Patrick et al., 2005). MPD inhibits DA and NE uptake through DAT and NET inhibition to increase extracellular monoamine concentrations. While the effect of

MPD is similar to that of cocaine, MPD exhibits decreased abuse liability due to different pharmacokinetic properties (Volkow et al., 1999; Yano and Steiner, 2007). Initial clinical trials examining the effect of MPD on AMPH abuse showed that MPD was efficacious in reducing intravenous AMPH use in patients with severe AMPH dependence (Tiihonen et al., 2007).

In addition to DAT and NET inhibitors, selective serotonin reuptake inhibitors (SSRIs) have been proposed as treatments for METH abuse. As discussed previously, METH interacts with SERT to increase extracellular 5-HT concentrations. Considering the role that SSRIs play in mood stabilization and the treatment of depression, the use of SSRIs in the treatment of withdrawal-associated depression is warranted (Karila et al., 2010). SSRIs have also been shown to alter DA signaling. Studies measuring the electrical activity of DA neurons showed that SSRIs such as sertaline, paroxetine and fluvoxamine inhibited DA firing rates and dopaminergic function (Di Mascio et al. 1998). Further, studies utilizing KO mice showed that SERT is involved in the rewarding effects of psychostimulants. Psychostimulants produced rewarding effects in DAT KO mice, but did not produce reward in mice deficient in both DAT and SERT, suggesting a role of SERT in the rewarding effects of psychostimulants (Rocha et al., 1998; Sora et al., 2001). Consistent with this hypothesis, fluoxetine, a SSRI, attenuated METH conditioned place preference and METH-induced locomotor sensitization (Takamatsu et al., 2006). Clinical trials determining the ability of fluoxetine to treat METH abuse revealed that fluoxetine failed to demonstrate efficacy in attenuating METH use (Karila et al., 2010).

Preliminary clinical studies with paroxetine found that paroxetine treatment reduced METH-associated cravings (Piasecki et al., 2002). Future studies will be needed to determine the efficacy of SSRIs in the treatment of METH dependence.

c. DA receptors as therapeutic targets

Modulation of DA receptors has been proposed as a potential treatment strategy for METH abuse (Karilla et al., 2010). Risperidone, an atypical antipsychotic, acts as a D2 and 5-HT_{2a} receptor antagonist and has been shown to improve cognitive function (Meredith et al., 2009). Clinical trials examining the efficacy of risperidone in the treatment of METH dependence were recently conducted and results indicated that risperidone was well tolerated and associated with a decrease in METH use and an increase in cognition and memory in METH users (Meredith et al., 2009). These results are promising but further studies are needed to determine the efficacy of risperidone in the treatment of METH abuse.

In addition to D2 receptor antagonists, D2 receptor partial agonists are proposed to be efficacious in the treatment of METH abuse. The idea behind the use of D2 partial agonism in METH dependence focuses on the dual use of partial agonists to increase DA signaling during METH abstinence (when withdrawal symptoms are present) and to act as an antagonist on D2 receptors when METH is used (relapse; Lile et al., 2005). Initial clinical trials determining the efficacy of aripiprazole, a D2 and 5-HT_{1a} partial agonist, in AMPH

dependence showed that ariprazole decreased the subjective effects of AMPH (Lile et al., 2005; Stoops et al., 2006). Results from more recent clinical trials with aripiprazole in the treatment of METH and AMPH dependence have shown that aripiprazole exacerbated METH-related cravings and increased AMPH use compared to placebo groups (Tiihonen et al., 2007; Newton et al., 2008). In contrast to ealier studies, the recent results suggest that aripiprazole increases METH cravings leading to increased use. While the subjective effects play an important role in predicting drug use, many other factors are involved in the manifestation of drug abuse. Thus, future studies to determine the utility of apiprazole as a pharmacotherapy for METH abuse are needed.

d. 5-HT receptors as therapeutic targets

5-HT increases DA release in NAc, prefrontal cortex, striatum and VTA through an interaction with 5-HT_1 and 5-HT_3 receptors (Guan and McBride, 1989; Arborelius et al., 1993; Benloucif et al., 1993; Parsons and Justice, 1993; Prisco et al., 1994). Thus, modulation of 5-HT signaling through 5-HT receptor antagonism could inhibit the effects of METH by decreasing DA release (Vocci and Appel, 2007; Karilla et al., 2010). Consistent with this hypothesis, mirtazapine, a 5-HT_3 and 5-HT_{2a} receptor antagonist, decreased METH-induced conditioned place preference, METH behavioral sensitization and cue-induced responding for METH in rats (McDaid et al., 2007; Herrold et al., 2009; Graves and Napier, 2011). However, clinical trials determining the effect of mirtazapine for the treatment of METH withdrawal symptoms failed to show efficacy

compared to placebo (Cruickshank et al., 2008). Even though mirtazapine did not affect METH withdrawal symptoms, future studies determining the effect of mirtazapine and other modulators of 5-HT neurotransmission on METH use should be investigated. In addition to importance of 5-HT in depression and mood balance as part of potential withdrawal symptoms, 5-HT also modulates DA signaling and could be a viable target for the development for treatments of METH abuse.

Ondansetron, a 5-HT_3 receptor antagonist has also been hypothesized to inhibit the rewarding effects of METH. Ondansetron, co-administered with DA agonist, pergolide inhibited METH-induced behavioral sensitization and METH-induced reinstatement in rats (Davidson et al., 2007). Moreover, ondansetron was shown to attenuate METH-induced reductions in food intake in mice (Ginawi et al., 2005). Clinical trials determining the efficacy of ondansetron in the treatment of METH dependence failed to reveal a significant effect of ondansetron to attenuate METH use or withdrawal symptoms (Johnson et al., 2008).

e. GABA neurotransmitter system as a therapeutic target

gamma-Aminobutyric acid (GABA) is an inhibitory neurotransmitter in the brain primarily functioning to modulate neuronal excitability (Cooper et al., 2003). GABA interacts with GABA receptors in the brain which are comprised of $GABA_A$ receptors that act as ligand gated ion channels, and $GABA_B$ receptors, which act as metabotrophic G-protein coupled receptors. $GABA_A$ receptor activation leads

to the opening of Cl^- channels, while $GABA_B$ receptor activation leads to the opening of K^+ channels, resulting in hyperpolarization of the cell membrane and a decrease in neuronal firing (Cooper et al., 2003). DA neurons in the ventral palladium receive GABA inputs from the NAc which play an important role drug reward and abuse (Zahm et al., 1985; Koob, 1992; Bardo, 1998). Specifically, activation of GABA receptors in the ventral palladium decreases DA release and signaling (Gong et al., 1998). Thus, by decreasing DA neurotransmission, modulation of GABA neurotransmission could attenuate the reinforcing effects of abused drugs. Consistent with this hypothesis, GABA receptor agonists have been used in the treatment of cocaine, heroin, nicotine, METH, and alcohol (Cousins et al., 2000; Vocci and Appel, 2007; Karila et al., 2010). Baclofen, a $GABA_B$ receptor agonist, decreased AMPH-induced increases in extracellular DA in the NAc and decreased AMPH self-administration in rats (Brebner et al., 2005). Further, baclofen improved METH-induced decreases in memory and cognition (Arai et al., 2008, 2009). Gabapentin, a nonselective GABA receptor agonist, attenuated METH-induced hyperlocomotion, conditioned place preference and behavioral sensitization (Itzhak and Martin, 2000; Kurokawa et al., 2011). Clinical trials however, revealed that baclofen and gabapentin were not effacious in decreasing METH use (Heinzerling et al., 2006). Vigabatrin (gamma-vinyl-GABA) increases GABA transmission through inhibition of GABA metabolism by GABA transaminase (Gerasimov et al., 1999). Vigabatrin pretreatment inhibited METH-induced increases in NAc DA release and reinstatement of METH-induced conditioned place preference (Gerasimov et al.,

1999; DeMarco et al., 2008). Results from clinical trials revealed that vigabatrin decreased METH use in METH-dependent users (Brodie et al., 2004). Thus, GABA neurotransmission may represent a useful therapeutic target in developing pharmacotherapies for METH abuse.

f. Acetylcholine neurotransmitter system as a therapeutic target

Acetylcholine (ACh) is a neurotransmitter involved in both the central and peripheral nervous systems (Cooper et al., 2003). In the peripheral nervous system, ACh functions to regulate the autonomic nervous system activity and skeletal muscle contraction. In the central nervous system, ACh is important in reward, learning, and memory (Miwa et al., 2011). Removal of cholinergic neurons in NAc by immunotoxin treatment decreased ACh signaling in the NAc, leading to an increase in the rewarding effects of cocaine (Hikida et al., 2001). Thus, an increase in ACh signaling is hypothesized to decrease the rewarding effects of psychostimulants (Karila et al., 2010). Cholinesterase inhibitors such as donepezil and rivastigmine inhibit acetylcholinesterase, the enzyme responsible for the degradation of acetylcholine, to increase the action of acetylcholine. Donepezil treatment attenuated cue- and drug-induced METH reinstatement in rats (Hiranita et al., 2006). Preliminary clinical trials examining the effects of rivastigmine on METH users revealed that rivastigmine reduced METH-induced increases in blood pressure as well as METH-induced cravings in METH users (De la Garza et al., 2008). Additional clinical trials are needed to determine the effectiveness of cholinesterase inhibitors for the treatment of

METH, but preliminary reports suggest a possible clinical benefit in the treatment of METH abuse (Karila et al. 2010).

g. Opioid receptors as therapeutic targets

Opioid receptors are G-protein coupled receptors found in the CNS and gastrointestinal tract, consisting of three main receptor subtypes (μ, δ, κ; Dhawan et al., 1996). Opioid receptors are involved in pain and interact with endogenous peptides such as enkephalins, dynorphins and endorphins, as well as other agonists such as morphine, sufentanil, and fentanyl (Dhawan et al., 1996). Antagonists such as naltrexone and naloxene inhibit the action of opioid peptides and stimulation by opioid receptor agonists (Dhawan et al., 1996). Morphine and endogenous opiates interact with opioid receptors to increase extracellular DA release in the NAc, leading to reward and abuse (Koob et al., 1998). Opioid receptors are also involved in psychostimulant reward and reinforcement (Chiu et al., 2006). Naltrexone pretreatment attenuated AMPH-induced increases in locomotor activity, and naloxone pretreatment decreased AMPH conditioned place preference (Trujillo et al., 1991; Balcells-Olivero and Vezina, 1997). Further, naltrexone treatment inhibited METH-induced behavioral sensitization in mice and cue-induced METH reinstatement in rats trained to self-administer METH (Chiu et al., 2005; Anggardiredja et al., 2004). Clinical trials report that naltrexone decreased the subjective effects of AMPH (Jayaram-Lindstrom et al., 2004). More recent results revealed that naltrexone decreased AMPH use and cravings in AMPH users (Jayaram-Lindstrom et al., 2008). Thus, antagonism of

opioid receptors may represent an effective therapeutic target in the treatment of METH abuse.

h. VMAT2 as therapeutic target

VMAT2 represents a primary target in the mechanism of action of METH (Sulzer et al., 2005). METH inhibits DA uptake at VMAT2 and promotes DA release from vesicles to increase cytosolic DA. Thus, pharmacological agents that modulate VMAT2 function or act to redistribute DA from presynaptic vesicles, thereby limiting vesicular and cytosolic DA available for METH-induced reverse transport, may be efficacious for the treatment of METH. Consistent with this hypothesis, VMAT2 heterzygous KO mice showed decreased AMPH-induced conditioned place preference (Takahashi et al., 1997). Further, VMAT2 inhibition by TBZ pretreatment decreased METH-induced hyperactivity (Kuribara, 1997). However, additional studies examining the effects of TBZ on METH have shown that high doses of TBZ nonspecifically inhibited METH self-administration in rats, while low doses increased METH self-administration (Meyer et al., 2011). Nevertheless, VMAT2 inhibition may represent a novel therapeutic target for the development of pharmacotherapies to treat METH abuse.

VII. Lobeline

a. Background and Historical Uses

(-)-Lobeline (2*R*,6*S*,10*S*-lobeline; Fig. 1) is the principal alkaloid found in *Lobelia inflata*, a biannual or annual flowering plant grown primarily in Eastern

North America. The herb was named after famous French botanist, Matthias de Lobel (Felpin and Lebreton, 2004). While the entire plant is harvested and used in the extraction of alkaloids, the seeds contain the highest percent of the alkaloid, lobeline (Krochmal and Krochmal, 1973; Dwoskin and Crooks, 2002). *Lobelia* has also been called “Indian tobacco” because Native Americans used to chew and smoke the dried leaves of *lobelia* to obtain the CNS effects of the alkaloids (Millspaugh et al., 1974) *Lobelia* is also known as “puke weed”, “gagroot”, and “vomit wort” presumably from its emetic side effects. While the species of plant was identified by Linneaus in 1741, *Lobelia* was not used medicinally until its introduction in 1813 for its use in the treatment of asthma by the botanic physician, Reverend D. Cutler (Millspaugh, 1974). In addition to the respiratory stimulant effects used for the treatment of asthma, *Lobelia* extracts have historically been used as an expectorant, emetic, anti-spamodic, diuretic and muscle relaxant (Dwoskin and Crooks, 2002).

Lobeline is the most biologically active alkaloid of more than 20 alkaloids found in *Lobelia* (Felpin and Lebreton, 2004). Structurally, lobeline is characterized by a central piperdine ring with two phenylethyl side chains attached at the 2- and 6-positions of the piperdine ring. Lobeline possesses a hydroxyl moiety on the 8-position and a keto moiety on the 10-position of the phenylethyl side chains. Lobeline has three chiral centers, at the 8-position on the side chain and the 2- and 6-positions of the piperdine ring.

The first known therapeutic use of lobeline was the treatment of asthma due to the powerful respiratory stimulant effect of lobeline (King et al., 1928). In addition to the respiratory stimulant effects, lobeline has been shown to offer expectorant benefits (Felpin and Lebreton, 2004). Due to these effects, lobeline has been used in treatment of pneumonia, whooping cough, bronchitis, and asphyxsia from narcotic, morphine, and alcohol poisoning (Dwoskin and Crooks, 2002). In addition, lobeline has also been tested for potential benefits as a smoking cessation agent. The earliest use of lobeline as a smoking cessation agent was shown in 1936 (Dorsey, 1936). Numerous pharmacological agents containing lobeline, such as CigArest, Nicoban, NicFit, Bantron and Smoker's Choice have been used as smoking cessation aids, but were deemed ineffective by the FDA (Felpin and Lebreton, 2004). Results from numerous clinical trials have shown that lobeline is not effective as a smoking cessation agent (Stead and Hughes, 2000). One potential reason for the ineffectiveness of lobeline as a smoking cessation agent is its poor bioavailability (Schneider and Olsson, 1996). As such, sublingual formulations of lobeline have been tested for their efficacy in attenuating nicotine use (Glover et al., 2010). Results from these studies however, demonstrated that lobeline is ineffective as a smoking cessation agent.

b. Pharmacology

While lobeline and nicotine are not structurally similar, they exhibit many similar effects. Lobeline interacts with the autonomic ganglia, producing various sympathetic and parasympathetic effects. Lobeline induces tachycardia and

hypertension, as well as increased salivation and gastric mobility (Dwoskin and Crooks, 2002). Lobeline acts at the emetic center in the CNS and directly irritates the gastrointestinal tract causing nausea and vomiting (Felpin and Lebreton, 2004). In addition, lobeline has been shown to improve learning and memory in rats, as well as improve performance in sustained attention tasks (Decker et al., 1993; Brioni et al., 1993; Terry et al., 1996).

Lobeline exhibits its nicotine-like effects through interactions with nicotinic acetylcholine receptors (nAChRs). Lobeline exhibits high affinity (Ki = 4 nM) at α4β2* nAChRs (* indicates putative nAChR assignment), as probed by [^{3}H]nicotine binding studies (Damaj et al., 1997). Unlike nicotine, repeated exposure to lobeline does not result in an upregulation of α4β2* nAChRs (Bhat et al., 1991). Further, studies have shown that lobeline acts as an antagonist at α4β2* nAChRs as lobeline inhibits nicotine-evoked Rb+ efflux from rat thalamic synaptosomes (Miller et al., 2000). Lobeline also displaces [^{3}H]methyllycaconitine (MLA) binding (Ki = 11.6 μM), suggesting an interaction with α7* nAChRs (Miller et al., 2004). Further, functional studies utilizing *Xenopus oocytes* demonstrated that lobeline was an antagonist at α7* nAChRs (Briggs and McKenna, 1998). In addition to antagonism at α4β2* and α7* nAChRs, lobeline also inhibits nicotine-evoked [^{3}H]NE release from cultured fetal rat locus coeruleus cells, suggesting antagonism at α3β4* nAChRs. Lobeline has also been shown to antagonize nAChRs mediating nicotine-evoked DA release, as lobeline inhibits nicotine-evoked [^{3}H]DA release from striatal slices (Miller et al., 2000). While the exact nAChR subunits responsible for nicotine-evoked DA

release are controversial, several nAChR subtypes are proposed to be involved including α4β2*, α6β2*, α4α6β2*, and α6β3β2* (Champtiaux et al., 2003; Salminen et al., 2004). Lobeline also evokes [^{3}H]DA and [^{3}H]NE release from striatal and hippocampal slices, respectively; however release was not mediated by nAChRs, as release was not sensitive to the noncompetitive nAChR antagonist, mecamylamine (Clarke and Reuben, 1996; Kiss et al., 2001).

In addition to an interaction at nAChRs, lobeline also interacts with VMAT2 (Fig 5). Lobeline inhibits [^{3}H]DTBZ binding in whole brain homogenates and [^{3}H]DA uptake in striatal vesicles with similar potency (IC_{50} ~ 0.9 µM; Teng et al., 1997, 1998). Lobeline also inhibits [^{3}H]DA uptake at DAT (IC_{50} = 80 µM), exhibiting 90-fold higher potency at VMAT2 compared to DAT (Teng et al.,1997). In addition to the inhibition of DA uptake at VMAT2, lobeline also releases [^{3}H]DA from preloaded synaptic vesicles (Nickell et al., 2011). Similar to METH, lobeline interacts with VMAT2 to redistribute DA from vesicles, increasing cytosolic DA concentrations. Unlike METH, however, lobeline does not inhibit MAO, as high concentrations of lobeline evoked DOPAC overflow, rather than DA (Teng et al., 1997). Lobeline redistributes DA from synaptic vesicles into the cytosol where it can then be metabolized by MAO into DOPAC, limiting the DA available for METH-induced reverse transport. Thus, due to the interaction with VMAT2, lobeline has been proposed to inhibit the neurochemical effects of METH (Dwoskin and Crooks, 2002). Consistent with this hypothesis, lobeline inhibited AMPH-evoked DA release from striatal slices in the same concentration range that lobeline interacted with VMAT2 (0.1 -1 µM; Miller et al., 2001). In respect to

behavioral experiments, lobeline pretreatment attenuated AMPH- and METH-induced hyperlocomotor activity and the discriminative stimulus effects of METH in rats (Miller et al., 2001). Further, lobeline decreased METH self-administration in rats and this inhibition was not surmounted by increasing concentrations of METH (Harrod et al., 2001). Importantly, lobeline is predicted to have low abuse liability, as lobeline is not self-administered and does not produce conditioned place preference in rats (Fudala and Iwamoto, 1986; Harrod et al., 2003). Based upon these preclinical findings, lobeline is currently undergoing clinical trials to determine effectiveness as a pharmacotherapy for METH abuse. Results from recently completed Phase Ib clinical trials demonstrated that sublingual lobeline was safe in METH addicted individuals (Jones et al, 2007). Despite these encouraging results, some problems with lobeline exist. The half-life of lobeline is relatively short however (~50 min), requiring multiple dosings (Miller et al., 2003). Further, lobeline interacts with multiple targets in the CNS such as nAChRs. Thus, recent focus has been on the development of lobeline analogs with better pharmacokinetic profiles and increased selectivity for VMAT2.

c. *meso*-Transdiene

meso-Transdiene (MTD) is a defunctionalized (i.e. keto and hydroxyl moieties removed), unsaturated analog of lobeline (Fig 1; Zheng et al., 2005a). MTD exhibited low affinity for α4β2* and α7* nAChRs, as probed by [^{3}H]nicotine and [^{3}H]MLA binding (Ki >100 μM for both subtypes; Miller et al., 2004). These results suggest that the hydroxyl and keto groups on the phenyethyl side chains

are important for potent nAChR binding affinity. Compared with lobeline, MTD was found to exhibit similar affinity for the [^{3}H]DTBZ binding site and [^{3}H]DA uptake site on VMAT2 (Ki = 9.88 and 0.54 μM, respectively; Zheng et al., 2005a; Nickell et al., 2010). Unfortunately, MTD exhibited high affinity for DAT (Ki = 0.58 μM), which has been associated with a potential for abuse liability (Miller et al., 2004). MTD inhibited METH-evoked DA overflow from rat striatal slices with potency not different from lobeline (IC_{50} = 0.44 and 0.42 μM, respectively; Nickell et al., 2010). Interestingly, MTD exhibited ~20% greater inhibitory activity compared to lobeline in inhibiting METH-evoked DA release (I_{max} = 76.3 and 56.1%, respectively; Nickell et al., 2010). The ability of MTD to decrease METH self-administration is unknown. Unfortunately, chemical defunctionalization decreased the water solubility of MTD compared to lobeline.

d. Lobelane

Lobelane is a defunctionalized, saturated analog of lobeline (Fig 1; Zheng et al., 2005a). Similar to MTD, lobelane exhibits low affinity for α4β2* and α7* nAChRs, as probed by [^{3}H]nicotine and [^{3}H]MLA binding (Ki = 77.3 and 43.1 μM, respectively; Miller et al., 2004). Lobelane exhibits affinity for [^{3}H]DTBZ binding (Ki = 0.97 μM) not different from lobeline (Zheng et al., 2005a). Interestingly, lobelane exhibits increased potency to inhibit [^{3}H]DA uptake at VMAT2 (Ki = 0.045 μM) compared to lobeline (Nickell et al., 2010). Compared to lobeline, lobelane exhibited higher affinity for DAT (Ki = 1.57 μM; Nickell et al., 2010). Lobelane inhibited METH-evoked DA release with potency not different from

lobeline (IC_{50} = 0.65; Nickell et al., 2010). Similar to MTD, lobelane exhibited ~20% greater inhibitory activity compared to lobeline in inhibiting METH-evoked DA release (I_{max} = 76.3 and 56.1%, respectively; Nickell et al., 2010). Further, lobelane pretreatment dose-dependently decreased METH self-administration in rats; however tolerance developed to this behavioral effect after repeated dosings (Neugebauer et al., 2007). Similar to MTD, chemical defunctionalization resulted in decreased water solubility compared to lobeline.

VIII. Hypothesis and Specific Aims

The purpose of the current research is to identify analogs of MTD and lobelane with improved selectivity for inhibition of VMAT2 function, in an effort to develop pharmacotherapies for METH abuse. This thesis describes the results from an iterative drug discovery effort consisting of two sets of analogs, 3,5-disubstituted MTD analogs and N-1,2-dihydroxypropyl (diol) lobelane analogs. Results from initial structure activity relationships (SAR) determining the ability of these analogs to interact with VMAT2, DAT, SERT, and nAChRs are reported. The ability of the most VMAT2 selective analogs to inhibit METH-evoked DA release was determined to select the lead analogs from each series (UKMH-106 and GZ-793A). In addition, mechanistic studies were conducted to further identify the effect of GZ-793A on VMAT2 and METH-evoked DA release. Finally, initial DA neurotoxicity evaluations were conducted with GZ-793A to determine the effect of GZ-793A on DA content.

The hypothesis of this thesis is that selective VMAT2 inhibition by lobeline analogs will inhibit the effects of METH. The specific hypotheses and aims for this project were:

Hypothesis 1: 3,5-Disubstituted MTD analogs inhibit VMAT2 function, and VMAT2-selective MTD analogs inhibit METH-evoked DA release from striatal slices.

Specific Aims:

1) Determine the ability of MTD to decrease METH self-administration in rats.
2) Determine the selectivity of MTD analogs to inhibit VMAT2 function *in vitro*.
3) Determine the ability of MTD analogs to inhibit METH-evoked DA release in striatal slices *in vitro*.

Hypothesis 2: N-1,2-Diol analogs of lobelane inhibit VMAT2 function, and VMAT2 selective analogs inhibit METH-evoked DA release from striatal slices.

Specific Aims:

1) Determine the selectivity of N-1,2-diol analogs to inhibit VMAT2 function *in vitro*.

2) Determine N-1,2-diol lobelane analogs to inhibit METH-evoked DA release in striatal slices *in vitro*.

Hypothesis 3: GZ-793A interacts with VMAT2 to release DA from striatal vesicles and inhibits METH-evoked DA release from striatal vesicles.

Specific Aims:

1) Determine the ability of GZ-793A to release DA from striatal vesicles *in vitro*.
2) Determine the ability of GZ-793A to inhibit METH-evoked DA release from striatal vesicles *in vitro*.

Hypothesis 4: VMAT2 inhibition by GZ-793A does not alter striatal DA content and GZ-793A protects against METH-induced DA depletions in striatal tissue and vesicles.

Specific Aims:

1) Determine the effect of acute and repeated GZ-793A on DA content in striatal tissue and vesicle preparations.
2) Determine the effect of acute and repeated GZ-793A pretreatment on acute and repeated METH-induced DA content depletion in striatal tissue and vesicle preparations.

Fig. 1. Chemical Structures (Chapter 1)

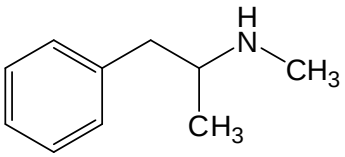

Methamphetamine

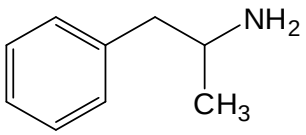

Amphetamine

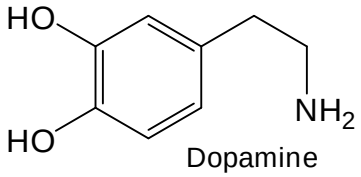

Dopamine

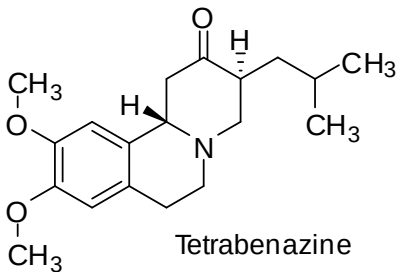

Tetrabenazine

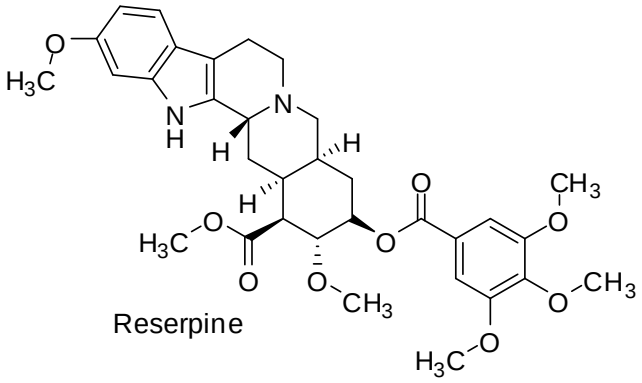

Reserpine

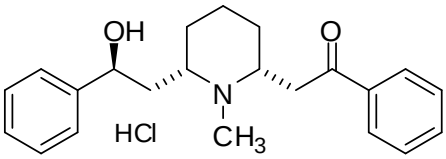

Lobeline

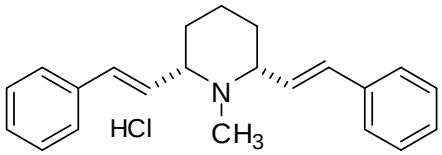

meso-Transdiene

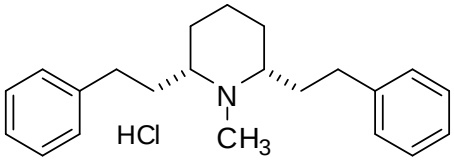

Lobelane

Fig. 2. Sagittal view of rodent brain showing DA pathways (as indicated by solid lines).

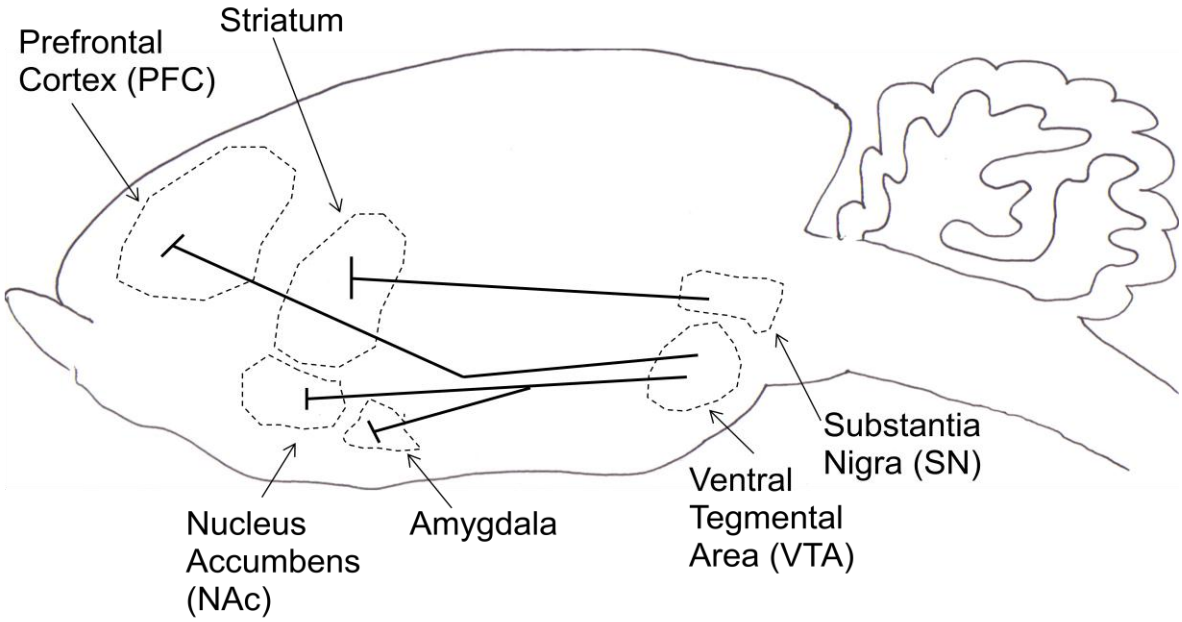

Fig. 3. Schematic diagram of DA nerve terminal.

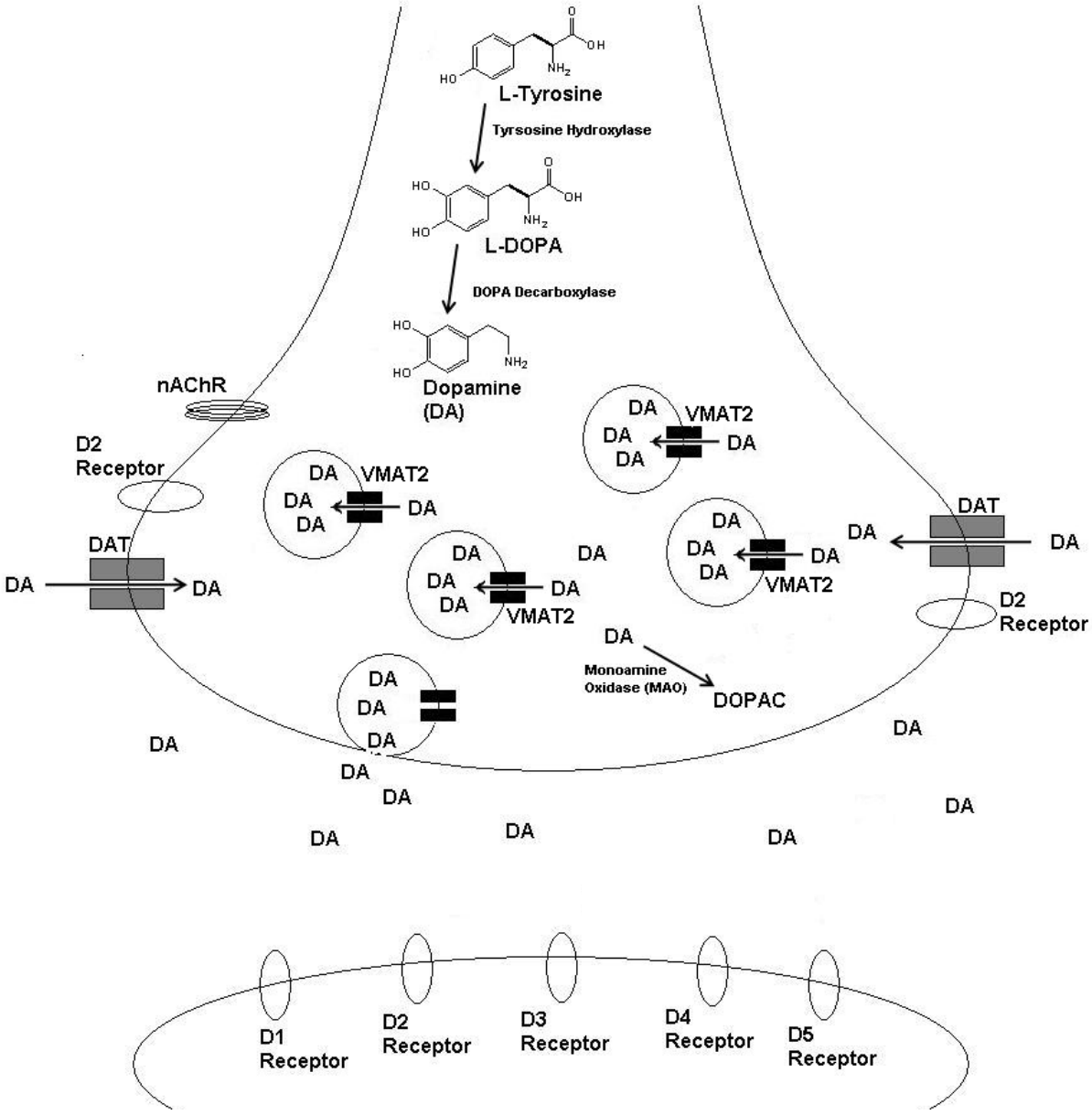

Fig. 4. Schematic diagram of DA nerve terminal in the presence of methamphetamine (METH).

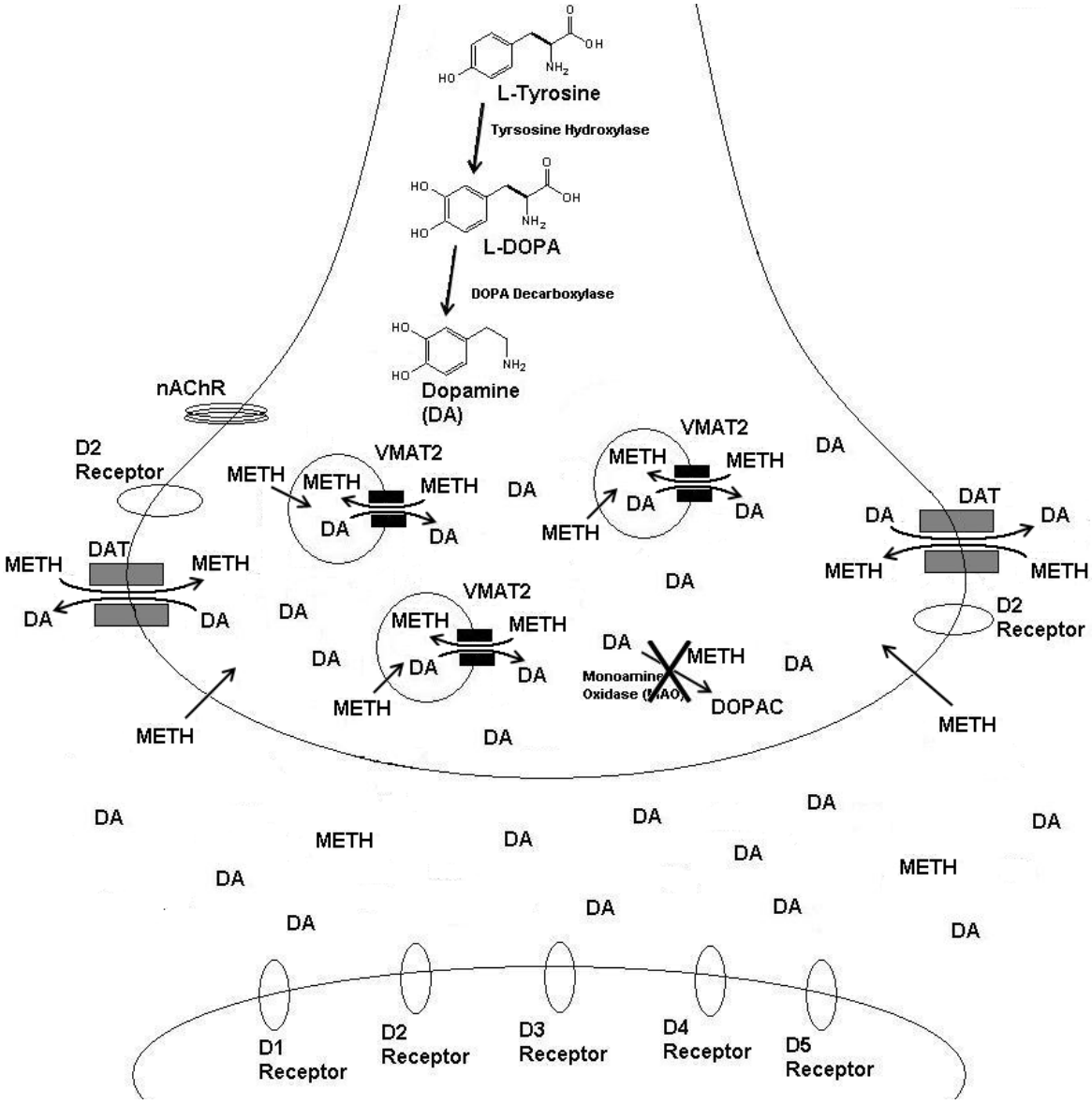

Fig. 5. Schematic diagram of DA nerve terminal in the presence of lobeline (LOB).

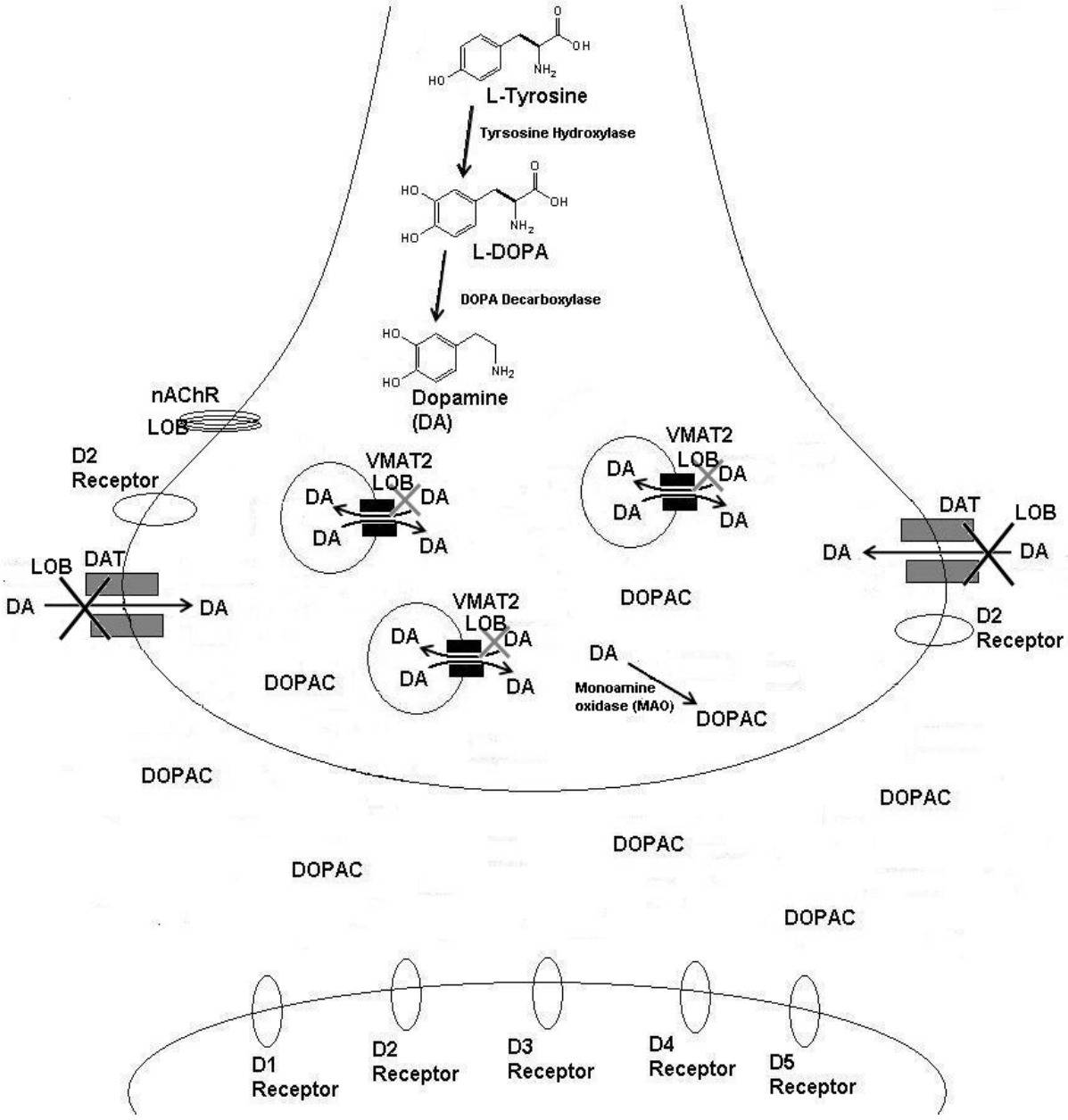

CHAPTER TWO

MTD Analogs Inhibit VMAT2 Function and METH-evoked DA Release

Portions of this chapter have been published in the manuscript:

Horton DB, Siripurapu KB, Norrholm SD, Deaciuc AG, Hojahmat M, Culver JP, Crooks PA, Dwoskin LP. Lobeline and *meso*-transdiene analogs: interaction at neurotransmitter transporters and nicotinic receptors. *J Pharm Exp Ther*, 336:940-951, 2011.

I. Introduction

METH abuse is a serious public health concern (NSDUH, 2008). Pharmacotherapies are not available to treat METH abuse. Efforts have focused on the DAT as a therapeutic target (Dar et al., 2005; Howell et al., 2007; Tanda et al., 2009), because METH interacts with DAT to increase extracellular DA concentrations, leading to its reinforcing properties (Wise and Bozarth, 1987; Di Chiara and Imperato, 1988; Di Chiara et al., 2004). DAT translocates DA from the extracellular space into presynaptic terminals, whereas METH reverses DAT translocation to increase DA extracellularly (Fischer and Cho, 1979; Liang and Rutledge, 1982; Sulzer et al., 1995). This approach has not led to therapeutic agents for METH abuse, although several DAT inhibitors currently are undergoing clinical trials.

A largely unexplored target of METH action is VMAT2. By interacting with VMAT2, METH increases cytosolic DA concentrations available for translocation by DAT to the extracellular compartment (Sulzer and Rayport, 1990; Sulzer et al., 1995; Pifl et al., 1995). The current research focuses on the discovery of novel compounds which interact with VMAT2 and inhibit the pharmacological effects of METH. Lobeline, the major alkaloid of *Lobelia inflata*, inhibits VMAT2 function (Teng et al., 1997, 1998), has high affinity for [^{3}H]DTBZ binding sites on VMAT2 (Kilbourn et al., 1995; Miller et al., 2004) and decreases AMPH-evoked DA release from rat striatal slices (Miller et al., 2001). However, lobeline is not selective for VMAT2, acting as a nAChR antagonist with low affinity for DAT and SERT (Damaj et al., 1997; Flammia et al., 1999; Miller et al., 2000, 2004). Lobeline also decreases METH-induced hyperactivity, behavioral sensitization and self-administration in rats (Harrod et al., 2001; Miller et al., 2001). Importantly, lobeline is not self-administered, indicating lack of abuse liability (Harrod et al., 2003). Based on these preclinical findings, lobeline is being evaluated as a treatment for METH abuse. Initial Phase Ib clinical trials report that lobeline is safe in METH addicts (Jones et al., 2007).

Lobeline has a central piperidine ring with phenyl rings attached at C-2 and C-6 of the piperidine ring by ethylene linkers containing hydroxyl and keto functionalities at the C8 and C10 positions on the linkers, respectively (Fig. 6). Potency and selectivity for VMAT2 were improved based on SARs, with the emergence of two new lead compounds, i.e., lobelane and MTD (Zheng et al., 2005a; Nickell et al., 2010). Lobelane is a lobeline analog with defunctionalized

(hydroxyl and keto groups of lobeline eliminated from the linkers) and saturated linkers. Subsequent reports described the preclinical evaluation of lobelane as well as analogs based on the lobelane structural scaffold (Beckmann et al., 2010; Nickell et al., 2011). MTD is a lobeline analog with defunctionalized and unsaturated (double bonds) linkers (Fig. 6). Compared with lobeline, MTD was found to exhibit similar affinity for the [^{3}H]DTBZ binding site on VMAT2 and decreased affinity for nAChRs, thus revealing increased selectivity for VMAT2 (Zheng et al., 2005a). Also, MTD inhibited METH-evoked DA overflow from rat striatal slices (Nickell et al., 2010). However, MTD exhibited high affinity for DAT (Miller et al., 2004), which has been associated with potential for abuse liability. Furthermore, MTD has limited solubility, diminishing its potential for development as a pharmacotherapy for METH abuse.

To extend the previous work, the current study determined if MTD decreases METH self-administration in rats. The current SAR also identified analogs based on the MTD scaffold that potently and selectively inhibit VMAT2 function, and had both low affinity for DAT and increased water solubility compared to MTD. These analogs were designed as more rigid, conformationally-restricted analogs of MTD, in which the phenylethylene substituents in the MTD structure were incorporated into the piperidine ring system (Fig. 7). This structural change reduces the molecular weight and the number of rotational carbon bonds from four in MTD to two in the current analogs. Other changes included: 1) altering the geometry of the C5 double bond from E to Z; 2) lengthening the linker units at C3 and C5 of the piperidine

ring; 3) adding aromatic substituents to the phenyl moieties; and 4) replacing the phenyl rings with heteroaromatic rings, such as thiophene or furan. Affinity for VMAT2 was retained despite these structural alterations, and importantly, selectivity for VMAT2 was improved. These novel analogs were evaluated further for their ability to inhibit METH-evoked DA release from superfused rat striatal slices, and constitute new leads in the discovery of novel treatments for METH abuse.

The hypothesis of this chapter is that 3,5-disubstituted MTD analogs will inhibit VMAT2 function and VMAT2 selective MTD analogs will inhibit METH-evoked DA release from striatal slices.

II. Methods

IIa. Animals. Male Sprague-Dawley rats (200–250 g, Harlan, Indianapolis, IN) were housed two per cage with *ad libitum* access to food and water in the Division of Laboratory Animal Resources at the University of Kentucky (Lexington, KY). Experimental protocols involving the animals were in accord with the 1996 *NIH Guide for the Care and Use of Laboratory Animals* and were approved by the Institutional Animal Care and Use Committee at the University of Kentucky.

IIb. Chemicals. [^{3}H]Nicotine (L-(-)-[N-methyl-^{3}H]; specific activity, 66.9 Ci/mmol), [^{3}H]dopamine ([^{3}H]DA; dihydroxyphenylethylamine, 3,4-[7-^{3}H]; specific activity, 28 Ci/mmol), and [^{3}H]5-hydroxytryptamine ([^{3}H]5-HT; hydroxytryptamine creatinine sulfate 5-[1,2-^{3}H(N)]; specific activity, 30 Ci/mmol) and Microscint 20

LSC-cocktail were purchased from PerkinElmer, Inc. (Boston, MA). [^{3}H]Dihydrotetrabenazine ([^{3}H]DTBZ; (±)alpha-[O-methyl-^{3}H]dihydrotetrabenazine; specific activity, 20 Ci/mmol) and [^{3}H]methyllycaconitine ([^{3}H]MLA; ([1α,4(S),6β,14α,16β]-20-ethyl-1,6,14,16-tetramethoxy-4-[[[2-([3-^{3}H]-methyl-2,5-dioxo-1-pyrrolidinyl)benzoyl]oxy]-methyl]aconitane-7,8-diol; specific activity, 100 Ci/mmol) were obtained from American Radiolabled Chemicals, Inc. (St. Louis, MO). Diazepam and ketamine were purchased from N.L.S. Animal Health (Pittsburgh, PA). Acetonitrile, ATP-Mg^{2+}, benzaldehyde, 2,4-dichlorobenzaldehyde, 4-methoxybenzaldehyde, 4-methylbenzaldehyde, furan-2-carbaldehyde, furan-3-carbaldehyde, trans-cinnamaldehyde, catechol, DA, DOPAC, disodium ethylenediamine tetraacetate (EDTA), ethylene glycol tetraacetate (EGTA), ethyl acetate, fluoxetine HCl, 1-(2-(bis-(4-fluorophenyl)methoxy)ethyl)-4-(3-phenylpropyl)piperazine (GBR 12909), α-D-glucose, N-[2-hydroxyethyl]piperazine-N'-[2-ethanesulfonic acid] (HEPES), hexane, $MgSO_4$, methanol, methylene chloride, 1-methyl-4-piperidone, pargyline HCl, polyethyleneimine (PEI), KOH, potassium tartrate, sodium borohydride, NaOH, Na_2SO_4, sucrose, silica gel (240-400 mesh), and trifluoroacetic acid were purchased from Sigma-Aldrich, Inc. (St. Louis, MO). L-Ascorbic acid and $NaHCO_3$ were purchased from Aldrich Chemical Co. (Milwaukee, WI). $CaCl_2$, KCl, K_2PO_4, $MgCl_2$, NaCl, and NaH_2PO_4 were purchased from Fisher Scientific Co. (Pittsburgh, PA). Thiophene-2-carbaldehyde and thiophene-3-carbaldehyde were purchased from Acros Organics USA (Morris Plains, NJ). Preparative TLC plates (250 µM silica layer, organic binder, no indicator) were purchased from

Dynamic Adsorbents Inc. (Atlanta, GA). Chloroform-D was purchased from Cambridge Isotope Laboratories, Inc. (Andover, MA). Complete counting cocktail 3a70B was purchased from Research Products International Corp. (Mount Prospect, IL). (2R,3S,11bS)-2-Ethyl-3-isobutyl-9,10-dimethoxy-2,2,4,6,7,11b-hexahydro-1H-pyrido[2,1-a]isoquinolin-2-ol (Ro-4-1284) was a generous gift from Hoffman-LaRoche Inc. (Nutley, NJ).

IIc. General Synthetic Methodology for the UKMH Analogs. A mixture of 1-methyl-4-piperidone (1.0 eq, 10.2 mmol), the appropriately substituted aromatic aldehyde (2.1 eq, 21.42 mmol), and potassium hydroxide (2.1 eq, 21.42 mmol) were stirred in methanol (20 ml) at ambient temperature for 4 h. The resulting yellow precipitate was collected by filtration and washed with cold methanol to yield the crude 3,5-disubstituted-1-methylpiperidin-4-one (9.17-9.83 mmol; 89.9-96.4% yield). Without further purification, the crude 3,5-disubstituted-1-methylpiperidin-4-one product was added to a pre-equilibrated mixture of sodium borohydride (4 eq.) and trifluoroacetic acid (16 eq.) in a 1:1 mixture of dichloromethane and acetonitrile. The mixture was stirred at ambient temperature for 4-8 h until TLC and GC-MS analysis revealed that all of the starting material was consumed. The reaction mixture was then diluted with dichloromethane, and 2 M aqueous sodium hydroxide solution was added drop-wise with stirring to afford a pH of 10. The organic layer was then separated, dried over anhydrous sodium sulfate, filtered, and the filtrate evaporated to dryness under vacuum. The reaction yielded a mixture of mainly the 3Z,5Z- and 3Z,5E-geometrical isomers of the 3,5-disubstituted-1-methylpiperidines, as well

as other minor geometric double bond combinations; both these isomers could be separated by silica gel column chromatography or by preparative TLC, utilizing a 10:1 hexane:ethyl acetate solvent mixture. Utilizing this general procedure, the UKMH series of analogs shown in Fig. 6 were prepared and fully characterized for structural identity and purity, as determined by TLC, GC-MS, ^{1}H NMR and ^{13}C NMR analysis.

IId. METH Self-administration. Behavioral experiments were conducted using previously described methods (Neugebauer et al., 2007). Operant conditioning chambers (ENV-008, MED Assoc., St. Albans, VT) were enclosed within sound-attenuating compartments (ENV-018M, MED Assoc.). Each chamber was connected to a personal computer interface (SG-502, MED Assoc.), and chambers were operated using MED-PC™ software. A 5 × 4.2 cm recessed food tray was located on the response panel of each chamber. Two retractable response levers were mounted on either side of the recessed food tray (7.3 cm above metal rod floor). A 28V, 3-cm diameter, white cue light was mounted 6 cm above each response lever.

Rats were trained briefly to respond on a lever for food reinforcement. Immediately after food training, rats were allowed free access to food for 3 days. Rats were anesthetized (100 mg/kg ketamine and 5 mg/kg diazepam, i.p.) and catheters were implanted into the right jugular vein, exiting through a dental acrylic head mount affixed to the skull via jeweler screws. Drug infusions were administered i.v. (0.1 ml over 5.9 sec) via a syringe pump (PHM-100, MED Assoc.) through a water-tight swivel attached to a 10 ml syringe via catheter

tubing, which was attached to the cannulae mounted to the head of the rat. Following a one-week recovery period from surgery, rats were trained to press one of two levers for an infusion of METH (0.05 mg/kg/infusion). Each infusion was followed by a 20-sec time out signaled by illumination of both lever lights. The response requirement was gradually increased to a terminal fixed ratio 5 (FR 5) schedule of reinforcement. Each session was 60 min in duration. Training continued until responding stabilized across sessions. Stable responding was defined as less than 20% variability in the number of infusions earned across 3 successive sessions, a minimum of a 2:1 ratio of active (drug) lever responses to inactive (no drug) lever responses, and at least 10 infusions per session. Once stability was reached, an acute dose (0, 3.0, 5.6, 10 or 17 mg/kg) of MTD was administered (s.c.) 15 min prior to the session according to a within-subject Latin square design. Two maintenance sessions (i.e., no pretreatment) were included between each test session to ensure stable responding throughout the experiment.

IIe. Food-Maintained Responding. Briefly, rats were trained to respond on one lever (active lever) for food pellet reinforcement (45 mg pellets, BIO-SERV, #F0021, Frenchtown, NJ), while responses on the other lever (inactive lever) had no programmed consequence. Location (left or right) of the active and inactive levers was counterbalanced across rats. The response requirement was gradually increased, terminating at an FR 5. Following lever training, a 20-sec signaled time out (illumination of both lever lights) was included following each pellet delivery. Time out following each pellet delivery was

instituted to be consistent with the METH self-administration procedure. Each food-reinforced session lasted 60 min. Training continued until responding stabilized across sessions. Stable responding was defined as less than 20% variability in the number of pellets earned across 3 successive sessions, and a minimum of a 2:1 ratio of active lever responses to inactive lever responses. After the stability criteria were reached, an acute dose of MTD (17 mg/kg) was administered (s.c.) 15 min prior to the 60-min session. Two maintenance sessions (i.e., no pretreatment) were included between test sessions to ensure stable responding throughout the experiment.

IIf. [^{3}H]Nicotine and [^{3}H]MLA Binding Assays. Analog-induced inhibition of [^{3}H]nicotine and [^{3}H]MLA binding was determined using published methods (Miller et al., 2004). Whole brain, excluding cortex and cerebellum, was homogenized using a Tekmar polytron (Tekmar-Dohrmann, Mason, OH) in 20 volume of ice-cold modified Krebs'-HEPES buffer, containing: 2 mM HEPES, 14.4 mM NaCl, 0.15 mM KCl, 0.2 mM $CaCl_2 \cdot 2H_2O$ and 0.1 mM $MgSO_4 \cdot 7H_2O$, pH 7.5. Homogenates were centrifuged at 31,000 g for 17 min at 4 ^oC (Avanti J-301 centrifuge, Beckman Coulter, Fullerton, CA). Pellets were resuspended by sonication (Vibra Cell, Sonics & Materials Inc, Danbury, CT) in 20 volumes of Krebs'-HEPES buffer and incubated at 37 ^oC for 10 min (Reciprocal Shaking Bath Model 50, Precision Scientific, Chicago, IL). Suspensions were centrifuged using the above conditions. Resulting pellets were resuspended by sonication in 20 volumes buffer and centrifuged at 31,000 g for 17 min at 4 ^oC. Final pellets were stored in incubation buffer, containing: 40 mM HEPES, 288 mM NaCl, 3.0

mM KCl, 4.0 mM $CaCl_2 \cdot 2H_2O$, and 2.0 mM $MgSO_4.7H_2O$, pH 7.5. Membrane suspensions (100-140 µg protein/100 µl) were added to duplicate wells containing 50 µl analog (7-9 concentrations, 1 nM – 0.1 mM, final concentration in assay buffer), 50 µl of buffer, and 50 µl of [^{3}H]nicotine or [^{3}H]MLA (3 nM; final concentration) for a final volume of 250 µl, and incubated for 1 h at room temperature. Nonspecific binding was determined in the presence of 10 µM cytisine or 10 µM nicotine for the [^{3}H]nicotine and [^{3}H]MLA assays, respectively. Reactions were terminated by harvesting samples on Unifilter-96 GF/B filter plates presoaked in 0.5% PEI using a Packard Filter Mate Harvester (Perkin Elmer, Inc.). Samples were washed 3 times with 350 µl of ice-cold buffer. Filter plates were dried for 60 min at 45 ^{o}C, bottom-sealed and each well filled with 40 µl of Microscint 20 cocktail. Bound radioactivity was determined via liquid scintillation spectmometry (TopCount NXT scintillation counter; PerkinElmer, Inc.).

IIg. Synaptosomal [^{3}H]DA and [^{3}H]5-HT Uptake Assays. Analog-induced inhibition of [^{3}H]DA and [^{3}H]5-HT uptake into rat striatal and hippocampal synaptosomes, respectively, was determined using modifications of a previously described method (Teng et al., 1997). Brain regions were homogenized in 20 ml of ice-cold 0.32 M sucrose solution containing 5 mM $NaHCO_3$ (pH 7.4) with 16 up-and-down strokes of a Teflon pestle homogenizer (clearance ~ 0.005”). Homogenates were centrifuged at 2,000 g for 10 min at 4 °C, and resulting supernatants centrifuged at 20,000 g for 17 min at 4 °C. Pellets were resuspended in 1.5 ml of Krebs’ buffer, containing: 125 mM NaCl, 5 mM KCl, 1.5

mM $MgSO_4$, 1.25 mM $CaCl_2$, 1.5 mM KH_2PO_4, 10 mM α-D-glucose, 25 mM HEPES, 0.1 mM EDTA, with 0.1 mM pargyline and 0.1 mM ascorbic acid saturated with 95% O_2/5% CO_2, pH 7.4). Synaptosomal suspensions (20 µg protein/50 µl) were added to duplicate tubes containing 50 µl analog (7-9 concentrations, 0.1 nM – 1 mM, final concentration in assay buffer) and 350 µl of buffer and incubated at 34 °C for 5 min in a total volume of 450 µl. Samples were placed on ice and 50 µl of [^{3}H]DA or [^{3}H]5-HT (10 nM; final concentration), was added to each tube for a final volume of 500 µl. Reactions proceeded for 10 min at 34°C and were terminated by the addition of 3 ml of ice-cold Krebs' buffer. Nonspecific [^{3}H]DA and [^{3}H]5-HT uptake were determined in the presence of 10 µM GBR 12909 and 10 µM fluoxetine, respectively. Samples were rapidly filtered through Whatman GF/B filters using a cell harvester (MP-43RS; Brandel Inc.). Filters were washed 3 times with 4 ml of ice-cold Krebs' buffer containing catechol (1 µM). Complete counting cocktail was added to the filters and radioactivity determined by liquid scintillation spectrometry (B1600 TR scintillation counter; PerkinElmer, Inc.).

IIh. [^{3}H]DTBZ Vesicular Binding Assays. Analog-induced inhibition of [^{3}H]DTBZ binding, a high affinity ligand for VMAT2, was determined using modifications of a previously published method (Teng et al., 1998). Rat whole brain (excluding cerebellum) was homogenized in 20 ml of ice-cold 0.32 M sucrose solution with 10 up-and-down strokes of a Teflon pestle homogenizer (clearance ~ 0.008"). Homogenates were centrifuged at 1,000g for 12 min at 4 °C and resulting supernatants were centrifuged at 22,000g for 10 min at 4 °C.

Resulting pellets were osmotically shocked by incubation in 18 ml of cold water for 5 min. Osmolarity was restored by adding 2 ml of 25 mM HEPES and 100 mM potassium tartrate solution. Samples were centrifuged (20,000g for 20 min at 4°C), and then 1 mM $MgSO_4$ solution was added to the supernatants. Samples were centrifuged at 100,000g for 45 min at 4°C. Pellets were resuspended in cold assay buffer, containing: 25 mM HEPES, 100 mM potassium tartrate, 5 mM $MgSO_4$, 0.1 mM EDTA, and 0.05 mM EGTA, pH 7.5. Assays were performed in duplicate in 96-well plates. Vesicular suspensions (15 µg protein/100 µl) were added to wells containing 50 µl analog (7-9 concentrations, 0.01 nM – 0.1 mM, final concentration in assay buffer), 50 µl of buffer, and 50 µl of [^{3}H]DTBZ (3 nM; final concentration) for a final volume of 250 µl and incubated for 1 hr at room temperature. Nonspecific uptake was determined in the presence of 50 µl of 20 µM Ro-4-1284. Reactions were terminated by filtration onto Unifilter-96 GF/B filter plates (presoaked in 0.5% PEI). Filters were washed 3 times with 350 µl of ice-cold buffer, containing: 25 mM HEPES, 100 mM potassium-tartrate, 5 mM $MgSO_4$, and 10 mM NaCl, pH 7.5. Filter plates were dried, bottom-sealed and each well filled with 40 µl of scintillation cocktail (MicroScint 20; PerkinElmer, Inc.). Radioactivity on the filters was determined by liquid scintillation spectrometry.

IIi. Vesicular [^{3}H]DA Uptake Assay. Analog-induced inhibition of [^{3}H]DA uptake into rat striatal vesicles was determined using modifications of a previously published method (Teng et al., 1997). Previous reports from our laboratory show that this vesicle preparation contains <1% contaminating

membrane fragments (Teng et al., 1997). Striata were homogenized in 14 ml of ice-cold 0.32 M sucrose solution containing 5 mM $NaHCO_3$ (pH 7.4) with 10 up-and-down strokes of a Teflon pestle homogenizer (clearance ~ 0.008”). Homogenates were centrifuged at 2,000 g for 10 min at 4 °C and resulting supernatants centrifuged at 10,000 g for 30 min at 4 °C. Pellets were resuspended in 2.0 ml of 0.32 M sucrose and were transferred to tubes containing 7 ml of milliQ water and homogenized with 5 up-and-down strokes. Homogenates were transferred to tubes containing 900 µl of 0.25 M HEPES and 900 µl of 1.0 M potassium tartrate solution and centrifuged at 20,000 g for 20 min at 4 ºC. Resulting supernatants were centrifuged at 55,000 g for 60 min at 4 ºC. Subsequently, 100 µl of 1 mM $MgSO_4$, 100 µl of 0.25 M HEPES and 100 µl of 1.0 M potassium tartrate were added to the supernatant and centrifuged at 100,000 g for 45 min at 4 ºC. Final pellets were resuspended in assay buffer, containing: 25 mM HEPES, 100 mM potassium tartrate, 50 µM EGTA, 100 µM EDTA, and 1.7 mM ascorbic acid, 2 mM ATP-Mg^{2+}, pH 7.4. Vesicular suspensions (10 µg protein/100 µl) were added to duplicate tubes containing 50 µl analog (7-9 concentrations, 1 nM – 0.1 mM, final concentration in assay buffer), 300 µl of buffer, and 50 µl of [^{3}H]DA (0.1 µM; final concentration) for a final volume of 500 µl and incubated for 8 min at 34 °C. Nonspecific [^{3}H]DA uptake was determined in the presence of 10 µM Ro-4-1284. Samples were filtered rapidly through Whatman GF/B filters using the cell harvester and washed 3 times with assay buffer containing 2 mM $MgSO_4$ in the absence of ATP. Radioactivity retained by the filters was determined as previously described.

IIj. Kinetics of Vesicular [^{3}H]DA Uptake. Vesicle suspensions were prepared as described above; striata were pooled from 2 rats. Vesicular suspensions (20 µg protein/50 µl) were added to duplicate tubes containing 25 µl analog (final concentration approximating the K_i), 150 µl of buffer, and 25 µl of [^{3}H]DA (1 nM – 5 µM; final concentration) for a final volume of 250 µl, and incubated for 8 min at 34 °C. Nonspecific [^{3}H]DA uptake was determined in samples containing 10 µM Ro4-1284. Samples were processed as previously described.

IIk. Endogenous DA Release Assay. HPLC-EC determination of DA release was performed by Kiran Siripurapu, Ph.D.. Rat coronal striatal slices (0.5 mm thick) were prepared and incubated in Krebs' buffer, containing: 118 mM NaCl, 4.7 mM KCl, 1.2 mM $MgCl_2$, 1.0 mM NaH_2PO_4, 1.3 mM $CaCl_2$, 11.1 mM α-D-glucose, 25 mM $NaHCO_3$, 0.11 mM L-ascorbic acid and 0.004 mM EDTA, pH 7.4, saturated with 95% O_2/5% CO_2 at 34 ºC in a metabolic shaker for 60 min (Teng et al., 1997). Each slice was transferred to a glass superfusion chamber and superfused at 1 ml/min for 60 min with Krebs' buffer before sample collection. Two basal samples (1 ml) were collected at 5-min and 10-min time points. Each slice was superfused for 30 min in the absence or presence of a single concentration of analog (0.1 -10 µM) to determine analog-evoked DA and DOPAC overflow, and remained in the buffer until the end of the experiment. METH (5 µM) was added to the buffer after 30 min of superfusion, and slices were superfused for 15 min, followed by 20 min of superfusion in the absence of METH. In each experiment, a striatal slice was superfused for 90 min in the

absence of both analog and METH, serving as the buffer control condition. In each experiment, duplicate slices were superfused with METH in the absence of analog, serving as the METH control condition. The concentration of METH was selected based on pilot concentration-response data showing a reliable response of sufficient magnitude to allow evaluation of analog-induced inhibition. Each superfusate sample (1 ml) was collected into tubes containing 100 μl of 0.1 M perchloric acid. Prior to HPLC-EC analysis, ascorbate oxidase (20 μl, 168 U/mg reconstituted to 81 U /ml) was added to 500 μl of each sample and vortexed for 30 s, and 100 μl of the resulting solution injected onto the HPLC-EC.

The HPLC-EC consisted of a pump (model 126 Beckman Coulter, Inc, Fullerton, CA) and autosampler (model 508 Beckman Coulter, Inc), an ODS Ultrasphere C18 reverse-phase 80 × 4.6 mm, 3-μm column and a Coulometric-II detector with guard cell (model 5020) maintained at +0.60 V and analytical cell (model 5011) maintained at potentials E1 = -0.05 V and E2 = +0.32 V (ESA Inc., Chelmsford, MA). HPLC mobile phase (flow rate, 1.5 ml/min) was 0.07 M citrate/0.1 M acetate buffer pH 4, containing: 175 mg/l octylsulfonic acid sodium salt, 650 mg/l NaCl and 7% methanol. Separations were performed at room temperature, and 5-6 min was required to process each sample. Retention times of DA or DOPAC standards were used to identify respective peaks. Peak heights were used to quantify the detected amounts of analyte based on standard curves. Detection limit for DA and DOPAC was 1-2 pg/100 μl.

III. Data Analysis. For the behavioral experiments, one-way ANOVA with dose as a within-subject factor was used to determine if MTD altered METH

self-administration. Dunnett's post-hoc tests were used to compare each MTD dose to the saline control. A single paired-sample *t*-test was used to determine the effects of MTD on food-maintained behavior.

For the neurochemical experiments, specific [^{3}H]nicotine, [^{3}H]MLA and [^{3}H]DTBZ binding and specific [^{3}H]DA and [^{3}H]5-HT uptake were determined by subtracting the nonspecific binding or uptake from the total binding or uptake. Analog concentrations producing 50% inhibition of specific binding or uptake (IC_{50} values) were determined from concentration effect curves via an iterative curve-fitting program (Prism 5.0; GraphPad Software Inc., San Diego, CA). Inhibition constants (K_i values) were determined using the Cheng-Prusoff equation (Cheng and Prusoff, 1973). For kinetic analyses, Km and Vmax were determined using one-site binding curves. Paired two-tailed t-tests were performed on the arithmetic Vmax and the log Km values to determine significant differences between analog and control conditions. Pearson's correlation analysis determined the relationship between affinity for the [^{3}H]DTBZ binding site and vesicular [^{3}H]DA uptake.

For endogenous neurotransmitter release assays, fractional release was defined as the DA or DOPAC concentration in each sample divided by the slice weight. Basal DA or DOPAC outflow was calculated as the average fractional release of the two basal samples collected 10 min prior to addition of analog to the buffer. Analog-evoked DA or DOPAC overflow was calculated as the average fractional release during the 30 min period of analog exposure prior to METH addition to the buffer. Analog-evoked DA or DOPAC overflow was

analyzed by one-way repeated-measures ANOVA. Time course for analog-induced inhibition of METH-evoked fractional DA or DOPAC release was analyzed by two-way ANOVA with concentration and time as repeated-measures factors. If a concentration x time interaction was found, one-way ANOVAs were performed at each time point at which METH-evoked DA release above basal outflow. When appropriate, one-way ANOVAs were followed by Dunnett's post hoc test to determine concentrations of analog that decreased METH-evoked DA fractional release. Furthermore, one-way ANOVA was performed on the peak response of METH-evoked fractional release at each analog concentration. The log IC_{50} value was generated using an iterative nonlinear least squares curve-fitting program (PRISM version 5.0). Statistical significance was defined as $p < 0.05$.

III. Results

IIIa. MTD decreases METH self-administration without altering food-maintained responding. The effect of MTD on METH self-administration is illustrated in Fig. 8 (top panel). One-way ANOVA revealed a dose-related effect of MTD on the number of METH infusions earned ($F_{4,16} = 4.86$, $p < 0.05$). Dunnett's test revealed that the high dose of MTD (17 mg/kg) decreased the number of METH infusions earned compared to control. Tolerance developed to the ability of MTD to decrease METH self-administration on the second day of treatment. The effect of the acute high dose of MTD (17 mg/kg) on food-maintained responding is illustrated in Fig. 8 (bottom panel). MTD did not decrease responding for food ($p = 0.414$). Thus, the high dose of MTD

specifically decreased METH self-administration; however, tolerance developed to this effect.

IIIb. MTD analogs do not inhibit [^{3}H]nicotine and [^{3}H]MLA binding.

Concentration-response curves and K_i values for lobeline, MTD, and the series of MTD analogs to inhibit [^{3}H]nicotine and [^{3}H]MLA binding to whole brain membranes, compared with nicotine (positive control), are provided in Fig 9 (top and bottom panels, respecitively) and Table 1. K_i values for nicotine were 3 nM and 370 nM at the [^{3}H]nicotine and [^{3}H]MLA binding sites, respectively, consistent with previous reports (Flammia et al., 1999). K_i values for lobeline were 4 nM and 6.26 µM at the [^{3}H]nicotine and [^{3}H]MLA binding sites, respectively, also consistent with previous reports (Zheng et al., 2005a). K_i values for MTD were >100 µM at both [^{3}H]nicotine and [^{3}H]MLA binding sites, as previously observed (Miller et al., 2004). None of the MTD analogs in this series inhibited [^{3}H]nicotine or [^{3}H]MLA binding.

IIIc. MTD analogs inhibit synaptosomal [^{3}H]DA uptake.

Concentration-response curves and K_i values for lobeline, MTD, and the series of MTD analogs to inhibit [^{3}H]DA uptake into striatal synaptosomes, compared with GBR 12909 (positive control), are provided in Fig. 10 and Table 1. The K_i value for GBR 12909 to inhibit [^{3}H]DA uptake was 0.97 nM, consistent with previous reports (Reith et al., 1994). The K_i value for lobeline to inhibit [^{3}H]DA uptake was 28.2 µM, whereas the defunctionalized unsaturated compound MTD exhibited a 200-fold higher potency (K_i = 100 nM) compared to lobeline, in agreement with previous observations (Miller et al., 2004). MTD analogs in the current series

exhibited 50-1000-fold lower potency (K_i > 5 µM) than MTD at DAT. Of note, the 2,4-dichlorophenyl analogs, UKMH-105 and UKMH-106, exhibited 60-fold lower potency (K_i = 6.27 and 6.90 µM, respectively) than MTD. Thus, this series of MTD analogs exhibited lower affinities for DAT compared to the parent compound.

IIId. MTD analogs inhibit synaptosomal [^{3}H]5-HT uptake.

Concentration-response curves and K_i values for lobeline, MTD, and the series of MTD analogs to inhibit [^{3}H]5-HT uptake into hippocampal synaptosomes, compared with fluoxetine (positive control), are provided in Fig. 11 and Table 1. The K_i value for fluoxetine to inhibit [^{3}H]5-HT uptake was 6.5 nM, consistent with previous reports (Owens, 2001). The K_i value for lobeline to inhibit [^{3}H]5-HT uptake was 46.8 µM, whereas MTD exhibited 6-fold higher potency (K_i = 7 µM) compared to lobeline, in agreement with previous observations (Miller et al., 2004). The majority of the MTD analogs had K_i values not different from MTD; of note, the 2,4-dichlorophenyl analogs, UKMH-105 and UKMH-106, exhibited low potency at SERT (K_i = 18.3 and 20.7 µM, respectively). Exceptions include UKMH-101 (no phenyl substituents), UKMH-107 (a 4-methoxyphenyl analog), UKMH-108 (a 4-methylphenyl analog), and UKMH-112 (a 3-furanyl analog), which exhibited 10-fold higher potency at SERT compared to MTD.

IIIe. MTD analogs inhibit [^{3}H]DTBZ binding at VMAT2.

Concentration-response curves and K_i values for lobeline, MTD, and the series of

MTD analogs to inhibit [^{3}H]DTBZ binding to whole brain membranes, compared with Ro-4-1284 (positive control), are provided in Fig. 12 and Table 1. The K_i value for Ro-4-1284 to inhibit [^{3}H]DTBZ binding was 28 nM, consistent with a previous report (Cesura et al., 1990). The K_i value for lobeline to inhibit [^{3}H]DTBZ binding was 2.04 µM, whereas MTD exhibited a 5-fold lower potency (K_i = 9.88 nM) compared to lobeline, consistent with previous observations (Zheng et al., 2005a). The majority of analogs in the series were equipotent inhibiting [^{3}H]DTBZ binding compared with MTD (Table 1). An exception was UKMH-109 (2-thiophenyl analog), which exhibited 10-fold lower potency at the [^{3}H]DTBZ binding site compared to MTD. Of note, UKMH-105 and UKMH-106, the 2,4-dichlorophenyl double bond isomers, exhibited geometrically specific inhibition of [^{3}H]DTBZ binding (K_i = 4.60 and 41.3 µM, respectively).

IIIf. MTD analogs inhibit [^{3}H]DA uptake by VMAT2. Concentration-response curves and K_i values for lobeline, MTD, and the series of MTD analogs to inhibit [^{3}H]DA uptake into striatal vesicles, compared with Ro-4-1284 (positive control), are provided in Fig. 13 and Table 1. The K_i value for Ro-4-1284 to inhibit [^{3}H]DA uptake was 18 nM, consistent with a previous report (Nickell et al., 2011). The K_i value for lobeline to inhibit [^{3}H]DA uptake by VMAT2 was 1.27 µM, which was not different from that for MTD (K_i = 0.46 µM), consistent with previous observations (Nickell et al., 2010). The majority of the analogs in this series were equipotent with MTD inhibiting [^{3}H]DA uptake at VMAT2 (Table 1). Of note, the 2,4-dichlorophenyl isomers, UKMH-105 and UKMH-106, were two of the most potent analogs in the series, with K_i values of 0.22 and 0.32 µM, respectively.

Fig. 14 illustrates K_i values for inhibition of vesicular [^{3}H]DA uptake as a function of K_i for inhibition of [^{3}H]DTBZ binding for lobeline, MTD and the series of MTD analogs. Correlation analysis revealed no relationship between these parameters probing VMAT2 (Pearson's correlation coefficient r = 0.42, p = 0.13).

IIIg. UKMH-105 and UKMH-106 competitively inhibit [^{3}H]DA uptake at VMAT2. UKMH-105 and UKMH-106 were 20- to 450-fold selective for VMAT2 over DAT, SERT and α4β2* and α7* nAChRs. UKMH-105 and UKMH-106 had 10- to 100-fold higher affinity in the VMAT2 functional assay compared with the VMAT2 binding assay. To further evaluate these two analogs, kinetic analyses of [^{3}H]DA uptake at VMAT2 were conducted to determine the mechanism of inhibition, i.e., competitive or noncompetitive, compared with parent compounds (MTD and lobeline). Kinetic assays revealed an increased Km value and no change in Vmax for each compound (Fig. 15) compared to control, indicating a competitive mechanism of action.

IIIh. UKMH-106 inhibits METH-evoked endogenous DA release, while UKMH-105 does not. The ability of UKMH-105 and UKMH-106 to evoke DA release from superfused striatal slices is illustrated in Figs. 16 and 17. Analysis of the effect of UKMH-105 on DA release prior to the addition of METH to the buffer (20-40 min of sample collection) showed no main effects of concentration ($F_{5,29} = 0.47$, $p > 0.05$) and time ($F_{4,29} = 1.01$, $p > 0.05$), and no concentration x time interaction ($F_{20,29} = 0.67$, $p > 0.05$). Thus, UKMH-105 alone did not evoke DA release. Similarly, UKMH-106 did not alter DA release (no main effect of concentration ($F_{4,43} = 0.12$, $p > 0.05$) and showed no time x

concentration interaction ($F_{16,43}$ = 1.57, $p > 0.05$)). A main effect of time was found ($F_{4,43}$ = 6.78, $p < 0.05$), revealing that fractional release increased slightly across the 20 min exposure period in both the absence and presence of UKMH-106. Both UKMH-105 and UKMH-106 also had no effect on DOPAC fractional release across the time period (Fig. 18).

The ability of UKMH-105 and UKMH-106 to decrease METH-evoked DA release is illustrated also in Figs. 16 and 17. A two-way repeated measures ANOVA on fractional DA release during exposure to UKMH-105 and METH revealed no main effect of concentration ($F_{5,29}$ = 0.65, $p > 0.05$) and no concentration x time interaction ($F_{25,29}$ = 0.45, $p > 0.05$); however, a main effect of time ($F_{5,29}$ = 15.4, $p < 0.0001$) was observed, which reflects the increase in fractional release evoked by METH in the absence and presence of UKMH-105. Similar results were obtained with DOPAC, although in the absence and presence of UKMH-105, DOPAC fractional release was decreased in response to METH (Fig. 18). Thus, UKMH-105 did not alter the effect of METH on DA or DOPAC fractional release.

In a concentration-dependent manner, UKMH-106 decreased METH-evoked DA release (Fig. 17). Two-way repeated-measures ANOVA on fractional DA release during exposure to UKMH-106 and METH revealed a main effect of concentration ($F_{4,43}$ = 7.61, $p < 0.0001$) and time ($F_{5,43}$ = 23.0, $p < 0.0001$), and a concentration x time interaction ($F_{20,43}$ = 1.68, $p < 0.05$). Post hoc analysis revealed that, UKMH-106 (1.0 and 3.0 µM) decreased METH-evoked DA release compared to control at 50-55 min and 50-60 min, respectively. The

concentration response for UKMH-106 to inhibit METH-evoked DA release at peak response is illustrated also in Fig 17. IC_{50} and Imax values were 0.38 ± 0.13 μM and 50.2 ± 15.5%, respectively. One-way ANOVA on peak response data revealed a concentration-dependent effect of UKMH-106 ($F_{4,43} = 3.11$, $p < 0.05$). Post hoc analysis revealed that 3 μM UKMH-106 inhibited the DA peak response. In contrast to the ability of UKMH-106 to decrease METH-evoked fractional DA release, fractional DOPAC release was not altered (Fig. 18).

IV. Discussion

In the current study, MTD was shown to decrease METH self-administration specifically, but only at the highest dose evaluated, and tolerance developed rapidly to this effect. Taking into account this encouraging finding, but tempered by the limitations associated with the development of tolerance, modifications to the MTD molecule were evaluated in search of preclinical candidates for the treatment of METH abuse. SAR identified several conformationally-restricted MTD analogs with high affinity and selectivity for VMAT2. Structural modifications included lengthening the linker units, introduction of 4-methoxy, 4-methyl, or 2,4-dichloro substituents into the phenyl rings, or replacement of the phenyl rings with thiophene or furan rings. Effects of altering the geometry of the double bond at the C5-position of the piperidine ring were evaluated in analogs with either a lengthened linker unit or an aromatic 2,4-dichloro substituted phenyl ring. Affinity for VMAT2 was retained, and increases

in selectivity for VMAT2 over DAT were found. The most selective analogs inhibited METH-evoked DA release in a geometrically specific manner.

Conformational restriction in combination with both E and Z geometries at the C5 position of the piperidine ring (UKMH-101 and UKMH-102, respectively) did not alter affinity for VMAT2 binding and uptake sites. Lengthening the linker units, regardless of E or Z geometry (UKMH-103 and UKMH-104, respectively), or adding aromatic 4-methoxy or 4-methyl substituents (UKMH-107 and UKMH-108, respectively), did not alter VMAT2 binding and function. Adding aromatic electron-withdrawing 2,4-dichloro groups in combination with E or Z geometries at the C5-postion on the piperidine ring (UKMH-105 and UKMH-106, respectively) afforded equipotent inhibition of uptake compared to MTD. In kinetic analyses, UKMH-105 and UKMH-106 increased Km, and did not alter Vmax, indicating competitive inhibition of DA uptake. Although no differences in affinity for VMAT2 uptake sites were observed, geometrically-specific inhibition of [^{3}H]DTBZ binding was observed. Specifically, UKMH-106 (3Z, 5*Z* geometry) had 10-fold lower affinity than UKMH-105 (3Z, 5E geometry) at the [^{3}H]DTBZ binding site. In contrast, double bond geometry was not a contributing factor to affinity for VMAT2 binding or uptake in analogs (UKMH-101 and UKMH-102) with no phenyl ring substituents, or analogs (UKMH-103 and UKMH-104) with lengthened linker units and no phenyl ring substituents. While E geometry was better tolerated than Z geometry at the VMAT2 binding site, double bond geometry was not a factor for affinity at the VMAT2 uptake site.

Substitution of the phenyl rings with thiophene or furan moieties afforded analogs with equipotent or 10-fold lower affinity for VMAT2 binding and uptake sites, compared with MTD. Position of the heteroaromatic ring was a factor influencing affinity. Specifically, 3-substituted analogs were equipotent at VMAT2 binding and uptake sites compared with MTD, whereas 2-substituted analogs exhibited 10-fold lower potency. These results suggest that VMAT2 can accommodate analogs in which furanyl and thiophenyl rings have been substituted for phenyl rings, with the 3-position better tolerated than the 2-position.

The current results provide examples of structural modifications that dissociate affinity for the VMAT2 binding site from that for the VMAT2 substrate site and support previous observations showing a lack of correlation between affinities for these sites (Nickell et al., 2011). The best examples from the current series of analogs are the 2,4-dichlorophenyl analogs (UKMH-105 and UKMH-106) which were equipotent at the VMAT2 uptake site, yet exhibited a 10-fold difference in affinity at the binding site. Thus, these findings support an interaction at two alternate sites on VMAT2 associated with distinct pharmacophores.

One goal was to discover MTD analogs with greater selectivity for VMAT2 over DAT. MTD had low affinity (K_i>100 μM) at α4β2* and α7* nAChRs, and inhibited DA uptake by DAT (K_i=500 nM) and 5-HT uptake by SERT (K_i=8.9 μM; Miller et al., 2004). Psychostimulant-induced inhibition of DAT function resulted in increases in extracellular DA, leading to reward and abuse (Ritz et al., 1987;

Williams and Galli, 2006). Affinity of MTD for DAT (K_i=100 nM; current study) is similar to that for cocaine and methylphenidate (K_i=300 and 100 nM, respectively; Han and Gu, 2006), suggesting that MTD may have abuse liability. Reducing affinity for DAT is imperative to avoiding abuse liability. Analogs in the current series had reduced affinity (50-1000-fold) at DAT compared to MTD. Substitution of the phenyl rings with 3-thiophenyl and 3-furanyl rings resulted in the greatest decreases in DAT affinity. Thus, the current analogs have increased selectivity for VMAT2 over DAT, compared to MTD, and would be predicted to have reduced abuse liability.

Since MTD had moderate affinity for SERT (Miller et al., 2004), affinity of the MTD analogs for SERT also was evaluated. Introduction of aromatic 4-methoxy or 4-methyl substituents into the phenyl rings of MTD resulted in a 5-10-fold increased affinity for SERT compared with MTD. The remaining structural changes to MTD did not alter affinity at SERT compared with MTD.

Since the 2,4-dichlorophenyl analogs, UKMH-105 and UKMH-106, exhibited high affinity and selectivity for inhibiting VMAT2 function, these compounds were evaluated for their ability to decrease METH-evoked DA release. Alone, these analogs did not evoke DA release. UKMH-106, but not UKMH-105, inhibited METH-evoked DA release. Inhibition of DA uptake by the analogs at the VMAT2 substrate site does not explain the C5 Z-selective inhibition of the effect of METH on VMAT2. UKMH-105 and UKMH-106 equipotently inhibited DA uptake by VMAT2, but exhibited C5 Z-selective inhibition of METH-evoked DA release, suggesting that these two geometrical

isomers interact with different sites on VMAT2 to inhibit DA uptake and METH-evoked DA release. Only, the Z double bond geometry at the C5 position of the piperidine ring (UKMH-106) was tolerated by the DA release site, whereas the DA uptake site also tolerated the C5 E geometry (UKMH-105). Thus, the VMAT2 site mediating METH-evoked DA release is restricted in its ability to accommodate both geometrical isomers compared to the VMAT2 uptake site.

While the mechanism by which METH releases DA from synaptic vesicles is not understood fully, potential mechanisms include weak base effects of METH, which disrupt vesicular proton gradients and METH effects at the VMAT2 substrate site (Sulzer et al., 2005). Although having different double bond geometries, UKMH-105 and UKMH-106 are expected to have comparable pKa's, inconsistent with the weak base hypothesis as an explanation for differential effects in decreasing METH-evoked DA release. However, current observations are consistent with a previous report showing differential effects of the AMPH optical isomers (Arnold et al., 1977; Fisher and Cho, 1979), despite having the identical pKa's, which again does not support the weak base hypothesis (Sulzer et al., 2005). Thus, UKMH-106 may inhibit METH-evoked DA release through an interaction with VMAT2 and not via a weak-base mechanism.

One caveat of the current study is that inhibitory effects of the analogs on DA uptake and METH-evoked DA release were evaluated using different preparations, isolated vesicles and more intact slices, respectively. One alternative is that the analogs may inhibit METH-evoked DA release by interacting with DAT in the slice. Cytosolic DA is transported to the extracellular

compartment through a METH-induced reversal of DAT (Fischer and Cho, 1979). However, UKMH-106 inhibited METH-evoked DA release 18-fold more potently than inhibition of DAT function, making it unlikely that inhibition of DAT is responsible for the decrease in METH-evoked DA release. If inhibition of DAT was responsible, then both UKMH-105 and UKMH-106 would be expected to decrease METH-evoked DA release, since they are equipotent inhibiting DAT.

A concern regarding the approach of developing VMAT2 inhibitors as treatments for METH abuse is the potential for neurotoxicity, as increased cytosolic DA levels can lead to oxidative stress. METH, inhibits DA uptake at VMAT2, promotes DA release from vesicles, inhibits monoamine oxidase, and produces DA deficits due to increased formation of reactive oxygen species (Fleckenstein et al., 2007). To the contrary, lobeline protects against METH-induced neurotoxicity (Eyerman and Yamamoto, 2005). Further, METH-addicted individuals given lobeline in phase II clinical trials exhibited no adverse effects (Jones, 2007), and TBZ (a classical VMAT2 inhibitor) is FDA-approved for the treatment of Huntington's chorea (Frank, 2010). Thus, precedent for the clinical use of VMAT2 inhibitors exists. Nevertheless, evaluation of the potential neurotoxicity of these analogs using animal models will be an integral component of the drug development process for these candidate treatments for METH abuse.

In summary, the current results extend our previous research by showing that MTD decreases METH self-administration without altering food-maintained responding, demonstrating that inhibition of VMAT2 function translates to a

promising behavioral result. However, MTD has relatively low water solubility, diminishing drug-likeness, and has high affinity (100 nM) for DAT, which may result in abuse liability. Current results show that incorporation of the phenylethylene moiety of MTD into the piperidine ring system, and the addition of aromatic dichloro substituents, results in a novel candidate compound, UKMH-106, which has improved water-solubility and reduced affinity for DAT, SERT, and nAChRs, thereby increasing selectivity for VMAT2. Moreover UKMH-106 decreased the effect of METH to evoke DA release. Thus, the current research utilizing a classical pharmacological approach has identified a novel lead compound that shows promise as a pharmacotherapy to treat METH abuse, a devastating problem for which there are no available treatments.

Table 1. Affinity values (K_i) of MTD analogs, lobeline, MTD and standard compounds for nicotinic receptors, DAT, SERT, and VMAT2 binding and function.

Compound	[^{3}H]Nicotine Binding K_i ± SEM (μM)	[^{3}H]MLA Binding K_i ± SEM (μM)	DAT [^{3}H]DA Uptake K_i ± SEM (μM)	SERT [^{3}H]5-HT Uptake K_i ± SEM (μM)	VMAT2 [^{3}H]DTBZ Binding K_i ± SEM (μM)	VMAT2 [^{3}H]DA Uptake K_i ± SEM (μM)
Nicotine	0.003 ± 0.0002 [a]	0.37 ± 0.08 [a]	ND[b]	ND[b]	ND[b]	ND[b]
GBR 12909	ND[b]	ND[b]	0.00097 ± 0.0001 [a]	ND	ND	ND
Fluoxetine	ND	ND	ND	0.0065 ± 0.0001 [a]	ND	ND
Ro-4-1284	ND	ND	ND	ND	0.028 ± 0.003 [a]	0.018 ± 0.002 [a]
Lobeline	0.004 ± 0.0001	6.26 ± 1.30	28.2 ± 6.73	46.8 ± 3.70	2.04 ± 0.26[c]	1.27 ± 0.46
MTD	>100[d]	>100[d]	0.10 ± 0.01	7.00 ± 1.30	9.88 ± 2.22[c]	0.46 ± 0.11
UKMH-101	>100	>100	11.5 ± 1.90	0.71 ± 0.09	31.8 ± 5.84	0.88 ± 0.19
UKMH-102	>100	>100	25.1 ± 2.93	1.37 ± 0.09	12.3 ± 4.70	0.22 ± 0.05
UKMH-103	>100	>100	16.2 ± 1.20	2.10 ± 0.51	20.3 ± 3.73	0.79 ± 0.18
UKMH-104	>100	>100	5.25 ± 0.46	2.67 ± 0.51	15.0 ± 5.22	0.88 ± 0.26
UKMH-105	>100	>100	6.27 ± 0.60	18.3 ± 7.50	4.60 ± 1.70	0.22 ± 0.01
UKMH-106	>100	>100	6.90 ± 1.10	20.7 ± 4.90	41.3 ± 14.3	0.32 ± 0.12
UKMH-107	>100	>100	68.2 ± 6.93	0.51 ± 0.05	7.27 ± 2.28	1.03 ± 0.19
UKMH-108	>100	>100	39.0 ± 16.3	0.61 ± 0.08	3.42 ± 0.26	0.33 ± 0.08
UKMH-109	>100	>100	>100	16.3 ± 4.10	91.3 ± 26.2	2.27 ± 1.13
UKMH-110	>100	>100	58.1 ± 18.7	13.4 ± 4.10	10.4 ± 2.62	0.36 ± 0.12
UKMH-111	>100	>100	>100	16.1 ± 2.91	32.6 ± 6.79	3.82 ± 1.99
UKMH-112	>100	>100	5.50 ± 0.26	0.71 ± 0.19	15.5 ± 1.61	0.58 ± 0.08

[a] n = 3-4 rats; [b]ND, not determined; [c] data taken from Zheng et al., 2005a; [d]data taken from Miller et al., 2001; (3*Z*,5*E*)-3,5-dibenzylidene-1-methylpiperidine (UKMH-101); (3*Z*,5*Z*)-3,5-dibenzylidene-1-methylpiperidine (UKMH-102); [(3*Z*,5*E*)-1-methyl-3,5-bis((*E*)-3-phenylallylidene)piperidine (UKMH-103); (3*Z*,5*Z*)-1-methyl-3,5-bis((*E*)-3-phenylallylidene)piperidine (UKMH-104); (3*Z*,5*E*)-3,5-bis(2,4-dichlorobenzylidene)-1-methylpiperidine (UKMH-105); (3*Z*,5*Z*)-3,5-bis(2,4-dichlorobenzylidene)-1-methylpiperidine (UKMH-106); (3*Z*,5*Z*)-3,5-bis(4-methoxybenzylidene)-1-methylpiperidine (UKMH-107); (3*Z*,5*Z*)-1-methyl-3,5-bis(4-methylbenzylidene)-piperidine (UKMH-108); (3*Z*,5*Z*)-1-methyl-3,5-bis(thiophen-2-ylmethylene)piperidine (UKMH-109); (3*Z*,5*Z*)-1-methyl-3,5-bis(thiophen-3-ylmethylene)piperidine (UKMH-110); (3*Z*,5*Z*)-3,5-bis(furan-2-ylmethylene)-1-methylpiperidine (UKMH-111); (3*Z*,5*Z*)-3,5-bis(furan-3-ylmethylene)-1-methylpiperidine (UKMH-112)

Fig. 6. Chemical structures of lobeline, MTD, and MTD analogs incorporating the phenyethylene moiety of MTD into the piperidine ring system with the addition of various phenyl ring substituents. For clarity of presentation, compounds are grouped according to structural similarity. (top) Lobeline, MTD and MTD analogs with no phenyl ring additions; (middle) MTD analogs with dichloro, methoxy, or methyl additions; (bottom) MTD analogs with heteroaromatic phenyl ring substitutions.

Lobeline, *meso*-transdiene, and MTD analogs with no phenyl ring substituents

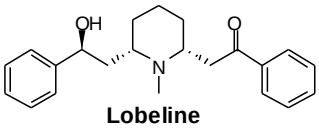

Lobeline

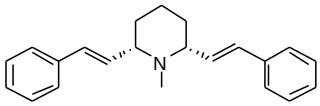

***meso*-transdiene (MTD)**

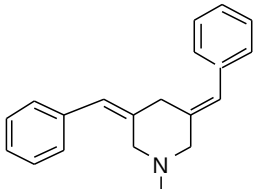

UKMH-101

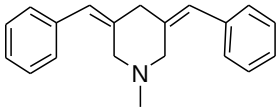

UKMH-102

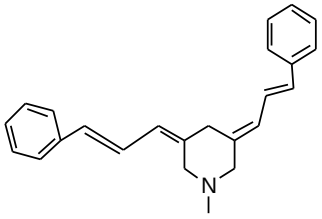

UKMH-103

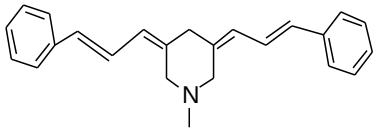

UKMH-104

MTD analogs with dichloro, methoxy, or methyl aromatic substituents

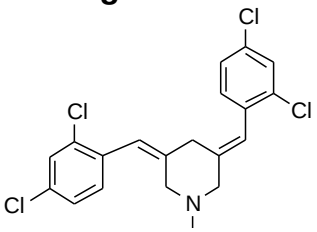

UKMH-105

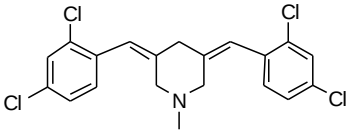

UKMH-106

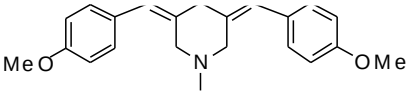

UKMH-107

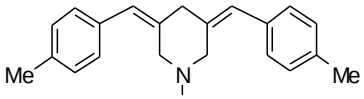

UKMH-108

MTD analogs containing heteroaromatic rings

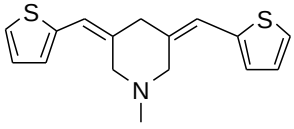

UKMH-109

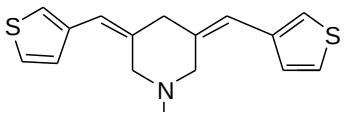

UKMH-110

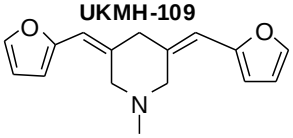

UKMH-111

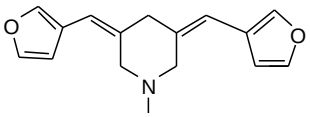

UKMH-112

Fig 7. Incorporating the phenylethylene moiety of MTD into the piperdine ring of the analogs affords a novel more rigid molecule. For all analogs in the series, the phenyethylene substituents in the MTD structure (left) were incorporated into the piperidine ring system to afford analogs (right) with a similar number of carbons between the piperidine nitrogen and the phenyl rings. This structural change reduces the molecular weight and the number of rotational carbon bonds (curved arrows) from four in MTD to two in the MTD analogs, affording a novel, more conformationally-restricted structure.

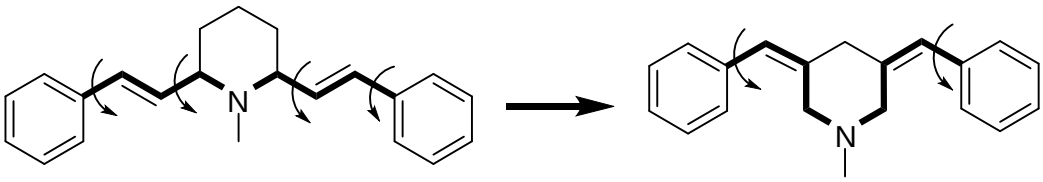

Fig 8. MTD decreases METH self-administration, however tolerance develops to this effect. MTD does not alter food-maintained responding. Effect of acute MTD (closed circles) and repeated MTD (open circles) on METH self-administration (top panel). Effect of the high dose of MTD (17.0 mg/kg) on food-maintained responding (bottom panel). Data are expressed as mean ± S.E.M. number of METH infusions (0.05 mg/kg/infusion) or number of pellets earned during 60-min sessions (n = 5-6). *indicates $p < 0.05$ compared to control.

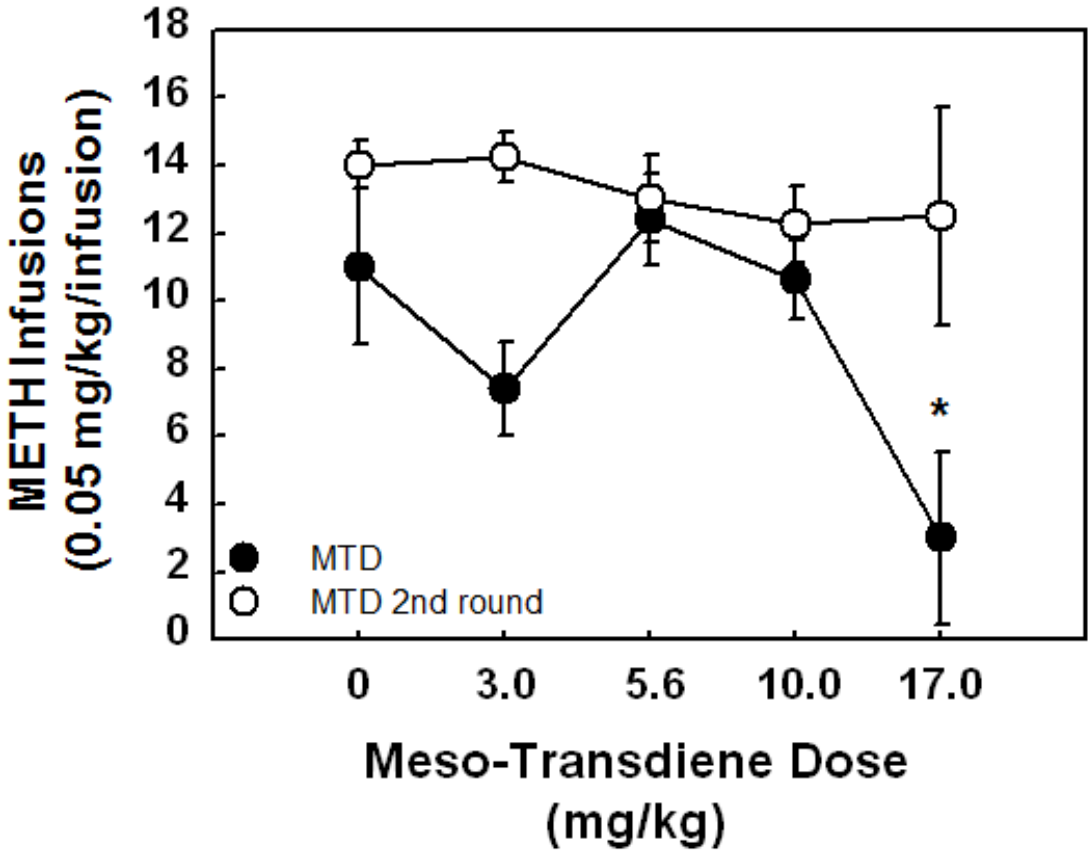

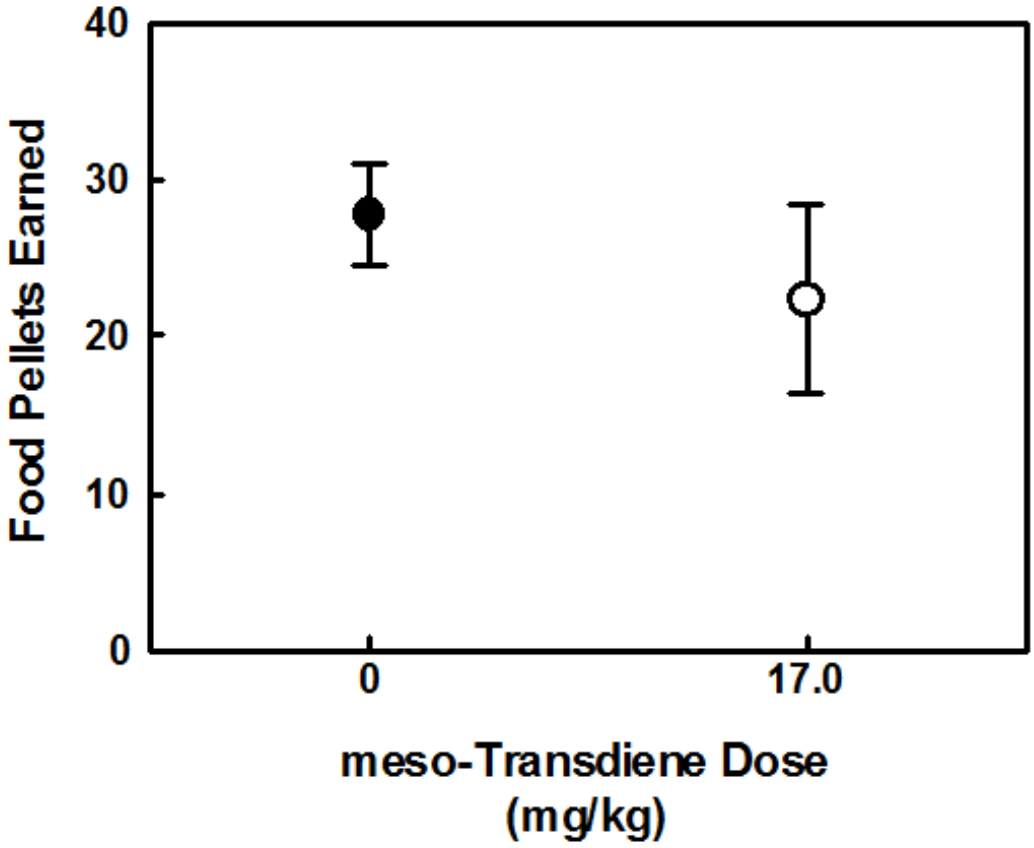
40
30
20
10
0
Food Pellets Earned
0
17.0
meso-Transdiene Dose
(mg/kg)

Fig 9. MTD analogs do not inhibit [^{3}H]nicotine binding and [^{3}H]MLA binding to whole brain membranes. Data represent the ability of analogs to displace [^{3}H]nicotine and [^{3}H]MLA binding (top and bottom panel, respectively). Nonspecific [^{3}H]nicotine binding and nonspecific [^{3}H]MLA binding were determined in the presence of 10 μM cytisine and 10 μM nicotine, respectively. Control represents [^{3}H]nicotine and [^{3}H]MLA binding in the absence of analog (56.8 ± 4.22 and 69.7 ± 2.67 fmol/mg protein, respectively). n = 3-4 rats/analog.

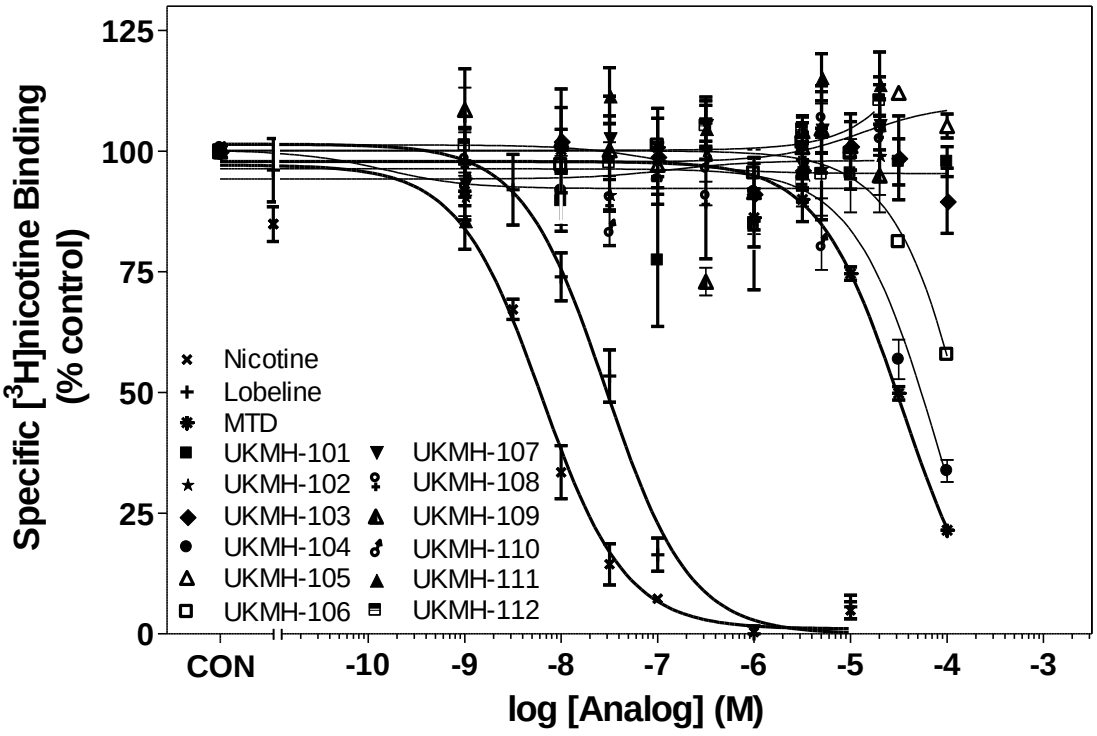

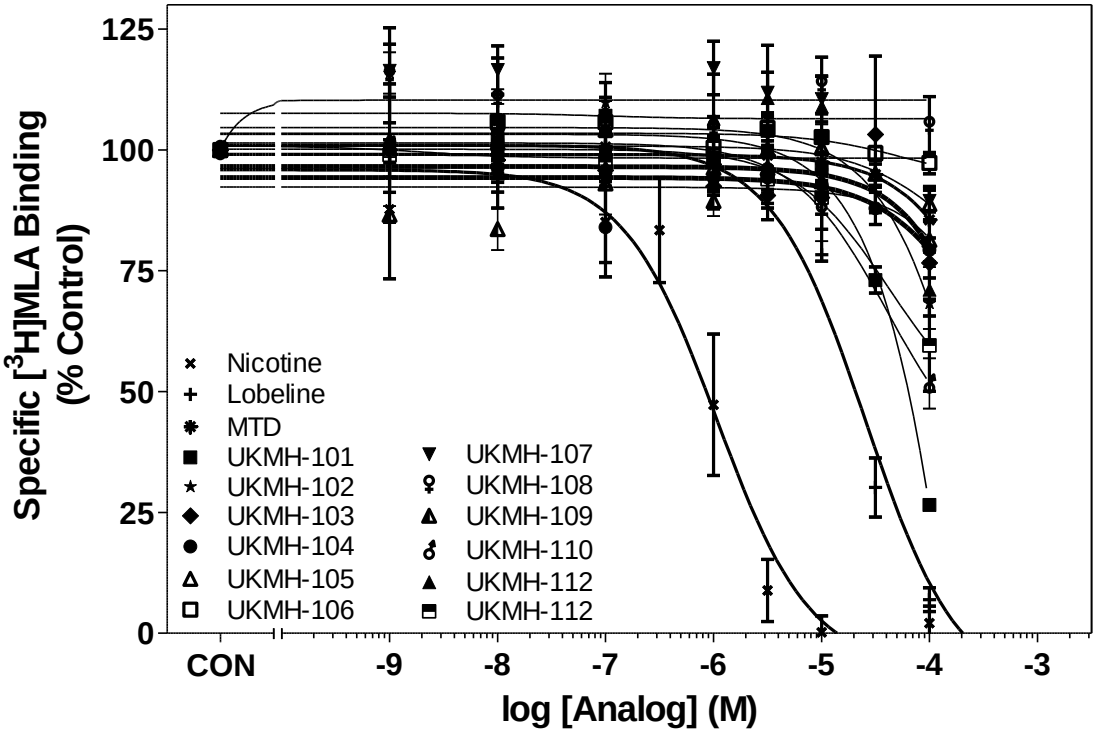
Specific [3H]MLA Binding
(% Control)
125
100
75
50
25
0
CON
-9
-8
-7
-6
-5
-4
-3
log [Analog] (M)
Nicotine
Lobeline
MTD
UKMH-101
UKMH-102
UKMH-103
UKMH-104
UKMH-105
UKMH-106
UKMH-107
UKMH-108
UKMH-109
UKMH-110
UKMH-112
UKMH-112

Fig. 10. Structural modifications to MTD afford analogs with decreased affinity for DAT. Analogs are grouped according to structural similarity of the aromatic rings. (top) Lobeline, MTD and MTD analogs with no aromatic ring substituents; (middle) MTD analogs with dichloro, methoxy, or methyl aromatic substituents; (bottom) MTD analogs containing heteroaromatic rings. MTD is repeated in all 3 panels for purpose of comparison. Nonspecific [^{3}H]DA uptake was determined in the presence of 10 μM GBR 12909. Control (CON) represents specific [^{3}H]DA uptake in the absence of analog (35.0 ± 1.55 pmol/mg/min). Legend provides analogs in order from highest to lowest affinity. n = 4 rats/analog.

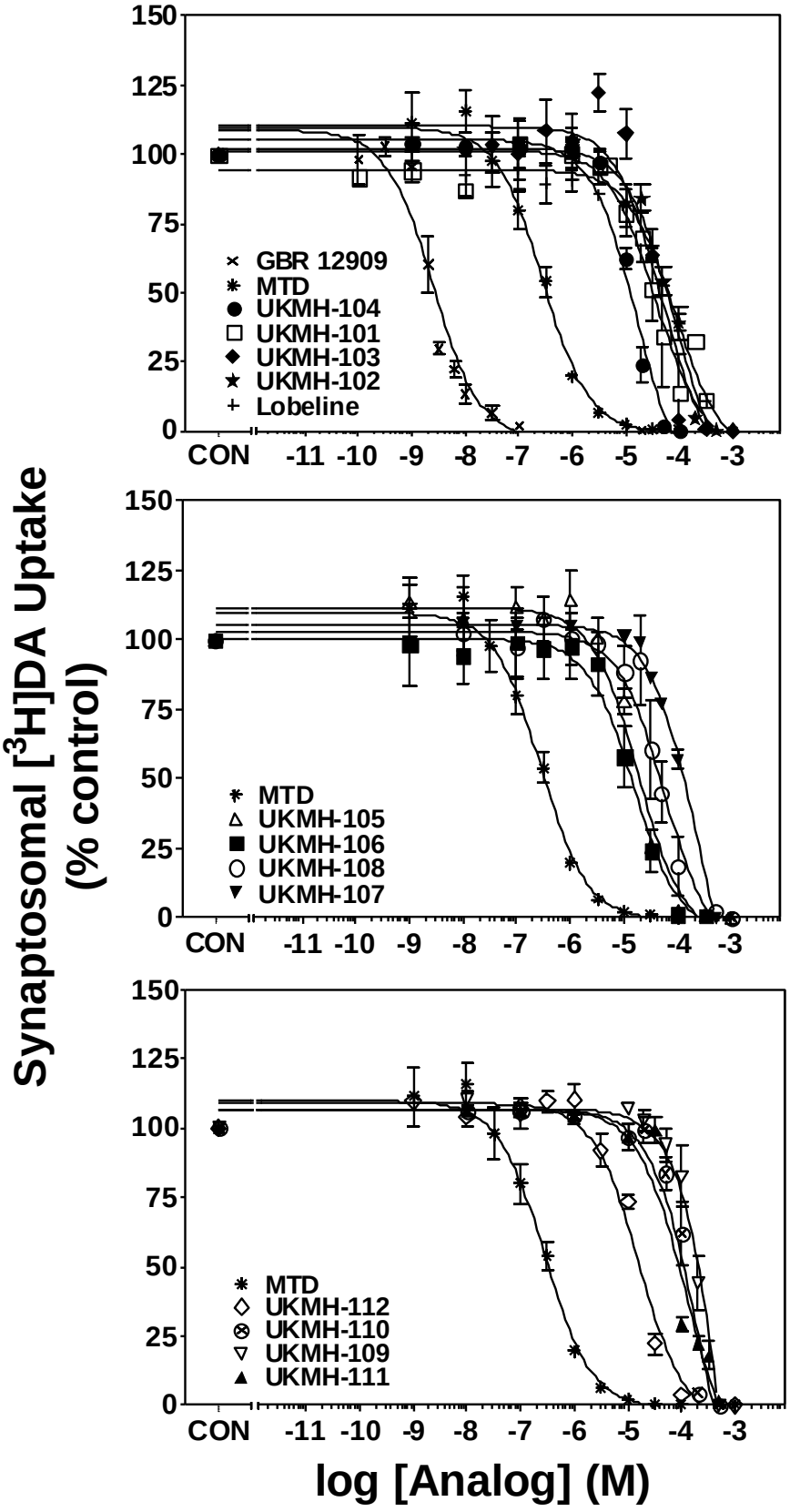
Synaptosomal [3H]DA Uptake
(% control)
150
125
100
75
50
25
0
CON
-11
-10
-9
-8
-7
-6
-5
-4
-3
GBR 12909
MTD
UKMH-104
UKMH-101
UKMH-103
UKMH-102
Lobeline
MTD
UKMH-105
UKMH-106
UKMH-108
UKMH-107
MTD
UKMH-112
UKMH-110
UKMH-109
UKMH-111
log [Analog] (M)

Fig. 11. MTD analogs inhibit [^{3}H]5-HT uptake into rat hippocampal synaptosomes. Analogs are grouped according to structural similarity of the aromatic rings. (top) Lobeline, MTD and MTD analogs with no aromatic ring substituents; (middle) MTD analogs with dichloro, methoxy, or methyl aromatic substituents; (bottom) MTD analogs containing heteroaromatic rings. MTD is repeated in all 3 panels for purpose of comparison. Nonspecific [^{3}H]5-HT uptake was determined in the presence of 10 μM fluoxetine. Control (CON) represents specific [^{3}H]5-HT uptake in the absence of analog (1.67 ± 0.09 pmol/mg/min). Legend provides compounds in order from highest to lowest affinity. n = 4 rats/analog.

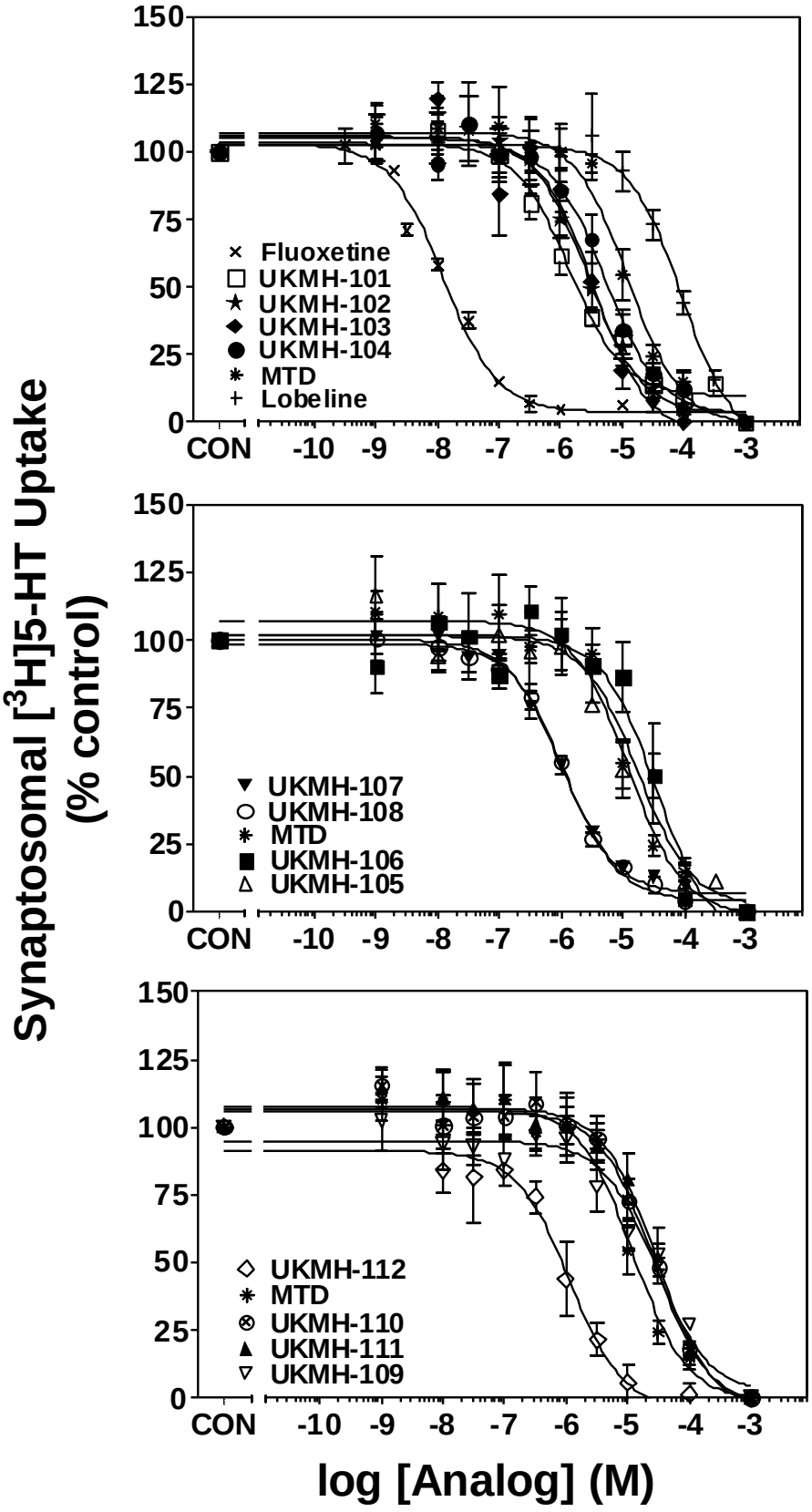
Synaptosomal [3H]5-HT Uptake
(% control)
150
125
100
75
50
25
0
CON
-10
-9
-8
-7
-6
-5
-4
-3
Fluoxetine
UKMH-101
UKMH-102
UKMH-103
UKMH-104
MTD
Lobeline
UKMH-107
UKMH-108
MTD
UKMH-106
UKMH-105
UKMH-112
MTD
UKMH-110
UKMH-111
UKMH-109
log [Analog] (M)

Fig 12. MTD analogs inhibit [^{3}H]DTBZ binding to vesicle membranes from rat whole brain preparations. Analogs are grouped according to structural similarity of the aromatic rings. (top) Lobeline, MTD and MTD analogs with no aromatic ring substituents; (middle) MTD analogs with dichloro, methoxy, or methyl aromatic substituents; (bottom) MTD analogs containing heteroaromatic rings. MTD is repeated in all 3 panels for purpose of comparison. Nonspecific [^{3}H]DTBZ binding was determined in the presence of 10 μM Ro-4-1284. Control (CON) represents specific [^{3}H]DTBZ binding in the absence of analog (5.01 ± 0.10 pmol/mg protein). Analogs are arranged in order from greatest potency to least potency. n = 4 rats/analog.

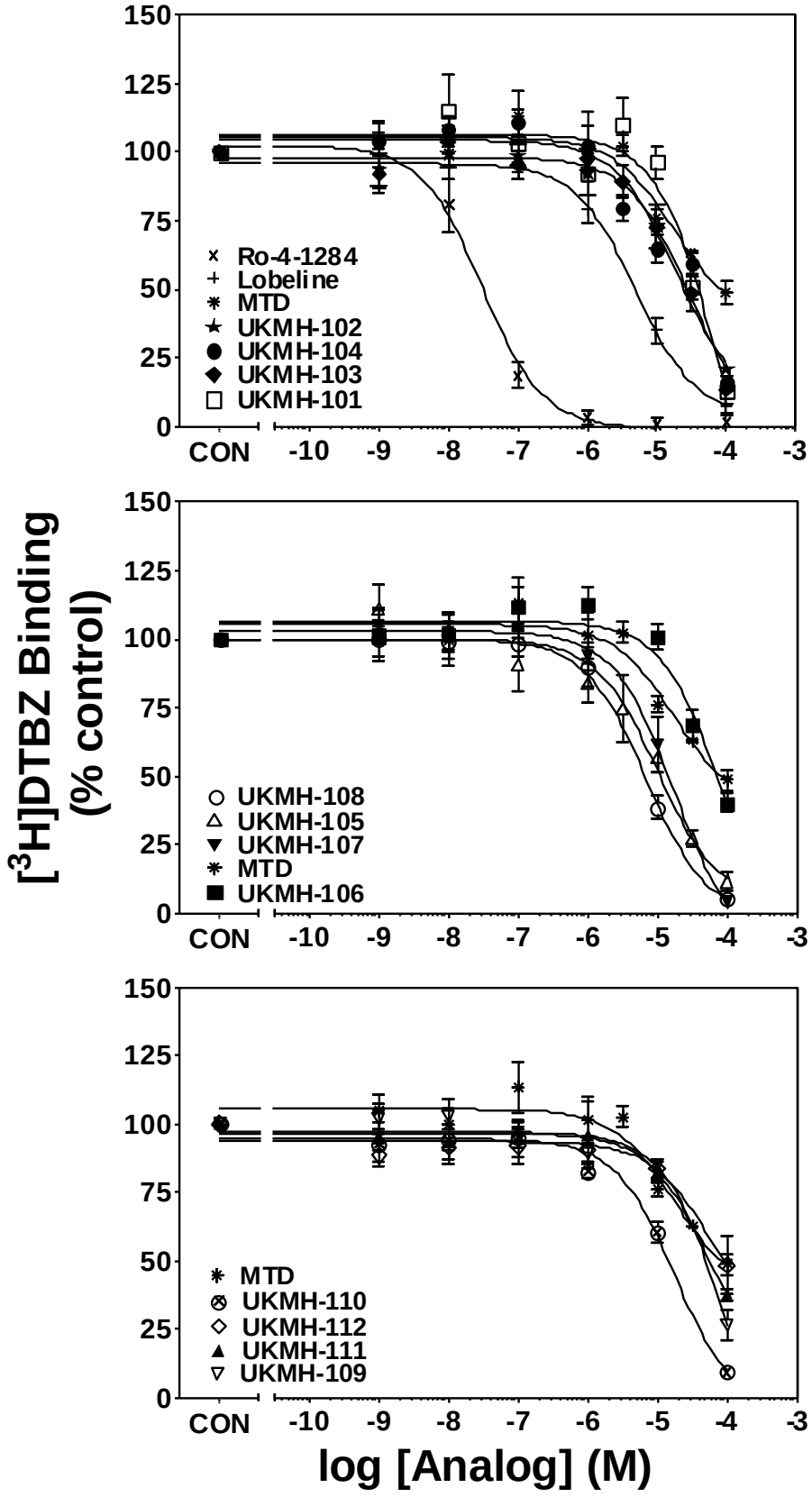
[3H]DTBZ Binding
(% control)
150
125
100
75
50
25
0
CON
-10
-9
-8
-7
-6
-5
-4
-3
Ro-4-1284
Lobeline
MTD
UKMH-102
UKMH-104
UKMH-103
UKMH-101
UKMH-108
UKMH-105
UKMH-107
MTD
UKMH-106
MTD
UKMH-110
UKMH-112
UKMH-111
UKMH-109
log [Analog] (M)

Fig 13. MTD analogs inhibit [^{3}H]DA uptake into rat striatal vesicles. Analogs are grouped according to structural similarity of the aromatic rings. (top) Lobeline, MTD and MTD analogs with no aromatic ring substituents; (middle) MTD analogs with dichloro, methoxy, or methyl aromatic substituents; (bottom) MTD analogs containing heteroaromatic rings. MTD is repeated in all 3 panels for purpose of comparison. Nonspecific [^{3}H]DA uptake was determined in the presence of 10 μM Ro-4-1284. Control (CON) represents specific vesicular [^{3}H]DA uptake in the absence of analog (29.3 ± 1.38 pmol/mg/min). Legend provides compounds in order from highest to lowest affinity. n = 4 rats/analog.

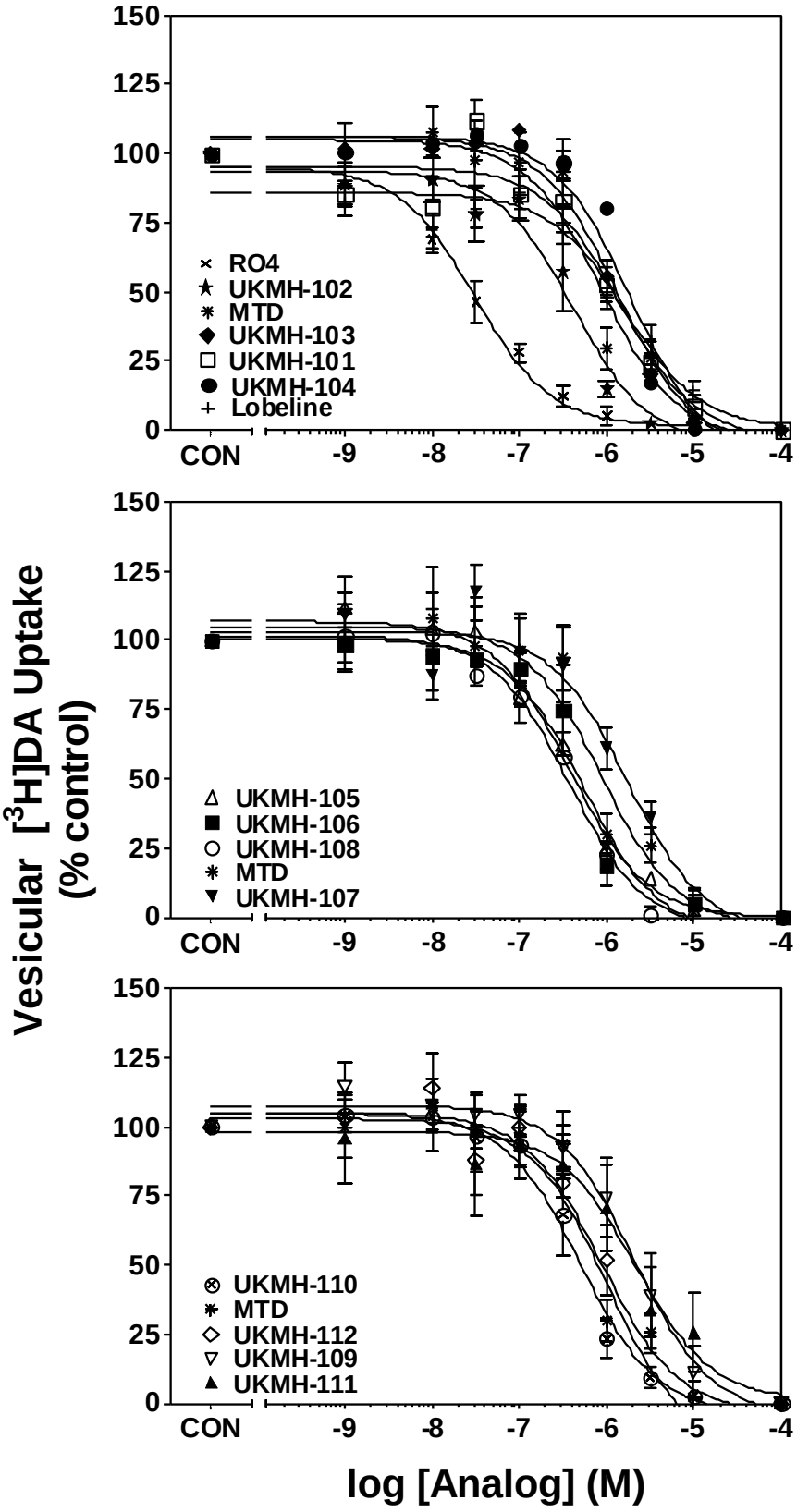
Vesicular [3H]DA Uptake (% control)
150
125
100
75
50
25
0
CON
-9
-8
-7
-6
-5
-4
RO4
UKMH-102
MTD
UKMH-103
UKMH-101
UKMH-104
Lobeline
UKMH-105
UKMH-106
UKMH-108
MTD
UKMH-107
UKMH-110
MTD
UKMH-112
UKMH-109
UKMH-111
log [Analog] (M)

Fig 14. Inhibition of [^{3}H]DTBZ binding does not predict inhibition of [^{3}H]DA uptake at VMAT2. Data presented are K_i values from analog-induced inhibition of [^{3}H]DTBZ binding and [^{3}H]DA uptake at VMAT2 (Figs. 12 and 13, respectively). Pearson's correlation analysis of these data revealed a lack of correlation (Pearson's r = 0.42; p = 0.13) between the ability of analogs to inhibit [^{3}H]DTBZ binding and [^{3}H]DA uptake at VMAT2.

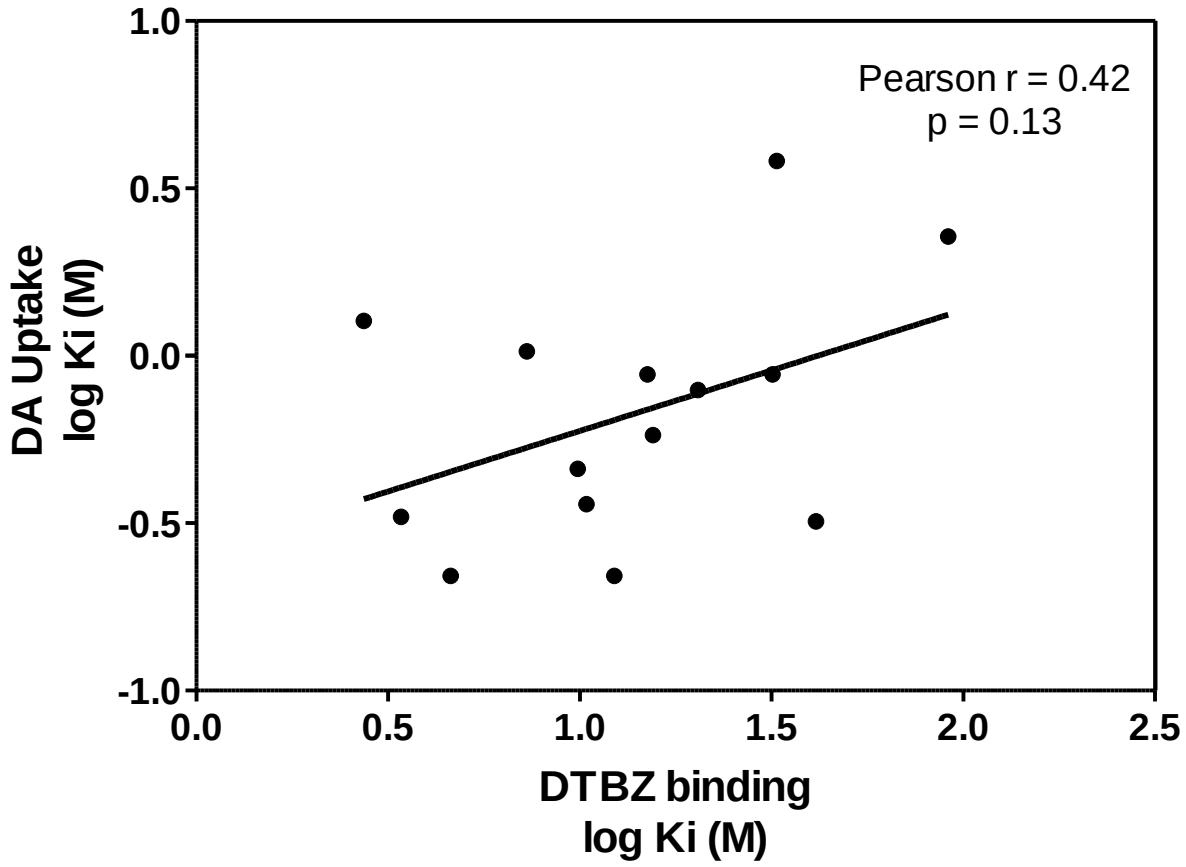

Fig 15. Lobeline, MTD and MTD analogs competitively inhibit [^{3}H]DA uptake into vesicles prepared from rat striatum. Concentrations of lobeline (0.25 µM), MTD (0.23 µM), UKMH-105 (0.11 µM), and UKMH-106 (0.16 µM) approximated the K_i values for inhibiting [^{3}H]DA uptake into isolated synaptic vesicles obtained from the data shown in Fig. 13. Km (top panel) and Vmax (bottom panel) values are mean ± S.E.M. (* $p < 0.05$ different from control; ** $p < 0.01$ different from control; n = 4-7 rats/analog)

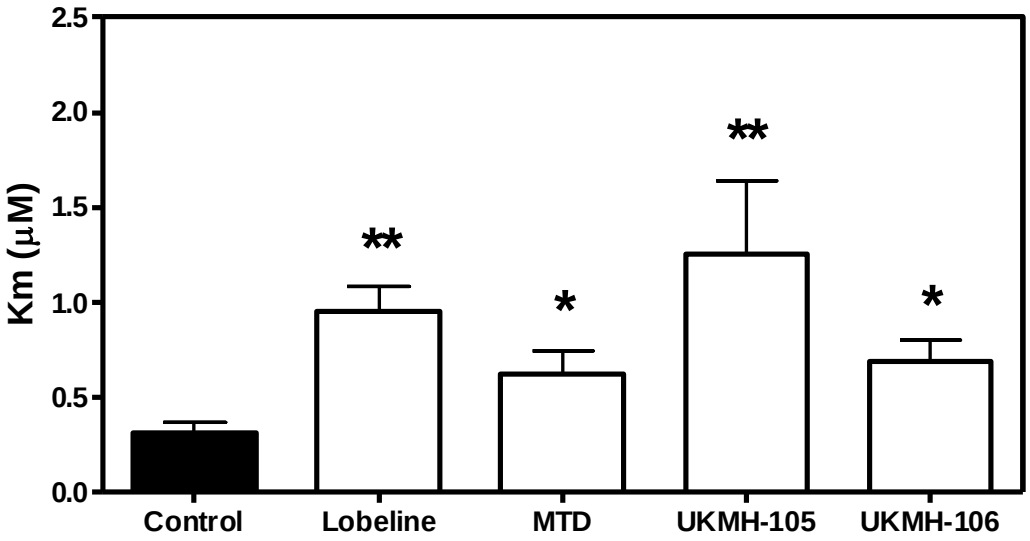

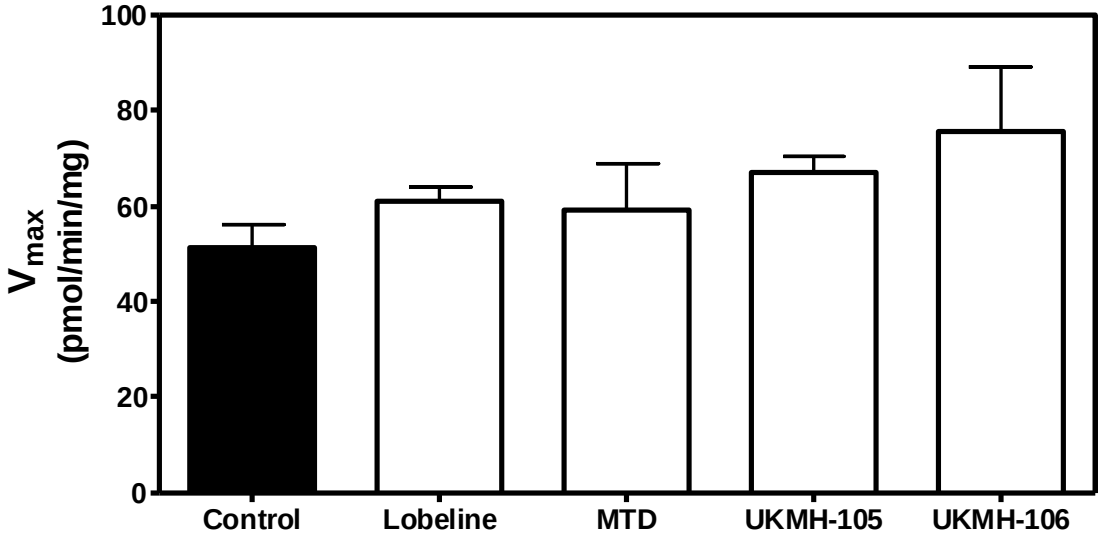
100
80
60
40
20
0
V_{max}
(pmol/min/mg)
Control
Lobeline
MTD
UKMH-105
UKMH-106

Fig 16. UKMH-105 does not inhibit METH-evoked endogenous DA release from striatal slices. Fractional DA release represents the amount of DA in each 5-min sample. Slices were superfused with UKMH-105 after 10 min collection of basal samples, as indicated by the arrow and analog remained in the buffer until the end of the experiment. METH (5 μM) was added to the buffer for 15 min as indicated by the horizontal bar. Fractional release data are expressed as mean ± S.E.M. pg/ml/mg of the slice weight. n = 5 rats.

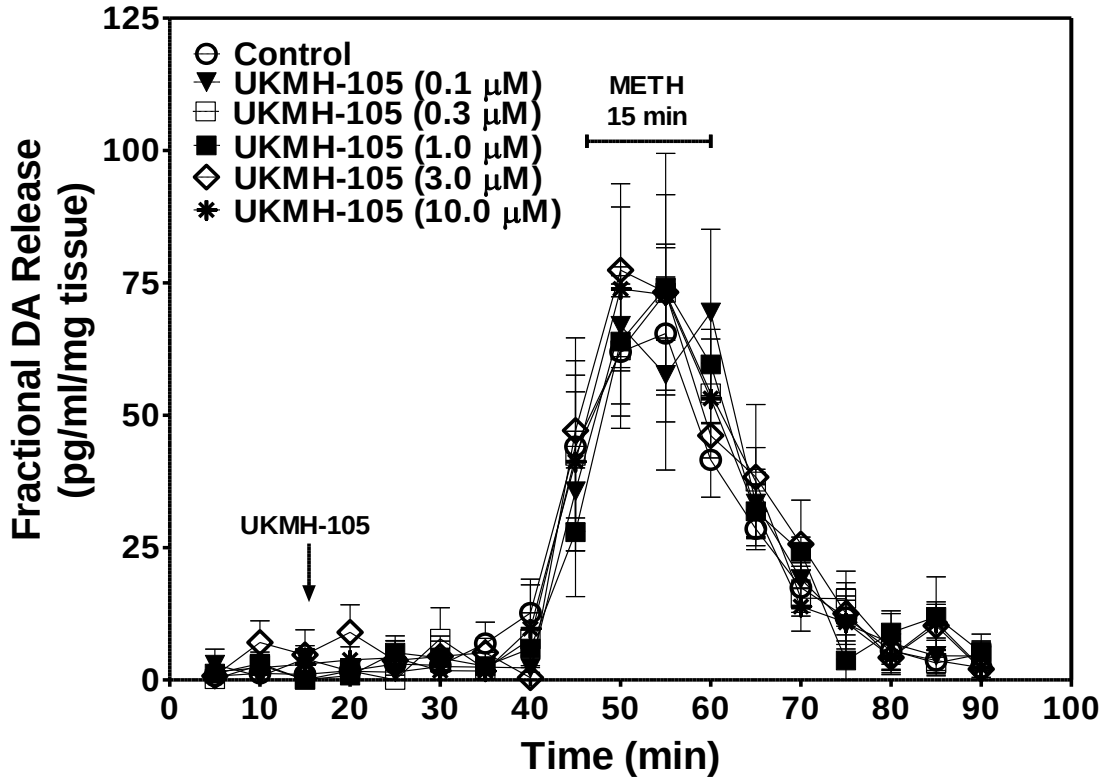

Fig 17. In a concentration-dependent manner, UKMH-106 inhibits METH-evoked DA release in striatal slices. Fractional DA release (top panel) represents the amount of DA in each 5-min sample. Slices were superfused with UKMH-106 after 10 min collection of basal samples, as indicated by the arrow and analog remained in the buffer until the end of the experiment. METH (5 μM) was added to the buffer for 15 min as indicated by the horizontal bar. Concentration-response curve (bottom panel) was derived from peak response data for each concentration of UKMH-106. Fractional release and peak response data are expressed as mean ± S.E.M. pg/ml/mg of the slice weight. For fractional release: *p < 0.05 different from METH alone. For peak response: *p < 0.05 different from peak response of METH alone (CON). n = 8 rats

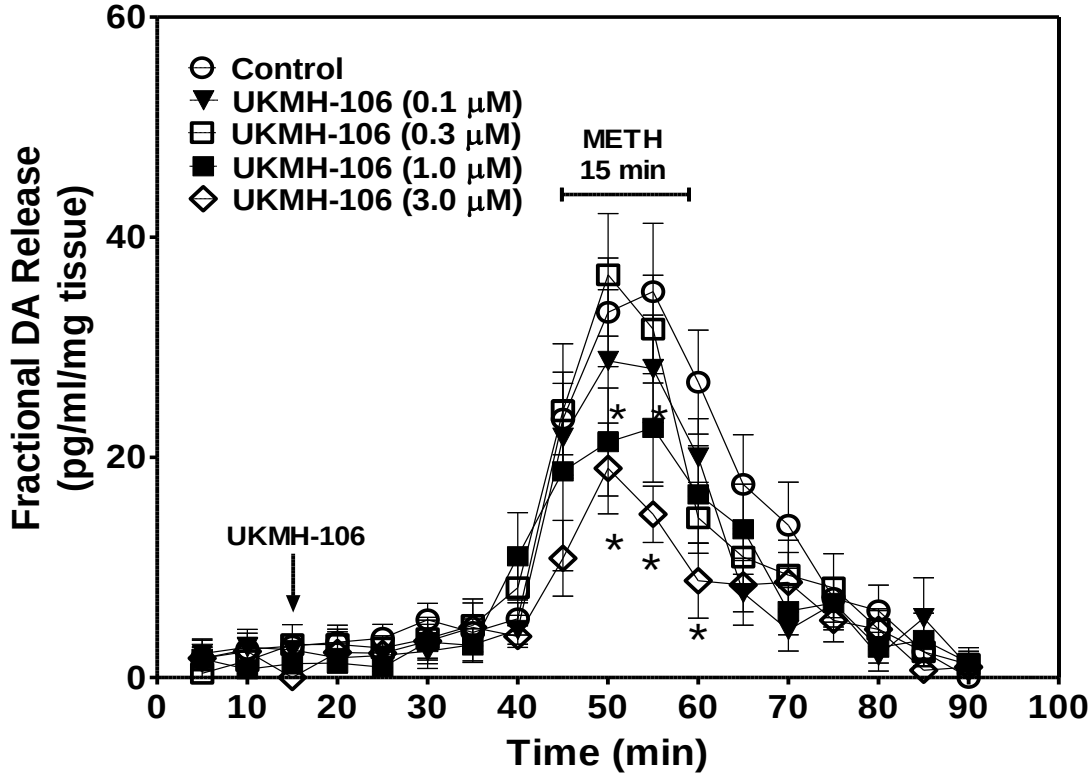

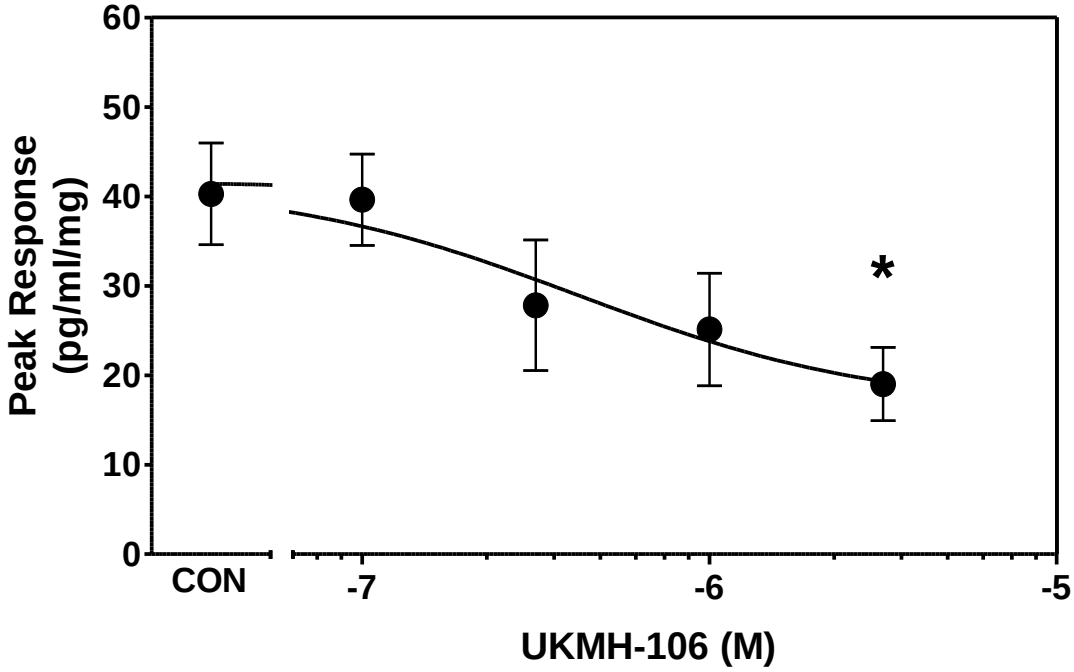
60
50
40
30
20
10
0
Peak Response
(pg/ml/mg)
*
CON
-7
-6
-5
UKMH-106 (M)

Fig 18. UKMH-105 and UKMH-106 do not alter DOPAC release. Fractional DOPAC release represents the amount of DOPAC in each 5-min sample. Slices were superfused with UKMH-105 (top panel) or UKMH-106 (bottom panel) after 10 min collection of basal samples, as indicated by the arrow and analog remained in the buffer until the end of the experiment. METH (5 µM) was added to the buffer for 15 min as indicated by the horizontal bar. Fractional release data is expressed as mean ± S.E.M. pg/ml/mg of the slice weight. n = 8 rats

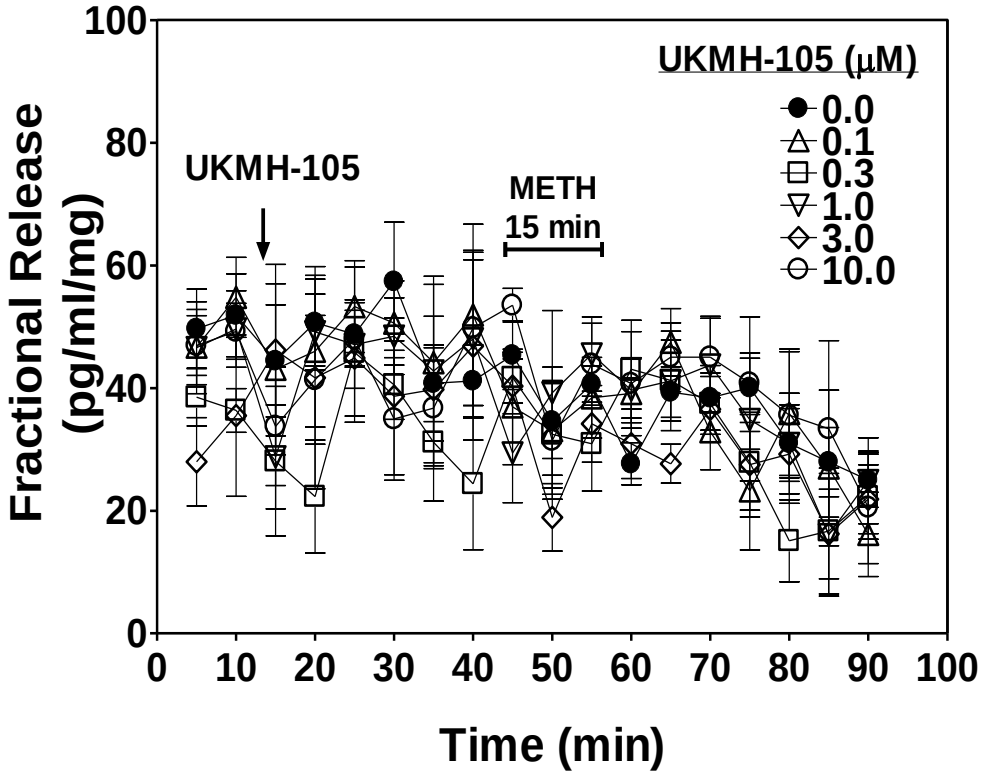

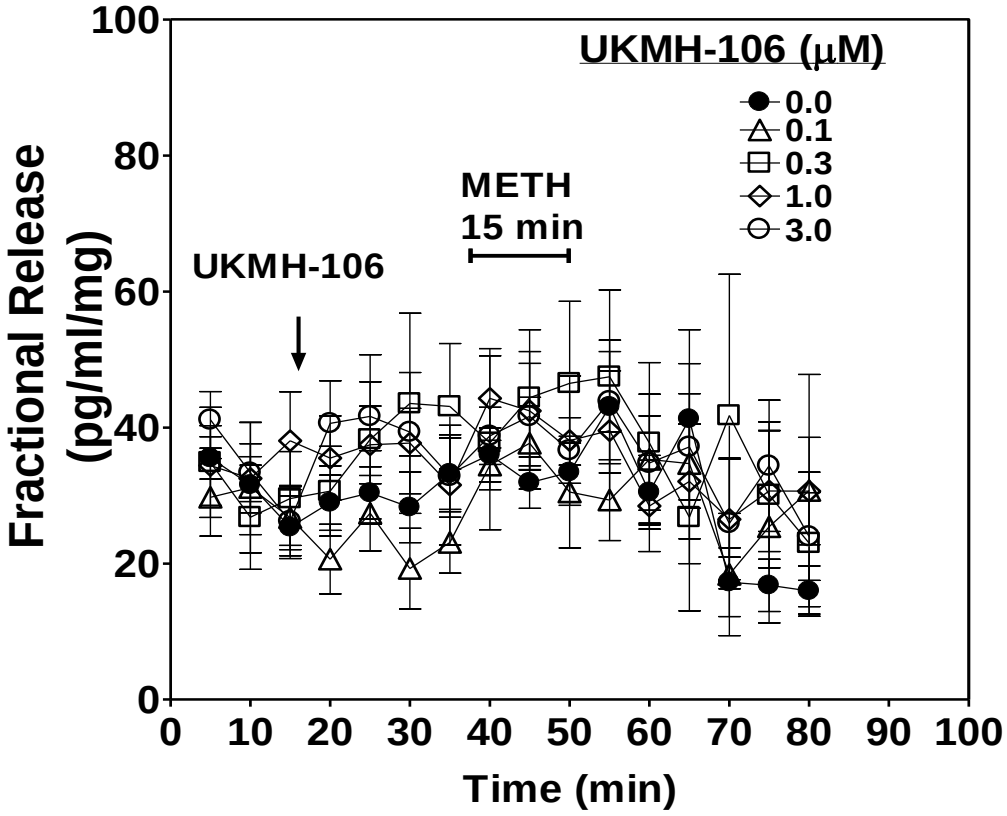

CHAPTER THREE

Novel N-1,2-Dihydroxypropyl Analogs of Lobelane Inhibit VMAT2 Function and METH-evoked DA Release

Portions of this chapter have been published in the manuscript:

> Horton DB, Zheng G, Siripurapu KB, Deaciuc AG, Crooks PA, Dwoskin LP. N-1,2 dihydroxylpropyl analogs of lobelane as novel vesicular monoamine transporter (VMAT2) inhibitors and potential treatments for methamphetamine abuse. *J Pharm Exp Ther,* 339: 286-297, 2011.

Chapter reprinted with permission of the American Society for Pharmacology and Experimental Therapeutics.

I. Introduction

METH is a highly addictive stimulant with robust rewarding properties leading to its abuse. METH use continues to be a major health concern in the United States, with 100,000 new users in the United States every year (NSDUH, 2008). To date, there are no approved therapeutics for METH abuse. METH acts at both the DAT and VMAT2 to increase extracellular DA concentrations (Sulzer et al., 2005). Specifically, METH reverses DA translocation by DAT to increase extracellular DA concentrations leading to reward (Fischer and Cho, 1979, Liang and Rutledge, 1982; Wise and Bozarth, 1987; Di Chiara and Imperato, 1988). Numerous studies have focused on DAT as a therapeutic target for the development of treatments for psychostimulant abuse (Grabowski et al., 1997, Dar et al., 2005; Howell et al., 2007; Tanda et al., 2009). However, this approach to drug discovery has thus far not resulted in viable efficacious therapeutics for METH abuse.

METH inhibits DA uptake at VMAT2 and stimulates DA release from presynaptic vesicles, which presumably increases cytosolic DA concentrations (Sulzer and Rayport, 1990; Sulzer et al., 1995; Pifl et al., 1995). Taking into account VMAT2 as a component of the mechanism of action of METH, our research focus has been the discovery of novel therapeutic agents that target VMAT2. SARs have been generated to elucidate novel pharmacophores that modify VMAT2 function with the aim of developing effective treatments for METH abuse (Zheng et al., 2005a,b; Nickell et al., 2010a,b; Horton et al., 2010; Crooks et al., 2010).

Lobeline (Fig. 19), the principal alkaloid in *Lobelia inflata*, inhibits the neurochemical and behavioral effects of METH through its interaction with VMAT2 (Teng et al., 1997, 1998; Miller et al., 2001, Harrod et al., 2001; Dwoskin and Crooks, 2002; Nickell et al., 2010). Lobeline inhibits [^{3}H]DTBZ binding to VMAT2 (Ki = 0.90 μM), [^{3}H]DA uptake at VMAT2 (Ki = 0.88 μM; Teng et al., 1997, 1998) and METH-evoked DA release (IC_{50} = 0.42 μM), supporting the tenet that VMAT2 is a viable therapeutic target for the development of treatments for METH abuse. In further support of this hypothesis, lobeline decreases METH self-administration in rats (Harrod et al., 2001). Importantly, lobeline is not self-administered (Harrod et al., 2003), suggesting that it will not have abuse liability. Recently, lobeline has completed Phase Ib clinical trials demonstrating safety in METH abusers (Jones, 2007).

Initial SAR around the lobeline pharmacophore revealed that lobelane (Fig. 19), a chemically defunctionalized, saturated analog of lobeline,

competitively inhibited DA uptake at VMAT2 and exhibited increased affinity and selectivity for VMAT2 compared with lobeline (Miller et al., 2001; Nickell et al., 2010). Lobelane inhibited METH-evoked DA release and decreased METH self-administration; however, tolerance developed to the latter behavior effects (Neugebauer et al., 2007; Nickell et al., 2010). Unfortunately, lobelane exhibits decreased water solubility and diminished drug likeness properties due to its decreased polarity resulting from removal of the keto and hydroxyl functionalities of lobeline.

In the current study, the N-methyl moiety of the central piperidine ring of lobelane was replaced with a chiral N-1,2-dihydroxypropyl (N-1,2-diol) moiety to improve water solubility and enhance drug-likeness properties. Based on computational modeling, this structural modification was predicted to enhance water solubility. VMAT2 binding and function was determined following 1) replacement of the N-methyl moiety with a chiral N-1,2-diol moiety, 2) alteration of the configuration of the N-1,2-diol moiety, and 3) incorporation of phenyl ring substituents into the analogs. Specifically, incorporation of 2-methoxy, 3-methoxy, 4-methoxy, 3-flouro, 2,4-dichloro, and 3,4-methylenedioxy substituents into both phenyl rings, or replacement of the phenyl rings with naphthalene or biphenyl rings, were evaluated. To assess VMAT2 selectivity, SAR was generated for inhibition of DAT and SERT function. Analogs with highest potency for inhibiting DA uptake at VMAT2 and with at least 10-fold selectivity were evaluated for inhibition of METH-evoked DA release from superfused

striatal slices. GZ-793A emerged as a potent, selective and drug-like VMAT2 inhibitor to be further developed as a treatment for METH abuse.

The hypothesis of this chapter is that N-1,2-diol analogs of lobelane will inhibit VMAT2 function and VMAT2 selective lobelane analogs will inhibit METH-evoked DA release from striatal slices.

II. Methods

IIa. Animals. Male Sprague-Dawley rats (200–250g, Harlan, Indianapolis, IN) were housed two per cage with *ad libitum* access to food and water in the Division of Laboratory Animal Resources at the University of Kentucky (Lexington, KY). Experimental protocols involving the animals were in accord with the 1996 *NIH Guide for the Care and Use of Laboratory Animals* and were approved by the Institutional Animal Care and Use Committee at the University of Kentucky.

IIb. Chemicals. [^{3}H]Dopamine ([^{3}H]DA; dihydroxyphenylethylamine, 3,4-[7-^{3}H]; specific activity, 28 Ci/mmol), and [^{3}H]5-hydroxytryptamine ([^{3}H]5-HT; hydroxytryptamine creatinine sulfate 5-[1,2-^{3}H(N)]; specific activity, 30 Ci/mmol) and Microscint 20 LSC-cocktail were purchased from PerkinElmer, Inc. (Boston, MA). [^{3}H]Dihydrotetrabenazine ([^{3}H]DTBZ; (±)alpha-[O-methyl-^{3}H]dihydrotetrabenazine; specific activity, 20 Ci/mmol) was obtained from American Radiolabled Chemicals, Inc. (St. Louis, MO). ATP-Mg^2, catechol, DA, disodiumethylenediamine tetraacetate (EDTA), ethylene glycol tetraacetate (EGTA), fluoxetine HCl, 1-(2-(bis-(4-fluorophenyl)methoxy)ethyl)-4-(3-

phenylpropyl)piperazine (GBR 12909), α-D-glucose, S-glycidol, R-glycidol, N-[2-hydroxyethyl]piperazine-N'-[2-ethanesulfonic acid] (HEPES), $MgSO_4$, pargyline HCl, polyethyleneimine (PEI), KOH, potassium tartrate and sucrose were purchased from Sigma-Aldrich, Inc. (St. Louis, MO). L-Ascorbic acid and $NaHCO_3$ were purchased from Aldrich Chemical Co. (Milwaukee, WI). Ammonium hydroxide, $CaCl_2$, diethyl ether, KCl, K_2PO_4, methylene chloride, methanol, $MgCl_2$, NaCl and NaH_2PO_4 were purchased from Fisher Scientific Co. (Pittsburgh, PA). Ethanol was purchased from Pharmco-AAPER Alcohol and Chemical Co., (Shelbyville, KY). Complete counting cocktail 3a70B was purchased from Research Products International Corp. (Mount Prospect, IL). (2R,3S,11bS)-2-Ethyl-3-isobutyl-9,10-dimethoxy-2,2,4,6,7,11b-hexahydro-1H-pyrido[2,1-a]isoquinolin-2-ol (Ro-4-1284) was a generous gift from Hoffman-LaRoche Inc. (Nutley, NJ).

IIc. General synthetic procedure for N-1,2-diol analogs. Based on computational modeling utilizing ACD/ADME algorithms (www.acdlabs.com), replacement of the N-methyl moiety on the central piperidine ring with a N-1,2-diol moiety was predicted to enhance water solubility. For example, a 365% increase in water solubility was predicted as a consequence of replacing the N-methyl group in para-methoxyphenyl lobelane (GZ-252C) with an *N*-1,2-diol moiety in GZ-793A (solubility of 2.0 and 7.3 mg/ml in water, respectively; structures in Fig. 19 and Nickell et al., 2011). Synthesis of (*R*)-3-(2,6-*cis*-diphenethylpiperidin-1-yl)propane-1,2-diol (GZ-745A), which contains a *N*-1,2(*R*)-dihydroxylpropyl group, and (*S*)-3-(2,6-*cis*-diphenethylpiperidin-1-yl)propane-1,2-

diol (GZ-745B), which contains a *N*-1,2(*S*)-dihydroxylpropyl group, was accomplished by reacting nor-lobelane with *S*-glycidol or *R*-glycidol in ethanol, respectively. The phenyl ring-modified nor-lobelane analogs were synthesized using previously reported methods (Zheng et al., 2005b), and the latter analogs served as intermediates for the synthesis of the current series of analogs via reaction with *S*-glycidol or *R*-glycidol in ethanol [i.e., (*R*)-3-[2,6-*cis*-di(3-methoxyphenethyl)piperidin-1-yl]propane-1,2-diol (GZ-790A), (*R*)-3-[2,6-*cis*-di(3-fluorophenethyl) piperidin-1-yl]propane-1,2-diol (GZ-791A), (*R*)-3-[2,6-*cis*-di(2-methoxyphenethyl) piperidin-1-yl]propane-1,2-diol (GZ-792A), GZ-793A, (*R*)-3-[2,6-*cis*-di(1-naphthylethyl)piperidin-1-yl]propane-1,2-diol (GZ-794A), (*R*)-3-[2,6-*cis*-di(2,4-dichlorophenethyl)piperidin-1-yl]propane-1,2-diol (GZ-795A), (*R*)-3-[2,6-*cis*-di(4-biphenylethyl)piperidin-1-yl]propane-1,2-diol (GZ-796A), and (*R*)-3-[2,6-*cis*-di(3,4-methylenedioxyphenethyl)piperidin-1-yl]propane-1,2-diol (GZ-797A), and the respective enantiomers (*S*)-3-[2,6-*cis*-di(3-methoxyphenethyl)piperidin-1-yl]propane-1,2-diol (GZ-790B), (*S*)-3-[2,6-*cis*-di(3-fluorophenethyl)piperidin-1-yl]propane-1,2-diol (GZ-791B), (*S*)-3-[2,6-*cis*-di(2-methoxyphenethyl)piperidin-1-yl]propane-1,2-diol (GZ-792B), (*S*)-3-[2,6-*cis*-di(4-methoxyphenethyl) piperidin-1-yl]propane-1,2-diol (GZ-793B), (*S*)-3-[2,6-*cis*-di(1-naphthylethyl)piperidin-1-yl]propane-1,2-diol (GZ-794B), (*S*)-3-[2,6-*cis*di(2,4-dichlorophenethyl)piperidin-1-yl]propane-1,2-diol (GZ-795B), (*S*)-3-[2,6-*cis*-di(4-biphenylethyl)piperidin-1-yl]propane-1,2-diol (GZ-796B), and (*S*)-3-[2,6-*cis*-di(3,4-methylenedioxyphenethyl)piperidin-1-yl]propane-1,2-diol (GZ-797B)]. The final products were purified by silica gel column chromatography [eluting with

methylene chloride/methanol/ammonium hydroxide, 30:1:0.2 (v/v/v)], followed by recrystallization from ethanol and diethyl ether after conversion into salt forms. Structures and purities of the analogs were determined by 1H-NMR, 13C-NMR, mass spectrometry, HPLC, and combustion analysis.

IId. Synaptosomal [^{3}H]DA and [^{3}H]5-HT uptake assays. Analog-induced inhibition of [^{3}H]DA and [^{3}H]5-HT uptake into rat striatal and hippocampal synaptosomes, respectively, was determined using modifications of a previously described method (Chapter 2, Horton et al., 2011a). Brain regions were homogenized in 20 ml of ice-cold 0.32 M sucrose solution containing 5 mM $NaHCO_3$ (pH 7.4) with 16 up-and-down strokes of a Teflon pestle homogenizer (clearance ~ 0.005”). Homogenates were centrifuged at 2,000 g for 10 min at 4 °C, and resulting supernatants centrifuged at 20,000 g for 17 min at 4 °C. Pellets were resuspended in 1.5 ml of Krebs’ buffer, containing: 125 mM NaCl, 5 mM KCl, 1.5 mM $MgSO_4$, 1.25 mM $CaCl_2$, 1.5 mM KH_2PO_4, 10 mM α-D-glucose, 25 mM HEPES, 0.1 mM EDTA, with 0.1 mM pargyline and 0.1 mM ascorbic acid, saturated with 95% O_2 /5% CO_2, pH 7.4). Synaptosomal suspensions (20 µg protein/50 µl) were added to duplicate tubes containing 50 µl analog (7-9 concentrations, 0.1 nM – 1 mM, final concentration in assay buffer) and 350 µl of buffer and incubated at 34 °C for 5 min in a total volume of 450 µl. Samples were placed on ice and 50 µl of [^{3}H]DA or [^{3}H]5-HT (10 nM; final concentration) was added to each tube for a final volume of 500 µl. Reactions proceeded for 10 min at 34°C and were terminated by the addition of 3 ml of ice-cold Krebs’ buffer. Nonspecific [^{3}H]DA and [^{3}H]5-HT uptake were determined in the presence of 10

µM GBR 12909 and 10 µM fluoxetine, respectively. Samples were rapidly filtered through Whatman GF/B filters using a cell harvester (MP-43RS; Brandel Inc.). Filters were washed 3 times with 4 ml of ice-cold Krebs' buffer containing catechol (1 mM). Complete counting cocktail was added to the filters and radioactivity determined by liquid scintillation spectrometry (B1600 TR scintillation counter; PerkinElmer, Inc.).

IIe. [^{3}H]DTBZ vesicular binding assays. Analog-induced inhibition of [^{3}H]DTBZ binding, a high affinity ligand for VMAT2, was determined using modifications of a previously published method (Chapter 2, Horton et al., 2011a). Rat whole brain (excluding cerebellum) was homogenized in 20 ml of ice-cold 0.32 M sucrose solution with 10 up-and-down strokes of a Teflon pestle homogenizer (clearance ~ 0.008"). Homogenates were centrifuged at 1,000 g for 12 min at 4 °C and resulting supernatants were centrifuged at 22,000 g for 10 min at 4 °C. Resulting pellets were osmotically lyzed by incubation in 18 ml of cold water for 5 min. Osmolarity was restored by adding 2 ml of 25 mM HEPES and 100 mM potassium tartrate solution. Samples were centrifuged (20,000 g for 20 min at 4°C), and then 1 mM $MgSO_4$ solution was added to the supernatants. Samples were centrifuged at 100,000 g for 45 min at 4°C. Pellets were resuspended in cold assay buffer, containing 25 mM HEPES, 100 mM potassium tartrate, 5 mM $MgSO_4$, 0.1 mM EDTA, and 0.05 mM EGTA, pH 7.5. Assays were performed in duplicate using 96-well plates. Vesicular suspensions (15 µg protein/100 µl) were added to wells containing 50 µl analog (7-9 concentrations, 0.01 nM – 0.1 mM, final concentration in assay buffer), 50 µl of buffer, and 50 µl

of [^{3}H]DTBZ (3 nM; final concentration) for a final volume of 250 µl and incubated for 1 hr at room temperature. Nonspecific binding was determined in the presence of 50 µl of 20 µM Ro-4-1284. Reactions were terminated by filtration onto Unifilter-96 GF/B filter plates (presoaked in 0.5% PEI). Filters were washed 3 times with 350 µl of ice-cold buffer containing: 25 mM HEPES, 100 mM potassium-tartrate, 5 mM $MgSO_4$, and 10 mM NaCl, pH 7.5. Filter plates were dried, bottom-sealed and each well filled with 40 µl of scintillation cocktail (MicroScint 20; PerkinElmer, Inc.). Radioactivity on the filters was determined by liquid scintillation spectrometry.

IIf. Vesicular [^{3}H]DA uptake assay. Analog-induced inhibition of [^{3}H]DA uptake into rat striatal vesicles was determined using modifications of a previously published method (Chapter 2, Horton et al., 2011a). Striata were homogenized in 14 ml of ice-cold 0.32 M sucrose solution containing 5 mM $NaHCO_3$ (pH 7.4) with 10 up-and-down strokes of a Teflon pestle (clearance ~ 0.008”). Homogenates were centrifuged at 2,000 g for 10 min at 4 °C and resulting supernatants centrifuged at 10,000 g for 30 min at 4 °C. Pellets were resuspended in 2.0 ml of 0.32 M sucrose and were transferred to tubes containing 7 ml of milliQ water and homogenized with 5 up-and-down strokes using the above homogenizer. Homogenates were transferred to tubes containing 900 µl of 0.25 M HEPES and 900 µl of 1.0 M potassium tartrate solution and centrifuged at 20,000 g for 20 min at 4 ºC. Resulting supernatants were centrifuged at 55,000 g for 60 min at 4 ºC. Subsequently, 100 µl of 1 mM $MgSO_4$, 100 µl of 0.25 M HEPES and 100 µl of 1.0 M potassium tartrate were

added to the supernatant and centrifuged at 100,000 g for 45 min at 4 ºC. Final pellets were resuspended in assay buffer, containing 25 mM HEPES, 100 mM potassium tartrate, 50 µM EGTA, 100 µM EDTA, and 1.7 mM ascorbic acid, 2 mM ATP-Mg^{2+}, pH 7.4. Vesicular suspensions (10 µg protein/100 µl) were added to duplicate tubes containing 50 µl analog (7-9 concentrations, 1 nM – 0.1 mM, final concentration in assay buffer), 300 µl of buffer, and 50 µl of [^{3}H]DA (0.1 µM; final concentration) for a final volume of 500 µl and incubated for 8 min at 34 °C. Nonspecific [^{3}H]DA uptake was determined in the presence of 10 µM Ro-4-1284. Samples were filtered rapidly through Whatman GF/B filters using the cell harvester and washed 3 times with assay buffer containing 2 mM $MgSO_4$ in the absence of ATP. Radioactivity retained by the filters was determined as previously described.

IIg. Kinetics of vesicular [^{3}H]DA uptake. Vesiclar suspensions were prepared as described above except that striata were pooled from 2 rats. Vesicular suspensions (20 µg protein/50 µl) were added to duplicate tubes containing 25 µl analog (final concentration approximating the Ki from inhibition curves for each analog), 150 µl of buffer, and 25 µl of various concentrations of [^{3}H]DA (1 nM – 5 µM; final concentration) for a final volume of 250 µl, and incubated for 8 min at 34 °C. Nonspecific [^{3}H]DA uptake was determined using 10 µM Ro4-1284. Samples were processed as previously described.

IIh. Endogenous DA release assay. HPLC-EC determination of DA release was performed by Kiran Siripurapu, Ph.D.. Rat coronal striatal slices of 0.5 mm thickness were prepared and incubated in Krebs' buffer, containing 118

mM NaCl, 4.7 mM KCl, 1.2 mM $MgCl_2$, 1.0 mM NaH_2PO_4, 1.3 mM $CaCl_2$, 11.1 mM α-D-glucose, 25 mM $NaHCO_3$, 0.11 mM L-ascorbic acid and 0.004 mM EDTA, pH 7.4, saturated with 95%O_2/5%CO_2 at 34 ºC in a metabolic shaker for 60 min (Chapter 2, Horton et al., 2011a). Each slice was transferred to a glass superfusion chamber and superfused with Krebs' buffer at 1 ml/min for 60 min before sample collection. Two basal samples (1ml) were collected at the 5-min and 10-min time points. To determine the ability of analog to evoke DA overflow, each slice was superfused for 30 min in the absence or presence of a single concentration of analog (0.3 -10 μM); analog was included in the buffer until the end of the experiment. METH (5 μM) was added to the buffer after 30 min of superfusion, and slices were superfused for an additional 15 min with METH, followed by 20 min of superfusion in the absence of METH. In each experiment, a striatal slice was superfused for 90 min in the absence of both analog and METH, serving as the buffer control condition. In each experiment, duplicate slices were superfused with METH in the absence of analog, serving as the METH control condition. The METH concentration was selected based on pilot concentration-response data showing a reliable response of sufficient magnitude to allow evaluation of analog-induced inhibition. Each superfusate sample (1 ml) was collected into tubes containing 100 μl of 0.1 M perchloric acid. Prior to HPLC-EC analysis, ascorbate oxidase (20 μl, 168 U/mg reconstituted to 81 U/ml) was added to 500 μl of each sample and vortexed for 30 s, and 100 μl injected onto the HPLC-EC. The HPLC-EC consisted of a pump (model 126, Beckman Coulter, Inc, Fullerton, CA) and autosampler (model 508 Beckman Coulter, Inc),

an ODS Ultrasphere C18 reverse-phase 80 × 4.6 mm, 3-µm column, a Coulometric-II detector with guard cell (model 5020) maintained at +0.60 V, and an analytical cell (model 5011) maintained at potentials E1 = -0.05 V and E2 = +0.32 V (ESA Inc., Chelmsford, MA). HPLC mobile phase (flow rate, 1.5 ml/min) was 0.07 M citrate/0.1 M acetate buffer pH 4, containing 175 mg/l octylsulfonic acid sodium salt, 650 mg/l NaCl and 7% methanol. Separations were performed at room temperature, and 5-6 min were required to process each sample. Retention times of DA standards were used to identify respective peaks. Peak heights were used to quantify the detected amounts of analyte based on standard curves. Detection limit for DA was 1-2 pg/100 µl.

IIi. Data analysis. Specific [^{3}H]DTBZ binding and specific [^{3}H]DA and [^{3}H]5-HT uptake were determined by subtracting the nonspecific binding or uptake from the total binding or uptake, respectively. Analog concentrations that produced 50% inhibition of the specific binding or uptake (IC_{50} values) were determined from the concentration-effect curves via an iterative curve-fitting program (Prism 5.0; GraphPad Software Inc., San Diego, CA). Inhibition constants (Ki values) were determined using the Cheng-Prusoff equation. For kinetic analyses, Km and Vmax were determined using one-site binding curves. Paired two-tailed t-tests were performed on the arithmetic Vmax and the log Km values to determine significant differences between analog and control (absence of analog). Pearson's correlation analysis determined the relationship between affinity for the [^{3}H]DTBZ binding site and vesicular [^{3}H]DA uptake.

For endogenous neurotransmitter release assays, fractional release is defined as the DA concentration in each sample divided by the slice weight. Basal DA outflow was calculated as the average fractional release of the two basal samples collected 10 min prior to addition of analog to the buffer. Intrinsic DA overflow was calculated as the sum of the increases in fractional release above basal outflow during superfusion with analog alone (in the absence of METH). One-way repeated-measures ANOVAs determined concentration-dependent effects on DA overflow. Peak DA fractional release evoked by METH was determined from the time course. Analog-induced inhibition of METH-evoked fractional DA release was evaluated using one-way repeated-measures ANOVA. When appropriate, Dunnett's post hoc test determined concentrations of analog that significantly decreased the effect of METH. Log IC_{50} value for each analog was generated using an iterative nonlinear least squares curve-fitting program (PRISM version 5.0). Statistical significance was defined as $p < 0.05$.

III. Results

IIIa. N-1,2-Diol analogs inhibit [^{3}H]DA uptake at DAT. Concentration-response curves for GBR 12909, cocaine, lobeline, lobelane, and the N-1,2-diol analogs to inhibit [^{3}H]DA uptake into striatal synaptosomes are illustrated in Fig. 20. Ki values for GBR 12909, cocaine, lobeline, and lobelane (Table 2) are consistent with previously reported findings (Reith et al., 1994; Han and Gu, 2006; Nickell et al., 2011). Replacement of the N-methyl in lobelane with a N-1,2-diol moiety generally afforded analogs that were 1 to 10-fold less potent (Ki = 1.43-9.5 μM) at DAT compared to lobelane. Alteration of the configuration of the

N-1,2-diol and incorporation of phenyl ring substitutents did not alter affinity for DAT. Of note, lead analogs, GZ-793A (4-methoxyphenyl-N-1,2(R)-diol analog) and GZ-794A (1-naphthalene-N-1,2(R)-diol analog) inhibited [^{3}H]DA uptake with potencies not different from lobelane.

IIIb. N-1,2-Diol analogs inhibit [^{3}H]5-HT uptake at SERT.

Concentration-response curves for fluoxetine, lobeline, lobelane, and the N-1,2-diol analogs to inhibit [^{3}H]5-HT uptake into hippocampal synaptosomes are illustrated in Fig. 21. Ki values for fluoxetine, lobeline and lobelane (Table 2) are consistent with previously reported findings (Owens, 2001; Miller et al., 2004). Generally, replacement of the N-methyl moiety with the N-1,2-diol moiety, alteration of the configuration of the N-1,2-diol and incorporation of phenyl ring substitutents did not alter affinity for SERT (Ki = 0.94 -11.0 μM vs 3.6 μM). Exceptions include the 1-naphthalene enantiomers, GZ-794A and GZ-794B (Ki = 0.31 and 0.16 μM, respectively), which afforded a 10-20-fold increase in potency compared with lobelane. Of note, the lead compound, GZ-793A, exhibited potency not different from lobelane.

IIIc. N-1,2-Diol analogs inhibit [^{3}H]DTBZ binding at VMAT2.

Concentration-response curves for Ro-4-1284, lobeline, lobelane, and the N-1,2-diol analogs to inhibit [^{3}H]DTBZ binding to whole brain membranes are illustrated in Fig. 22, and Ki values are provided in Table 2. The Ki value for Ro-4-1284 to inhibit [^{3}H]DTBZ binding is consistent with previously reported results (Cesura et al., 1990). Generally, replacement of the N-methyl moiety with the N-1,2-diol moiety, alteration of the configuration of the N-1,2-diol and incorporation of

phenyl ring substitutents did not alter affinity for the DTBZ site on VMAT2 (Ki = 0.46-5.6 μM vs 0.97 μM). Of note, GZ-794A (1-naphthalene N-1,2(R)-diol analog) exhibited potency not different from lobelane. Exceptions include the 4-methoxyphenyl enantiomers (GZ-793A and GZ-793B) and the 2,4-dichlorophenyl enantiomers (GZ-795A and GZ-795B), which exhibited 8-10-fold lower potency compared with lobelane. Also, GZ-796A and GZ-796B, the 4-biphenyl enantiomers, exhibited 90-100-fold lower potency than lobelane.

IIId. N-1,2-Diol analogs inhibit [^{3}H]DA uptake at VMAT2.

Concentration-response curves for Ro-4-1284, lobeline, lobelane, and the N-1,2-diol analogs to inhibit [^{3}H]DA uptake into striatal vesicles are illustrated in Fig. 23. Ki values for Ro-4-1284, lobeline and lobelane (Table 2) are consistent with previous reports (Nickell et al., 2011). Replacement of the N-methyl moiety with the N-1,2-diol and incorporation of the phenyl ring substituents resulted in a 5-45 fold lower potency inhibiting [^{3}H]DA uptake at VMAT2 compared to lobelane. Exceptions include GZ-793A (4-methoxyphenyl N-1,2(R)-diol analog) and GZ-794A (1-naphthalene N-1,2(R)-diol analog), which were equipotent with lobelane. Generally, the R-configuration of the N-1,2-diol analogs was more potent than the S-configuration inhibiting VMAT2 function. Correlation analysis revealed no correlation between the Ki values for inhibiting [^{3}H]DA uptake at VMAT2 and [^{3}H]DTBZ binding at VMAT2 (Pearson's correlation coefficient $r = 0.37$, $p = 0.13$, Fig. 24).

IIIe. N-1,2-Diol analogs inhibit [^{3}H]DA uptake at VMAT2 competitively.

To elucidate the mechanism of inhibition at VMAT2, i.e.

competitive or noncompetitive, kinetic analyses of [^{3}H]DA uptake at VMAT2 were conducted using the most potent analog inhibitors of VMAT2 function, i.e., GZ-793A and GZ-794A. GZ-793A had relatively low affinity for the [^{3}H]DTBZ binding site, whereas GZ-794A had high affinity for this site. For comparison, kinetic analysis of GZ-796A was performed to evaluate the mechanism of inhibition of an analog with moderate potency inhibiting DA uptake at VMAT2, but low potency at the [^{3}H]DTBZ binding site. Results show an increased Km value with no change in Vmax for each analog compared to control (Fig. 25), indicating a competitive mechanism of action.

IIIf. N-1,2-Diol analogs inhibit METH-evoked endogenous DA release. In the absence of METH, GZ-793A, GZ-794A and GZ-796A did not evoke DA overflow above basal outflow (one-way repeated measures ANOVA: $F_{5,29} = 0.31$, $F_{5,29} = 1.32$, $F_{5,29} = 0.48$, respectively, ps > 0.05). Importantly, GZ-793A, GZ-794A and GZ-796A inhibited METH-evoked DA release in a concentration-dependent manner (Fig. 26; repeated measures one-way ANOVAs: $F_{5,29} = 4.55$, $F_{5,29} = 3.16$, and $F_{5,29} = 3.03$, respectively, ps < 0.05). Even though GZ-793A and GZ-794A inhibited DA uptake at VMAT2 equipotently, GZ-793A was 25-fold less potent than GZ-794A inhibiting METH-evoked DA release. Further, GZ-793A exhibited ~35% greater inhibitory activity compared with GZ-794A. Although GZ-796A had 25-fold lower potency than either GZ-793A or GZ-794A inhibiting DA uptake at VMAT2, GZ-796A was equipotent with GZ-794A and 10-fold less potent than GZ-793A inhibiting METH-evoked DA

release. Inhibitory activity of GZ-796A (I_{max} = 56%) was not different than that exhibited by GZ-794A.

IV. Discussion

The current study reports on an iterative process of drug discovery aimed at identifying a novel lead candidate for the treatment of METH abuse. Rationale for VMAT2 as the pharmacological target evolved from the observation that METH interacts with this presynaptic protein to inhibit DA uptake into presynaptic vesicles. Inhibition of VMAT2 increases cytosolic DA levels available for METH-induced reverse transport by DAT, leading to an increase in extracellular DA (Sulzer, 2005). Through an interaction with VMAT2, lobeline inhibits the neurochemical and behavioral effects of METH (Teng et al., 1997, 1998; Miller et al., 2001, Harrod et al., 2001; Dwoskin and Crooks, 2002; Nickell et al., 2010). Lobelane, a lobeline analog with greater selectivity for VMAT2, decreased both METH-evoked DA release (IC_{50} = 0.65 µM; I_{max} = 73.2%; same experimental conditions as the current work) and METH self-administration (Zheng et al., 2005a; Neugebauer et al., 2007; Beckmann et al., 2010; Nickell et al., 2010, 2011). Unfortunately, further development of lobelane as an effective pharmacotherapy was hindered by unacceptable drug-likeness properties. The current study identified novel analogs of lobelane incorporating a N-1,2-diol moiety into the molecule to specifically enhance its drug-likeness properties. GZ-793A emerged as a potent, VMAT2-selective, drug-like lead candidate for the treatment of METH abuse.

The current SAR provided several insights regarding the optimization of the pharmacophore for inhibition of VMAT2 function (Tables 2 and 3). Merely replacing the N-methyl group of lobelane with a N-1,2(R)-diol moiety (GZ-745A) resulted in a 4-fold decrease in VMAT2 inhibitory potency. Also, the specific configuration of the N-1,2-diol moiety is a factor determining potency to inhibit DA uptake at VMAT2. The R enantiomer of N-1,2-diol analogs bearing no phenyl substituents, and those containing 3-flourophenyl, 3-methoxyphenyl, 4-methoxyphenyl or 3,4-methylenedioxyphenyl moieties exhibited 4-6-fold higher inhibitory potency compared to the corresponding S enantiomer. These results indicate that the pharmacophore for inhibition of VMAT2 function has a configurational restriction at the chiral N-1,2-diol moiety in the current series of analogs. Furthermore, N-1,2-diol analogs of lobelane with 3-fluoro, 2,4-dichloro, 2-methoxy, 3-methoxy, or 3,4-methylenedioxy substituents in both phenyl rings, or in which the phenyl rings were replaced with 1-naphthalene or 4-biphenyl rings, exhibited a 4 to 34-fold lower potency compared to lobelane, and a 3 to 66-fold lower potency compared to the corresponding N-methyl substituted analog. Thus, although N-methyl analogs with substituents on the phenyl rings retained potency as inhibitors of VMAT2 relative to lobelane, introduction of these substituents into the phenyl rings in the N-1,2-diol analogs resulted in reduced potency. Exceptions include the two lead N-1,2(R)-diol analogs, GZ-793A (4-methoxyphenyl analog) and GZ-794A (1-naphthalene analog), which inhibited VMAT2 with potencies not different from either lobelane or the corresponding N-methyl analogs. These results indicate that for GZ-793A and GZ794A, structural

modifications which enhanced drug-likeness did not alter VMAT2 inhibitory potency.

The use of [^{3}H]DTBZ to probe interaction with VMAT2 has been established in rodent models and in evaluation of patients with specific pathologies (Lehericy et al., 1994; Kilbourn et al., 1995). However, studies have reported that inhibition of VMAT2 function does not correlate with affinity for the [^{3}H]DTBZ binding site on VMAT2 (Chapter 2, Horton et al., 2011a; Nickell et al., 2011). These studies evaluated the SAR for conformationally restricted MTD analogs and for a series of phenyl ring substituted lobelane analogs. Results obtained from the current series of novel N-1,2-diol analogs are consistent with the latter observations, i.e., a correlation was not observed between VMAT2 binding and uptake. Together, the SAR indicates that [^{3}H]DTBZ binding site is more tolerant of structural alterations relative to the uptake site on VMAT2. One analog in the current series (GZ-796A, the 4-biphenyl N-1,2(R)-diol analog) inhibited DA uptake at VMAT2, but did not inhibit [^{3}H]DTBZ binding, consistent with previous results that 4-biphenyl nor-lobelane as well as several extensively aromatized N-methyl lobelane analogs inhibited VMAT2 function, but not [^{3}H]DTBZ binding (Nickell et al., 2011). Thus, analogs in these structural series appear to interact with two distinct sites on VMAT2.

Although VMAT2 and plasma membrane transporters (e.g., DAT and SERT) belong to two different transporter families and exhibit little structural homology (Liu and Edwards, 1997), these proteins are promiscuous and translocate DA and 5-HT (Norrholm et al., 2007), suggesting that there are

similarities in the substrate sites between these transporters. Since the parent compound lobelane exhibited only 15-fold selectivity for VMAT2 over DAT and SERT, it was imperative to assess interaction of the N-1,2-diol analogs with DAT and SERT to ascertain selectivity for VMAT2. Only the 1-naphthalene analogs exhibited a 10-fold higher potency inhibiting SERT compared with lobelane, whereas the remainder of the series of N-1,2-diol analogs exhibited affinity not different from lobelane at both DAT and SERT. Configuration of the N-1,2-diol moiety influenced potency to inhibit VMAT2 function, but did not influence potency at DAT and SERT.

The next critical step in our drug discovery approach is to determine the ability of the lead compounds to inhibit the neurochemical effects of METH. Representative analogs of the N-1,2(R)-diol series were evaluated for their ability to decrease METH-evoked DA release in striatum. The leads, GZ-793A and GZ-794A, which exhibited the highest potency for inhibition of VMAT2 function, and GZ-796A, which inhibited VMAT2 function but not [^{3}H]DTBZ binding, were chosen for evaluation. All three N-1,2(R)-diol analogs did not evoke DA overflow in the absence of METH (had no intrinsic activity) and inhibited METH-evoked DA release in a concentration-dependent manner. These preclinical results support the further evaluation of these analogs for development as potential pharmacotherapies for METH abuse.

The current results suggest that GZ-793A, GZ-794A and GZ-796A interact with VMAT2 to inhibit the pharmacological effects of METH. However, the order of potency for inhibition of VMAT2 function (GZ-793A = GZ-794A > GZ-796A)

was different from the order of potency for inhibition of METH-evoked DA release (GZ-794A > GZ-796A > GZ-793A). Furthermore, correlation analysis with a limited number of structurally-related compounds (GZ-793A, GZ-794A, GZ-796, lobelane, lobeline, MTD, UKCP-110; , *cis*-2,5-di-(2-phenethyl)-pyrrolidine hydrochloride and UKMH-106) for which data are available from both assays (current study; Miller et al., 2001, 2004; Nickell et al., 2010; Beckmann et al., 2010; Chapter 2, Horton et al., 2011a) reveal a lack of correlation between affinity for inhibition of DA uptake at VMAT2 and ability to inhibit METH-evoked DA release. There are several alternative explanations for this lack of correlation. First, variability in the physicochemical properties between the analogs may explain the lack of correlation between affinity for VMAT2 and efficacy for inhibition of METH-evoked DA release from slices. Such physicochemical properties are expected to differentially affect the ability of the analogs to distribute across cell membranes to reach its intracellular target. Further, VMAT2 has greater accessibility in the vesicular preparation compared to the more intact slice preparation in which cell membranes impede analog accessibility.

Another possibility is that the analogs may be interacting with an alternate site on VMAT2 other than the DA uptake site to inhibit METH-evoked DA release. Research demonstrates that the extracellular and intracellular faces of DAT expresses distinct sites for DA translocation that are regulated differentially (Gnegy, 2003), which provides precedence for alternate recognition sites on VMAT2 that mediate uptake of DA and METH-evoked release of DA from the vesicle. Thus, the analogs may have different affinities for these alternative sites

on VMAT2 which may explain the lack of correlation between affinity for VMAT2 and efficacy for inhibition of METH-evoked DA release from slices.

Further, the analogs may be interacting with an alternative target other than VMAT2, i.e., nicotinic receptors, to inhibit METH-evoked DA release. Lobeline interacts with both α4β2* and α7* nicotinic receptors; however, chemical defunctionalization (i.e., removal of the keto and hydroxyl groups from the phenyl ring side chains) of the lobeline molecule (affording analogs such as lobelane and the N-1,2-diol analogs) exhibit little or no affinity for α4β2* and α7* nicotinic receptors (Miller et al., 2001; Zheng et al., 2005a; Beckmann et al., 2010; Chapter 2, Horton et al., 2011a). Further, GZ-793A does not inhibit nicotinic receptors mediating nicotine-evoked DA release (unpublished observations). An alternative potential site of analog interaction is DAT. GZ-793A, GZ-794A and GZ-796A exhibit affinity for DAT within the concentration range that inhibits METH-evoked DA release. However, the observation that GZ-793A is not self-administered in rats diminishes support for an interaction with DAT as its mechanism of action (Beckman et al., 2011). Finally, the observation that these analogs are 10 to 50-fold more potent at VMAT2 than at DAT provides support for VMAT2 as the pharmacological target.

Of the series, GZ-793A, the 4-methoxyphenyl N-1,2(R)-diol analog, exhibited the best profile with the greatest selectivity (50-fold) for VMAT2 and maximal inhibition (86%) of the effect of METH. The N-1,2(R)-diol moiety in GZ-793A improved water solubility compared with its N-methyl counterpart, GZ-252C. Importantly, GZ-793A has been shown recently to decrease METH self-

administration and METH conditioned-place preference, without altering food maintained responding (Beckmann et al., 2011), providing preclinical data which support its potential utility as a novel pharmacotherapy for METH abuse. Results from these preclinical studies provide support for GZ-793A as a lead compound in the search for pharmacotherapies to treat METH abuse.

Table 2. Affinity values (K_i) of N-1,2-diol analogs, lobeline, lobelane and standard compounds for DAT, SERT, and VMAT2 binding and function

Compound	DAT [^{3}H]DA Uptake Ki ± SEM (μM)	SERT [^{3}H]5-HT Uptake Ki ± SEM (μM)	VMAT2 [^{3}H]DTBZ Binding Ki ± SEM (μM)	VMAT2 [^{3}H]DA Uptake Ki ± SEM (μM)
Standards				
GBR 12909	0.0009 ± 0.0001 [a]	ND[b]	ND[b]	ND[b]
Cocaine	0.48 ± 0.07	ND	ND	ND
Fluoxetine	ND[b]	0.007 ± 0.0001 [a]	ND	ND
Ro-4-1284	0.04 ± 0.005	0.02 ± 0.003	0.03 ± 0.003 [a]	0.02 ± 0.002 [a]
Lobeline, lobelane and N-1,2-diol analogs				
Lobeline	28.2 ± 6.73	46.8 ± 3.70	2.04 ± 0.26[c]	1.27 ± 0.46
Lobelane	1.05 ± 0.03	3.60 ± 0.35	0.97 ± 0.19[c]	0.067 ± 0.007
GZ-745A	0.60 ± 0.06	8.43 ± 2.80	0.56 ± 0.08	0.19 ± 0.05
GZ-745B	1.08 ± 0.12	11.0 ± 3.12	1.28 ± 0.13	0.86 ± 0.12
N-1,2-Diol analogs containing 1-naphthyl or 4-biphenyl substituents				
GZ-794A	1.43 ± 0.14	0.31 ± 0.08	0.31 ± 0.07	0.033 ± 0.002
GZ-794B	1.57 ± 0.16	0.16 ± 0.04	0.13 ± 0.01	0.08 ± 0.01
GZ-796A	8.33 ± 1.46	5.30 ± 0.96	>100	0.79 ± 0.23
GZ-796B	3.43 ± 0.63	2.55 ± 0.77	90.2 ± 9.70	2.25 ± 1.30
N-1,2-Diol analogs containing aromatic methoxy or methylene-dioxy substituents				
GZ-790A	3.80 ± 0.69	3.14 ± 1.18	0.46 ± 0.22	0.14 ± 0.02
GZ-790B	6.67 ± 2.15	8.03 ± 2.30	2.73 ± 0.68	0.52 ± 0.04
GZ-792A	2.90 ± 0.23	1.33 ± 0.46	1.04 ± 0.73	0.49 ± 0.06
GZ-792B	4.77 ± 1.03	0.94 ± 0.14	1.87 ± 0.69	0.79 ± 0.08
GZ-793A	1.44 ± 0.27	9.36 ± 2.74	8.29 ± 2.79	0.029 ± 0.008
GZ-793B	3.40 ± 0.82	10.4 ± 2.75	7.74 ± 2.34	0.18 ± 0.04
GZ-797A	2.46 ± 0.16	2.10 ± 0.70	1.30 ± 0.05	0.16 ± 0.04
GZ-797B	2.21 ± 0.31	2.63 ± 0.60	5.61 ± 0.62	0.76 ± 0.04
N-1,2-Diol analogs containing aromatic halogeno substituents				

GZ-791A	**0.25 ± 0.07**	**1.32 ± 0.46**	**1.00 ± 0.16**	**0.19 ± 0.06**
GZ-791B	**0.62 ± 0.05**	**2.87 ± 0.50**	**1.08 ± 0.38**	**1.03 ± 0.16**
GZ-795A	**3.87 ± 0.89**	**2.15 ± 0.38**	**10.4 ± 0.65**	**0.14 ± 0.04**
GZ-795B	**9.50 ± 2.53**	**1.86 ± 0.39**	**13.9 ± 0.38**	**0.09 ± 0.04**

[a] n = 3-4 rats; [b]ND, not determined; [c] data for [^{3}H]DTBZ binding for lobeline and lobelane taken from Nickell et al., 2010

Table 3. Summary of comparisons between phenyl ring substituted N-1,2-diol and respective N-methyl analog.

Compound	Phenyl Ring Substituent	Configuration of the N-1,2-diol	VMAT2 [^{3}H]DA Uptake (Ki; µM)	Selectivity for VMAT over DAT or SERT	N-Methyl Analog	VMAT2 [^{3}H]DA Uptake (Ki; µM)	Ratio of VMAT2 Uptake for the N-1,2-diol relative to the N-methyl analog	Ratio of VMAT2 Uptake for the N-1,2-diol relative to lobelane
Lobelane	NA[a]	NA[a]	0.067	15.6	NA[a]	NA[a]	NA[a]	NA[a]
GZ-745A	No Change	R	0.19	3.16	Lobelane	0.067	2.84	2.84
GZ-745B	No Change	S	0.86	1.26			12.8	12.8
GZ-794A	Naphthalene	R	0.033	9.39	GZ-258C[b]	0.091[b]	0.36	0.49
GZ-794B	Naphthalene	S	0.080	2.00			0.88	1.19
GZ-796A	Biphenyl	R	0.79	6.70	GZ-272C[b]	0.034[b]	23.2	11.8
GZ-796B	Biphenyl	S	2.25	1.13			66.2	33.6
GZ-790A	3-Methoxy	R	0.14	22.4	GZ-261C[b]	0.030[b]	4.67	2.09
GZ-790B	3-Methoxy	S	0.52	12.8			17.3	7.76
GZ-792A	2-Methoxy	R	0.19	2.71	GZ-273C[b]	0.026[b]	7.31	2.84
GZ-792B	2-Methoxy	S	0.79	1.19			30.4	11.8
GZ-793A	4-Methoxy	R	0.029	49.7	GZ-252C[b]	0.015[b]	1.93	0.43
GZ-793B	4-Methoxy	S	0.18	18.9			12	2.69
GZ-797A	3,4-Methylene Dioxy	R	0.16	13.1	GZ-250C[b]	0.043[b]	3.72	2.39
GZ-797B	3,4-Methylene Dioxy	S	0.76	2.90			17.7	11.3
GZ-791A	3-Flouro	R	0.19	1.32	GZ-275C[b]	0.093[b]	2.04	2.84
GZ-791B	3-Flouro	S	1.03	0.60			11.1	15.4
GZ-795A	2,4-Dichloro	R	0.14	15.4	GZ-260C[b]	0.016[b]	8.75	2.09
GZ-795B	2,4-Dichloro	S	0.090	20.7			5.63	1.34

[a] NA, Not Applicable; [b] data taken from Nickell et al., 2011; GZ-250C, 2,6-bis(2-(3,4-methylenedioxyphenyl)ethyl)-1-methylpiperidine hydrochloride;GZ-252C, paramethoxy-phenyl lobelane or 2,6-bis(2-(4-methoxyphenyl)ethyl)-1-methylpiperidine hydrochloride; GZ-260C, 2,6-bis(2-(2,4-dichlorophenyl)ethyl)-1-methylpiperidine hydrochloride; GZ-261C, 2,6-bis(2-(3-methoxyphenyl)ethyl)-1-methylpiperidine hydrochloride; GZ-272C, 2,6-bis(2-(biphenyl-4-yl)ethyl)-1-methylpiperidine hydrochloride; GZ-273C, 2,6-bis(2-(2-methoxyphenyl)ethyl)-1-methylpiperidine hydrochloride; GZ-275C, 2,6-bis(2-(3-fluorophenyl)ethyl)-1-methylpiperidine hydrochloride

.

Fig. 19. Chemical structures of lobeline, lobelane and N-1,2-diol analogs.

For clarity of presentation, compounds are grouped according to structural similarity of substituent additions to the phenyl rings: lobeline, lobelane and N-1,2-diol; N-1,2-diol analogs containing 1-naphthyl or 4-biphenyl substituents; N-1,2-diol analogs containing aromatic methoxy or methylenedioxy substituents; N-1,2-diol analogs containing aromatic halogeno substituents.

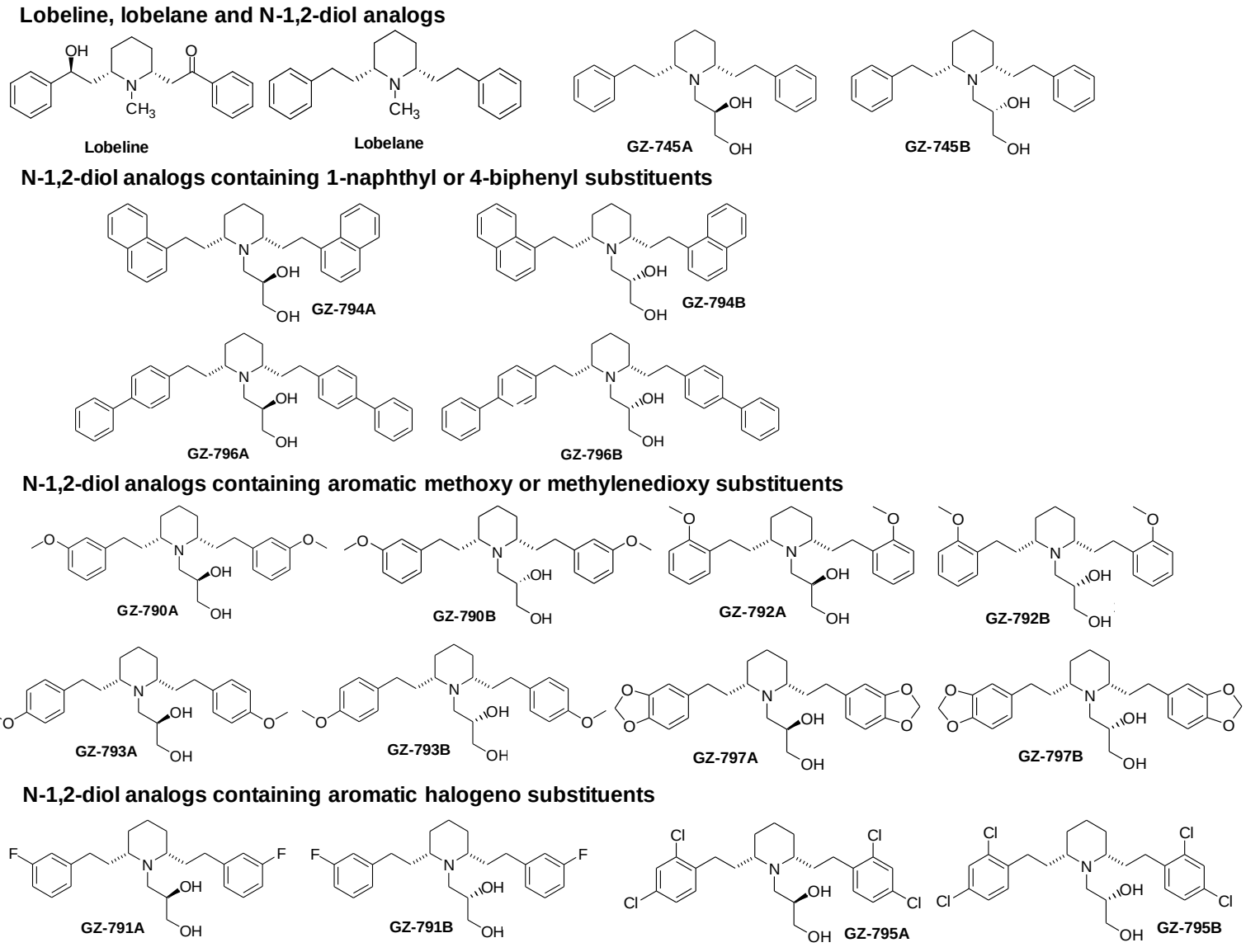

Fig. 20. N-1,2-Diol analogs inhibit [^{3}H]DA uptake into rat striatal synaptosomes. For clarity of presentation, compounds are grouped according to structural similarity of substituent additions to the phenyl rings: standards, lobeline, lobelane and N-1,2-diol analogs (top left panel), N-1,2-diol analogs containing 1-naphthyl or 4-biphenyl substituents (top right panel), N-1,2-diol analogs containing aromatic methoxy or methylenedioxy substituents (bottom left panel), or N-1,2-diol analogs containing aromatic halogeno substituents (bottom right panel). Nonspecific [^{3}H]DA uptake was determined in the presence of 10 μM GBR 12909. Control (CON) represents specific [^{3}H]DA uptake in the absence of analog (19.3 ± 0.94 pmol/mg/min). Legend provides compounds in order from highest to lowest affinity. n = 4 rats/analog.

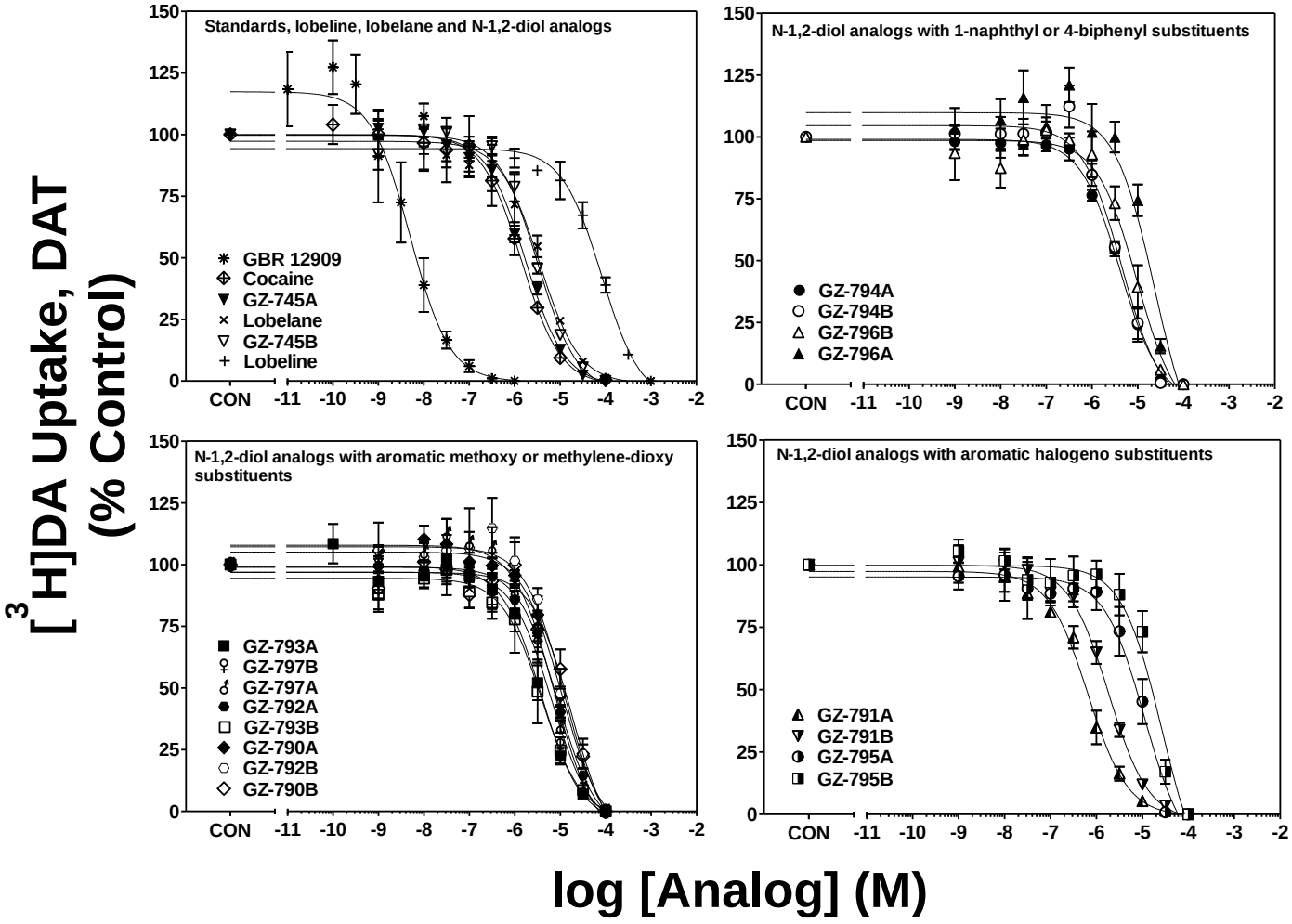
[3H]DA Uptake, DAT (% Control)
Standards, lobeline, lobelane and N-1,2-diol analogs
GBR 12909
Cocaine
GZ-745A
Lobelane
GZ-745B
Lobeline
N-1,2-diol analogs with 1-naphthyl or 4-biphenyl substituents
GZ-794A
GZ-794B
GZ-796B
GZ-796A
N-1,2-diol analogs with aromatic methoxy or methylene-dioxy substituents
GZ-793A
GZ-797B
GZ-797A
GZ-792A
GZ-793B
GZ-790A
GZ-792B
GZ-790B
N-1,2-diol analogs with aromatic halogeno substituents
GZ-791A
GZ-791B
GZ-795A
GZ-795B
CON
-11
-10
-9
-8
-7
-6
-5
-4
-3
-2
0
25
50
75
100
125
150
log [Analog] (M)

Fig. 21. N-1,2-Diol analogs inhibit [^{3}H]5-HT uptake into rat hippocampal synaptosomes. For clarity of presentation, compounds are grouped according to structural similarity of additions to the phenyl rings: standards, lobeline, lobelane and N-1,2-diol analogs (top left panel), N-1,2-diol analogs containing 1-naphthyl or 4-biphenyl substituents (top right panel), N-1,2-diol analogs containing aromatic methoxy or methylenedioxy substituents (bottom left panel), or N-1,2-diol analogs containing aromatic halogeno substituents (bottom right panel). Nonspecific [^{3}H]5-HT uptake was determined in the presence of 10 μM fluoxetine. Control (CON) represents specific [^{3}H]5-HT uptake in the absence of analog (0.56 ± 0.06 pmol/mg/min). Legend provides compounds in order from highest to lowest affinity. n = 4 rats/analog.

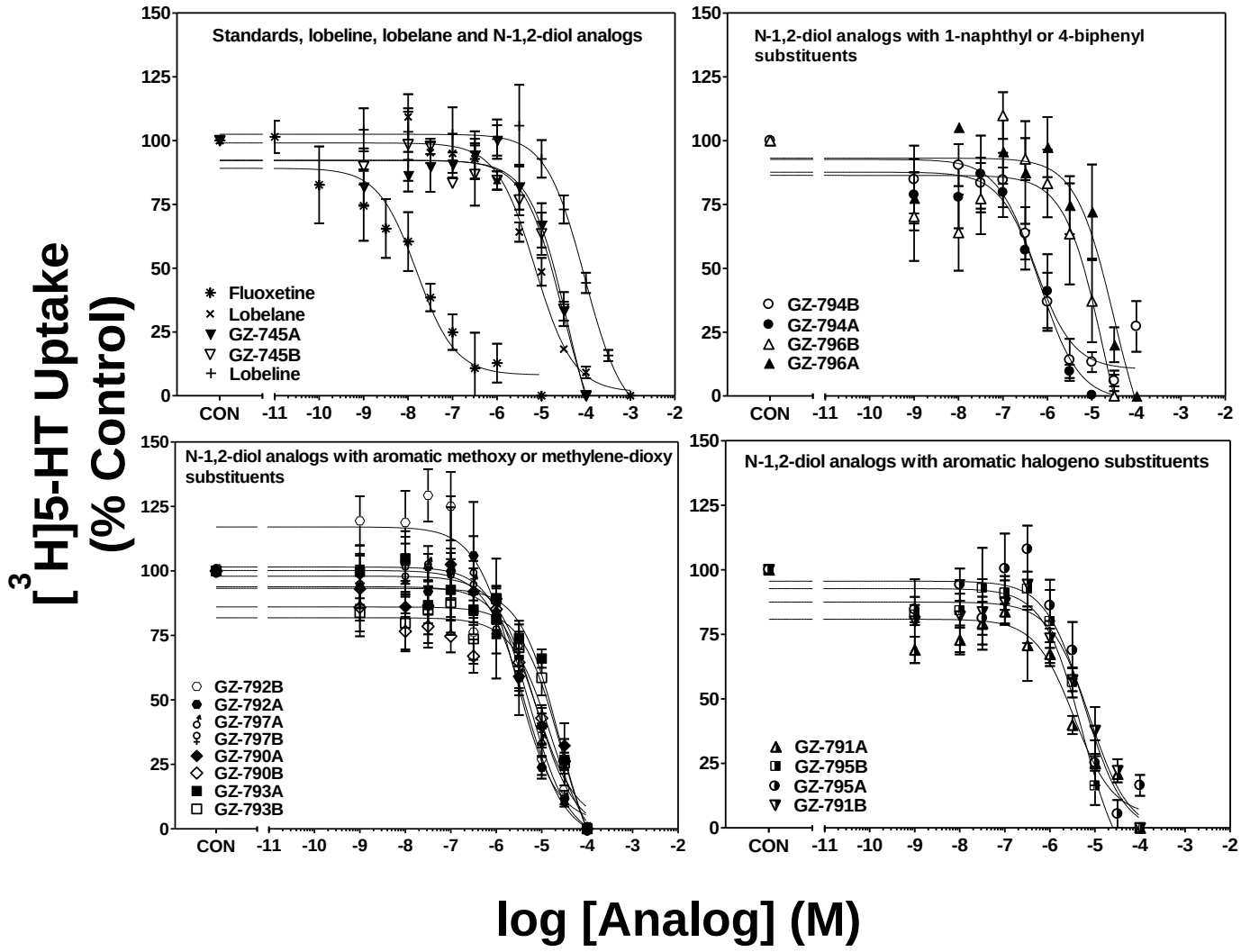
[3H]5-HT Uptake (% Control)
Standards, lobeline, lobelane and N-1,2-diol analogs
Fluoxetine
Lobelane
GZ-745A
GZ-745B
Lobeline
N-1,2-diol analogs with 1-naphthyl or 4-biphenyl substituents
GZ-794B
GZ-794A
GZ-796B
GZ-796A
N-1,2-diol analogs with aromatic methoxy or methylene-dioxy substituents
GZ-792B
GZ-792A
GZ-797A
GZ-797B
GZ-790A
GZ-790B
GZ-793A
GZ-793B
N-1,2-diol analogs with aromatic halogeno substituents
GZ-791A
GZ-795B
GZ-795A
GZ-791B
CON
-11
-10
-9
-8
-7
-6
-5
-4
-3
-2
0
25
50
75
100
125
150
log [Analog] (M)

Fig 22. N-1,2-diol analogs inhibit [^{3}H]DTBZ binding to vesicle membranes from rat whole brain preparations. For clarity of presentation, compounds are grouped according to structural similarity of additions to the phenyl rings: standards, lobeline, lobelane and N-1,2-diol analogs (top left panel), N-1,2-diol analogs containing 1-naphthyl or 4-biphenyl substituents (top right panel), N-1,2-diol analogs containing aromatic methoxy or methylenedioxy substituents (bottom left panel), or N-1,2-diol analogs containing aromatic halogeno substituents (bottom right panel). Nonspecific [^{3}H]DTBZ binding was determined in the presence of 10 μM Ro-4-1284. Control (CON) represents specific [^{3}H]DTBZ binding in the absence of analog (0.41 ± 0.01 pmol/mg protein). Legend provides compounds in order from highest to lowest affinity. n = 4 rats/analog. Previous results for lobeline and lobelane were obtained from Nickell et al., 2010.

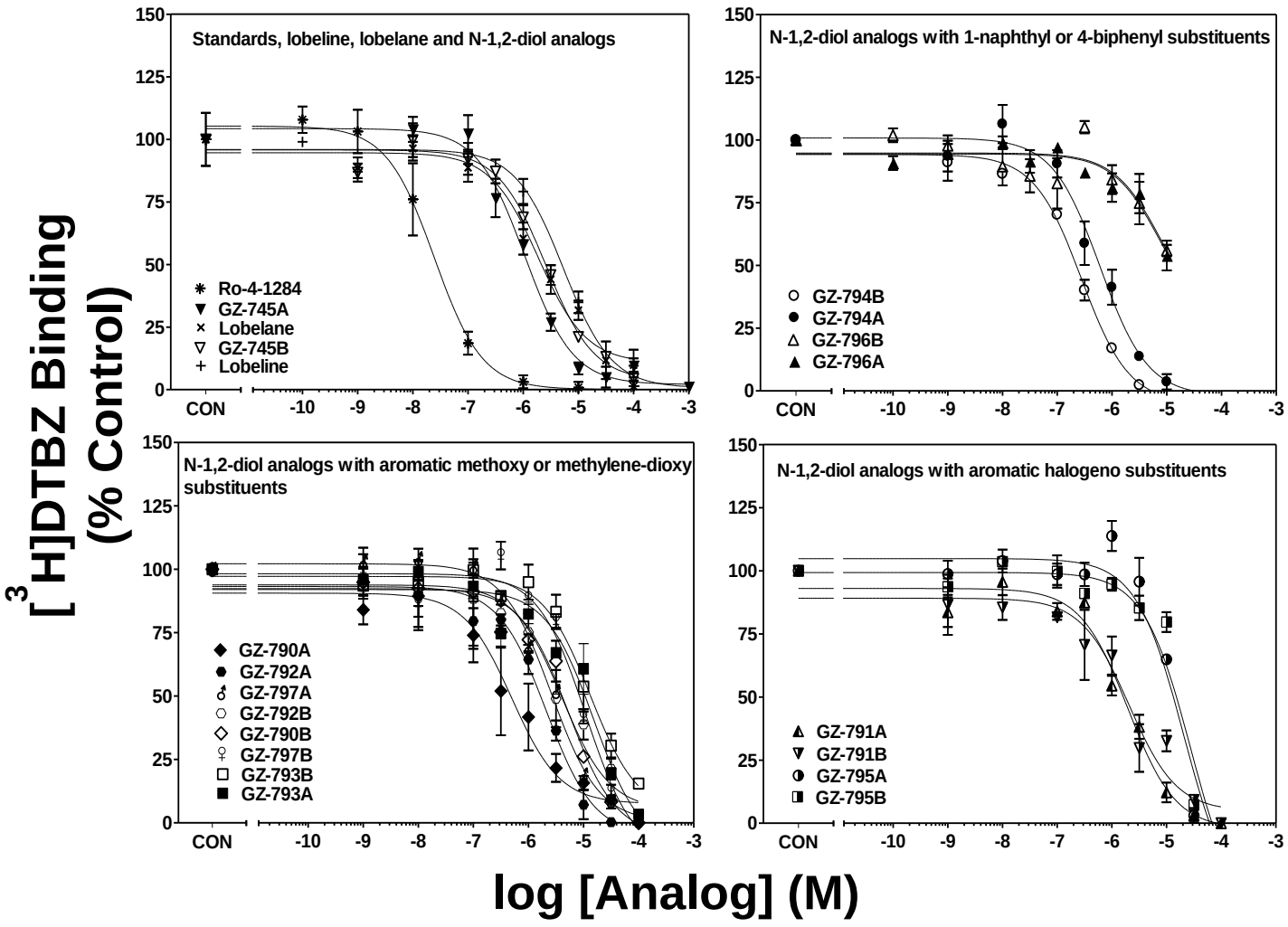
[3H]DTBZ Binding (% Control)
Standards, lobeline, lobelane and N-1,2-diol analogs
Ro-4-1284
GZ-745A
Lobelane
GZ-745B
Lobeline
N-1,2-diol analogs with 1-naphthyl or 4-biphenyl substituents
GZ-794B
GZ-794A
GZ-796B
GZ-796A
N-1,2-diol analogs with aromatic methoxy or methylene-dioxy substituents
GZ-790A
GZ-792A
GZ-797A
GZ-792B
GZ-790B
GZ-797B
GZ-793B
GZ-793A
N-1,2-diol analogs with aromatic halogeno substituents
GZ-791A
GZ-791B
GZ-795A
GZ-795B
CON
-10
-9
-8
-7
-6
-5
-4
-3
0
25
50
75
100
125
150
log [Analog] (M)

Fig 23. N-1,2-diol analogs inhibit [^{3}H]DA uptake into vesicles prepared from rat striatum. For clarity of presentation, compounds are grouped according to structural similarity of additions to the phenyl rings: standards, lobeline, lobelane and N-1,2-diol analogs (top left panel), N-1,2-diol analogs containing 1-naphthyl or 4-biphenyl substituents (top right panel), N-1,2-diol analogs containing aromatic methoxy or methylenedioxy substituents (bottom left panel), or N-1,2-diol analogs containing aromatic halogeno substituents (bottom right panel). Nonspecific [^{3}H]DA uptake was determined in the presence of 10 μM Ro-4-1284. Control (CON) represents specific vesicular [^{3}H]DA uptake in the absence of analog (34.1 ± 1.18 pmol/mg/min). Legend provides compounds in order from highest to lowest affinity. n = 4 rats/analog.

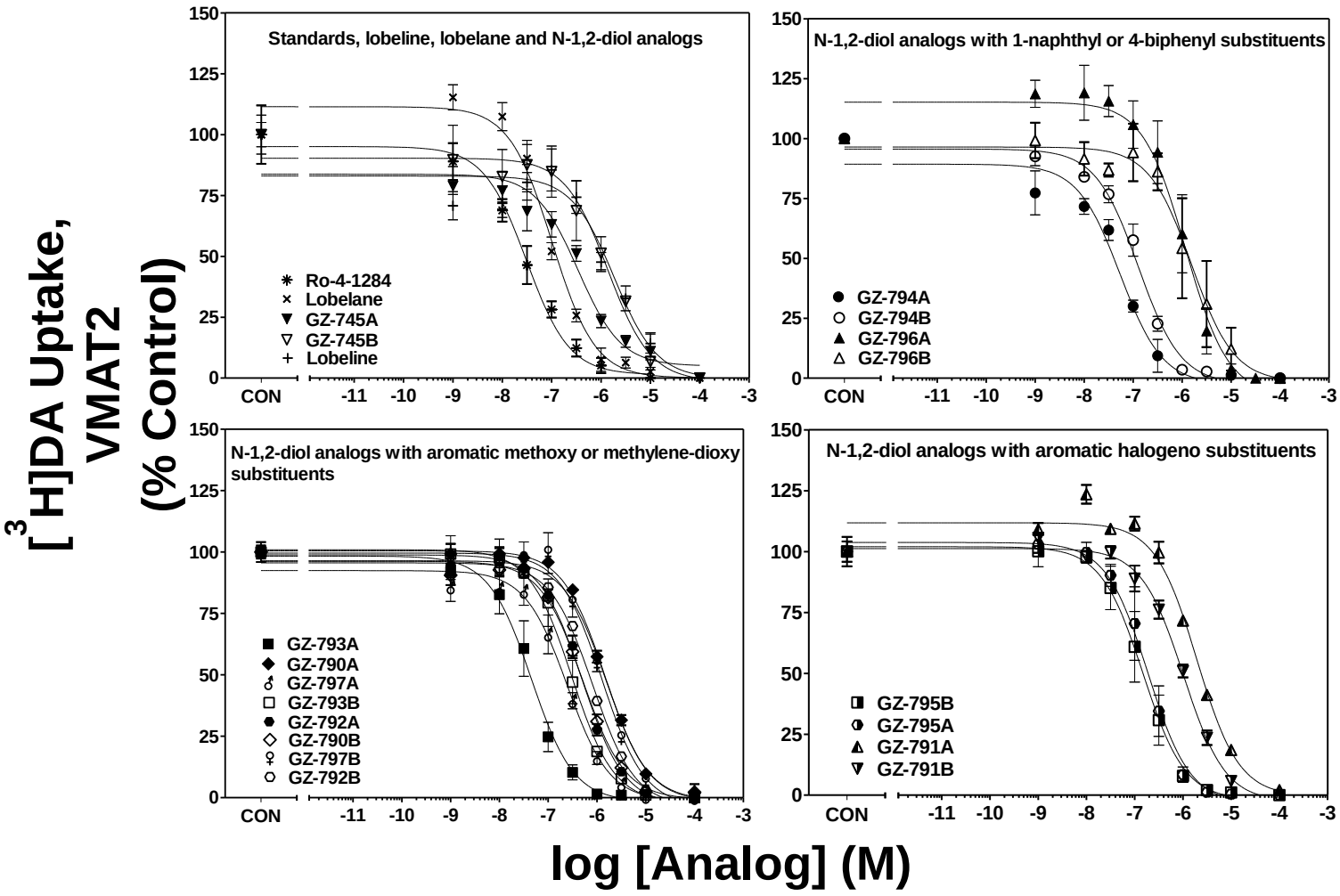
[3H]DA Uptake, VMAT2 (% Control)
Standards, lobeline, lobelane and N-1,2-diol analogs
Ro-4-1284
Lobelane
GZ-745A
GZ-745B
Lobeline
N-1,2-diol analogs with 1-naphthyl or 4-biphenyl substituents
GZ-794A
GZ-794B
GZ-796A
GZ-796B
N-1,2-diol analogs with aromatic methoxy or methylene-dioxy substituents
GZ-793A
GZ-790A
GZ-797A
GZ-793B
GZ-792A
GZ-790B
GZ-797B
GZ-792B
N-1,2-diol analogs with aromatic halogeno substituents
GZ-795B
GZ-795A
GZ-791A
GZ-791B
CON
-11 -10 -9 -8 -7 -6 -5 -4 -3
0 25 50 75 100 125 150
log [Analog] (M)

Fig 24. Lack of correlation between N-1,2-diol analogs inhibition of [^{3}H]DTBZ binding and [^{3}H]DA uptake at VMAT2. Data presented are Ki values obtained from concentration-response curves for analog-induced inhibition of [^{3}H]DTBZ binding and [^{3}H]DA uptake at VMAT2 (Figs. 21 and 22, respectively). Pearson's correlation analysis revealed a lack of correlation (Pearson's correlation coefficient r = 0.37; p = 0.13) between the ability of N-1,2-diol analogs to inhibit [^{3}H]DTBZ binding to VMAT2 and to inhibit [^{3}H]DA uptake at VMAT2.

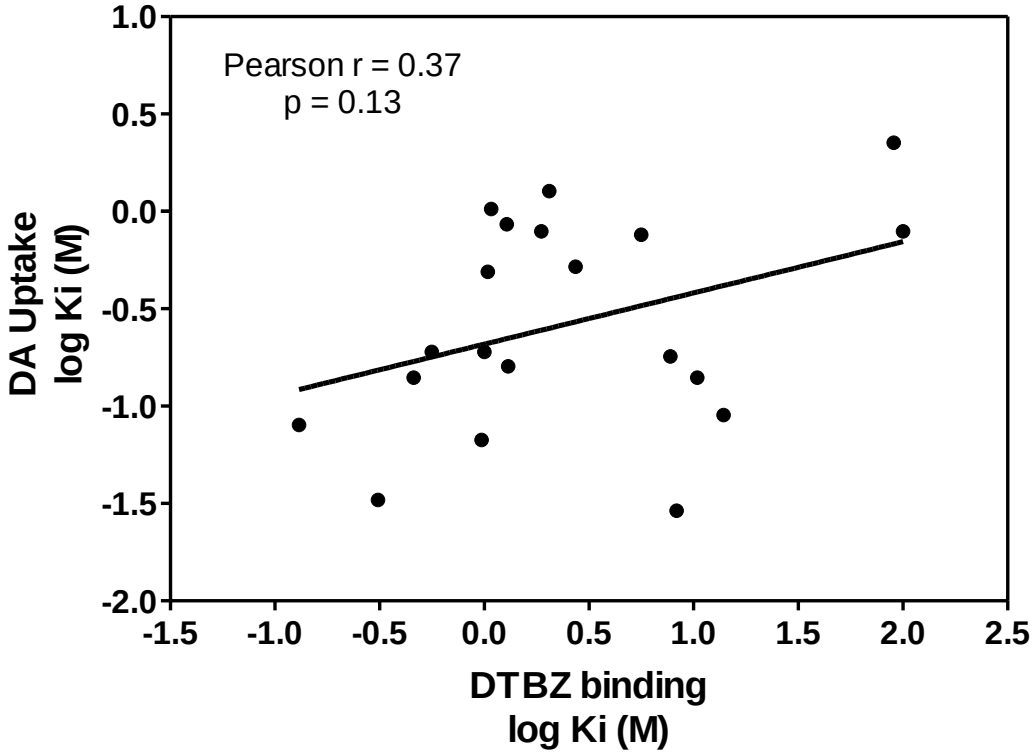

Fig 25. N-1,2-Diol analogs competitively inhibit [^{3}H]DA uptake into vesicles prepared from rat striatum. Concentrations of GZ-793A (0.029 µM), GZ-794A (0.060 µM), and GZ-796A (0.79 µM) approximated the Ki values for inhibiting [^{3}H]DA uptake into isolated synaptic vesicles obtained from the data shown in Fig. 22. K_m (top panel) and V_{max} (bottom panel) values are mean ± S.E.M. (** $p < 0.01$ different from control; *** $p < 0.001$ different from control; n = 4 - 7 rats/analog)

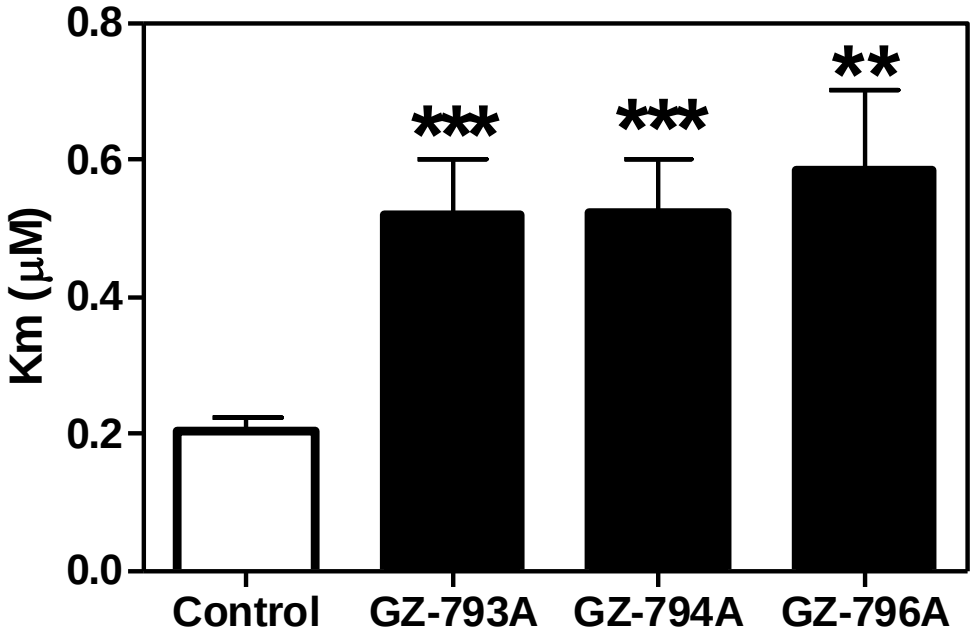

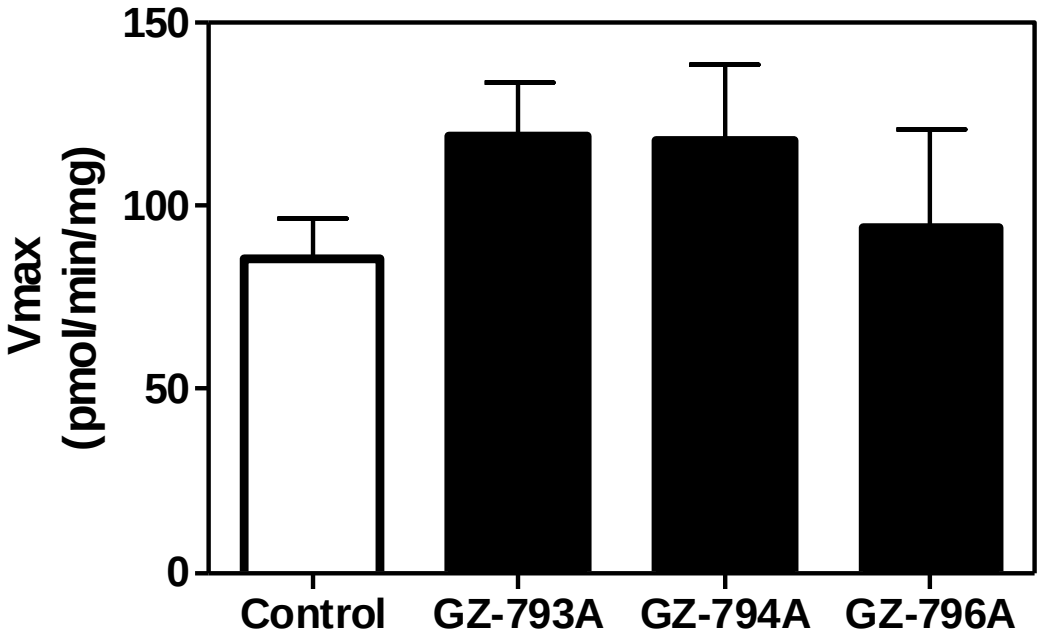
150
100
50
0
Vmax
(pmol/min/mg)
Control
GZ-793A
GZ-794A
GZ-796A

Fig 26. In a concentration-dependent manner, GZ-793A, GZ-794A, and GZ-796A inhibit METH-evoked peak DA fractional release from striatal slices. Peak response data are expressed as mean ± S.E.M. pg/ml/mg of the slice weight. Slices were superfused with analog (10 nM – 10 µM) and after a 10 min collection to determine intrinsic activity, METH (5 µM) was added to the buffer for 15 minutes. Analog remained in the buffer until the end of the experiment. *p < 0.05 different from METH alone (CON). n = 5 rats

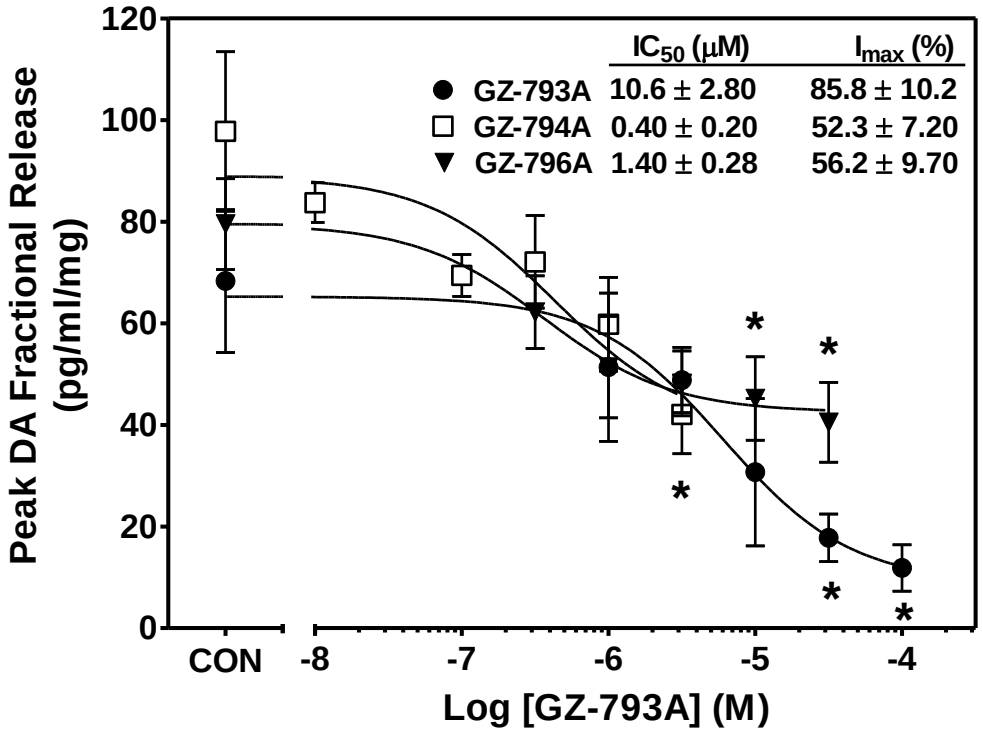

CHAPTER FOUR

GZ-793A, a Novel VMAT2 Inhibitor that Probes Multiple Sites on VMAT2 as a Potential Treatment for METH Abuse

Portions of this chapter have been submitted for publication in the manuscript:

Horton DB, Zheng G, Crooks PA, Dwoskin LP. GZ-793A interacts with the vesicular monoamine transporter-2 to inhibit the effect of methamphetamine. *J Neurochem,* submitted, 2011.

I. Introduction

METH abuse is a serious public health concern. According to the 2010 National Survey on Drug Use and Health, over 350,000 people in the United States reported using METH in the past month (NSDUH, 2011). Currently, no FDA-approved pharmacotherapies are available to treat METH abuse. METH produces reward by increasing extracellular DA concentrations through DAT-mediated reverse transport (Fischer and Cho, 1979; Wise and Bozarth, 1987; Di Chiara and Imperato, 1988). METH is transported into the synaptic vesicles via VMAT2 and/or passively diffuses across the vesicular membrane (Peter et al. 1995). METH inhibits DA uptake at VMAT2, promotes DA release from synaptic vesicles and inhibits monoamine oxidase leading to increases in cytosolic DA available for DAT-mediated reverse transport (Sulzer and Rayport 1990; Pifl et al. 1995; Sulzer et al. 2005). METH is transported into vesicles through VMAT2 and simultaneously releases DA from synaptic vesicles, similar to the facilitated diffusion exchange model of DA release at DAT (Fischer and Cho, 1979; Sulzer et al. 2005). Thus, the primary site of METH action is VMAT2, which increases

cytosolic DA available for reverse transport of DAT to increase extracellular DA concentrations leading to reward.

Based on the role of VMAT2 in METH effects, drug discovery efforts have focused on VMAT2 as a pharmacological target for the development of novel compounds to treat METH abuse. Lobeline (Fig. 27), the principal alkaloid of *Lobelia inflata*, inhibits [^{3}H]DTBZ binding to VMAT2, [^{3}H]DA uptake at VMAT2, and METH-evoked DA release from striatal slices (Teng et al. 1997, 1998; Nickell et al. 2010). Lobeline inhibits METH-induced hyperactivity, behavioral sensitization and METH self-administration in rats, supporting its potential as a treatment for METH abuse (Harrod et al. 2001, 2003; Dwoskin and Crooks, 2002). Lobeline has been evaluated in clinical trials for this indication (Jones, 2007). Importantly, lobeline has limited selectivity for VMAT2, also having high affinity for nicotinic acetylcholine receptors (Damaj et al. 1997; Miller et al. 2004).

Structure activity relationships revealed that lobelane (Fig. 27), a saturated, chemically defunctionalized lobeline analog, exhibited low affinity for nicotinic receptors and enhanced affinity and selectivity for VMAT2 compared to its parent compound (Miller et al. 2004; Nickell et al. 2010). Lobelane also inhibited METH-evoked DA release from striatal slices and decreased METH self-administration in rats (Neugebauer et al. 2007; Nickell et al. 2010). However, tolerance developed to the behavioral effects of lobelane (Neugebauer et al. 2007). The physicochemical properties of lobelane were not optimal, including low water solubility, which limited development with respect to clinical investigation.

Structural modification of lobelane was pursued with the aim of improving water solubility. Replacement of the N-methyl group of lobelane with a N-propan-1,2-diol moiety afforded the lead analog, GZ-793A [*R*-*N*-(1,2-dihydroxypropyl)-2,6-*cis*-di-(4-methoxyphenethyl)piperidine hydrochloride] (Fig. 27). GZ-793A potently and selectively inhibited DA uptake at VMAT2, increasing the K_m value with no change in V_{max}, indicative of a competitive mechanism of inhibition (Chapter 3, Horton et al. 2011). Further, GZ-793A decreased METH-evoked DA release from striatal slices, without altering field stimulation- and nicotine-evoked DA release, indicating specific inhibition of the effects of METH (Chapter 3, Horton et al., 2011; unpublished observations). Importantly, GZ-793A specifically decreased METH self-administration without altering food-maintained responding (Beckmann et al. 2011). Thus, the ability of GZ-793A to inhibit METH *in vitro* translated into efficacy against METH in the *in vivo* animal model. However, the cellular mechanism underlying the GZ-793A-induced inhibition of METH both *in vitro* and *in vivo* has not been evaluated fully. The current study determined the ability of GZ-793A to inhibit the effects of METH to release DA from isolated synaptic vesicles. Considering that VMAT2 is a primary target for the mechanism of action of METH, the ability of GZ-793A to evoke [^{3}H]DA release and inhibit METH-evoked [^{3}H]DA release from vesicles was investigated, and these effects were compared to those of the classical VMAT2 inhibitors, TBZ and reserpine.

The hypothesis of this chapter is that GZ-793A interacts with VMAT2 to release DA from striatal vesicles and inhibit METH-evoked DA release from striatal vesicles.

II. Methods

IIa. Animals. Male Sprague-Dawley rats (200–250g, Harlan, Indianapolis, IN) were housed two per cage with *ad libitum* access to food and water in the Division of Laboratory Animal Resources at the University of Kentucky (Lexington, KY). Experimental protocols involving the animals were in accord with the 1996 NIH Guide for the Care and Use of Laboratory Animals and were approved by the Institutional Animal Care and Use Committee at the University of Kentucky.

IIb. Materials. [^{3}H]Dopamine ([^{3}H]DA; dihydroxyphenylethylamine, 3,4-[7-^{3}H]; specific activity, 28 Ci/mmol) was purchased from PerkinElmer, Inc. (Boston, MA, USA). ATP-Mg^{2+}, DA, EDTA, EGTA, HEPES, $MgSO_4$, polyethyleneimine (PEI), KOH, potassium tartrate, reserpine and sucrose were purchased from Sigma-Aldrich, Inc. (St. Louis, MO, USA). Ascorbic acid and $NaHCO_3$ were purchased from Aldrich Chemical Co. (Milwaukee, WI, USA). Complete counting cocktail 3a70B was purchased from Research Products International Corp. (Mount Prospect, IL, USA). TBZ was a generous gift from Hoffman-LaRoche Inc. (Nutley, NJ, USA).

IIc. Vesicular [^{3}H]DA release assay. GZ-793A- and METH-evoked vesicular [^{3}H]DA release were determined using previously described methods (Nickell et al., 2011). Briefly, striata were homogenized in 14 ml of ice-cold 0.32 M sucrose solution containing 5 mM $NaHCO_3$ (pH 7.4) with 10 up-and-down strokes of a Teflon pestle homogenizer (clearance, ~ 0.008”). Homogenates were

centrifuged at 2,000 × *g* for 10 min at 4 °C and resulting supernatants centrifuged at 10,000 × *g* for 30 min at 4 °C. Pellets were resuspended in 2.0 ml of 0.32 M sucrose and were transferred to tubes containing 7 ml of milliQ water and homogenized with 5 up-and-down strokes of the Teflon pestle homogenizer. Homogenates were transferred to tubes containing 900 µl of 0.25 M HEPES and 900 µl of 1.0 M potassium tartrate solution and centrifuged at 20,000 × *g* for 20 min at 4 ºC. Resulting supernatants were centrifuged at 55,000 × *g* for 60 min at 4 ºC. Subsequently, 100 µl of 1 mM $MgSO_4$, 100 µl of 0.25 M HEPES and 100 µl of 1.0 M potassium tartrate were added to the supernatant and centrifuged at 100,000 × *g* for 45 min at 4 ºC. Pellets were resuspended in 2.7 ml of assay buffer, containing: 25 mM HEPES, 100 mM potassium tartrate, 50 µM EGTA, 100 µM EDTA, and 1.7 mM ascorbic acid, 2 mM ATP-Mg^{2+} (pH 7.4). Then, [^{3}H]DA (300 µl of 0.3 µM) was added and samples incubated for 8 min at 37 ºC. Following incubation, samples were centrifuged at 100,000 × *g* for 45 min at 4 ºC and resulting pellets were resuspended in a final volume of 4.2 ml of assay buffer. [^{3}H]DA-preloaded vesicles (180 µl) were added to duplicate tubes in the absence or presence of various concentrations (1 nM – 1 mM; 20 µl) of GZ-793A, METH or reserpine, for a final volume of 200 µl and incubated for 8 min at 37 °C. Reactions were terminated by the addition of 2.5 ml of ice-cold assay buffer and rapid filtration through Whatman GF/B filters. Samples were washed 3 times with assay buffer containing 2 mM $MgSO_4$ in the absence of ATP. Radioactivity retained by the filters was determined by liquid scintillation spectrometry (B1600 TR scintillation counter; PerkinElmer, Inc.). GZ-793A-, METH- or reserpine-

evoked [^{3}H]DA release was calculated for each test compound concentration by subtracting the radioactivity remaining on the filter in the presence of compound from the amount of radioactivity remaining on the filter in the absence of compound (control samples).

To determine if GZ-793A-induced [^{3}H]DA release from striatal synaptic vesicles was inhibited by TBZ (TBZ-sensitive) or reserpine (reserpine-sensitive), [^{3}H]DA-preloaded synaptic vesicles (180 µl) were added to duplicate tubes containing a range of concentrations (1 nM – 1 mM) of GZ-793A in the absence and presence of TBZ (35 nM) or reserpine (50 nM), and incubated (final volume, 200 µl) for 8 min at 37 ºC. Samples were processed as previously described.

To determine if METH-induced [^{3}H]DA release from striatal synaptic vesicles was TBZ- or GZ-793A-sensitive, [^{3}H]DA-preloaded synaptic vesicles (180 µl) were added to duplicate tubes containing a range of concentrations (1 nM – 1 mM) of METH in the absence and presence of TBZ (30 nM – 10 µM) or GZ-793A (7 nM - 1µM), and incubated (final volume, 200 µl) for 8 min at 37 ºC. Samples were processed as previously described.

To determine if GZ-793A-induced inhibition of METH-evoked DA release was the result of a rate-dependent slow-offset dissociation, [^{3}H]DA-preloaded synaptic vesicles (180 µl) were added to duplicate tubes containing a range of concentrations (1 µM – 1 mM) of METH in the absence and presence of GZ-793A (1 µM), and incubated (final volume, 200 µl) for either 8 min or 15 min at 37 ºC. Samples were processed as previously described.

IId. Data analysis. EC_{50} values for GZ-793A, METH and reserpine were determined from the concentration-effect curves via an iterative curve-fitting program (Prism 5.0; GraphPad Software Inc., San Diego, CA). EC_{50} values for GZ-793A evoked [^{3}H]DA release in the presence of TBZ or reserpine were determined also using the Prism 5.0 curve-fitting program TBZ-induced and GZ-793A-induced inhibition of METH-evoked [^{3}H]DA release were analyzed using separate two-way repeated-measures ANOVA. If significant TBZ x METH or GZ-793A x METH interactions were found, one-way ANOVAs followed by Dunnetts's *post hoc* test were performed at each METH concentration to determine the concentrations that decreased METH-evoked [^{3}H]DA release. To determine if the various concentrations of TBZ or GZ-793A increased the log EC_{50} value or decreased the E_{max} for METH compared to the values for these parameters in the absence of inhibitor (control), one-way ANOVAs were conducted followed by Dunnett's post hoc test. Schild analyses were performed using the dose ratios (DR) obtained by dividing the EC_{50} for METH-evoked [^{3}H]DA release in the presence of inhibitor by that in the absence of inhibitor. Log (DR-1) was plotted as a function of log inhibitor concentration to provide the Schild regression. The data were fit by linear regression and the slope determined and linearity was assessed using Prism 5.0. Significant difference from unity was concluded if the 95% confidence intervals (CI) of the slope did not include unity (Kenakin, 2006).

To determine if the effect of GZ-793A to inhibit METH was rate dependent, a three-way repeated-measures ANOVA was performed. If significant interactions were found, follow-up ANOVAs were performed to identify the source

of the interaction. Differences between EC_{50} values and between E_{max} values were determined using repeated-measures two-way ANOVAs. For all analyses, significance was defined as $p < 0.05$.

III. Results

IIIa. GZ-793A evoked [^{3}H]DA release from striatal vesicles. GZ-793A-evoked [^{3}H]DA release from isolated striatal synaptic vesicles is illustrated in Fig. 28. Nonlinear regression of the GZ-793A concentration-response revealed a two-site model of GZ-793A interaction with VMAT2 ($R^2 = 0.89$, $p < 0.001$; Hi and Low EC_{50} = 14.3 ± 4.46 nM and 33.0 ± 4.00 µM, respectively; Hi and Low E_{max} = 37.5 ± 4.32% and 86.1 ± 2.69% vesicular [^{3}H]DA content, respectively). To evaluate inhibition of the effect of GZ-793A on DA release, the highest concentration (35 nM) of TBZ that did not evoke DA release from isolated vesicles was chosen (Nickell et al., 2011). TBZ inhibited only the effect of GZ-793A to release DA via the Hi affinity sites on VMAT2 (Fig. 28). Nonlinear regression revealed a one-site model of GZ-793A interaction with VMAT2 in the presence of TBZ ($R^2 = 0.95$, $p < 0.001$; EC_{50} = 23.7 ± 6.53 µM).

The effect of reserpine to increase [^{3}H]DA release from vesicles was determined (Fig. 29). Nonlinear regression of the reserpine concentration response revealed a significant fit to a one-site model ($R^2 = 0.25$, $p < 0.001$; EC_{50} = 1.44 ± 0.47 µM, E_{max} = 28.4 ± 7.48%). The highest concentration (50 nM) of reserpine that did not evoke DA release from isolated vesicles was chosen to evaluate if GZ-793A-evoked [^{3}H]DA release was reserpine sensitive.

Concentration response for GZ-793A-evoked [^{3}H]DA release from striatal vesicles in the absence and presence of reserpine (50 nM) is illustrated in Fig. 28. Reserpine inhibited only the effect of GZ-793A to release DA via the Hi affinity sites on VMAT2. Nonlinear regression revealed a one-site model of GZ-793A interaction with VMAT2 in the presence of reserpine (R^2 = 0.92, $p < 0.001$; EC_{50} = 20.2 ± 3.17 µM).

IIIb. TBZ inhibits METH-evoked [^{3}H]DA release from striatal vesicles.

The concentration response for METH to evoke [^{3}H]DA release from synaptic vesicles was analyzed using nonlinear regression and a significant fit to a single site model was found (R^2 = 0.95, $p < 0.001$;Fig. 30). The EC_{50} value for METH was 8.93 ± 1.36 µM and E_{max} was 87.4 ± 1.37% (Table 4), consistent with our previous findings (Nickell et al., 2011). Based on our previous concentration response (Nickell et al., 2011), a full range of TBZ concentrations were chosen to evaluate the ability of TBZ to decrease METH-evoked [^{3}H]DA release from synaptic vesicles. TBZ produced a rightward shift in the METH concentration-response, consistent with surmountable inhibition. A linear fit (r^2 = 0.79, $p < 0.001$) to the Schild regression revealed a slope (s = 0.92 ± 0.33) not significantly different from unity, consistent with competitive inhibition (Fig. 30, inset). Two-way repeated measures ANOVA revealed a main effect of METH ($F_{11,209}$ = 435, $p < 0.0001$) and TBZ ($F_{4,19}$ = 7.61, $p < 0.001$), and a METH × TBZ interaction [$F_{44,209}$ = 12.8, $p < 0.0001$). To further evaluate the interaction, one-way ANOVAs were conducted at each METH concentration to determine the TBZ concentration which decreased release (Table 5; METH 3 µM, $F_{4,20}$ = 3.96, $p < 0.05$; 10 µM,

$F_{4,20} = 18.2$, $p < 0.0001$; 30 µM, $F_{4,20} = 31.1$, $p < 0.0001$; 100 µM, $F_{4,20} = 46.4$, $p < 0.0001$; 300 µM, $F_{4,19} = 29.3$, $p < 0.0001$; 1 mM, $F_{4,30} = 9.39$, $p < 0.001$). Post hoc analyses revealed that at 3 µM METH, only 10 µM TBZ significantly decreased METH-evoked [^{3}H]DA release. At 10 µM - 1 mM METH, TBZ (100 nM, 1 µM, and 10 µM) significantly decreased METH-evoked [^{3}H]DA release. Analysis of the log EC_{50} for METH-evoked [^{3}H]DA release revealed that TBZ (100 nM - 10 µM) increased the METH EC_{50} value (Table 4; $F_{4,20} = 43.6$, $p < 0.0001$).

IIIc. GZ-793A inhibits METH-evoked [^{3}H]DA release from striatal vesicles. The concentration response for METH to evoke [^{3}H]DA release from synaptic vesicles is illustrated in Fig. 31. Using nonlinear regression a significant fit to a one-site model was obtained for the METH concentration response ($R^2 = 0.90$, $p < 0.001$). The EC_{50} value for METH was 19.5 ± 5.19 µM and E_{max} was 88.0 ± 1.21% (Table 4), in agreement with our previous findings (Nickell et al., 2011). Fig. 31 also illustrates that concentrations of GZ-793A, which selectively interact with the Hi-affinity site on VMAT2 (Fig. 28), inhibited the METH-evoked [^{3}H]DA release. A rightward shift in the METH concentration-response curve was evident with increasing concentrations of GZ-793A, consistent with surmountable inhibition. A linear fit ($r^2 = 0.95$, $p < 0.001$) to the Schild regression revealed a slope ($s = 0.49 \pm 0.08$) significantly different from unity based on the 95% confidence interval (CI: 0.15 to 0.83), consistent with allosteric inhibition (Fig. 31, inset). Analysis of the concentration response by two-way repeated measures ANOVA revealed main effects of METH ($F_{11,308} = 821$, $p < 0.001$) and GZ-793A ($F_{4,28} = 8.82$, $p < 0.001$), and a METH × GZ-793A interaction ($F_{44,308} = 8.13$, $p <$

0.001). To further evaluate the interaction, one-way ANOVAs were conducted at each METH concentration to determine the GZ-793A concentrations which decreased release (Table 5; METH 1 µM, $F_{4,30} = 3.31$, $p < 0.05$; 3 µM, $F_{4,30} = 9.10$, $p < 0.0001$; 10 µM, $F_{4,30} = 12.9$, $p < 0.0001$; 30 µM, $F_{4,30} = 20.4$, $p < 0.0001$; 100 µM, $F_{4,30} = 25.1$, $p < 0.0001$; 300 µM, $F_{4,28} = 15.6$, $p < 0.0001$; 1 mM, $F_{4,30} = 7.12$, $p < 0.001$). Post hoc analyses revealed that at 1 µM METH, only 1 µM GZ-793A significantly decreased [^{3}H]DA release and at 3 µM METH, GZ-793A (70 nM, 100 nM, and 1 µM) significantly decreased [^{3}H]DA release. At higher concentrations of METH, GZ-793A (70 nM – 1 µM) significantly decreased METH-evoked [^{3}H]DA release. Analysis of the log EC_{50} for METH-evoked [^{3}H]DA release revealed that GZ-793A (70 nM - 1 µM) increased the METH EC_{50} value (Table 4; $F_{4,30} = 26.6$, $p < 0.0001$).

IIId. GZ-793A-induced inhibition of METH-evoked [^{3}H]DA release was not rate-dependent. To provide further evidence regarding the mechanism of GZ-793A inhibition of the effect of METH at synaptic vesicles, additional experiments determined if the GZ-793A-induced inhibition of METH-evoked [^{3}H]DA release was rate-dependent. The highest concentration of GZ-793A (1 µM), shown to selectively interact with the Hi-affinity site on VMAT2 (Fig. 28), was evaluated for inhibition of METH-evoked [^{3}H]DA release after 8- and 15-min incubation (Fig. 32). Three-way repeated measures ANOVA revealed a main effect of METH $F_{4,32} = 498$, $p < 0.0001$) and GZ-793A ($F_{1,8} = 62.2$, $p < 0.0001$), and a METH × GZ-793A interaction ($F_{4,32} = 39.2$, $p < 0.0001$); however, no main effect of time or interactions of METH × time, GZ-793A × time or METH × GZ-

793A × time were observed. Increasing the incubation time from 8 to 15 min did not alter EC_{50} or E_{max} for METH-evoked [^{3}H]DA release.

IV. Discussion

METH inhibits DA uptake at VMAT2 and evokes DA release from synaptic vesicles increasing intracellular DA concentrations available for METH-induced reverse transport via DAT to ultimately increase extracellular DA concentrations (Sulzer et al., 2005). The lead compound emerging from our iterative drug discovery approach, GZ-793A, decreases METH-evoked DA release from superfused striatal slices and decreases METH self-administration in rats (Beckmann et al. 2011; Chapter 3, Horton et al. 2011b). The cellular mechanism underlying the GZ-793A-induced inhibition of METH's effects has not been elucidated fully. The current results show that GZ-793A potently released [^{3}H]DA from isolated striatal synaptic vesicles. GZ-793A-induced release was mediated by two sites on VMAT2, i.e., a Hi-affinity, TBZ- and reserpine-sensitive site, and a Low-affinity, TBZ- and reserpine-insensitive site. Moreover, GZ-793A inhibited METH-evoked [^{3}H]DA release from vesicles by interacting with the Hi-affinity VMAT2 site. Thus, GZ-793A inhibits the effects of METH at VMAT2, which may underlie the previously reported GZ-793A-induced decrease in METH self-administration.

Previous research from our laboratories demonstrated that GZ-793A potently (Ki = 29 nM) and competitively inhibits [^{3}H]DA uptake at VMAT2 using isolated synaptic vesicle preparations. Interestingly, GZ-793A exhibited a 285-fold higher affinity for the DA translocation site compared with the [^{3}H]DTBZ

binding site (Ki = 8.29 μM), suggesting that the inhibition of DA uptake is not via an interaction at the DTBZ site on VMAT2 (Chapter 3, Horton et al. 2011b). TBZ and reserpine have been shown to act at two different sites on VMAT2 (Yelin and Schuldiner, 2000). Relative to the classical VMAT2 inhibitors, GZ-793A was found to be equipotent with TBZ and reserpine inhibiting DA uptake at VMAT2, but was 1-2-orders of magnitude less potent than TBZ and reserpine at the [^{3}H]DTBZ binding site (Partilla et al., 2006; Chapter 3, Horton et al., 2011b; Meyer et al., 2011; Nickell et al., 2011), consistent with these sites being different.

Since GZ-793A exhibited a higher affinity for the DA translocation site compared with the [^{3}H]DTBZ binding site on VMAT2, GZ-793A inhibition of METH-evoked [^{3}H]DA release appeared to be due to inhibition of DA uptake at VMAT2. However, GZ-793A was significantly more potent (365-fold) inhibiting [^{3}H]DA uptake into vesicles than it was inhibiting METH-evoked DA release from striatal slices, warranting further evaluation of the cellular mechanism underlying the pharmacological effects of GZ-793A. Our working hypothesis was based on the idea that METH interacts with an extravesicular site on VMAT2 to inhibit DA uptake into the vesicle, and with an intravesicular site on VMAT2 to evoke DA release from the vesicle (Fig. 33). The current results show that GZ-793A also releases DA from the synaptic vesicle, presumably by interacting with intravesicular sites on VMAT2. Moreover, the biphasic concentration-response curve for GZ-793A to release [^{3}H]DA supports an interaction with two different intravesicular sites, a Hi-affinity site and a Low-affinity site (Fig. 28). The current

results also show that the intravesicular Hi-affinity site for GZ-793A was both TBZ- and reserpine-sensitive. The Low-affinity site was insensitive to both TBZ and reserpine, suggesting that the Low-affinity site may represent a nonspecific effect of GZ-793A, e.g., disruption of the proton gradient responsible for retention of DA in the synaptic vesicle (Sulzer et al. 2005). The ability of TBZ and reserpine to inhibit GZ-793A-evoked DA release at the intravesicular Hi-affinity site appears to be via an allosteric interaction, since TBZ and reserpine act at different sites on VMAT2 (Pletscher, 1977; Darchen et al., 1989; Yelin and Schuldiner, 2000). Thus, TBZ and reserpine may conformationally change the VMAT2 protein resulting in inhibition of GZ-793A-evoked DA release.

Concentration-response curves for both TBZ and reserpine to release DA were consistent with a one-site model of interaction (current results; Nickell et al., 2011), further indicating that GZ-793A acts differently than the classical VMAT2 standards at the DA release site on VMAT2. Although GZ-793A, TBZ and reserpine were equipotent at the extravesicular DA translocation site on VMAT2, the order of potency for DA release via the intravesicular site on VMAT2 was GZ-793A > TBZ > reserpine, suggesting that DA uptake and DA release are mediated by two different sites on VMAT2. Of note, GZ-793A interacts with the Hi affinity site mediating DA release across the same concentration range that it inhibits DA uptake by VMAT2 (Hi affinity DA release site, EC_{50} = 15 nM; DA uptake site, Ki = 29 nM; current results; Chapter 3, Horton et al., 2011b). Differential protein kinase C regulation of DA uptake and release sites on DAT (Gnegy, 2003) provides precedence for alternate recognition sites on VMAT2

that mediate DA uptake into and DA release from the vesicle. Thus, GZ-793A interacts with at least 3 sites on VMAT2 (Fig. 33), i.e., the intravesicular DA release site, the extravesicular DA uptake site and the extravesicular DTBZ binding site.

The goal of the current work was to identify compounds which have efficacy decreasing the neurochemical effects of METH as potential pharmacotherapeutics to treat METH abuse. METH evokes DA release from synaptic vesicles increasing the concentration of cytosolic DA available for reverse transport by DAT, leading to an increase in DA in the extracellular space (Sulzer et al. 2005). The current results demonstrate that low concentrations of the lead compound GZ-793A, that selectively interact with Hi-affinity sites on VMAT2 to evoke DA release, inhibit METH-evoked DA release from striatal synaptic vesicles. Results show that increasing concentrations of GZ-793A produced a rightward shift in the METH concentration response; however, the Schild regression revealed a slope different from unity, consistent with surmountable allosteric inhibition. Precedence for surmountable allosteric inhibition has been provided by previous research on nicotinic and muscarinic acetylcholine receptor antagonists (Tucek and Proska, 1995; Kukkonen et al., 2004; Wooters et al., 2011). Interpretations of concentration-response curves using Schild regression analysis are unambiguous with receptor binding data relative to functional data (Kenakin, 1993). However, the distinction between ligand-gated ion channel receptors and transporters has become blurred with a greater understanding of these proteins (Sonders and Amara, 1996; Galli et al.,

1996; Sonders et al., 1997). In accordance with the characteristics of an allosteric mechanism of inhibition (Kenakin, 2006), the shift to the right in the concentration response for METH-evoked DA release via VMAT2 should be diminished, as the allosteric site becomes saturated with increasing GZ-793A concentrations. Current results show a 5-fold shift in EC_{50} as the GZ-793A concentration progressed from 7 to 70 nM, but only a 1-2-fold shift was apparent with GZ-793A concentrations ranging from 70 to 1000 nM, consistent with an allosteric mechanism. Further support for surmountable allosteric inhibition of METH-evoked DA release by GZ-793A is derived from the current observation that the inhibitory effect of GZ-793A was not rate dependent, as evidenced by no differences in the METH concentration-response curves in the presence of GZ-793A with increasing incubation time. Thus, GZ-793A inhibits METH by producing a conformational change in the VMAT2 protein, reducing the affinity of METH for the intravesicular DA release site, without altering efficacy of METH to release DA.

While GZ-793 shares pharmacological characteristics with the classical VMAT2 inhibitors, TBZ and reserpine, there are also notable differences in their interaction with VMAT2. First, although GZ-793A, TBZ and reserpine are equipotent and completely inhibit DA uptake at the extravesicular site on VMAT2 (Partilla et al., 2006; Chapter 3, Horton et al., 2011b; Nickell et al., 2011), the inhibition produced by reserpine is irreversible (Rudnick et al., 1990), whereas inhibition produced by TBZ and GZ-793A is not (Near, 1986; data not shown). TBZ has been classified as a noncompetitive inhibitor of the DA uptake site on

VMAT2 (Scherman and Henry, 1984); however, our results indicate that TBZ inhibits DA uptake through a surmountable allosteric mechanism (Nickell et al., 2011). GZ-793A inhibition of DA uptake at VMAT2 also has been shown to be surmountable (Chapter 3, Horton et al., 2011b); although a Schild analysis has not been carried out to determine if GZ-793A-induced inhibition of DA uptake is via an allosteric or orthosteric mechanism. Second, these compounds differ in the order of potency for interaction at the extravesicular DTBZ binding site on VMAT2 (TBZ>reserpine>GZ-793A; Partilla et al., 2006; Chapter 3, Horton et al., 2011), supporting the interpretation that GZ-793A acts differently than TBZ and reserpine. Third, with respect to the intravesicular DA release sites, GZ-793A exhibited a different pattern for the concentration response compared to that for TBZ and reserpine. Specifically, the concentration-response curves for GZ-793A to evoke DA release from synaptic vesicles fit a two-site model of interaction, while those for TBZ and reserpine fit a one-site model. Further, GZ-793A released DA with greater efficacy (E_{max} = 88%) than either TBZ or reserpine (E_{max} = 48.5 and 28.4%, respectively), suggesting that GZ-793A has greater access to the ATP-associated pool of DA within the synaptic vesicles. Moreover, GZ-793A inhibited METH-evoked DA release at the Hi affinity DA release site via a surmountable allosteric mechanism, while TBZ-induced inhibition of METH-evoked DA release is consistent with a competitive mechanism of action. Taken together, GZ-793A exhibits a unique pharmacological profile in terms of its interaction with VMAT2.

In summary, GZ-793A likely interacts with at least three distinct sites on VMAT2: 1) the extravesicular DTBZ binding site (low affinity), 2) the extravesicular DA uptake site (high affinity) and 3) intravesicular DA release sites (high and low affinity). GZ-793A inhibits METH-evoked DA release from synaptic vesicles via a surmountable allosteric mechanism. As such, GZ-793A inhibits METH-induced increases in cytosolic DA by interacting with VMAT2. There are a limited number of available compounds that interact with VMAT2. The addition of GZ-793A to our armamentarium has augmented our understanding of VMAT2 function and has identified a specific pharmacological target to prevent METH's neurochemical action. GZ-793A represents a lead in the development of novel therapeutics for the treatment of METH abuse.

Table 4. Summary of EC_{50} and E_{max} for METH-evoked [^{3}H]DA release in the absence and presence of TBZ or GZ-793A

	EC_{50} (μM)	E_{max} (%)
TBZ on METH-evoked [^{3}H]DA release		
TBZ (0 nM)	8.93 ± 1.36	82.1 ± 1.21
TBZ (30 nM)	9.89 ± 2.44	83.4 ± 1.23
TBZ (100 nM)	45.5 ± 12.7 *	72.0 ± 1.39
TBZ (1 μM)	185 ± 31.1 *	88.1 ± 4.55
TBZ (10 μM)	366 ± 115 *	91.9 ± 10.3
GZ-793A on METH-evoked [^{3}H]DA release		
GZ-793A (0 nM)	18.9 ± 5.21	85.7 ± 1.22
GZ-793A (7 nM)	11.6 ± 1.37	86.2 ± 0.90
GZ-793A (70 nM)	56.3 ± 6.16 *	80.7 ± 3.50
GZ-793A (100 nM)	62.4 ± 8.10 *	82.7 ± 2.33
GZ-793A (1 μM)	119 ± 12.2 *	79.1 ± 4.02

*$p<0.05$ different from [^{3}H]DA release in the presence of METH alone and absence of TBZ or GZ-793A.

Table 5. Summary of TBZ and GZ-793A concentrations that significantly decreased METH-evoked [^{3}H]DA release compared to control.

METH	TBZ	GZ-793A
1 nM	-	-
10 nM	-	-
100 nM	-	-
300 nM	-	-
1 μM	-	1 μM
3 μM	10 μM	70 nM, 100 nM, 1 μM
10 μM	100 nM, 1 μM, 10 μM	70 nM, 100 nM, 1 μM
30 μM	100 nM, 1 μM, 10 μM	70 nM, 100 nM, 1 μM
100 μM	100 nM, 1 μM, 10 μM	70 nM, 100 nM, 1 μM
300 μM	100 nM, 1 μM, 10 μM	100 nM, 1 μM
1 mM	100 nM, 1 μM, 10 μM	100 nM, 1 μM

Fig. 27. Chemical structures of lobeline, lobelane, GZ-793A, TBZ, reserpine. Lobeline is the principal alkaloid found in *lobelia inflata*. Lobelane is the chemically defunctionalized, saturated analog of lobeline. GZ-793A is a *para*-methoxy analog of lobelane incorporating an N-propan-1,2-diol moiety. TBZ is a benzoquinolizine compound and VMAT2 inhibitor proposed to interact with a site distinct from the DA uptake site on VMAT2. Reserpine is an indole alkaloid and VMAT2 inhibitor, proposed to interact with the DA uptake site on VMAT2.

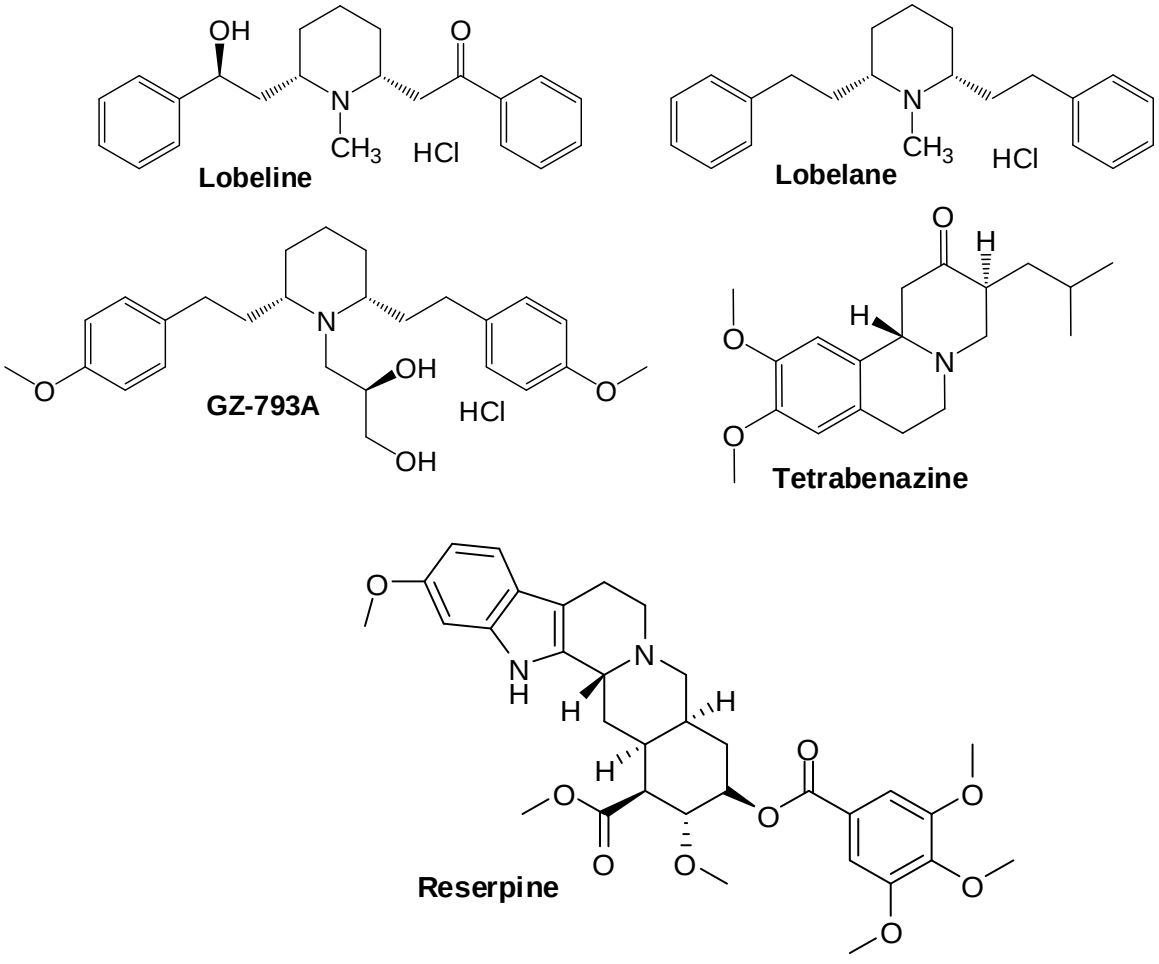

Fig. 28. GZ-793A-evoked [^{3}H]DA release from striatal vesicles fits a two-site model; DA release mediated by the high affinity site is TBZ- and reserpine-sensitive. Data represents the ability of GZ-793A to evoke [^{3}H]DA release from striatal vesicles in the absence (closed circles) and presence of TBZ (35 nM; open squares) or reserpine (50 nM, closed triangle). Control (CON) represents [^{3}H]DA release in the absence of GZ-793A. Data are mean (± S.E.M) [^{3}H]DA release as a percentage of the control. n = 4-8 rats/experiment.

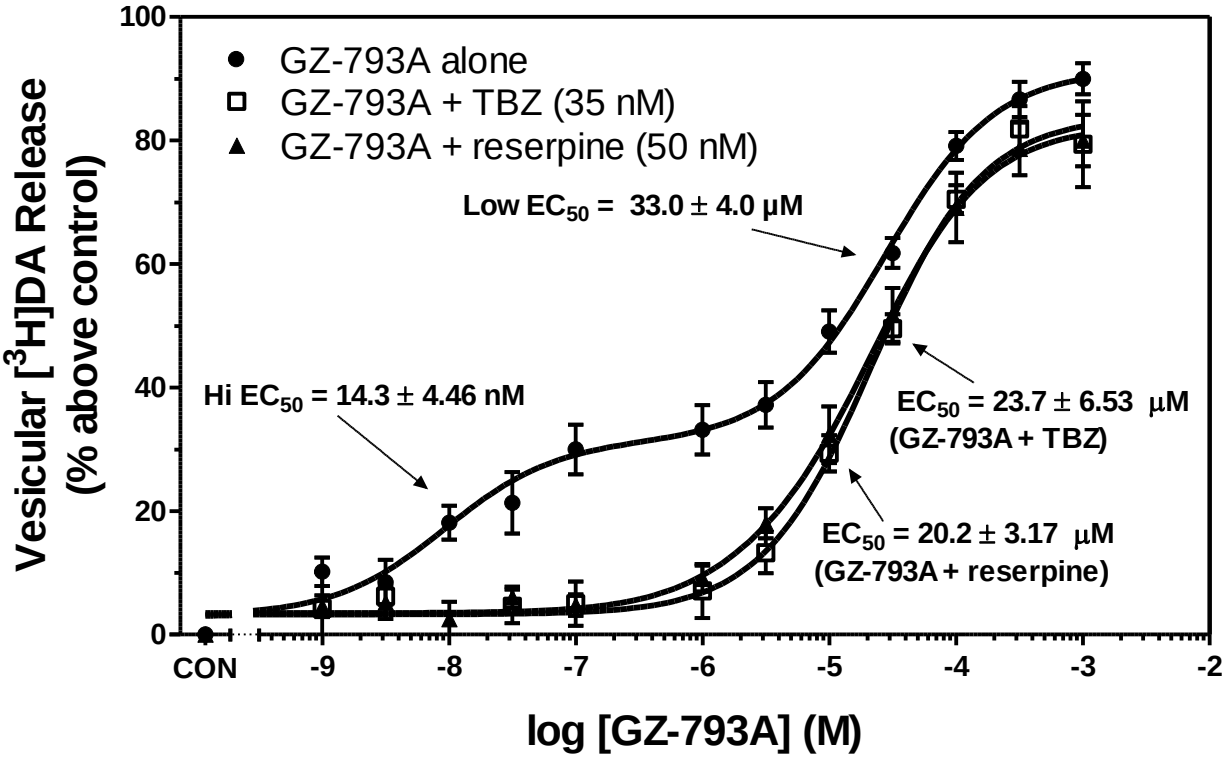

Fig. 29. Reserpine evoked [^{3}H]DA release from striatal synaptic vesicles. Data represents the ability of reserpine to evoke [^{3}H]DA release from striatal vesicles. GZ-793A-evoked [^{3}H]DA release (10 µM and 100 µM) was included as a positive control in the experiment (data not shown). Control (CON) represents [^{3}H]DA release in the absence of reserpine. Data are mean (± S.E.M) [^{3}H]DA release as a percentage of the control. n = 5 rats.

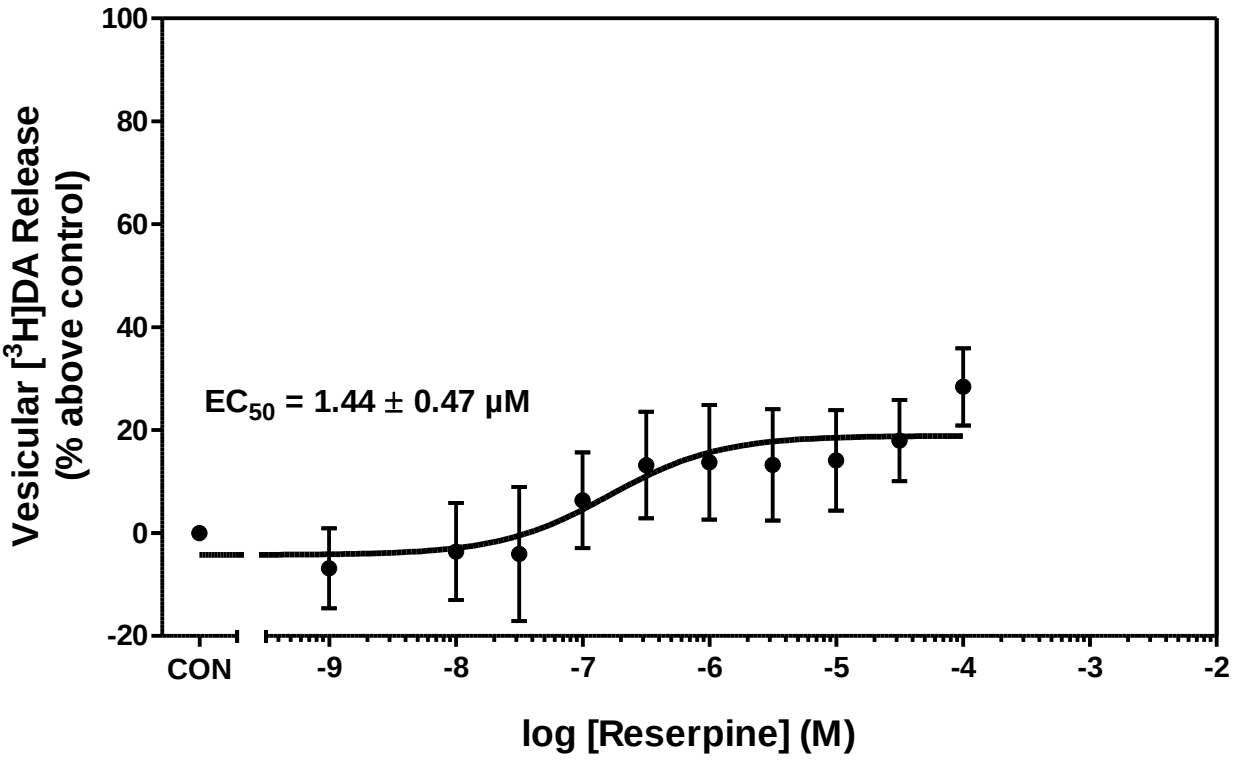

Fig. 30. TBZ inhibits METH-evoked [^{3}H]DA release from striatal vesicles. Data represents the ability of TBZ to inhibit METH-evoked [^{3}H]DA release from striatal vesicles. Control represents [^{3}H]DA release in the absence of METH and TBZ. Data are mean (± S.E.M) [^{3}H]DA release as a percentage of the control. n = 4-9 rats/experiment. Inset shows the Schild regression; log of DR−1 is plotted as a function of log of TBZ concentration.

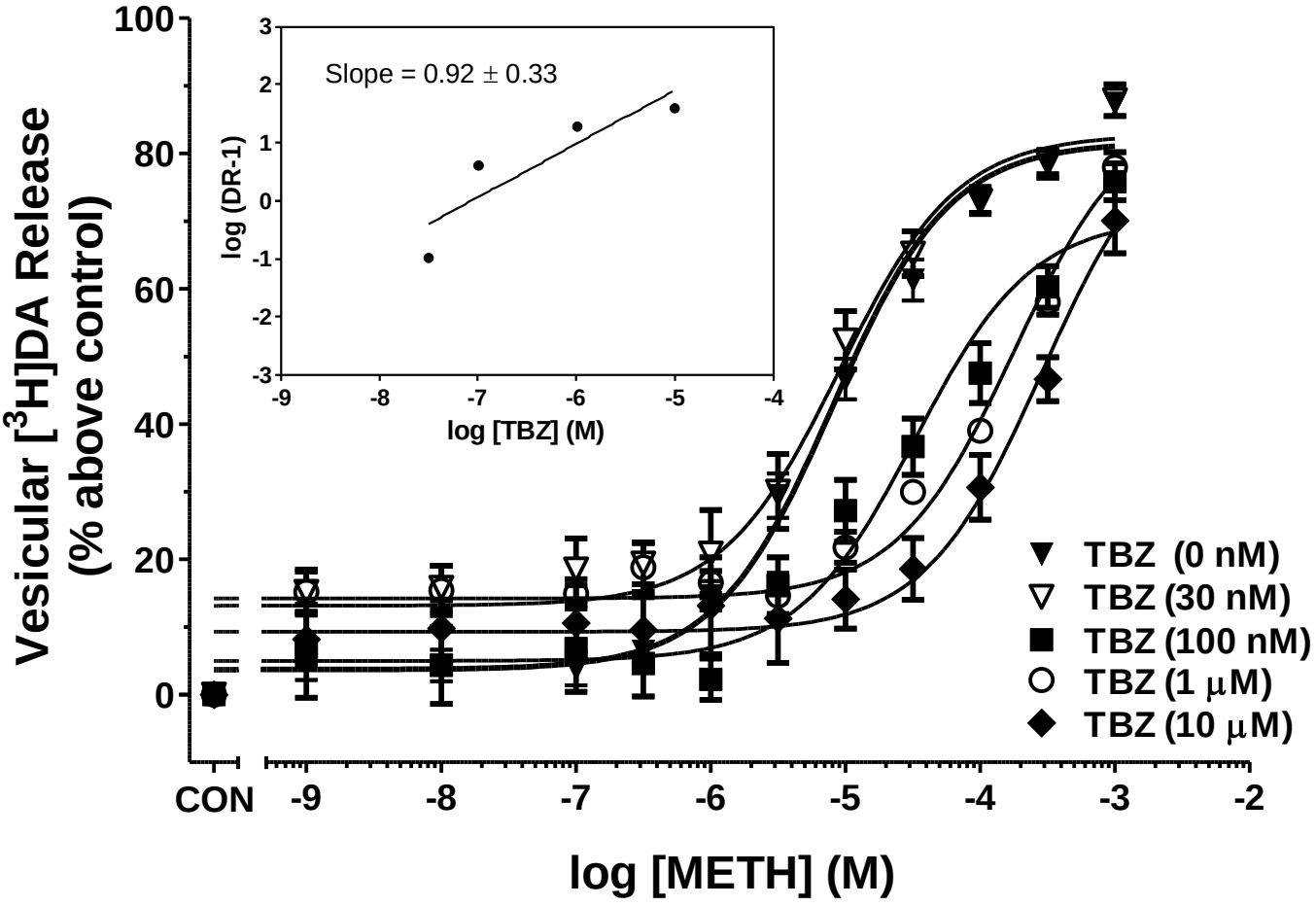

Fig. 31. GZ-793A inhibits METH (METH)-evoked [^{3}H]DA release from striatal vesicles. Data represents the ability of GZ-793A to inhibit METH-evoked [^{3}H]DA release from striatal vesicles. Control represents [^{3}H]DA release in the absence of METH and GZ-793A. Data are mean (± S.E.M) [^{3}H]DA release as a percentage of the control. n = 4-10 rats/experiment. Inset shows the Schild regression; log of DR−1 is plotted as a function of log of GZ-793A concentration.

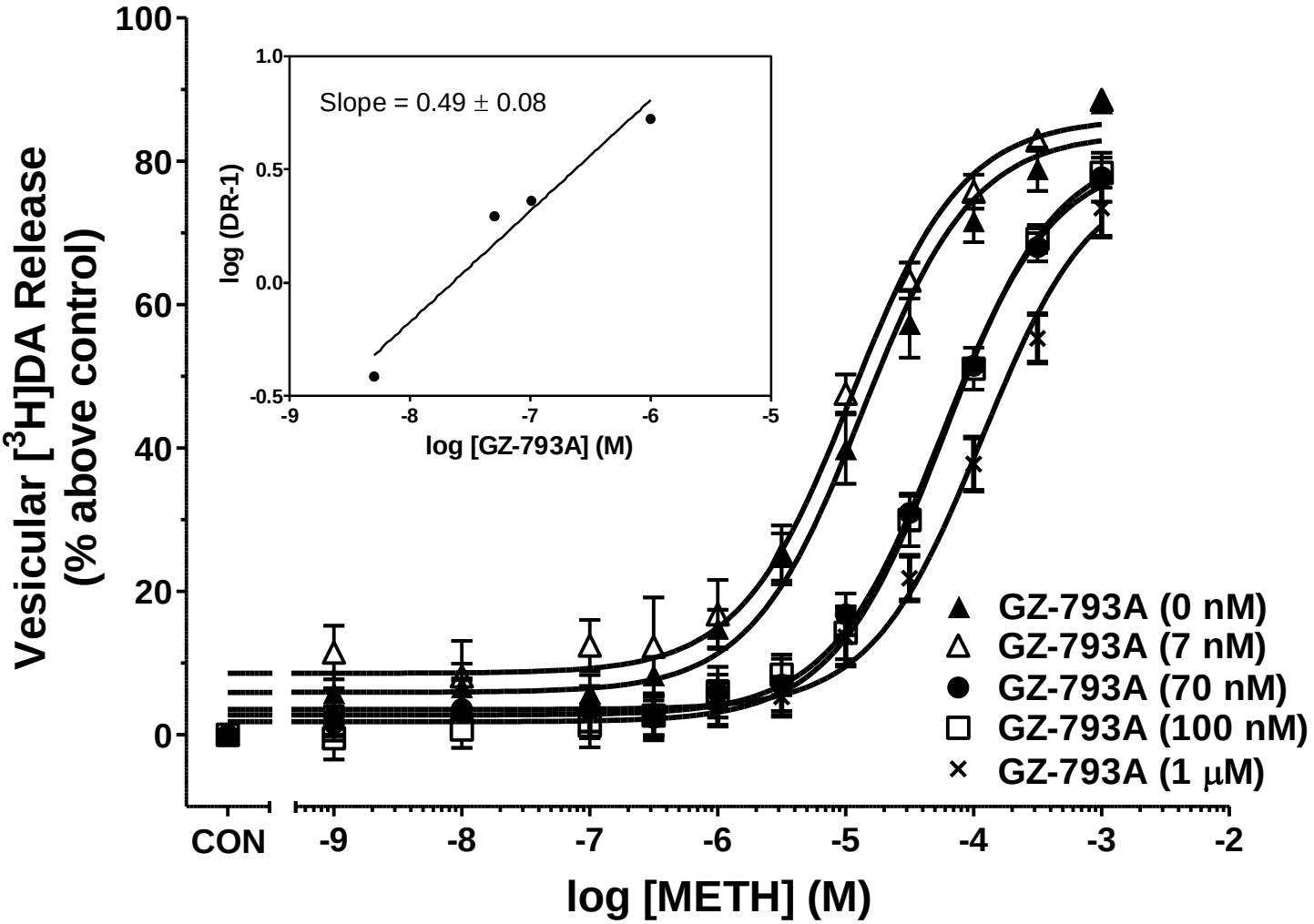

Fig 32. GZ-793A-induced inhibition of METH-evoked DA release is not rate-dependent. Data represents the ability of METH to evoke [^{3}H]DA release from striatal vesicles following 8 min incubation in the absence (closed circle) and presence of GZ-793A (1 μM; closed square) or following 15 min incubation in the absence (open circles) and presence of GZ-793A (1 μM; open square). Control (CON) represents [^{3}H]DA release in the absence of METH and GZ-793A. Data are mean (± S.E.M) [^{3}H]DA release as a percentage of the control. n = 3 rats.

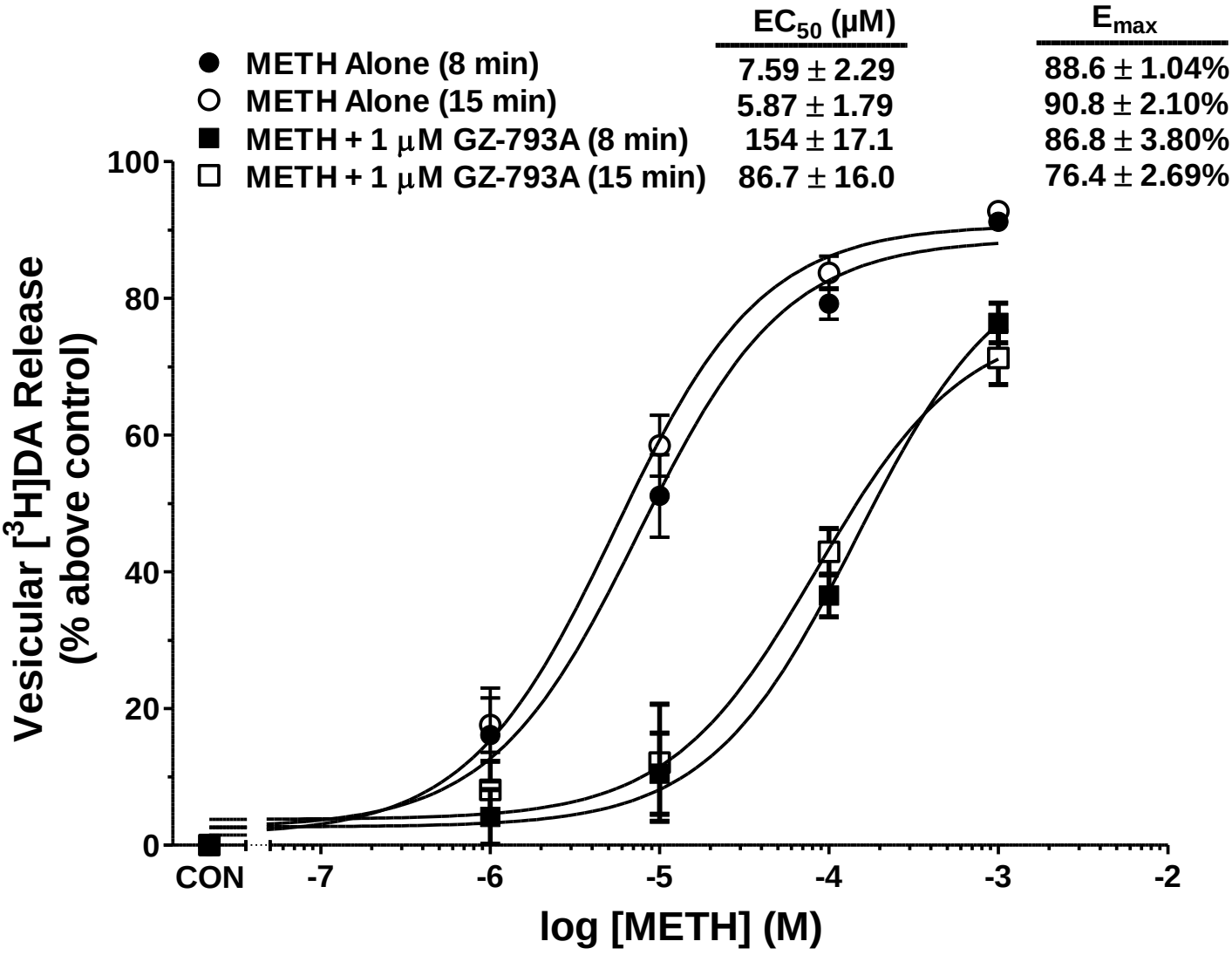

Fig 33. GZ-793A interacts with multiple sites on VMAT2. GZ-793A interacts with the extravesicular [^{3}H]DTBZ binding site (open square) with low affinity, the extravesicular [^{3}H]DA uptake site (closed circle) with high affinity, and intravesicular [^{3}H]DA release sites (TBZ- and reserpine-sensitive Hi-affinity site, closed triangle; TBZ- and reserpine-insensitive Low-affinity site, open triangle). Also illustrated is the proposed intravesicular site mediating GZ-793A-induced inhibition of METH-evoked DA release.

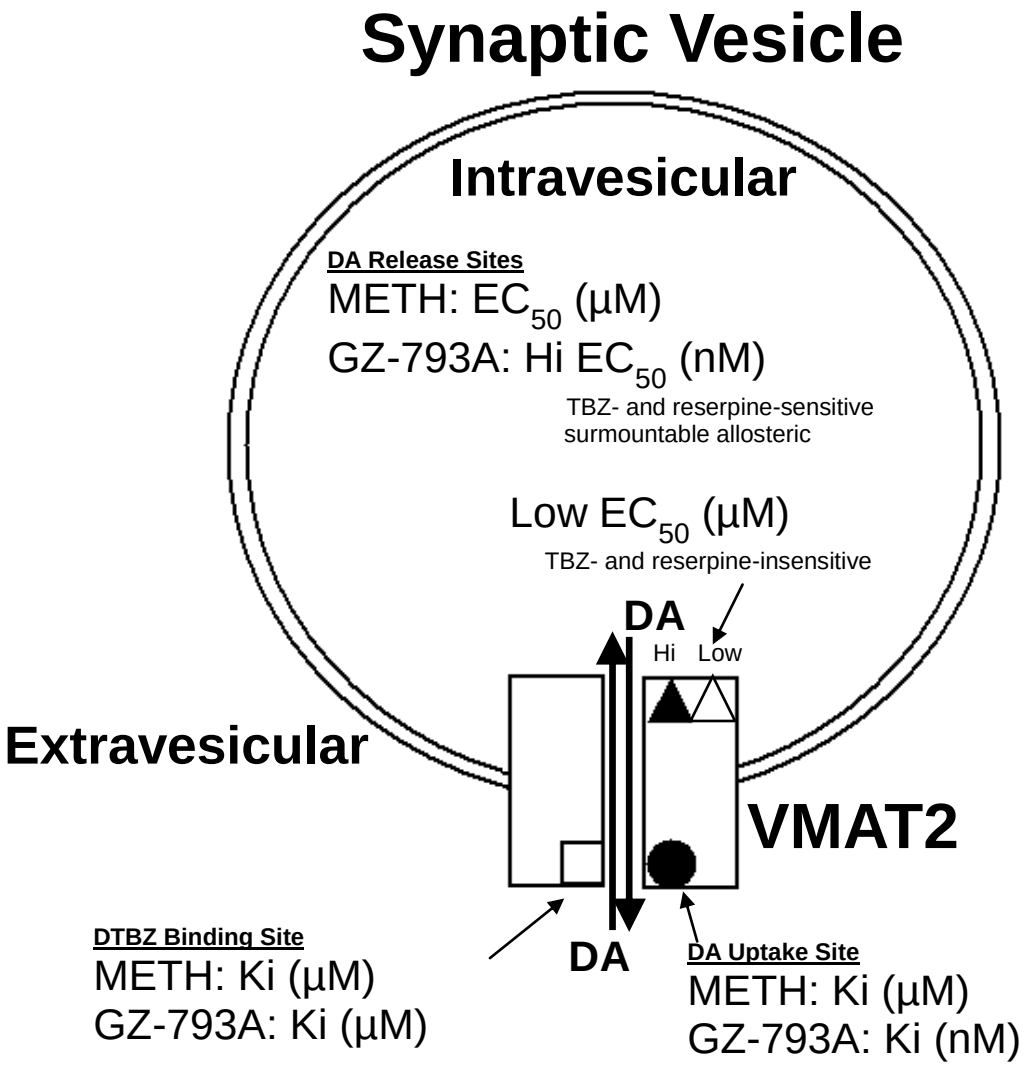

CHAPTER FIVE

Acute and Repeated GZ-793A Does Not Alter DA Content and GZ-793A Pretreatment Protects Against METH-Induced DA Content Depletion

Portions of this chapter have been submitted for publication in the manuscript:

Siripurapu KB, Horton DB, (co-first authors) Zheng G, Crooks PA, Dwoskin LP. GZ-793A does not exacerbate methamphetamine-induced dopamine depletions in striatal tissue and striatal vesicles. *Eur J Pharmacol*, submitted, 2011.

I. Introduction

METH is a highly addictive psychostimulant and currently no pharmacotherapies have been approved to treat its abuse. METH produces reward by increasing extracellular DA levels via VMAT2 and DAT interactions (Di Chiara and Imperato, 1988; Sulzer et al., 2005). Cytosolic DA levels are increased via inhibition of DA uptake at VMAT2 and by stimulation of vesicular release (Sulzer et al., 1995; Pifl et al., 1995). Reverse transport through DAT releases the cytosolic DA into the extracellular space (Fischer and Cho, 1979; Liang and Rutledge, 1982). Considerable effort has focused on VMAT2 as a pharmacological target in the discovery of compounds for treatment of METH abuse (Dwoskin and Crooks, 2002; Crooks et al., 2011; Wimalasena et al., 2011).

Lobeline, the major alkaloid of *Lobelia inflata*, interacts with VMAT2 to inhibit the neurochemical and behavioral effects of METH (Fig. 34; Miller et al., 2001; Harrod et al., 2001; Dwoskin and Crooks, 2002). However, lobeline is

nonselective, exhibiting high affinity for nicotinic receptors (Damaj et al., 1997). Structure-activity relationships revealed that chemical defunctionalization of lobeline affords lobelane, an analog with decreased water solubility, but increased potency and selectivity for VMAT2 (Fig. 34; Miller et al., 2004). Furthermore, lobelane decreased METH-induced DA release from striatal slices and METH self-administration in rats (Neugebauer et al., 2007; Nickell et al., 2010). Unfortunately, tolerance developed to the behavioral effects of lobelane (Neugebauer et al., 2007).

Structural modification of lobelane afforded GZ-793A (Fig. 34), which has increased water solubility, while retaining potency and selectivity for VMAT2 (Chapter 3, Horton et al., 2011b). GZ-793A inhibits METH-evoked DA release from striatal slices without altering electrical field stimulation- or nicotine-evoked DA release, indicating specific inhibition of METH. Also, GZ-793A decreases METH self-administration and conditioned place preference without altering food maintained responding (Beckmann et al., 2011). Thus, GZ-793A represents a new lead in the discovery of novel pharmacotherapeutics to treat METH abuse.

Classical VMAT2 inhibitors (e.g., reserpine, an irreversible VMAT2 inhibitor) deplete striatal DA content (Cleren et al., 2003), suggesting that GZ-793A may produce similar effects. METH also depletes striatal DA content, which serves as an index of dopaminergic neurotoxicity (Krasnova and Cadet, 2009). Furthermore, VMAT2 heterozygous knockout mice exhibit increased METH-induced neurotoxicity compared to wild-type mice (Fumagalli et al., 1999). Conversely, reversible VMAT2 inhibitors are neuroprotective against

dopaminergic toxicity. For example, tetrabenazine and lobeline attenuate dopaminergic neurotoxicity (Cleren et al., 2003; Eyerman and Yamamoto, 2005). As such, since GZ-793A interacts with VMAT2, it is imperative to evaluate the potential of this compound for both exacerbation and/or neuroprotection of METH-induced dopaminergic neurotoxicity. The outcome of these studies will provide important insights regarding the further development of GZ-793A as a lead compound for the treatment of METH abuse.

The hypothesis of this chapter is that VMAT2 inhibition by GZ-793A will not alter striatal DA content and GZ-793A pretreatment will protect against METH-induced DA content depletions in striatal tissue and vesicles.

II. Materials and Methods

IIa. Animals. Male Sprague-Dawley rats (200-250g, Harlan, Indianapolis, IN) were housed two per cage with *ad libitum* access to food and water in the Division of Laboratory Animal Resources at the University of Kentucky (Lexington, KY, USA). Experimental protocols involving the animals were in accord with the 1996 *NIH Guide for the Care and Use of Laboratory Animals* and were approved by the Institutional Animal Care and Use Committee at the University of Kentucky.

IIb. Chemicals. $CaCl_2$, citric acid, $MgCl_2$, KCl, K_2PO_4, $NaHCO_3$ and NaH_2PO_4 were purchased from Fisher Scientific Co. (Pittsburgh, PA, USA). Ascorbic acid, ascorbate oxidase, DA, EDTA, EGTA, d-glucose, HEPES, METH, $MgSO_4$, octane sulphonic acid, potassium tartrate, NaCl and sucrose were

purchased from Sigma-Aldrich (St. Louis, MO, USA). GZ-793A was synthesized according to previously reported methods (Chapter 3, Horton et al., 2011b).

IIc. Experimental Design. To determine the effect of acute GZ-793A on DA content in striatal tissue and vesicles, GZ-793A (15 mg/kg; s.c) or saline was administered. The GZ-793A dose was selected based upon behavioral studies showing efficacy to decrease METH self-administration and conditioned place preference (Beckmann et al., 2011). To determine the effect of acute GZ-793A alone on DA content, GZ-793A or saline was administered s.c. and striata (8 and 65 mg) were obtained 0.3, 1.3, 8, or 24 hr post-injection for tissue and vesicular DA content assays, respectively. To determine the interaction of acute GZ-793A with METH, GZ-793A (15 mg/kg; s.c.) or saline was injected 20 min prior to METH (0, 5 or 10 mg/kg; i.p.), and 3 days later, striata were obtained for tissue and vesicular DA content assays. Doses of METH and the time point following administration were chosen based on previous findings (Xi et al., 2009).

The effect of repeated 7-day pre-treatment with GZ-793A (15 mg/kg, once daily; s.c) on the acute METH (10 mg/kg; i.p) induced depletion of DA content was determined. METH was administered 20 min after the last GZ-793A dose on Day 7. Striata were obtained 3 days subsequently. The effect of GZ-793A (15 mg/kg; s.c) pre-treatment on striatal DA depletion induced by a METH treatment regimen (7.5 mg/kg x 4, 2-hr injection intervals; i.p.) traditionally used to deplete DA (Stephans and Yamamoto, 1996; Chapman et al., 2001; Eyerman and Yamamoto, 2005) was determined. GZ-793A or saline was administered 20 min prior to each dose of METH. Striata were obtained 7 days after the last

treatment. Doses of METH and the pre-treatment time point following administration were chosen based on previous findings (Eyerman and Yamamoto, 2005). Also, the effect of GZ-793A (15 mg/kg; s.c) post-treatment on striatal DA depletion induced by METH (7.5 mg/kg x 4 at 2 hr injection intervals; i.p) was determined. GZ-793A or saline was administered 5 and 7 hr after each dose of METH. Striata were obtained 7 days after the last treatment. Doses of METH and the post-treatment time point following administration were chosen based on previous findings (Eyerman and Yamamoto, 2005).

IId. Tissue and vesicle preparation for DA content assay. Striata from each rat were used to prepare both tissue (8 mg) and vesicle (65 mg) preparations for the content assay. Striata were sonicated in 1 ml of 0.1 M perchloric acid and the suspension centrifuged at 20,000 g for 30 min. Supernatants (50 µl) were injected into the HPLC with electrochemical detection to determine tissue DA content.

Striatal vesicle preparations were prepared as previously reported (Chapter 2, Horton et al., 2011a). Striata were homogenized in 14 ml of ice-cold 0.32 M sucrose solution containing 5 mM $NaHCO_3$ (pH 7.4) with 10 up-and-down strokes of a Teflon pestle homogenizer (clearance = 0.008”). Homogenates were centrifuged at 2,000 g for 10 min at 4 °C and resulting supernatants centrifuged at 10,000 g for 30 min at 4 °C. Pellets were resuspended in 2.0 ml of 0.32 M sucrose and were transferred to tubes containing 7 ml of milliQ water and homogenized with 5 up-and-down strokes. Homogenates were transferred to tubes containing 900 µl of 0.25 M HEPES and 900 µl of 1.0 M potassium tartrate

solution and centrifuged at 20,000 g for 20 min at 4 ºC. Resulting supernatants were centrifuged at 55,000 g for 60 min at 4 ºC. Subsequently, 100 µl of 1 mM $MgSO_4$, 100 µl of 0.25 M HEPES and 100 µl of 1.0 M potassium tartrate were added to the supernatant and centrifuged at 100,000 g for 45 min at 4 ºC. Final pellets were resuspended in 1.2 ml of milliQ water. Vesicle suspensions were sonicated at 4^{o} C for 5 min and centrifuged at 20,000 g for 15 min. Supernatants (50 µl) were injected into the HPLC with electrochemical detection for determination of vesicular DA content.

IIe. DA content determination by HPLC with electrochemical detection. HPLC-EC determination of DA content was performed by Kiran Siripurapu, Ph.D.. HPLC with electrochemical detection consisted of a pump and auto-sampler (508 Beckman Coulter, Inc., Fullerton, CA, USA) and an ODS ultrasphere C18 reverse-phase column (80 × 4.6 mm, 3-µm ESA Inc., Chelmsford, MA, USA). Analytes were detected with a coulometric-II detector with guard cell (model 5020) maintained at +0.60 V and an analytical cell (model 5011) maintained at potentials E1 = 0.05 V & E2 = +0.32 V (ESA, Inc). The mobile phase was 0.07 M citrate/0.1 M acetate buffer (pH 4) containing, 175 mg/l octylsulfonic acid-sodium salt, 650 mg/l of NaCl and 7% methanol. Separations were performed at room temperature at a flow rate of 1.5 ml/min, and 5-6 min were required to process each sample. Retention times of DA and dihydroxyphenylacetic acid (DOPAC) standards were used to identify peaks. Peak heights were used to quantify detected amounts on the basis of standard curves. Detection limits for DA and DOPAC were 1 and 2 pg/100 µl, respectively.

Peak integrations and analyses were performed by using 32 karat software (Beckman Coulter, Inc.).

IIf. Data analysis. DA content was expressed as mean ± S.E.M. ng/mg wet weight for striatal tissue content assays and ng/mg protein for vesicular content assays. The effect of acute GZ-793A on DA content was analyzed using a two-way ANOVA with GZ-793A treatment and time as between-subjects factors.

Both the concentration effect of METH to deplete striatal DA content and the effect of acute GZ-793A pre-treatment on METH depletion were analyzed using a two-way ANOVA, with GZ-793A pre-treatment and METH dose as between-subject factors.

The effect of repeated GZ-793A pre-treatment on depletion of DA content induced by acute METH treatment was analyzed using a two-way ANOVA followed by Tukey's *post hoc* analysis to determine significant differences between the treatment groups and respective controls. The effect of GZ-793A pre-treatment on DA depletion induced by repeated METH was analyzed using a two-way ANOVA, followed by Tukey's *post hoc* analysis to determine differences between treatment groups and respective controls. The effect of repeated METH treatment followed by GZ-793A was analyzed using a two-way ANOVA followed by Tukey's *post hoc* analysis to determine differences between treatment groups and respective controls. Statistical analyses were conducted using SPSS (version 17.0; SPSS Inc., Chicago, IL, USA) and GraphPad PRISM (version 5.0;

Graph Pad Software, Inc., San Diego, CA, USA). Statistical significance was defined as $p < 0.05$.

III. Results

IIIa. GZ-793A does not alter striatal DA content. DA content in striatal tissue and vesicles 0.3, 1.3, 8 and 24 hr following GZ-793A treatment is provided in Table 6. Analysis of striatal DA content by two-way ANOVA failed to reveal a main effect of GZ-793A treatment ($F_{1,56} = 1.45$, $p > 0.05$] or a GZ-793A treatment x time interaction $F_{3,56} = 0.06$, $p > 0.05$); however a main effect of time ($F_{3,56} = 10.6$, $p < 0.05$) was observed. Analysis of vesicular DA content by two-way ANOVA also failed to reveal main effects of GZ-793A treatment ($F_{1,56} = 0.04$, $p > 0.05$) and time ($F_{3,56} = 1.25$, $p > 0.05$), and no GZ-793A treatment x time interaction ($F_{3,56} = 0.76$, $p > 0.05$).

IIIb. Acute GZ-793A pre-treatment attenuates the acute METH-induced decrease in striatal tissue and vesicular DA content. Fig. 35 illustrates the effect of GZ-793A pre-treatment on METH-induced decreases in striatal tissue and vesicular DA content (top and bottom panel, respectively). Analysis of DA content in striatal tissue by two-way ANOVA failed to reveal a main effect of GZ-793A pre-treatment $F_{1,42} = 3.39$, $p > 0.05$) and no GZ-793A x METH interaction ($F_{2,42} = 1.66$, $p > 0.05$); however, a main effect of METH dose ($F_{2,42} = 6.96$, $p < 0.05$) was found.

Analysis of vesicular DA content by two-way ANOVA revealed main effects of GZ-793A pre-treatment ($F_{1,42} = 4.56$, $p < 0.05$) and METH dose $F_{2,42} =$

3.54, $p < 0.05$) and a GZ-793A x METH interaction ($F_{2,42} = 3.31$, $p < 0.05$). Further evaluation of the effect of METH in saline pre-treated rats by one-way ANOVAs revealed a main effect of METH dose ($F_{2,21} = 9.51$, $p < 0.05$). *Post hoc* analysis revealed that METH (5 and 10 mg/kg) significantly decreased DA content in striatal vesicles compared to the respective saline control. Also, one-way ANOVA on the dose effect of METH following GZ-793A pre-treatment did not reveal a main effect of METH dose ($F_{2,21} = 0.44$, $p > 0.05$). The latter result demonstrates that GZ-793A pre-treatment attenuated the METH-induced decrease in DA content in striatal vesicles.

IIIc. Repeated GZ-793A pre-treatment attenuates the acute METH-induced decrease in striatal tissue or vesicular DA content. The effect of repeated GZ-793A pre-treatment on the acute METH (10 mg/kg) induced decrease in striatal tissue and vesicular DA content is illustrated in Fig. 36 (top panel and bottom panel, respectively). Analysis of DA content in striatal tissue following GZ-793A pre-treatment and acute METH by two-way ANOVA revealed a main effect of METH treatment ($F_{1,35} = 4.29$, $p < 0.05$) and a GZ-793A x METH interaction ($F_{1,35} = 6.58$, $p < 0.05$); however, a main effect of GZ-793A pre-treatment ($F_{1,35} = 0.60$, $p > 0.05$) was not found. *Post hoc* analysis revealed that DA content was decreased in the saline + METH group compared to the saline control group. Also, striatal DA content in both the GZ-793A + saline and the GZ-793A + METH groups were not different from the saline control group. Thus, repeated GZ-793A alone did not decrease striatal DA content and repeated GZ-793A attenuated the METH-induced decrease in striatal DA content.

Analysis of vesicular DA content following GZ-793A pre-treatment and acute METH treatment by two-way ANOVA revealed a GZ-793A x METH interaction ($F_{1,36} = 4.87$, $p < 0.05$); however, main effects of GZ-793A pre-treatment ($F_{1,36} = 0.54$, $p > 0.05$) and METH treatment ($F_{1,36} = 3.51$, $p > 0.05$) were not found. *Post hoc* analysis revealed that vesicular DA content in the saline + METH group was decreased relative to the saline control group. Furthermore, vesicular DA content for both the GZ-793A + saline group and the GZ-793A + METH group was not different from that for the saline control group. Thus, repeated GZ-793A alone did not alter vesicular DA content and repeated GZ-793A pre-treatment attenuated the METH-induced decrease in vesicular DA content.

IIId. GZ-793A pre-treatment does not exacerbate DA depletion in striatal tissue or vesicles induced by METH (7.5 mg/kg x 4). The effect of GZ-793A pre-treatment on striatal DA depletion induced by METH (7.5 mg/kg x 4, 2-hr injection intervals) is provided in Fig. 37 and Table 7. Analysis of DA content in striatal tissue by two-way ANOVA revealed a main effect of METH treatment ($F_{1,36} = 14.2$, $p < 0.05$); however, no main effect of GZ-793A pre-treatment ($F_{1,36} = 0.21$, $p > 0.05$) and no GZ-793A x METH interaction ($F_{1,36} = 2.94$, $p > 0.05$) was observed. Striatal DA content was decreased in both the saline + METH and GZ-793A + METH treatment groups compared to the saline control group; and moreover, the GZ-793A + METH group was not different from the saline + METH group. Thus, repeated GZ-793A pre-treatment (15 mg/kg x 4) did not alter the

depletion in striatal DA content induced by a METH regimen traditionally employed to deplete striatal DA.

Analysis of vesicular DA content by two-way ANOVA failed to reveal main effects of GZ-793A pre-treatment ($F_{1,36} = 0.86$, $p > 0.05$), METH ($F_{1,36} = 2.15$, $p > 0.05$), and GZ-793A x METH interaction ($F_{1,36} = 1.00$, $p > 0.05$).

IIIe. GZ-793A post-treatment does not exacerbate depletion of striatal tissue or vesicular DA content induced by METH (7.5 mg/kg x 4). The effect of GZ-793A treatment 5 hrs and 7 hrs after METH (7.5 mg/kg x 4, 2-hr injection intervals) on striatal tissue and vesicular DA content is provided in Fig. 38 and Table 8, respectively. Analysis of DA content in striatal tissue by two-way ANOVA revealed a main effect of METH ($F_{1,19} = 52.0$, $p < 0.05$), but no main effect of GZ-793A post-treatment ($F_{1,19} = 0.18$, $p > 0.05$) and no GZ-793A x METH interaction ($F_{1,19} = 0.32$, $p >0.05$). Striatal DA content was decreased in both the METH + saline and METH + GZ-793A treatment groups compared to the saline control group; and moreover, the GZ-793A + METH group was not different from the saline + METH group. Thus, repeated post-treatment with GZ-793A (15 mg/kg) did not alter the depletion in striatal DA content induced by METH (7.5 mg/kg x 4).

Analysis of vesicular DA content by two-way ANOVA failed to reveal main effects of GZ-793A pre-treatment ($F_{1,19} = 0.19$, $p > 0.05$), METH treatment ($F_{1,19} = 0.22$, $p > 0.05$) and no GZ-793A x METH interaction effect ($F_{1,19} = 1.25$, $p > 0.05$) was observed.

IV. Discussion

In a concentration-dependent manner, GZ-793A potently and selectively inhibits VMAT2 function and evokes DA release from vesicles (Chapter 3, Horton et al., 2011a; Chapter 4, Horton et al.,2011c). Despite the ability of GZ-793A to alter VMAT2 function, the current results show that GZ-793A administered acutely and repeatedly did not alter striatal DA content across a 24 hr time period following treatment with a behaviorally relevant dose. Importantly, GZ-793A inhibits METH-evoked DA release from striatal vesicles and slices (Chapter 3, Horton et al., 2011b; Chapter 4, Horton et al., 2011c). Moreover, these *in vitro* observations translated to the whole animal model, since GZ-793A decreased METH self-administration (Beckmann et al., 2011). The current results further show that acute and repeated GZ-793A pre-treatment attenuated the acute METH-induced decrease in striatal DA content. Pertinent to the development of GZ-793A as a lead compound for the treatment of METH abuse, GZ-793A did not exacerbate DA depletion induced by a repeated high dose regimen of METH. Thus, the ability of GZ-793A to decrease METH self-administration is not accompanied by an exacerbation of METH-induced dopaminergic neurotoxicity. These results further advance GZ-793A as a preclinical lead in the development of pharmacotherapies to treat METH abuse.

GZ-793A is a structural synthetic analog of lobeline, the major alkaloid from *Lobelia inflata*. Similar to the current findings with GZ-793A, previous work showed that lobeline, across a wide dose range, did not alter striatal DA content during the 24-hr period following its acute or repeated administration (Miller et al.,

2001). Importantly, both lobeline pre-treatment and post-treatment was shown to attenuate DA depletion induced by a neurotoxic regimen of METH (Eyerman and Yamamoto, 2005).

In the current study, acute METH (5 and 10 mg/kg) decreased striatal tissue and vesicular DA content consistent with previous results (Xi et al., 2009). Acute and repeated GZ-793A pre-treatment attenuated the DA depletion induced by acute METH treatment (5 and 10 mg/kg). Recent studies show that GZ-793A decreases METH-evoked DA release from vesicles via a surmountable allosteric mechanism (Chapter 4, Horton et al., 2011c), which thereby may have limited the METH-induced striatal DA depletion. An alternative explanation is that GZ-793A may interact with DAT to attenuate the METH-induced DA depletion. DAT inhibitors, including GBR-12909, buproprion and mazindol, attenuate METH-induced depletion of striatal DA content by inhibiting METH-evoked DA release (Marek et al., 1990; Stephans and Yamamoto, 1994). Similarly, GZ-793A may interact with DAT to inhibit METH-induced reverse transport (release) of DA and the METH-induced decrease in striatal DA content. However, GZ-793A is 50-fold more potent inhibiting VMAT2 function than inhibiting DAT function (Chapter 3, Horton et al., 2011b). Furthermore, the observation that GZ-793A is not self-administered in rats (Beckmann et al., 2011), diminishes support for an interaction with DAT as the underlying mechanism for its ability to attenuate METH toxicity.

Although GZ-793A attenuated the DA depletion induced by acute METH, GZ-793A did not alter DA depletion in striatal tissue induced by a neurotoxic

regimen of METH in contrast with the neuroprotection afforded by lobeline. This difference in neuroprotection between GZ-793A and lobeline may be due to the doses chosen to evaluate the interaction with METH. The GZ-793A dose (15 mg/kg) was chosen due to its behavioral relevance, i.e., this dose decreased METH self-administration in rats (Beckmann et al., 2011). Conversely, a high dose (10 mg/kg) of lobeline was evaluated for interaction with METH (Eyerman and Yamamoto, 2005); this high dose was shown to nonspecifically decrease METH self-administration (Harrod et al., 2001). In this regard, a higher dose of GZ-793A also may attenuate the dopaminergic depletion induced by the neurotoxic regimen of METH. Another potential explanation for the difference in neuroprotection between GZ-793A and lobeline may be that lobeline also acts as a nicotinic receptor antagonist, whereas GZ-793A does not (Damaj et al., 1997; Flammia et al., 1999; Miller et al., 2004; Siripirapu et al., 2011). Furthermore, support for the involvement of nicotinic receptors in lobeline neuroprotection is the observation that methyllycaconitine, an α7 nicotinic receptor antagonist, protected against METH-induced dopaminergic neurotoxicity (Northrop et al., 2011). Thus, the selectivity of GZ-793A for VMAT2 and the lack of interaction with nicotinic receptors could explain the difference between GZ-793A and its parent compound to attenuate the dopaminergic neurotoxicity induced by METH.

Although the neurotoxic regimen of METH (7.5 mg/kg x 4) depleted DA in striatal tissue content, vesicular DA content was not depleted significantly. Furthermore, although vesicular DA was depleted by ~40% three days following acute METH (10 mg/kg), striatal vesicles were not depleted significantly seven

days after the neurotoxic regimen of METH. These results support the concept that vesicular DA stores are more resilient to depletion induced by METH compared with striatal tissue DA, and that compensation may have occurred by 7 days to restore vesicular DA levels. The current results are in contrast with a recent study reporting that vesicular DA was depleted by 50% 7 days following METH (10 mg/kg x 4) administration (Northrop et al., 2011). Methodological differences between the studies may be responsible for the contrasting observation, i.e., different doses of METH employed, and different procedures for vesicle preparation. Nonetheless, GZ-793A did not potentiate the ability of METH to deplete vesicular DA content. Furthermore, the METH regimen (7.5 mg/kg x 4) employed in the current study depleted DA content in the striatal tissue, and this depletion was not exacerbated by GZ-793A pre-treatment or post-treatment. Thus, GZ-793A did not protect, but also did not exacerbate, the dopaminergic neurotoxicity induced by repeated high dose METH.

In summary, results from the current study demonstrate that acute or repeated GZ-793A alone does not alter DA content in striatal tissue or vesicles. Furthermore, GZ-793A pre-treatment attenuates the acute METH-induced decrease in DA content, and importantly, does not exacerbate DA depletion following repeated high dose METH administration. Thus, behaviorally relevant doses of GZ-793A did not alter DA content when administered alone, and did not exacerbate striatal DA depletion induced by METH. In conclusion, GZ-793A represents an exciting preclinical lead candidate for the treatment of METH abuse.

Table 6. Striatal tissue and vesicular DA content at various time points following saline or GZ-793A (15 mg/kg) treatment.

Time (hrs)	Tissue DA Content (ng/mg tissue)		Vesicular DA Content (ng/mg protein)	
	Saline	GZ-793A	Saline	GZ-793A
0.3	3.03 ± 0.58	2.36 ± 0.49	0.28 ± 0.06	0.32 ± 0.14
1.3	4.65 ± 0.77	4.15 ± 0.61	0.18 ± 0.01	0.14 ± 0.05
8	1.97 ± 0.52	1.75 ± 0.32	0.09 ± 0.003	0.08 ± 0.01
24	5.25 ± 0.59	4.56 ± 0.87	0.07 ± 0.01	0.06 ± 0.01

Data are mean ± S.E.M.; n = 8 rats/treatment

Table 7. The effect of GZ-793A pretreatment (15 mg/kg) 20 minutes prior to a traditional regimen of METH administration (7.5 mg/kg x 4; every 2 hrs) on striatal vesicular DA content.

Treatment Group	Vesicular DA Content (ng/mg protein)
Saline/Saline	0.11 ± 0.01
GZ-793A/Saline	0.13 ± 0.01
Saline/METH	0.10 ± 0.01
GZ-793A/METH	0.09 ± 0.1

Data are mean ± S.E.M.; n = 10 rats/treatment

Table 8. The effect of GZ-793A post-treatment (15 mg/kg) 5 and 7 hrs after a traditional regimen of METH administration (7.5 mg/kg x 4; every 2 hrs) on striatal vesicular DA content.

Treatment Group	Vesicular DA Content (ng/mg protein)
Saline/Saline	0.10 ± 0.01
Saline/GZ-793A	0.08 ± 0.01
METH/Saline	0.08 ± 0.01
METH/GZ-793A	0.09 ± 0.01

Data are mean ± S.E.M.; n = 5-6 rats/treatment

Fig. 34. Chemical structures of lobeline, lobelane, and GZ-793A. Lobeline is the principle alkaloid found in *Lobelia inflata*. Lobelane is the defunctionalized, saturated analog of lobeline. GZ-793A is a 4-methoxyphenyl analog of lobelane incorporating an N-1,2-diol moiety.

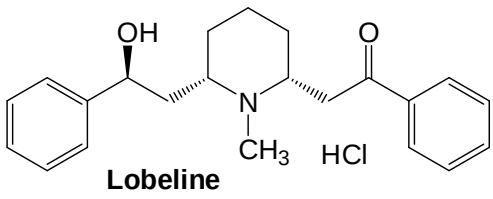

Lobeline

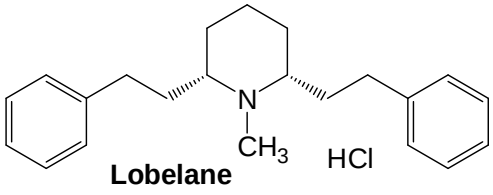

Lobelane

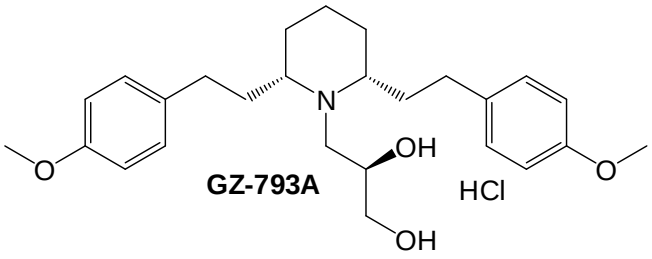

GZ-793A

Fig. 35. Acute GZ-793A pre-treatment attenuates acute methamphetamine-induced decreases in striatal tissue or vesicular dopamine content. Data are shown as ng/mg tissue and ng/mg protein for tissue (top panel) and vesicles (bottom panel), respectively and expressed as mean ± S.E.M. *p < 0.05 different from saline control. n = 8-12 rats/treatment.

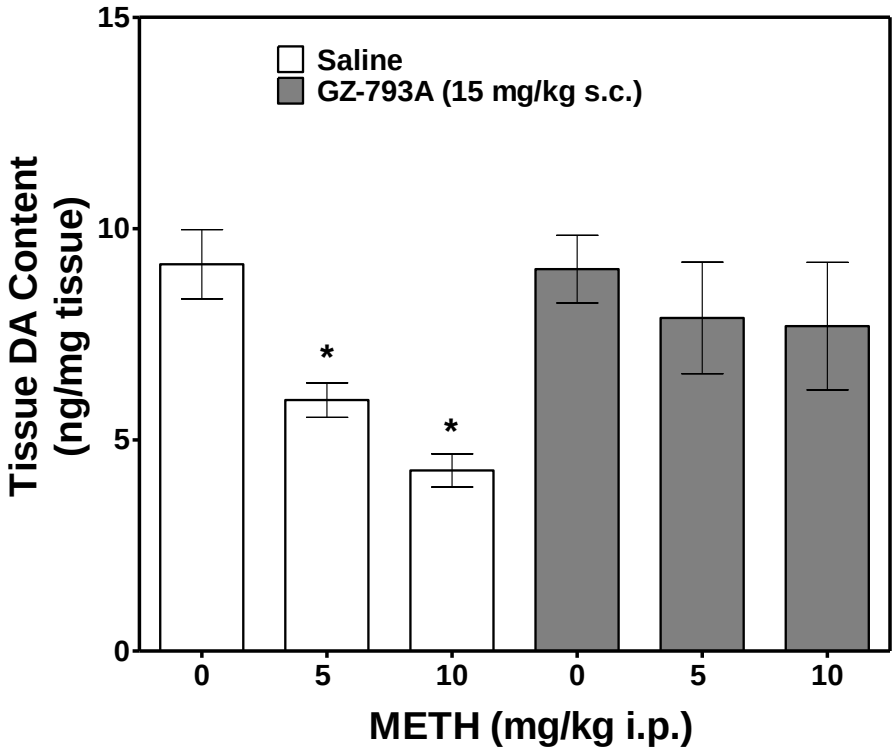

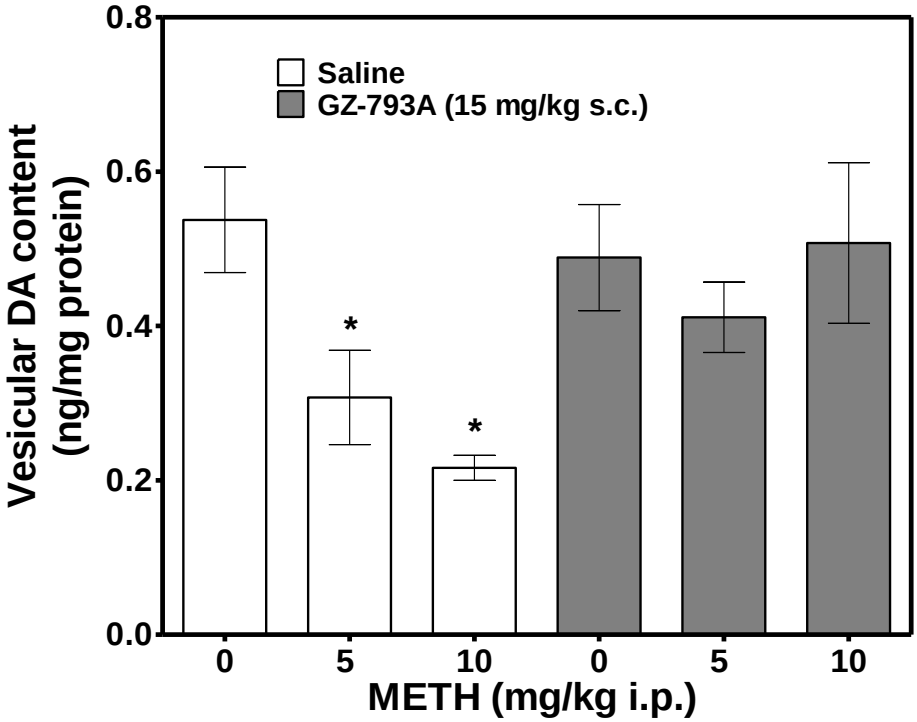
Saline
GZ-793A (15 mg/kg s.c.)
Vesicular DA content
(ng/mg protein)
0.0
0.2
0.4
0.6
0.8
*
*
0
5
10
0
5
10
METH (mg/kg i.p.)

Fig. 36. Repeated GZ-793A pre-treatment attenuates acute methamphetamine-induced decreases in striatal tissue or vesicular dopamine content. Data are shown as ng/mg tissue and ng/mg protein for tissue (top panel) and vesicles (bottom panel), respectively and expressed as mean ± S.E.M. *p < 0.05 different from saline control. n = 10 rats/treatment.

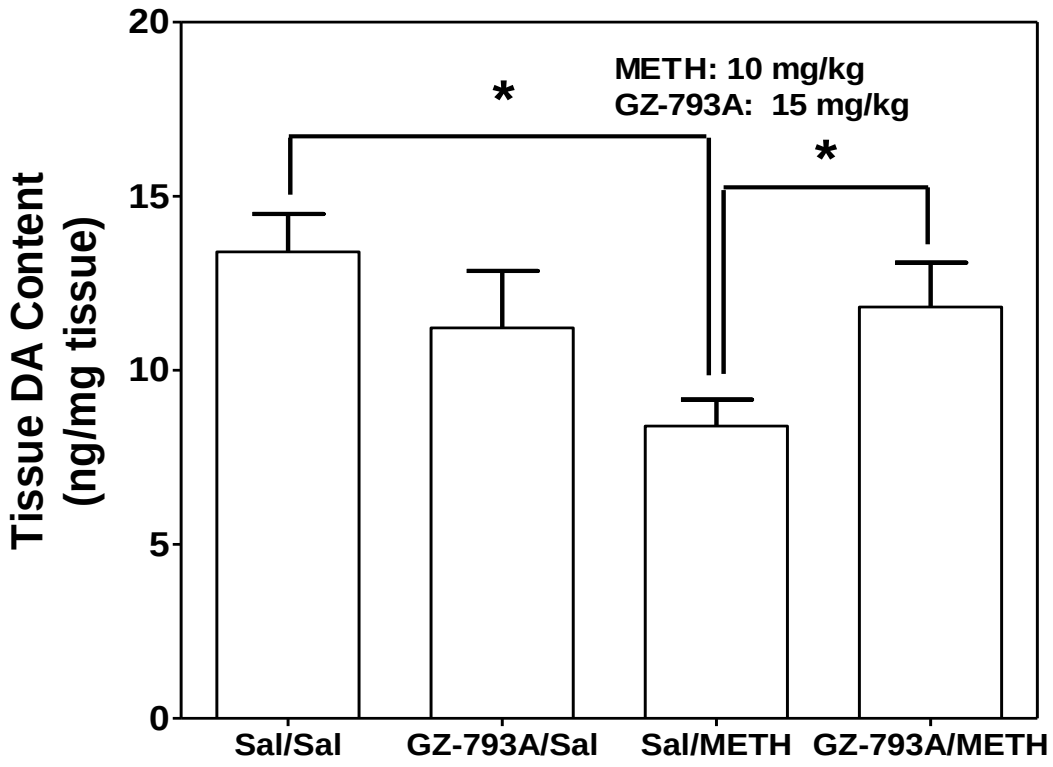

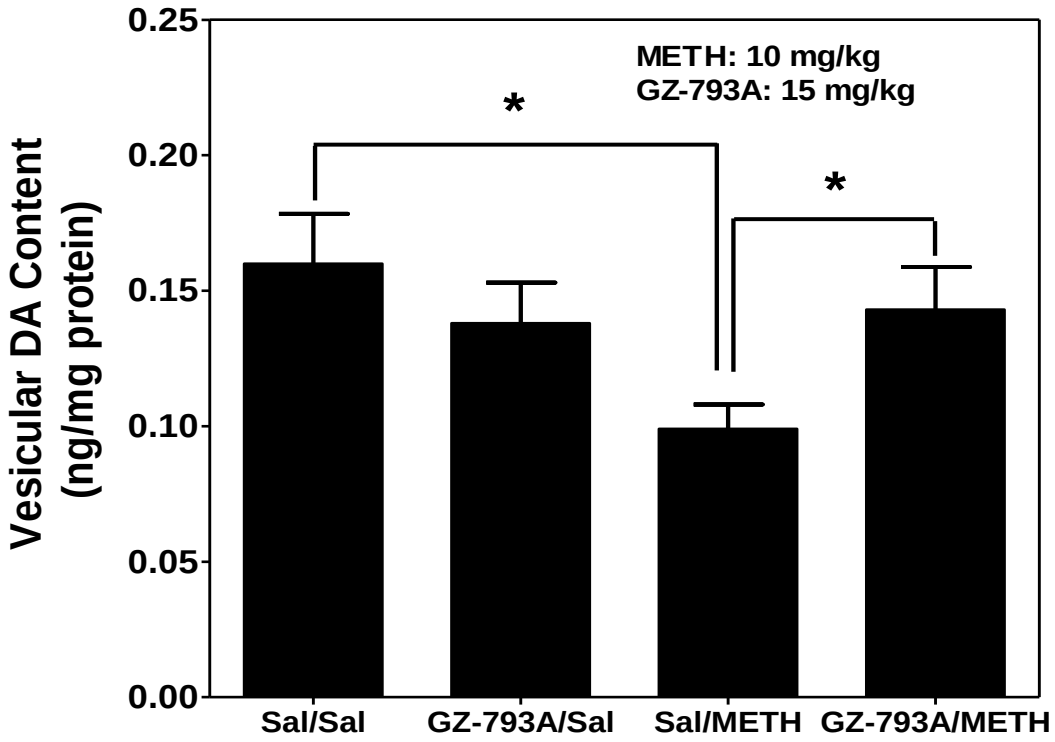
METH: 10 mg/kg
GZ-793A: 15 mg/kg
Vesicular DA Content
(ng/mg protein)
0.25
0.20
0.15
0.10
0.05
0.00
*
*
Sal/Sal
GZ-793A/Sal
Sal/METH
GZ-793A/METH

Fig. 37. GZ-793A pre-treatment (15 mg/kg) 20 min prior to a traditional regimen of methamphetamine administration (7.5 mg/kg x 4, 2-hr injection intervals) does not exacerbate methamphetamine-induced decreases in striatal tissue dopamine content. Data are shown as ng/mg tissue and expressed as mean ± S.E.M. *p < 0.05 different from saline control. n = 10 rats/treatment.

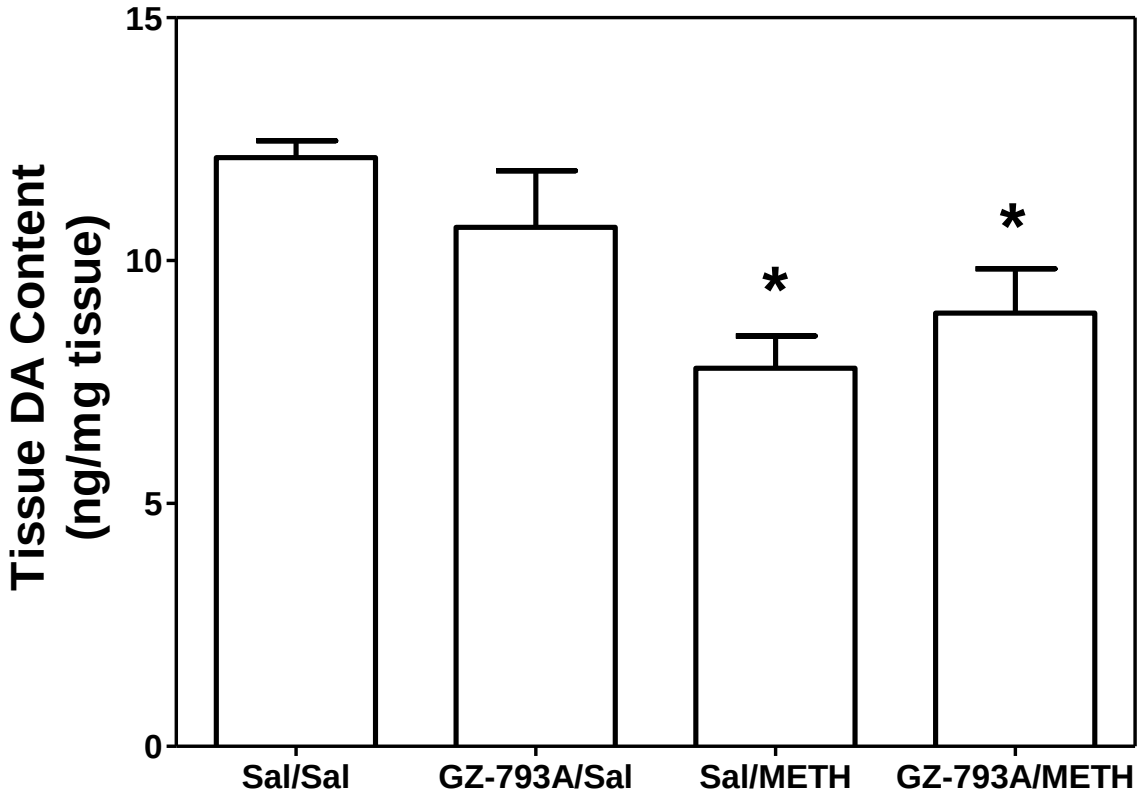

Fig. 38. GZ-793A post-treatment (15 mg/kg) 5 and 7 hrs after a traditional regimen of methamphetamine administration (7.5 mg/kg x 4, 2-hr injection intervals) does not exacerbate methamphetamine-induced decreases in striatal tissue dopamine content. Data are shown as ng/mg tissue for tissue and expressed as mean ± S.E.M. *p < 0.05 different from saline control. n = 5-6 rats/treatment.

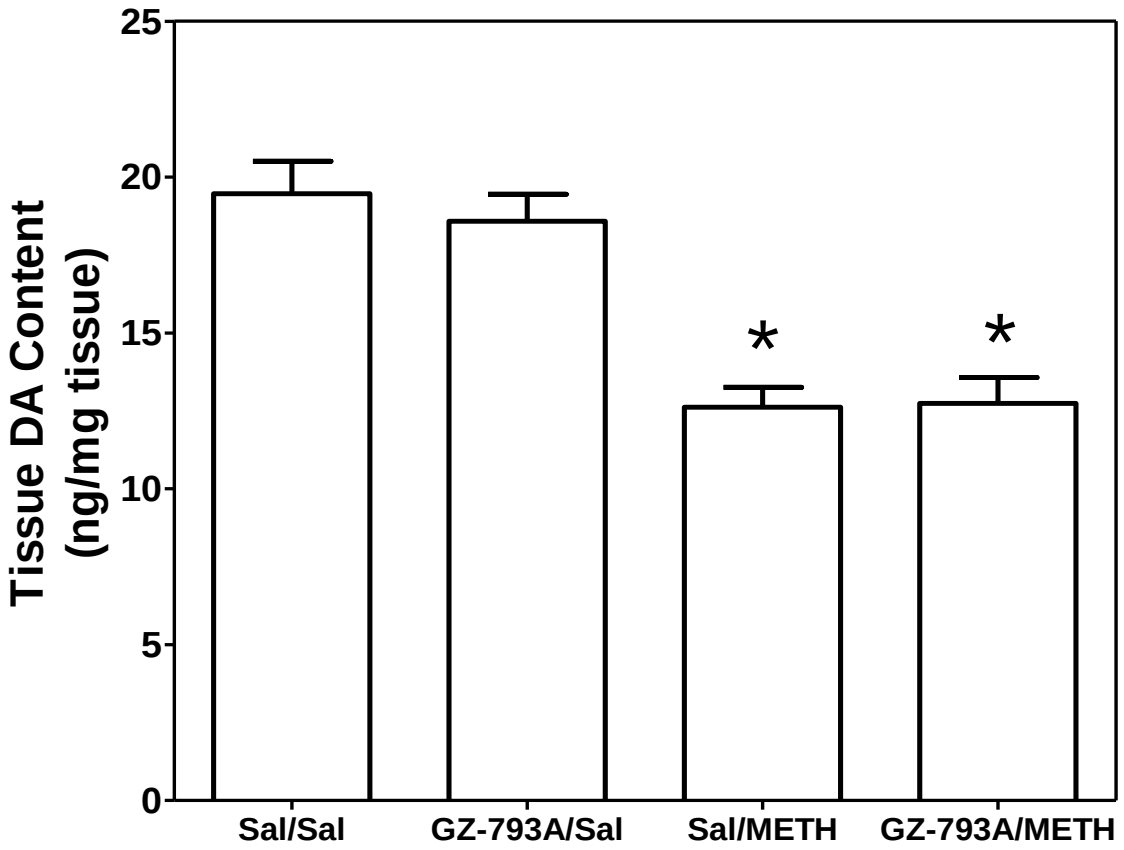

CHAPTER SIX

Discussion and Conclusions

I. Review

METH is the second most abused illicit drug in the world after marijuana, with over 25 million METH abusers worldwide (United Nations Office on Drugs and Crime, 2007; Cadet and Krasnova, 2009; Cruickshank and Dyer, 2009). METH is the most commonly synthesized illegal drug in the U.S., contributing to its widespread use (Cadet and Krasnova, 2009). AMPHs were the primary cause of over 170,000 substance abuse emergency room admissions, with over 80% of these cases involving METH (DASIS, 2008). METH abuse also represents a significant financial burden, costing the U.S. $23.4 billion in 2005 due to health care, law enforcement, and social welfare costs (Gonzales et al., 2010). In 2009, the number of people using METH in the past month increased 59% (NSDUH, 2009). Despite increased METH use, there are currently no pharmacotherapies approved for the treatment of METH abuse. Thus, METH abuse presents a serious public health concern.

METH elicits its rewarding and stimulant effects by increasing extracellular DA levels in the brain through an interaction with DAT and VMAT2 (Fischer and Cho, 1979; Seiden et al., 1993; Pifl et al., 1995; Sulzer et al., 1995; Jones et al., 1998; Sulzer et al., 2005). Specifically, METH acts as a substrate for DAT, inhibiting DA uptake into the presynaptic terminal. In the presynaptic terminal,

METH inhibits DA uptake at VMAT2 and promotes DA release from vesicles, leading to an increase in cytosolic DA concentrations available for reverse transport through DAT. Taking into consideration the role DAT plays in the mechanism of action of METH, numerous studies have been conducted examining the potential utility of DAT inhibitors such as buproprion and methylphenidate in the treatment of METH dependence. Unfortunately, results regarding the effectiveness of these treatments are inconclusive (Newton et al., 2006; Tiihonen et al., 2007; Vocci and Appel et al., 2007; Gonzales et al., 2009; Karila et al., 2010). Recent studies have focused on VMAT2 as a therapeutic target for the development of treatments for METH abuse (Dwoskin and Crooks, 2002; Zheng et al., 2005a; Vocci and Appel et al., 2007; Karila et al., 2010).

Lobeline, the principal alkaloid of *Lobelia inflata*, inhibits [^{3}H]DTBZ binding and [^{3}H]DA uptake at VMAT2 (Teng et al., 1997, 1998). In addition to inhibiting VMAT2 function, lobeline promotes a release of DA from preloaded synaptic vesicles (Nickell et al., 2011). Similar to METH, lobeline redistributes DA from vesicles to the cytosol. Unlike METH however, lobeline does not inhibit MAO and does not reverse DAT (Teng et al., 1997; Dwoskin and Crooks, 2002). Through the interaction with VMAT2 and redistribution of DA in the presynaptic terminal, lobeline is hypothesized to limit the DA available for reverse transport by METH. In support of this hypothesis, lobeline inhibited AMPH-evoked DA release from striatal slices in the same concentration range that lobeline interacts with VMAT2. Further, lobeline pretreatment inhibited METH-induced increases in locomotor activity and METH self-administration in rats (Miller et al., 2001;

Harrod et al., 2001). Importantly, lobeline is not self-administered in rats and does not produce conditioned place preference, suggesting limited abuse liability (Harrod et al., 2003). Recently, lobeline has passed Phase Ib clinical trials, demonstrating safety in METH users (Jones et al., 2007). Unfortunately, lobeline exhibits a short half-life and lacks selectivity for VMAT2 over nAChRs.

Structure activity relationships revealed that chemical defunctionalization of the lobeline molecule (i.e. removal of keto and hydroxyl groups) afforded analogs, MTD and lobelane which exhibited increased affinity for VMAT2 and decreased affinity for nAChRs (Miller et al., 2004; Zheng et al., 2005a; Nickell et al., 2011). In addition to exhibiting increased selectivity for inhibition of VMAT2 function, MTD and lobelane inhibited METH-evoked DA release from striatal slices (Nickell et al., 2011). To extend these findings, results from the current research revealed that MTD decreased METH self-administration without altering food maintained responding. However, MTD inhibited METH self-administration only at the highest dose tested and tolerance developed to this effect. Considering the high affinity of MTD for DAT (Ki = 0.10 µM), it is likely that the MTD-induced attenuation of METH self-administration was a result of high affinity inhibition of DAT function by MTD. Through inhibiting DAT function, MTD could act to inhibit METH-induced reverse transport of DA through DAT. Similar to MTD, lobelane pretreatment decreased METH self-administration in rats, but tolerance developed to this behavioral effect after repeated treatment (Neugebauer et al., 2007). In addition, both MTD and lobelane exhibited decreased water solubility compared to lobeline due to the removal of the keto

and hydroxyl moieties of the lobeline molecule. Thus, the purpose of this dissertation research was to identify analogs of MTD and lobelane that exhibited increased water solubility and VMAT2 selectivity in an effort to develop novel therapeutics to treat METH abuse.

The first aim of this dissertation was to determine the selectivity of 3,5-disubstituted MTD analogs to inhibit VMAT2 function over DAT, SERT, and nAChRs. Conformationally restricting the MTD molecule by incorporating the phenylethylene substituents into the piperdine ring afforded analogs with increased selectivity for VMAT2 compared to the parent analog, MTD. Unlike MTD, MTD analogs in this series exhibited decreased affinity for DAT, suggesting a decreased potential for abuse liability compared to MTD. UKMH-106, a 2,4-dichlorophenyl MTD analog competitively inhibited VMAT2 function with over 20-fold selectivity for VMAT2 over DAT, SERT and nAChRs. Furthermore, UKMH-106 decreased METH-evoked DA release from striatal slices in a concentration-dependent manner. Interestingly, UKMH-105, a 2,4-dichlorophenyl MTD analog and geometrical isomer of UKMH-106, did not inhibit METH-evoked DA release from striatal slices despite exhibiting equipotency for inhibition of VMAT2 function compared to UKMH-106. These results suggest that the site on VMAT2 mediating METH-evoked DA release is less accommodating to the double bond geometry of MTD analogs compared to the DA uptake site on VMAT2. Nonetheless, conformationally restricting the MTD molecule afforded

analogs with increased selectivity for inhibition of VMAT2 function compared to MTD and UKMH-106 decreased METH-evoked DA release from striatal slices.

The second aim was to determine the selectivity of N-1,2-diol lobelane analogs to inhibit VMAT2 function over DAT and SERT. Replacement of the N-methyl moiety with a chiral N-1,2-diol moiety on the piperdine nitrogen of lobelane afforded analogs with increased water solubility compared to lobelane. GZ-793A, the 4-methoxyphenyl N-1,2(*R*)-diol analog, and GZ-794A, the 1-naphthalene N-1,2(*R*)-diol analog, competitively inhibited [^{3}H]DA uptake at VMAT2 with affinity not different from that exhibited by lobelane. Further, both analogs inhibited METH-evoked DA release from striatal slices in a concentration-dependent manner, however GZ-793A exhibited ~35% greater inhibitory activity compared to GZ-794A. Thus, GZ-793A emerged as the lead analog of the series, exhibiting over 50-fold selectivity for inhibition of VMAT2 function and inhibiting METH-evoked DA release from striatal slices.

To further identify the cellular mechanism underlying GZ-793A-induced inhibition of the effects of METH, the third aim determined the ability of GZ-793A to release DA from vesicles and inhibit METH-evoked DA release from vesicles. GZ-793A evoked [^{3}H]DA release from synaptic vesicles with high affinity and the concentration-response curve fit a two-site model of interaction. GZ-793A-evoked DA release at the Hi affinity site was TBZ- and reserpine-sensitive, while release at the Low affinity site was TBZ- and reserpine-insensitive. GZ-793A concentrations that interact with the Hi affinity site inhibited METH-evoked [^{3}H]DA release from striatal synaptic vesicles. Increasing concentrations of GZ-793A

produced a rightward shift in the METH concentration-response and Schild regression analysis revealed a slope significantly different from unity, consistent with a surmountable allosteric mechanism of action. Thus, GZ-793A likely interacts with at least three distinct sites on VMAT2: 1) the extravesicular DTBZ binding site (low affinity), 2) the extravesicular DA uptake site (high affinity) and 3) intravesicular DA release sites (high and low affinity).

The fourth aim was to determine the effect of GZ-793A on striatal DA content and the ability of GZ-793A to protect against METH-induced DA content depletion. Results from this initial DA neurotoxicity evaluation revealed that acute or chronic GZ-793A did not alter DA content from striatal tissue or vesicles, suggesting that the ability of GZ-793A to inhibit the neurochemical and behavioral effects of METH is not due to a GZ-793A-induced neurotoxicity effect on DA content. GZ-793A pretreatment (15 mg/kg) prior to acute METH (5 and 10 mg/kg) attenuated METH-induced depletion of DA content. Conversely, GZ-793A pretreatment prior to repeated high doses of METH (4 x 10 mg/kg) did not protect against nor exacerbate METH-induced decreases in DA content. These preliminary studies suggest that GZ-793A may offer neuroprotective benefits against acute METH-induced depletions in DA content.

II. Comparisons Between 3,5-Disubstituted MTD analogs and N-1,2-Diol Lobelane Analogs.

The current research reports on the findings from an iterative drug discovery approach with the goal of identifiying selective VMAT2 inhibitors to

inhibit the rewarding effects of METH. This dissertation research focused on two sets of lobeline analogs, 3,5-disubstituted MTD analogs and N-1,2-diol lobelane analogs. MTD, the parent of the first series of analogs, exhibited high affinity for DAT, limiting selectivity for VMAT2. Conformational restriction of the MTD molecule, as well as various structural changes to the phenyl rings including the addition of 4-methoxy, 4-methyl, and 2,4-dichloro to the phenyl ring or replacement of the phenyl rings with thiophene or furan rings, afforded analogs with 50-1000-fold decreased affinity for DAT compared to MTD. Importantly, structural modifications did not alter affinity for the DA uptake site on VMAT2, thereby increasing selectivity for VMAT2 compared to MTD. UKMH-106 emerged as the lead analog of the series exhibiting the highest potency and selectivity to inhibit VMAT2 function. UKMH-106 decreased METH-evoked DA release from striatal slices in a concentration-dependent manner. UKMH-106 exhibited poor water solubility however, similar to that of MTD, which limited further development. Thus, the focus of the research project shifted to identifying analogs with increased water solubility in addition to VMAT2 selectivity.

Replacement of the N-methyl moiety of lobelane with a chiral N-1,2-diol moiety on the piperdine nitrogen of lobelane afforded analogs with increased water solubility compared to lobelane. In addition to the incorportation of the N-1,2-diol moiety, various structural modifications to the phenyl rings were performed including the addition of 2-methoxy, 3-methoxy, 4-methoxy, 3-flouro, 2,4-dichloro, or 3,4-methylenedioxy moieties to both phenyl rings or replacement of both phenyl rings with naphthalene or biphenyl moieties. While the analogs

exhibited similar affinity for DAT and SERT compared to lobelane, most analogs exhibited decreased potency to inhibit VMAT2 function. Exceptions included GZ-793A, the 4-methoxyphenyl N-1,2(*R*)-diol analog, and GZ-794A, the 1-naphthalene N-1,2(*R*)-diol analog, which exhibited potency to inhibit VMAT2 function not different from lobelane. Both GZ-793A and GZ-794A decreased METH-evoked DA release from striatal slices, however GZ-793A exhibited ~35% greater inhibitor activity compared to GZ-794A. Further, GZ-793A exhibited 5-fold greater selectivity for inhibition of VMAT2 function compared to GZ-794A. Thus, GZ-793A emerged as the lead analog of the series.

Compared to UKMH-106, GZ-793A exhibited 2.5-fold greater selectivity for inhibition of VMAT2 function and 35% greater inhibitory activity to inhibit METH-evoked DA release from striatal slices. Additionally, GZ-793A exhibited increased water solubility compared to UKMH-106 due to the incorportation of the N-1,2-diol moiety. Thus, GZ-793A emerged as the lead analog of both series of analogs and became the focus of the mechanistic vesicular DA release experiments and DA content studies.

III. Mechanisms Underlying GZ-793A-induced Inhibition of METH-evoked DA Release from Synaptic Vesicles.

GZ-793A concentrations that interacted with the Hi affinity site on VMAT2 inhibited METH-evoked DA release from striatal synaptic vesicles. Increasing concentrations of GZ-793A produced a rightward shift in the METH concentration response without altering maximal DA release suggesting a surmountable

mechanism of inhibition. Further, Schild regression analysis revealed a slope significantly different from unity, suggesting an allosteric mechanism. Thus, GZ-793A produces a conformational change in the VMAT2 protein which reduces the affinity of METH for the intravesicular DA release site without altering the efficacy of METH to release DA. Precendence for surmountable allosteric inhibition is seen with nicotinic and muscarinic acetylcholine receptor antagonists (Tucek and Proska, 1995; Kukkonen et al., 2004; Wooters et al., 2011).

One hallmark characteristic of allosteric inhibiton is saturability (Kenakin, 2006). The effect of allosteric inhibitors to shift the concentration-response curve of the agonist to the right is diminished as the allosteric site is saturated with increasing concentrations of inhibitor. The current results show that a 5-fold shift in EC50 was seen between GZ-793A concentrations of 7 and 70 nM, however, only a 1-2 fold shift was seen between GZ-793A concentrations of 70 nM to 1000 nM. Thus, the effect of GZ-793A to decrease the potency of METH to evoke vesicular DA release became saturated with increasing concentrations of GZ-793A, consistent with allosteric modulation. Further support for an allosteric inhibition mechanism is given by the finding that the inhibitory effect of GZ-793A was not rate dependent, as increasing the incubation time did not alter METH-evoked DA release in the presence of GZ-793A.

Interpretations of concentration-response curves and Schild regression analyses used in the classification of antagonists are considerably more straightforward in binding studies compared to functional data (Kenakin, 1993). In the current study, agonist response was measured as METH-evoked [^{3}H]DA

release from synaptic vesicles through an interaction with VMAT2. Considering the differences between receptors and transporters, the use of receptor-based models to interpret antagonism derived from experiments measuring transporter-mediated release is ambiguous. However, studies measuring electrochemical currents have demonstrated that substrate flux through transporters is accompanied by ion flow and electrical current, suggesting that transporters exhibit functions similar to ligand-gated ion channels (Sonders and Amara, 1996; Galli et al., 1996; Sonders et al., 1997). Thus, precedence exists for the use of receptor based models in the classification of antagonist mechanisms at transporters.

Alternatively, VMAT2 could exist in multiple conformations that exhibit different affinities for METH. GZ-793A could preferentially bind an outward-facing transporter conformation, which decreases affinity for METH, without altering DA release. By selectively binding to the outward-facing conformation, GZ-793A stabilizes the GZ-793A-bound transporter conformation, which would allow for a shift in the potency of METH to evoke DA release, without altering maximal response. Evidence for different confirmations of VMAT2 has been shown for the differential binding of reserpine and TBZ on VMAT2 (Darchen et al*.,* 1989).

An alternative explanation for GZ-793A-induced inhibition of METH-evoked DA release is through an interaction with the [^{3}H]DA uptake site. GZ-793A exhibits high affinity for the [^{3}H]DA uptake site on VMAT2 (Ki = 29 nM) and through this interaction, GZ-793A could elicit a conformational change in the VMAT2 protein which decreases the affinity of the DA release site for METH, but

does not alter the efficacy of METH to release DA. In addition to allosterically modulating the DA release site, GZ-793A could be inhibiting METH-evoked DA release from vesicles through a blockade of VMAT2 function. DAT inhibitors, such as nomifensine, inhibit METH-evoked DA release though blockade of reverse transport through DAT (Sulzer et al., 1993, 1995). In a similar manner, GZ-793A could be interacting with the [^{3}H]DA uptake site to inhibit the uptake of METH into vesicles, thereby decreasing METH-evoked DA release. METH acts as a substrate at VMAT2, being taken up into vesicles in a manner similar to DA (Peter et al., 1994; Erickson et al., 1996). In the facilitated diffusion mechanism of DA release, the uptake of METH through VMAT2 elicits a conformational change in VMAT2 that exposes DA binding sites on the inner-facing side of the transporter and enables the reverse transport of DA into the cytosol (Sulzer et al., 2005). Thus, GZ-793A could decrease METH-induced reverse transport of DA through VMAT2 through inhibiting the uptake of METH into vesicles. This explanation is unlikely, however, as GZ-793A-induced inhibition of the DA uptake site was consistent with competitive inhibition, while Schild regression analysis revealed that GZ-793A-induced inhibition of METH-evoked DA release was not consistent with a competitive inhibition.

GZ-793A-induced inhibition of uptake of METH into vesicles could presumably decrease METH-induced DA release by the weak base effect as well. Decreasing accumulation of METH in synaptic vesicles would prevent the alkanalization of the vesicular lumen, preventing the disruption of the pH gradient by METH and subsequently, METH-evoked DA release. Even though GZ-793A

inhibited the active transport of METH through VMAT2, METH can also passively diffuse across the vesicular membrane. As a lipophilic weak base, high concentrations of METH diffuse across the vesicular membrane to alkanalize the vesicular lumen, disrupt the pH gradient and release DA (Peter et al., 1995; Sulzer et al., 2005). This explanation is supported by the finding that even higher concentrations of GZ-793A (1µM) that completely inhibit VMAT2 function did not completely inhibit METH-evoked DA release. Thus, METH-evoked DA release that is not inhibited by GZ-793A could be occurring non-specifically through a weak base effect.

An alternative site of interaction for the GZ-793A-induced inhibition of METH-evoked DA release is the [^{3}H]DTBZ binding site. TBZ inhibited METH-evoked DA release from striatal vesicles across a similar concentration range compared to GZ-793A. However, Schild regression analysis of TBZ-induced inhibition of METH-evoked DA release was consistent with a competitive mechanism of inhibition, unlike GZ-793A. Further, GZ-793A and TBZ inhibited METH-evoked DA release from vesicles in the same concentration range even though GZ-793A exhibits 600-fold lower affinity for inhibiting [^{3}H]DTBZ binding compared to TBZ. If GZ-793A-induced inhibition of METH-evoked DA release was mediated through an interaction with the DTBZ binding site, then TBZ would be expected to inhibit METH-evoked DA release from vesicles at much lower concentrations, considering the significant difference in affinity for the [^{3}H]DTBZ binding site between GZ-793A and TBZ. Moreover, GZ-793A inhibited METH-evoked DA release from striatal vesicles at concentrations lower than the

concentrations that GZ-793A interacts with the [^{3}H]DTBZ binding site. GZ-793A exhibits low affinity at the [^{3}H]DTBZ binding site (Ki = 8.29 µM), but inhibits METH-evoked DA release at concentrations around 70 nM. Thus, it is unlikely that the GZ-793A- and TBZ-induced inhibition of METH-evoked DA release was through an interaction with the DTBZ binding site on VMAT2.

Interestingly, the in vitro finding that GZ-793A-induced inhibition of METH-evoked DA release from striatal synaptic vesicles was surmounted by increasing concentrations of METH did not translate to the in vivo behavioral model as GZ-793A-induced inhibition of METH self-administration in rats was not surmounted by increasing the dose of METH (Beckmann et al., 2011). The vesicular DA release studies were performed as a mechanistic approach *in vitro* allowing us to use extreme concentrations of METH that are not going to be realized *in vivo*. Importantly, however, GZ-793A inhibited METH-evoked DA release from vesicles at concentrations that are proposed to be realized *in vivo*.

IV. Mechanisms Underlying GZ-793A-induced Inhibition of METH-evoked DA Release from Striatal Slices.

GZ-793A inhibits METH-evoked DA release from striatal slices in a concentration-dependent manner. Consistent with these results, GZ-793A was found to decrease METH self-administration in rats, without affecting food-maintained responding. Thus, GZ-793A is inhibiting METH-evoked DA release to decrease the rewarding effects of METH. One mechanism by which GZ-793A could inhibit METH-evoked DA release is through the redistribution of DA in the

presynaptic terminal. Similar to lobeline, GZ-793A inhibits DA uptake at VMAT2 and evokes DA release from synaptic vesicles, increasing cytosolic DA concentrations (Chapter 3, Horton et al., 2011b; Chapter 4, Horton et al., 2011c). In the presence of GZ-793A, cytosolic DA is metabolized into DOPAC since GZ-793A is not expected to inhibit MAO as evidenced by the finding that high concentrations of GZ-793A increased DOPAC release in striatal slices rather than DA (unpublished observations). Thus, GZ-793A could be interacting with VMAT2 to increase cytosolic DA for metabolism, thereby limiting DA available for METH-evoked DA release through DAT.

The observation that GZ-793A does not inhibit MAO activity is based upon the finding that GZ-793A treatment increases DOPAC concentrations. While this is an indirect determination of a GZ-793A-MAO interaction, further enzymatic studies are needed to accurately assess the ability of GZ-793A to inhibit MAO activity. Furthermore, determination of the drug-drug interaction between METH and GZ-793A on MAO activity would be beneficial in further elucidating the underlying mechanism of GZ-793A-induced inhibition of METH's effects. Unlike GZ-793A, which is not expected to inhibit MAO, pargyline increases DA content in striatal tissue and vesicles (Fekete et al., 1979; Buu and Lussier, 1989). Thus, pargyline is not expected to be a suitable treatment to inhibit the effects of METH. Furthermore, pargyline would be expected to exacerbate the effect of METH since pargyline administration would increase DA available for release by METH. Consistent with this hypothesis, previous research has shown that

pargyline pretreatment exacerbates METH-induced DA content depletion (Kita et al., 1995).

In addition to redistributing DA from vesicles and increasing DA available for metabolism, GZ-793A could be inhibiting the ability of METH to release DA from vesicles, thereby limiting DA available for METH-induced reverse transport through DAT. Results from the current study demonstrate that GZ-793A-induced inhibition of METH-evoked [^{3}H]DA release from synaptic vesicles was consistent with a surmountable allosteric mechanism as discussed in the section above. Thus, GZ-793A interacts with VMAT2 to inhibit METH-evoked DA release from vesicles, resulting in decreased cytosolic DA available for METH-induced reverse transport through DAT.

In addition to VMAT2, GZ-793A could be interacting with other presynaptic targets to inhibit METH-evoked DA release from striatal slices. One alternative explanation could be that GZ-793A is inhibiting METH-evoked DA release through an interaction with nAChRs. Lobeline acts as an antagonist at both α4β2* and α7* nAChRs (Briggs and McKenna, 1998; Miller et al., 2000; Dwoskin and Crooks, 2002). Further, lobeline antagonizes the nAChRs mediating [^{3}H]DA and [^{3}H]NE release (Gallardo and Leslie, 1998; Miller et al., 2000; Miller et al., 2005). Chemical defunctionalization of the lobeline molecule afforded analogs, MTD and lobelane with diminished activity at nAChRs compared to lobeline (Miller et al., 2004). GZ-793A, a lobelane analog exhibits low affinity for α4β2* and α7* nAChRs (Ki > 100 μM), as probed by displacement of [^{3}H]NIC and [^{3}H]MLA binding, respectively (unpublished observations). Further, GZ-793A did

not alter nicotine-evoked DA release from striatal slices, demonstrating a lack of interaction with nAChRs mediating DA release. Thus, it is unlikely that GZ-793A is interacting with nAChRs to inhibit METH-evoked DA release from striatal slices.

An alternative explanation could be that GZ-793A is interacting with DAT to inhibit METH-evoked DA release from striatal slices. GZ-793A exhibits affinity for DAT (Ki = 1.44 μM) within the same concentration range that inhibits METH-evoked DA release from striatal slices. Similar to DAT inhibitors such as cocaine and nomifensine, GZ-793A could decrease METH-evoked DA release through an inhibition of METH-induced reverse transport through DAT. Unlike DAT inhibitors, however, GZ-793A does not support self-administration in rats, suggesting that inhibition of DAT is not the mechanism of action of GZ-793A (Beckman et al., 2011). In addition, GZ-793A is 50-fold more potent at VMAT2 compared to DAT, providing support for VMAT2 as the pharmacological target. Thus, it is unlikely that GZ-793A-induced inhibition of METH-evoked DA release is due to inhibition of DAT.

An alternative explanation for the ability of GZ-793A to inhibit METH-evoked DA release could involve a redistribution of VMAT2 containing vesicles in the presynaptic terminal. VMAT2-containing vesicles are thought to be localized to two distinct pools, a readily releasable pool located near the active zone of the synaptic cleft and a non-readily releasable pool located away from the synapse (Hua et al., 2011). Readily releasable pools are involved in the release of DA following stimulation, while non-readily releasable pools are unaffected by

stimulation (Hua et al., 2011). Through a redistribution in VMAT2 containing vesicles, METH treatment rapidly (within 1 hr) decreases [^{3}H]DA uptake in striatal vesicles (Brown et al., 2000; Riddle et al., 2002). The effect of GZ-793 on VMAT2 immunoreactivity and vesicular trafficking is not known. GZ-793A could redistribute VMAT2-containing vesicles out of the presynaptic terminal thereby limiting the ability of METH to interact with VMAT2 to increase cytosolic DA available for reverse transport through DAT. Future studies determining the effect of GZ-793A and METH on the localization of VMAT2-containing vesicles within the presynaptic terminal are needed. Studies utilizing western blot analysis of VMAT2 immunoreactivity following GZ-793A and METH administration would be beneficial in determining the mechanism underlying GZ-793A-induced inhibition of METH-evoked DA release from striatal slices.

V. Mechanisms underlying the increase in food-maintained responding following repeated GZ-793A treatment.

While acute and repeated GZ-793A treatment did not decrease food-maintained responding, repeated GZ-793A treatment significantly increased food-maintained responding (Beckmann et al., 2011). One mechanism underlying the orexigenic effects of GZ-793A could be that GZ-793A increases metabolism to stimulate food intake. GZ-793A could interact with ghrelin signaling to increase food intake. Ghrelin, a gut peptide hormone, stimulates energy metabolism and increase food intake (Patterson et al., 2011). Further, GZ-793A could be interacting with melanocortin (MC3/4) receptors to stimulate food intake. Previous research has shown that antagonism of the MC3/4

receptor increased food intake in rats (Hagan et al., 2000). Another potential explanation for the orexigenic effect of GZ-793A is that GZ-793A could be increasing food intake through a serotinergic mechanism. The role of the serotonin system in food intake and appetite has long been established (for review, Halford et al., 2011). While, GZ-793A inhibits SERT function with moderate potency (Ki = 9.36 µM; Chapter 3, Horton et al., 2011b), the ability of GZ-793A to interact with 5-HT receptors is not known. Further studies determining the ability of GZ-793A to interact with 5-HT receptors would be beneficial in elucidating the potential mechanisms underlying the orexigenic effects of GZ-793A.

VI. Mechanisms underlying the finding that GZ-793A-induced inhibition of METH-evoked DA release from synaptic vesicles was surmountable while GZ-793A-induced inhibition of METH self-administration was not surmounted by increasing doses of METH.

Interestingly, GZ-793A-induced inhibition of METH-evoked DA release from synaptic vesicles was consistent with an allosteric, surmountable mechanism of inhibition (Chapter 4, Horton et al., 2011c), while systemic GZ-793A pretreatment decreased METH self-administration which was not surmounted by increasing the METH dose (Beckmann et al., 2011). One explanation for this is that other mechanisms could be involved in the ability of GZ-793A to inhibit the effects of METH. The *in vitro* experiments in this study are performed in vesicle preparations while the *in vivo* experiments where conducted in the whole animal model. In the whole animal model GZ-793A could interact

with multiple targets to inhibit the effects of METH. While GZ-793A inhibits the action of METH at VMAT2 in a surmountable manner, GZ-793A could inhibit the effects of METH through different mechanisms which are not surmounted by increasing doses of METH in the whole animal. In addition to the abililty of GZ-793A to inhibit the effects of METH on VMAT2, other mechanisms by which GZ-793A inhibit the effects of METH may be involved.

VII. Mechanisms Underlying the Finding that GZ-793A Treatment Does Not Alter Striatal DA Content.

Acute and repeated treatment of a behaviorally active dose of GZ-793A (15 mg/kg; s.c.) did not alter DA content in striatal tissue and vesicles. Even though GZ-793A inhibits [^{3}H]DA uptake at VMAT2 with high affinity and promotes [^{3}H]DA release from striatal vesicles, systemic GZ-793A treatment had no effect on DA content. One possible explanation for this finding is that GZ-793A could act as a reversible inhibitor of VMAT2. Unlike GZ-793A, reserpine acts as an irreversible inhibitor of DA uptake at VMAT2, which cannot be surmounted by increasing substrate concentrations (Yelin and Schuldiner, 2000). As a result, in vivo treatment of reserpine corresponds to a long-lasting decrease in DA content (Yelin and Schuldiner, 2000). Conversely, GZ-793A-induced inhibition of DA uptake at VMAT2 was surmounted by increasing concentrations of DA. Thus, unlike reserpine, GZ-793A-induced inhibition of VMAT2 function is short-lasting. Consistent with this hypothesis, GZ-793A treatment did not alter DA content in striatal tissue or vesicles 0.3, 1, 8 and 24 hrs following treatment. These results were similar to results found in DA content studies conducted with lobeline that

demonstrate that acute or repeated lobeline treatment (1-30 mg/kg, s.c.) did not alter striatal DA content (Miller et al., 2001).

An alternative explanation for the lack of DA content depletion following GZ-793A treatment could be the effect of GZ-793A on DA synthesis. GZ-793A could increase DA synthesis in presynaptic terminals to compensate for a presumed decrease in synaptic DA content resulting from DA release from vesicles and inhibition of DA uptake at VMAT2. While an increase in DA content was not seen following GZ-793A treatment, studies examining the effect of GZ-793A on TH activity would be beneficial to determine if GZ-793A is increasing DA synthesis.

VIII. Mechanisms Underlying Attenuation of METH-induced Depletion of Striatal DA Content by GZ-793A Pretreatment.

Acute and repeated GZ-793A pretreatment (15 mg/kg, s.c.) attenuated METH-induced depletion of striatal DA content. One explanation is that GZ-793A interacts with VMAT2 to inhibit METH-evoked DA release. GZ-793A interacts with VMAT2 to inhibit METH-evoked DA release from striatal vesicles decreasing cytosolic DA concentrations available for METH-induced reverse-transport through DAT. Thus, GZ-793A inhibits METH-evoked DA release through an interaction with VMAT2, attenuating METH-induced depletions of DA content.

Another explanation for GZ-793A-induced attenuation of METH-induced DA depletion could be a redistribution of VMAT2-containing vesicles within the presynaptic terminal. Recent studies have shown that methylphenidate protects

DA neurons from METH-induced toxicity (Volz et al., 2008). Methylphenidate acts primarily to increase extracellular DA concentrations though an inhibition of DAT (Schweri et al., 1985). In addition, methylphenidate increases VMAT2 immunoreactivity in cytoplasmic fractions in rat synaptosomes (Sandoval et al., 2002). Through an increase in vesicular trafficking to the cytoplasmic fraction, methylphenidate increases vesicular DA content to compensate for the DA depleted by METH. Additionally, methylphenidate augments DA sequestration through an increase in VMAT2 function in the membrane-associated vesicles to protect against METH-induced decreases in DA content (Volz et al., 2007, 2008). In a similar manner, GZ-793A treatment could increase VMAT2 function and VMAT2 immunoreactivity to attenuate METH-induced DA content depletion. Additional studies determining the effect of systemic GZ-793A treatment on changes in VMAT2 function and localization of VMAT2-containing vesicles are needed.

An alternative explanation is that GZ-793A could be inhibiting DAT to protect against METH-induced DA content depletion. Through an inhibition of DAT function, GZ-793A could inhibit the transport of METH into presynaptic terminals and METH-induced reverse transport of DA through DAT. Precedence for this mechanism of action is given by Marek and colleagues in demonstrating that DAT inhibitors, amfonelic acid, mazindol and buproprion protected against striatal DA content depletions by high doses of METH (100 mg/kg, s.c.; Marek et al., 1990). Moreover, pretreatment with GBR-12909, a high affinity DAT inhibitor, protected against striatal DA content depletions following a neurotoxic regimen of

METH (Stephans and Yamamoto, 1994). In a similar manner, GZ-793A could inhibit METH uptake and METH-evoked DA release through DAT to protect against METH-induced depletions in DA content. Unlike DAT inhibitors, however, GZ-793A does not support self-administration in rats (Beckmann et al., 2011), suggesting that DAT is not the pharmacological target involved in the mechanism of action of GZ-793A.

Another possible explanation for GZ-793A-induced attenuation of METH-induced striatal DA content depletion is that GZ-793A could protect against METH-induced hyperthermia. METH administration induces hyperthermia, leading to striatal DA content depletion (Bowyer et al., 1994). GZ-793A could inhibit the effect of METH to increase body temperature thereby attenuating the effect of METH to deplete DA content through this mechanism. This explanation is unlikely however, as the ability of the parent analog, lobeline to attenuate METH-induced DA content depletion is not due to an effect on METH-induced hyperthermia (Eyerman and Yamamoto, 2005). Nonetheless, the effect of GZ-793A on METH-induced increases in body temperature is unknown and future studies determining the effect of GZ-793A on METH-induced changes in body temperature would be beneficial in determining the underlying mechanism of GZ-793A-induced attenuation of METH-induced DA content depletion.

IX. Implications

The results from this dissertation research imply that VMAT2 represents a pharmacological target to prevent the effects of METH in the development of

treatments for METH abuse. GZ-793A selectively inhibits DA uptake at VMAT2 and promotes a DA release from synaptic vesicles, resulting in a redistribution of DA from vesicles to the cytosol. In addition, GZ-793A decreases METH-evoked DA release from synaptic vesicles through an interaction with VMAT2, thereby reducing cytosolic DA concentrations available for METH-induced reverse transport through DAT. GZ-793A selectively inhibits METH-evoked DA release from striatal slices and GZ-793A pretreatment decreases METH self-administration without altering food-maintained responding in rats (Beckmann et al., 2011). GZ-793A-induced inhibition of METH self-administration is not surmounted by increasing the dose of METH and tolerance does not develop following repeated GZ-793A dosings (Beckmann et al., 2011). Moreover, GZ-793A pretreatment prevents the development of METH-induced conditioned place preference and inhibits METH cue-induced reinstatement (Beckmann et al., 2011; unpublished observations). Thus, GZ-793A would be expected to inhibit METH-induced cravings in METH-addicted individuals. In addition to inhibiting the behavioral effects of METH, GZ-793A does not support self-administration in rats, suggesting limited abuse potential. Thus, selective inhibition of VMAT2 by GZ-793A represents a valid target for the development of pharmacotherapies for METH abuse.

GZ-793A exhibits a different pharmacological profile for interaction of VMAT2 compared to classic VMAT2 inhibitors, TBZ and reserpine. First, while GZ-793A, TBZ and reserpine exhibited similar affinity for the DA uptake site on VMAT2, inhibition by GZ-793A and TBZ is surmountable (Chapter 3, Horton et

al., 2011b; Nickell et al., 2011), while reserpine-induced inhibition of DA uptake is not (Rudnick et al., 1990). Second, these compounds interact with the DTBZ binding site on VMAT2 with different affinities (TBZ > reserpine > GZ-793A). Third, concentration-response curves for GZ-793A-evoked DA release was consistent with a two-site model of interaction, while the concentration-response curves for TBZ and reserpine to release DA fit a one-site model of interaction. To our knowledge, GZ-793A is the first compound shown to evoke vesicular DA release through an interaction with a Hi and Low affinity site. Concentrations of GZ-793A that selectively interacted with the Hi affinity DA release site on VMAT2 inhibited METH-evoked DA release through a surmountable allosteric mechanism. While GZ-793A and TBZ inhibited METH-evoked DA release across similar concentration ranges, TBZ-induced inhibition of METH-evoked DA release is consistent with a competitive mechanism of action, unlike GZ-793A. Thus, GZ-793A exhibits a different pharmacological profile to interact with VMAT2 compared to TBZ and reserpine.

Additional results from this research imply that selective inhibition of VMAT2 function by GZ-793A did not deplete striatal DA content. Acute and repeated GZ-793A treatment, of a dose that inhibited the behavioral effects of METH (15 mg/kg), did not alter DA content in striatal tissue or vesicles. These results suggest that GZ-793A acts differently than reserpine to inhibit VMAT2 function, presumably in a short-acting, reversible manner. Further, results showed that inhibition of VMAT2 function by GZ-793A did not exacerbate acute METH-induced depletions of DA content. In fact, acute and repeated GZ-793A

pretreatment attenuated acute METH-induced DA content depletions. With respect to multiple high doses of METH, GZ-793A pretreatment did not protect against nor exacerbate METH-induced striatal DA content depletions. Thus, GZ-793A treatment alone did not alter striatal DA content and GZ-793A pretreatment might offer neuroprotective benefits against the neurotoxic effects of METH.

X. Limitations

One limitation of the current research was the limited water solubility exhibited by UKMH-106, GZ-794A, and GZ-796A. In determining the ability of the forementioned analogs to inhibit METH-evoked DA release from striatal slices, higher concentrations of analogs were needed to establish a full concentration-response curve. As such, the I_{max} of these analogs to inhibit METH-evoked DA release has been estimated with the highest soluble analog concentration. The use of other vehicles (such as PEG or DMSO), which would allow higher concentrations of analogs to be reached which would be beneficial in determining the ability of these analogs to inhibit METH-evoked DA release.

Another limitation of the current research was that METH exhibited low potency (EC_{50} = 18.9 µM) to evoke [^{3}H]DA release from striatal vesicles. Due to the low potency of METH to release vesicular DA, maximal DA release occurs close to the highest METH concentrations tested (10 mM). Since higher METH concentrations cannot be tested, the experiment is limited in the ability to fully characterize the plateau of maximal DA release. Therefore our estimation of the E_{max} is limited in that it is based upon only 1 or 2 data points. Since GZ-793A-

induced inhibition of METH-evoked DA release from vesicles is characterized by a rightward shift in potency, the E_{max} of METH-evoked DA release in the presence of GZ-793A is even more difficult to ascertain than METH alone. Since the E_{max} is difficult to determine in the presence of GZ-793A, it is therefore difficult to determine if the inhibitory effect of GZ-793A is surmounted by increasing concentrations of METH. Thus, the low potency of METH to release DA from striatal vesicles limits the ability to classify inhibition as surmountable or unsurmountable in determining the mechanisms of action of inhibitors.

The current research utilized *in vitro* models to determine the effect of lobeline analogs on VMAT2 selectivity and METH-evoked DA release from striatal vesicles and slices. As such, assumptions are made that the analogs tested are reaching the pharmacological targets following systemic treatment, e.g., in striatal synaptosome preparations analogs will have greater access to plasma membrane transporters compared to striatal slice preparations. Mechanistic studies such as the vesicular DA release assay are performed *in vitro* which allows us to use extreme concentrations that are not going to be realized *in vivo*. Further, when considering affinity of analogs for transporters, it is important to note that these values were obtained via *in vitro* and *ex vivo* models characterized by tissue functioning in buffer and not in fully intact, physiological systems and conditions.

XI. Future Directions

One of the main findings of this dissertation is that GZ-793A evokes [^{3}H]DA release at low concentrations through an interaction with the Hi affinity site on VMAT2. Support for this tenet arises from the finding that inhibition of VMAT2 function through known inhibitors TBZ and resepine inhibit GZ-793A evoked [^{3}H]DA release at the Hi affinity site. GZ-793A evoked DA release at the Low affinity site on VMAT2 is unaffected by TBZ or reserpine, however. Presumably, higher concentration of GZ-793A (> 1 µM) evoked [^{3}H]DA release through a non-specific mechanism such as the weak base effect. To test this hypothesis, the vesicular pH could be measured to determine if GZ-793A alkalinized the vesicular lumen leading to a disruption of pH gradients. Recently, Sulzer and colleagues have developed pH-responsive fluorescent false neurotransmitters (FFNs) to measure vesicular pH in intact presynaptic terminals (Lee et al., 2010). These FFNs act as VMAT2 substrates, being taken up into synaptic vesicles. FFNs contain a built-in ratiometric fluorescent pH sensor which allows the optical *in situ* measurement of intravesicular pH. By utilizing FFNs, the ability of high concentrations of GZ-793A to alter vesicular pH and non-specifically release vesicular DA from synaptic vesicles could be determined.

In addition to using FFNs to determine the effect of GZ-793A on vesicular pH, the effect of GZ-793A on METH-induced changes of vesicular pH could also be determined. METH is known to evoke DA release from vesicles at least in part through a weak base effect. As a lipophilic weak base, METH gets protonated inside the vesicle, alkalinizing the interior pH and disrupting the pH gradient which is responsible for DA transport through VMAT2 (Sulzer et al.,

2005). By inhibiting the uptake of METH into synaptic vesicles, GZ-793A could inhibit the ability of METH to alter vesicular pH and thereby release vesicular DA. Utilizing FFNs, the ability of METH to alter vesicular pH could be measured in the absence and presence of GZ-793A. While results from these experiments could be confounded by the ability of high concentrations of METH to passively diffuse across the vesicular membrane, these results could provide additional information about METH-evoked DA release through non-specific mechanisms.

While results from the current research suggest that GZ-793A inhibits METH-evoked DA release primarily through an interaction with VMAT2, the effect of GZ-793A on DAT and VMAT2 trafficking is unknown. Considering that METH interacts with DAT and VMAT2 to increase extracellular DA, modulating the expression and localization of these proteins could be a viable mechanism for inhibition of the effects of METH. For example, GZ-793A could downregulate DAT surface expression through a trafficking-mediated mechanism, thereby decreasing the availability of one of the pharmacological targets of METH. Further, GZ-793A could increase VMAT2 function through an increase in trafficking of VMAT2-containing vesicles in the cytosol to inhibit the effects of METH and protect against METH-induced neurotoxicity, similar to the neuroprotective mechanism of methylphenidate (Volz et al., 2008). Thus the ability of GZ-793A to modulate DAT and VMAT2 function through trafficking would be beneficial in elucidating the mechanism of GZ-793A-induced inhibition of the effects of METH.

Considering the finding that METH administration increases body temperature leading to striatal DA content depletion, one potential mechanism underlying GZ-793A-induced attenuation of METH-induced striatal DA content depletion is the effect of GZ-793A on body temperature. GZ-793A could be inhibiting the effect of METH to deplete DA content by protecting against METH-induced increases in body temperature. As such, additional studies determining the effect of GZ-793A pretreatment on METH-induced changes in body temperature would be beneficial in further elucidating the underlying mechanism of GZ-793A-induced attenuation of METH-induced striatal DA content depletion.

XII. Final Comments

The results from this dissertation research report on the findings from an iterative drug discovery approach with the aim of developing VMAT2 selective lobeline analogs as treatments for METH abuse. The current results demonstrate that the lead analog, GZ-793A inhibits the neurochemical effects of METH through a selective interaction with VMAT2. This research shows that GZ-793A potently and selectively inhibits DA uptake at VMAT2 and promotes a release of DA from vesicles to redistribute DA from vesicles into the cytosol. Further, GZ-793A inhibits METH-evoked DA release from synaptic vesicles decreasing the cytosolic DA available for METH-induced reverse transport through DAT. Despite potent and selective inhibition of VMAT2 function, acute and repeated GZ-793A treatment does not alter striatal DA content. Importantly, GZ-793A pretreatment protects against acute METH-induced DA content depletions. Thus, results from this dissertation demonstrate that GZ-793A

represents an exciting preclinical lead in the development of novel pharmacotherapies to treat METH abuse.

LIST OF ABBREVIATIONS

U.S., United States; DA, dopamine; DAT, dopamine transporter; METH, methamphetamine; AMPH, amphetamine; VMAT2, vesicular monoamine transporter-2; nAChRs, nicotinic acetylcholine receptors; MTD, *meso*-transdiene; CNS, central nervous system; NAc, nucleus accumbens; TH, tyrosine hydroxylase; L-DOPA, L-dihydroxylphenylalanine; LDVC, large dense core vesicles; SSV, small synaptic vesicles; TMD, transmembrane domain; cAMP, cyclic adensosine monophosphate; COMT, catechol-O-methyl transferase; MAO, monoamine oxidase; DOPAC, dihydroxyphenylacetic acid; MPP+, 1-methyl-4-phenylpyridinium; NET, norepinephrine transporter; VTA, ventral tegmental area; SERT, serotonin transporter; KO, knock-out; WT, wild-type; PKC, protein kinase C; PKA, protein kinase A; 5-HT, serotonin; NE, norepinephrine; E, epinephrine; TBZ, tetrabenazine; AMPT, α-methyl-p-tyrosine; BBB, blood-brain barrier; CBT, cognitive behavioral therapy; CM, contingency management; MPD, methylphenidate; ADHD, attention deficit hyperactivity disorder; SSRIs, selective serotonin reuptake inhibitors; GABA, *gamma*-aminobutyric acid; ACh, acetylcholine; MLA, methyllycaconitine; DTBZ, dihydrotetrabenazine; diol, dihydroxypropyl; SAR, structure-activity relationships; EDTA, disodium ethylenediamine tetraacetate; EGTA, ethylene glycol tetraacetate; GBR 12909, 1-(2-(bis-(4-fluorophenyl)methoxy)ethyl)-4-(3-phenylpropyl)piperazine; GBR 12935, 1-(2-(diphenylmethoxy)ethyl)-4-(3-phenylpropyl)piperazine;WIN 35,428, [^{3}H](–)-2-β-carbomethoxy-3-β-(4-fluorophenyl)tropane-1,5-napthalenedisulfonate; HEPES, N-[2-hydroxyethyl]piperazine-N'-[2-ethanesulfonic acid]; $MgSO_4$, magnesium sulfate; PEI, polyethyleneimine; Ro-4-1284, (2R,3S,11bS)-2-ethyl-3-isobutyl-9,10-dimethoxy-2,2,4,6,7,11b-hexahydro-1H-pyrido[2,1-a]isoquinolin-2-ol; 6-OHDA, 6-hydroxydopamine; $CaCl_2$, calcium chloride; MgCl2, magnesium chloride; KCl, potassium chloride; K_2PO_4, potassium phosphate; $NaHCO_3$, sodium bicarbonate; NaH_2PO_4, sodium phosphate; UKMH-101, (3*Z*,5*E*)-3,5-dibenzylidene-1-methylpiperidine; UKMH-102, (3*Z*,5*Z*)-3,5-dibenzylidene-1-methylpiperidine; UKMH-103, [(3*Z*,5*E*)-1-methyl-3,5-bis((*E*)-3-phenylallylidene)piperidine; UKMH-104, (3*Z*,5*Z*)-1-methyl-3,5-bis((*E*)-3-phenylallylidene)piperidine; UKMH-105, (3*Z*,5*E*)-3,5-bis(2,4-dichlorobenzylidene)-1-methylpiperidine; UKMH-106, (3*Z*,5*Z*)-3,5-bis(2,4-dichlorobenzylidene)-1-methylpiperidine; UKMH-107, (3*Z*,5*Z*)-3,5-bis(4-methoxybenzylidene)-1-methylpiperidine; UKMH-108, (3*Z*,5*Z*)-1-methyl-3,5-bis(4-methylbenzylidene)-piperidine; UKMH-109, (3*Z*,5*Z*)-1-methyl-3,5-bis(thiophen-2-ylmethylene)piperidine; UKMH-110, (3*Z*,5*Z*)-1-methyl-3,5-bis(thiophen-3-ylmethylene)piperidine; UKMH-111, (3*Z*,5*Z*)-3,5-bis(furan-2-ylmethylene)-1-methylpiperidine; UKMH-112, (3*Z*,5*Z*)-3,5-bis(furan-3-ylmethylene)-1-methylpiperidine GZ-252C, para-methoxyphenyl lobelane; GZ-745A, (*R*)-3-(2,6-*cis*-diphenethylpiperidin-1-yl)propane-1,2-diol; GZ-745B, (*S*)-3-(2,6-*cis*-diphenethylpiperidin-1-yl)propane-1,2-diol; GZ-790A, (*R*)-3-[2,6-*cis*-di(3-methoxyphenethyl)piperidin-1-yl]propane-1,2-diol; GZ-790B, (*S*)-3-[2,6-*cis*-di(3-methoxyphenethyl)piperidin-1-yl]propane-1,2-diol; GZ-791A, (*R*)-3-[2,6-*cis*-di(3-

fluorophenethyl)piperidin-1-yl]propane-1,2-diol; GZ-791B, (*S*)-3-[2,6-*cis*-di(3-fluorophenethyl)piperidin-1-yl]propane-1,2-diol; GZ- 792A, (*R*)-3-[2,6-*cis*-di(2-methoxyphenethyl)piperidin-1-yl]propane-1,2-diol; GZ-792B, (*S*)-3-[2,6-*cis*-di(2-methoxyphenethyl)piperidin-1-yl]propane-1,2-diol; GZ-793A, (*R*)-3-[2,6-*cis*-di(4-methoxyphenethyl)piperidin-1-yl]propane-1,2-diol; GZ-793B, (*S*)-3-[2,6-*cis*-di(4-methoxyphenethyl)piperidin-1-yl]propane-1,2- diol; GZ-794A, (*R*)-3-[2,6-*cis*-di(1-naphthylethyl)piperidin-1-yl]propane-1,2-diol; GZ-794B, (*S*)-3-[2,6-*cis*-di(1-naphthylethyl)piperidin-1-yl]propane-1,2-diol; GZ- 795A, (*R*)-3-[2,6-*cis*-di(2,4-dichlorophenethyl)piperidin-1-yl]propane-1,2-diol; GZ-795B, (*S*)-3-[2,6-*cis*-di(2,4-dichlorophenethyl)piperidin-1-yl]propane-1,2-diol; GZ-796A, (*R*)-3-[2,6-*cis*-di(4-biphenylethyl)piperidin-1-yl]propane-1,2-diol; GZ-796B, (*S*)-3-[2,6-*cis*-di(4-biphenylethyl)piperidin-1-yl]propane-1,2-diol; GZ-797A, (*R*)-3-[2,6-*cis*-di(3,4-methylenedioxyphenethyl)piperidin-1-yl]propane-1,2-diol; GZ-797B, (*S*)-3-[2,6-*cis*-di(3,4-methylenedioxyphenethyl)piperidin-1-yl]propane-1,2-diol; UKCP-110, *cis*-2,5-di-(2-phenethyl)-pyrrolidine hydrochloride; GZ-250C, 2,6-bis(2-(3,4-methylenedioxyphenyl)ethyl)-1-methylpiperidine hydrochloride; GZ-252C, para-methoxyphenyl lobelane or 2,6-bis(2-(4-methoxyphenyl)ethyl)-1-methylpiperidine hydrochloride; GZ-260C, 2,6-bis(2-(2,4-dichlorophenyl)ethyl)-1-methylpiperidine hydrochloride; GZ-261C, 2,6-bis(2-(3-methoxyphenyl)ethyl)-1-methylpiperidine hydrochloride; GZ-272C, 2,6-bis(2-(biphenyl-4-yl)ethyl)-1-methylpiperidine hydrochloride; GZ-273C, 2,6-bis(2-(2-methoxyphenyl)ethyl)-1-methylpiperidine hydrochloride; GZ-275C, 2,6-bis(2-(3-fluorophenyl)ethyl)-1-methylpiperidine hydrochloride

REFERENCES

ACD/ADME Suit, version 5.0, Advanced Chemistry Development, Inc., Toronto, ON, Canada, www.acdlabs.com, 2010.

Adam et al., 2008 Anglin MD, Burke C, Perrochet B, Stamper E, Dawud-Noursi S (2000) Expression and function of the rat vesicular monoamine transporter 2. *Am J Physiol Cell Physiol*. **294:** 1004-1011.

Ahnert-Hilger G, Nurnberg B, Exner T, Schafer T, Jahn R (1998) The heterotrimeric G protein Go2 regulates catecholamine uptake by secretory vesicles. *EMBO J*. **17:** 406-413.

Ali SF, Newport GD, Holson RR, Slikker W Jr, Bowyer JF (1994) Low environmental temperatures or pharmacologic agents that produce hypothermia decrease methamphetamine neurotoxicity in mice. *Brain Res.* **658:** 33-38.

Almers W, Breckenridge LJ, Iwata A, Lee AK, Spruce AE, Tse FW (1991) Millisecond studies of single membrane fusion events. *Ann N Y Acad Sci*. **635:** 318-327.

Anggardiredja K, Nakamichi M, Hiranita T, Tanaka H, Shoyama Y, Watanabe S, Yamamoto T (2004) Naltrexone attenuates cue- but not drug-induced methamphetamine seeking: a possible mechanism for the dissociation of primary and secondary reward. *Brain Res*. **1021:** 1470-1478.

Anglin MD, Burke C, Perrochet B, Stamper E, Dawud-Noursi S (2000) History of the methamphetamine problem. *J Psychoactive Drugs*. **32:** 137-142.

Arai S, Takuma K, Mizoguchi H, Ibi D, Nagal T, Takahashi K, Kamei H, Nabeshima T, Yamada K (2008) Involvement of pallidotegmental neurons in methamphetamine- and MK-801-induced impairment of prepulse inhibition of the acoustic startle reflex in mice: reversal by GABAB receptor agonist baclofen. *Neuropsychopharmacology*. **33:** 3164-3175.

Arai S, Takuma K, Mizoguchi H, Ibi D, Nagal T, Kamei H, Kim HC, Yamada K (2009) GABAB receptor agonist baclofen improves methamphetamine-induced cognitive deficit in mice. *Eur J Pharmacol*. **602:** 101-104.

Arborelius L, Chergui K, Murase S, Nomikos GG, Hook BB, Chouvet G, Hacksell U, Svensson TH (1993) The 5-HT1A receptor selective ligands, (R)-8-OH-DPAT and (S)-UH-301, differentially affect the activity of midbrain dopamine neurons. *Naunyn Schmiedebergs Arch Pharmacol*. **347:** 353-362.

Armstrong BD and Noguchi KK (2004) The neurotoxic effects of 3,4-methylenedioxymethamphetamine (MDMA) and methamphetamine on serotonin, dopamine, and GABA-ergic terminals: an in-vitro autoradiographic study in rats. *Neurotoxicology*. **25:** 905-914.

Arnold EB, Molinoff PB, Rutledge CO (1977) The release of endogenous norepinephrine and dopamine from cerebral cortex by amphetamine. *J Pharmacol Exp Ther* **202:** 544-557.

Baker A, Lee NK, Claire M, Lewin TJ, Grant T, Pohlman S, Saunders JB, Kay-Lambkin, Constable P, Jenner L, Carr VJ (2005) Brief cognitive behavioral

interventions for regular amphetamine users: a step in the right direction. *Addiction* **100:** 367-378.

Bakhit C, Morgan ME, Peat MA, Gibb JW (1981) Long-term effects of methamphetamine on the synthesis and metabolism of 5-hydroxytryptamine in various regions of the rat brain. *Neuropharmacology* **20:** 1135-1140.

Balcells-Olivero M and Vezina P (1997) Effects of naltrexone on amphetamine-induced locomotion and rearing: acute and repeated injections. *Psychopharmacology (Berl)* **131:** 230-238.

Bardo MT (1998) Neuropharmacological mechanisms of drug reward: beyond dopamine in the nucleus accumbens. *Exp Clin Psychopharmacol*. **6:** 131-138

Barr AM, Panenka WJ, MacEwan GW, Thornton AE, Lang DJ, Honer WG, Lecomte T (2006) The need for speed: an update on methamphetamine addiction. *J Psychiatry Neurosci* **31:** 301-313.

Beckmann JS, Denehy ED, Zheng G, Crooks PA, Dwoskin LP, Bardo MT (2011) The effect of a novel VMAT2 inhibitor, GZ-793A, on methamphetamine reward in rats. *Psychopharmacology* Epub Sept. 21.

Beckmann JS, Siripurapu KB, Nickell JR, Horton DB, Denehy ED, Vartak A, Crooks PA, Dwoskin LP, Bardo MT (2010) The novel pyrrolidine nor-lobelane analog UKCP-110 [cis-2,5-di-(2-phenethyl)-pyrrolidine hydrochloride] inhibits VMAT2 function, methamphetamine-evoked

dopamine release and methamphetamine self-administration in rats. *J Pharmacol Exp Ther* **335:** 841-851.

Benloucif S, Keegan MJ, Galloway MP (1993) Serotonin-facilitated dopamine release in vivo: pharmacological characterization. *J Pharmacol Exp Ther* **265**: 373-377.

Berman SM, Kuczenski R, McCracken JT, London ED (2009) Potential adverse effects of amphetamine treatment on brain and behavior: a review. Mol Psychiatry. 14: 123-142.

Bhat RV, Turner SL, Selvaag SR, Marks MJ, Collins AC (1991) Regulation of brain nicotinic receptors by chronic agonist infusion. *J Neurochem*. **56:** 1932-1939.

Bjorklund A and Dunnett SB (2007) Dopamine neurons systems in the brain: an update. *Trends Neurosci.* **30:** 194-202.

Bonisch H (1984) The transport of (+)-amphetamine by the neuronal noradrenaline carrier. *Naunyn-Schmiedeberg's Arch Pharmacol* **327:** 262-272.

Bowyer JF and Ali S (2006) High doses of methamphetamine that cause disruption of the blood-brain barrier in limbic regions produce extensive neuronal degeneration in mouse hippocampus. *Synapse* **60:** 521-532.

Bowyer JF, Davies DL, Schmued L, Broening HW, Newport GD, Slikker W Jr, Holson RR (1994) Further studies of the role of hyperthermia in methamphetamine neurotoxicity. *J Pharmacol Exp Ther.* **268:** 1571-80.

Brebner K, Ahn S, Phillips AG (2005) Attenuation of d-amphetamine self-administration by baclofen in the rat: behavioral and neurochemical correlates. *Psychopharmacology (Berl).* **177:** 409-417.

Briggs CA and McKenna DG (1998) Activation and inhibition of the human alpha7 nicotinic acetylcholine receptor by agonists. *Neuropharmacology* **37:** 1095-1102

Brioni JD, O'Neill AB, Kim DJ, Decker MW (1993) Nicotinic receptor agonists exhibit anxiolytic-like effects on the elevated plus-maze test. *Eur J Pharmacol.* **238:** 1-8.

Brodie BB, Cho AK, Stefano FJ, Gessa GL (1969) On mechanisms of norepinephrine release by amphetamine and tyramine and tolerance to their effects. *Adv Biochem Psychopharmacol.* **1:** 219-238.

Brodie JD, Figueroa E, Laska EM, Dewey SL (2005) Safety and efficacy of gamma-vinyl GABA (GVG) for the treatment of methamphetamine and/or cocaine addiction. *Synapse* **55:** 122-125.

Brown JM, Hanson GR, Fleckenstein AE (2000) Methampehtamine rapidly decreases vesicular dopamine uptake. *J Neurochem.* **74:** 2221-2223.

Brunk I, Blex C, Rachakonda S, Holtje M, Winter S, Pahner I, Walther DJ, Ahnert-Hilger G (2006) The first luminal domain of vesicular monoamine transporters mediates G-protein-dependent regulation of transmitter uptake. *J Biol Chem.* **281:** 33373-33385.

Buck KJ and Amara SG (1995) Structural domains of catecholamine transporter chimeras involved in selective inhibition by antidepressants and psychomotor stimulants. *Mol Pharmacol.* **48:** 1030-1037.

Budygin EA, Brodie MS, Sotnikova TD, Mateo Y, John CE, Cyr M, Gainetdinov RR, Jones SR (2004) Dissociation of rewarding and dopamine transporter-mediated properties of amphetamine. *Proc Natl Acad Sci U S A* **101:** 7781-7786.

Burn JH and Rand MJ (1958) The action of sympathomimetic amines in animals treated with reserpine. *J Physiol.* **144:** 314-336.

Buu NT and Lussier C (1989) Consenquences of monoamine oxidase inhibition: increased vesicular accumulation of dopamine and norepinephrine and increased metabolism by catechol-O-methyltransferase and phenolsulfotransferase. *Prog Neuropsychopharmacol Biol Psychiatry*. **13:** 536-568.

Cadet JL and Brannock C (1998) Free radicals and the pathobiology of brain dopamine systems. *Neurochem Int.* **32:** 117-131.

Cadet JL and Krasnova IN (2009) Molecular bases of methamphetamine-induced neurodegeneration. *Int Rev Neurobiol*. **88:** 101-119.

Carboni E, Sielewoy C, Vacca C, Nosten-Bertrand M, Giros B, Di Chiara G (2001) Cocaine and amphetamine increase extracellular dopamine in the nucleus accumbens of mice lacking the dopamine transporter gene*. J Neurosci*. **21:** 1-4.

Cass WA and Zahniser NR (1991) Potassium channel blockers inhibit D2 dopamine, but not A1 adenosine, receptor-mediated inhibition of striatal dopamine release. *J Neurochem.* **57:** 147-152.

Cervinksi MA, Foster JD, Vaughan RA (2005) Psychoactive substrates stimulate dopamine transporter phosphorylation and down-regulation by cocaine-sensitive and protein kinase C-dependent mechanisms. *J Biol Chem*. **280:** 40442-40449.

Champtiaux N, Gotti C, Cordero-Erausquin M, David DJ, Przybylski C, Lena C, Clementi F, Moretti M, Rossi FM, Le Novere N, McIntosh JM, Gardier AM, Changeux JP (2003) Subunit composition of functional nicotinic receptors in dopaminergic neurons investigated with knock-out mice. *J Neurosci.* **23:** 7820-7829.

Chen N and Reith ME (2008) Substrates dissociate dopamine transporter oligomers. *J Neurochem.* **105:** 910-920.

Cheng Y and Prusoff WH (1973) Relationship between the inhibition constant (KI) and the concentration of inhibitor which causes 50 per cent inhibition (I50) of an enzymatic reaction. *Biochem Pharmacol* **22:** 3099-3108.

Chen N, Vaughan RA, Reith ME (2001) The role of conserved tryptophan and acidic residues in the human dopamine transporter as characterized by site-directed mutagenesis. *J Neurochem*. **77:** 1116-1127.

Chen BT, Hopf FW, Bonci A (2010) Synaptic plasticity in the mesolimbic system: therapeutic implications for substance abuse. *Ann N Y Acad Sci* **1187:** 129-139.

Chiu CT, Ma T, Ho IK (2006) Methamphetamine-induced behavioral sensitization in mice: alterations in mu-opioid receptor. *J Biomed Sci.* **13:** 797-811.

Ciliax BJ, Heilman C, Demchyshyn LL, Pristupa ZB, Ince E, Hersch SM, Niznik HB, Levey AI (1995) The dopamine transporter: immunochemical characterization and localization in brain. *J Neurosci.* **15:** 1714-1723.

Clarke PB and Reuben M (1996) Release of [^{3}H]-noradrenaline from rat hippocampal synaptosomes by nicotine: mediation by different nicotinic receptor subtypes from striatal [^{3}H]-dopamine release. *Br J Pharmacol.* **117:** 595-606.

Cleren C, Naudin B, Costentin J (2003) Apparent opposite effects of tetrabenazine and reserpine on the toxic effects of 1-methyl-4-phenylpyridinium or 6-hydroxydopamine on nigro-striatal dopaminergic neurons. *Brain Res.* **989:** 187-195.

Cooper JR, Bloom FE, Roth RH (2003) The biochemical basis of neuropharmacology. 8th ed. University Press: New York.

Cousins MS, Roberts DC, de Wit H (2002) GABA(B) receptor agonists for the treatment of drug addiction: a review of recent findings. *Drug Alcohol Depend.* **65:** 209-220.

Coyle JT and Snyder SH (1969) Antiparkinsonian drugs: inhibition of dopamine uptake in the corpus striatum as a possible mechanism of action. *Science* **166:** 899-901.

Crooks PA, Zheng G, Vartak AP, Culver JP, Zheng F, Horton DB, Dwoskin LP (2010) Design, synthesis and interaction at the vesicular monoamine

transporter-2 of lobeline analogs: potential pharmacotherapies for the treatment of psychostimulant abuse. *Curr Top Med Chem* **11:** 1103-27.

Cruickshank CC, Montebello ME, Dyer KR, Quigley A, Blaszczyk J, Tomkins S, Shand D (2008) A placebo-controlled trial of mirtazapine of the management of methamphetamine withdrawal. *Drug Alcohol Rev.* **27:** 326-333.

Cruickshank CC and Dyer KR (2009) A review of the clinical pharmacology of methamphetamine. *Addiction*. **104:** 1085-1099.

DASIS, Drug and Alcohol Services Information System (2008) Substance Abuse and Mental Health Services Administration, Office of Applied Studies. *National Survey of Substance Abuse Treatment Services (N-SSATS): 2008. Data on Substance Abuse Treatment Facilities*, DASIS Series: S-49, HHS Publication No. (SMA) 09-4451, Rockville, MD, 2009.

Damaj MI, Patrick GZ, Creasy KR, Martin BR (1997) Pharmacology of lobeline, a nicotinic receptor ligand. *J Pharmacol Exp Ther*. **282:** 410-419.

Daniels GM and Amara, SG (1999) Regulated trafficking of the human dopamine transporter. Clathrin-mediated internalization and lysosomal degradation in response to phorbol esters. *J Biol Chem.* **274:** 35794-35801.

Dar DE, Thiruvazhi M, Abraham P, Kitayama S, Kopajtic TA, Gamliel A, Slusher BS, Carrol FI, Uhl GR (2005) Structure-activity relationship of trihexyphenidyl analogs with respect to the dopamine transporter in the on-going search for a cocaine inhibitor. *Eur J Med Chem* **40:** 13-21.

Darchen F, Scherman D, Henry JP (1989) Reserpine binding to chromaffin granules suggests the existence of two conformaitons of the monoamine transporter. *Biochemistry* **28:** 1692-1697.

Darke S, Kaye S, McKetin R, Duflou J (2008) Major physical and psychological harms of methamphetamine use. *Drug Alcohol Rev* **27:** 253-262.

Davidson C, Gopalan R, Ahn C, Chen Q, Mannelli P, Patkar AA, Weese GD, Lee TH, Ellinwood EH (2007) Reduction in methamphetamine induced sensitization and reinstatement after combined pergolide plus ondansetron treatment during withdrawal. *Eur J Pharmacol.* **565:** 113-118.

Decker MW, Majchrzak MJ, Arneric SP (1993) Effects of lobeline, a nicotinic receptor agonist, on learning and memory. *Pharmacol Biochem Behav.* **45:** 571-576.

De la Garza R, Shoptaw S, Newton TF (2008) Evaluation of the cardiovascular and subjective effects of rivastigmine in combination with methamphetamine in methamphetamine-dependent human volunteers. *Int J Neuropsychophamacol*. **11:** 729-741.

DeMarco A, Dalal RM, Pai J, Aquilina SD, Mullapudi U, Hammel C, Kothari SK, Kahanda M, Liebling CN, Patel V, Schiffer WK, Brodie JD, Dewey SL (2008) Racemic gamma vinyl-GABA (R,S-GVG) blocks methamphetamine-triggered reinstatement of conditioned place preference. *Synapse* **63:** 87-94.

Demarest KT, Lawson-Wendling KL, Moore KE (1993) *d*-amphetamine and γ-butyrolactone alteration of dopamine synthesis in the terminals of

nigrostriatal and mesolimbic neurons: Possible role of various autoreceptor sensitivities *Biochem Pharmacol.* **32:** 691-697.

Derlet RW and Heischober B (1990) Methamphetamine. Stimulant of the 1990s? *West Med* **153:** 625-628.

Dhawan BN, Cesselin F, Raghubir R, Reisine T, Bradley PB, Portoghese PS, Hamon M (1996) International Union of Pharmacology. XII. Classification of opioid receptors. *Pharmacol Rev.* **48:** 567-592.

Di Chiara G and Imperato A (1988) Drugs abused by humans preferentially increase synaptic dopamine concentrations in the mesolimbic system of freely moving rats. *Proc Natl Acad Sci USA* **85:** 5274-5278.

Di Chiara G, Bassareo V, Fenu S, De Luca MA, Spina L, Cadoni C, Acquas E, Carboni E, Valentini V, Lecca D (2004) Dopamine and drug addiction: the nucleus acumens shell connection. *Neuropharmacology* **47:** 227-241.

Di Mascio M, Di Giovanni G, Di Matteo V, Prisco S, Esposito E (1998) Selective serotonin reuptake inhibitors reduce the spontaneous activity of dopaminergic neurons in the ventral tegmental area. *Brain Res Bull*. **46:** 547-54.

Dorsey JL (1936) Control of the tobacco habit. *Ann Int Med.* **10:** 628-631.

Dwoskin LP and Crooks PA (2002) A novel mechanism of action and potential use for lobeline as a treatment for psychostimulant abuse. *Biochem Pharmacol* **63:** 89-98.

Egaña LA, Cuevas RA, Baust TB, Parra LA, Leak RK, Hochendoner S, Peña K, Quiroz M, Hong WC, Dorostkar MM, Janz R, Sitte HH, Torres GE (2009)

Physical and functional interaction between the dopamine transporter and the synaptic vesicle protein synaptogyrin-3. *J Neurosci.* **29:** 4592-4604.

Eiden LE and Weihe E (2011) VMAT2: a dynamic regulator of brain monoaminergic neuronal function interacting with drug of abuse. *Ann N Y Acad Sci.* **1216:** 86-98.

Eiden LE, Schafer MK, Weihe E, Schutz B (2004) The vesicular amine transporter family (SLC18): amine/proton antiporters required for vesicular accumulation and regulated exocytotic secretion of monoamines and acetylcholine. *Pflugers Arch.* **447:** 636-640.

Eisenhofer G (2001) The role of neuronal and extraneuronal plasma membrane transporters in the inactivation of peripheral catecholamines. *Pharmacol Ther.* **91:** 35-62.

Erickson JD, Schafer MKH, Bonner TI, Eiden LE, Weihe E (1996) Distinct pharmacological properties and distribution in neurons and endocrine cells of two isoforms of the human vesicular monoamine transporter. *Proc. Natl. Acad. Sci.* **93**:5166-5171.

Eriksen J, Bjorn-Yoshimoto WE, Jorgensen TN, Newman AH, Gether U (2010) Postendocytic sorting of constitutively internalized dopamine transporter in cell lines and dopaminergic neurons. *J Biol Chem.* **285:** 27289-27301.

Everitt BJ and Robbins TW (2005) Neural systems of reinforcement for drug addiction: from actions to habits to compulsion. *Nat Neurosci*. **8:** 1481-1489.

Eyerman DJ and Yamamoto BK (2005) Lobeline attenuates methamphetamine-induced changes in vesicular monoamine transporter 2 immunoreactivity and monoamine depletions in the striatum. *J Pharmacol Exp Ther* **312:** 160-169.

Eyerman DJ and Yamamoto BK (2007) A rapid oxidation and persistent decrease in the vesicular monoamine transporter 2 after methamphetamine. *J Neurochem*, **103**: 1219-1227.

Fekete MIK, Herman JP, Kanyicska B, Palkovits M (1979) Dopamine, noradrenaline and 3,4-dihydroxypheylacetic acid (DOPAC) levels of individual brain nuclei, effects of haloperidol and pargyline. *J Neural Transmission*. **45:** 207-218.

Felpin F and Lebreton J (2000) History, chemistry and biology of alkaloids from Lobelia inflata. *Tetrahedron* **60:** 10127-10153.

Fischer JF and Cho AK (1979) Chemical release of dopamine from striatal homogenates: Evidence for an exchange diffusion model. *J Pharmacol Exp Ther* **208:** 203-209.

Flammia D, Dukat M, Damaj MI, Martin B, Glennon RA (1999) Lobeline: structure-affinity investigation of nicotinic acetylcholinergic receptor binding. *J Med Chem* **42:** 3726-3731.

Fleckenstein AE, Metzger RR, Wilkins DG, Gibb JW, Hanson GR (1997) Rapid and reversible effects of methamphetamine on dopamine transporters. *J Pharmacol Exp Ther.* **282:** 834-838.

Fleckenstein AE, Volz TJ, Riddle EL, Gibb JW, Hanson GR (2007) New insights into the mechanism of action of amphetamines. *Annu Rev Pharmacol Toxicol* **47:** 681-698.

Floor E and Meng L (1996) Amphetamine releases dopamine from synaptic vesicles by dual mechanisms. *Neurosci Lett.* **215:** 53-56.

Floor E, Leventhal PS, Wang Y, Meng L, Chen W (1995) Dynamic storage of dopamine in rat brain synaptic vesicles in vitro. *J Neurochem.* **64:** 689-699.

Fon EA, Pothos EN, Sun BC, Killeen N, Sulzer D, Edwards RH (1997) Vesicular transport regulates monamine storage and release but is not essential for amphetamine action. *Neuron.* **19:** 1281-1283.

Frank S (2010) Tetrabenazine: the first approved drug for the treatment of chorea in US patients with Huntington disease. *Neuropsychiatr Dis Treat* **6:** 657-665.

Freese TE, Miotto K, Reback CJ (2002) The effects and consequences of selected club drugs. *J Subst Abuse Treat* **23:** 151-156.

Fudala PJ and Iwamoto ET (1986) Further studies on nicotine-induced conditioned place preference in the rat. *Pharmacol. Biochem. Behav.* **25:** 1041-1049

Fumagalli F, Gainetdinov RR, Valenzano K, Caron MG (1998) Role of dopamine transporter in methamphetamine-induced neurotoxicity: Evidence from mice lacking the transporter. *J. Neurosci.* **18:** 4861-4869.

Fumagalli F, Gainetdinov RR, Wang YM, Valenzano KJ, Miller GW, Caron MG (1999) Increased methamphetamine neurotoxicity in heterozygous vesicular monoamine transporter 2 knock-out mice. *J Neurosci* **19:**2424-2431.

Gainetdinov RR, Jones SR, Fumagalli F, Wightman RM, Caron MG (1998) Re-evaluation of the roleof the dopamine transporter in dopamine system homeostasis. *Brain Res Brain Res Rev*. **26:** 148-153.

Gainetdinov RR (2008) Dopamine transporter mutant mice in experimental neuropharmacology. *Naunyn Schmiedebergs Arch Pharmacol.* **377:** 301-313.

Galli A, Blakely RD, DeFelice LJ (1998) Patch-clamp and amperometric recordings from norepinephrine transporters: channel activity and voltage-dependent uptake. *Proc Natl Acad Sci U S A* **95:** 13260-13265.

Gerasimov MR, Ashby CR Jr, Gardner EL, Mills MJ, Brodie JD, Dewey SL (1999) Gamma-vinyl GABA inhibits methamphetamine, heroin, or ethanol-induced increases in nucleus accumbens dopamine*. Synapse* **34:** 11-19.

Gettig JP, Grady SE, Nowosadzka I (2006) Methamphetmaine: putting the brakes on speed. *J Sch Nurs.* **22:** 66-73.

Ginawi OT, Al-Majed AA, Al-Suwailem AK (2005) Ondansetron, a selective 5-HT3 antagonist, antagonizes methamphetamine-induced anorexia in mice. *Pharmacol Res.* **51:** 255-259.

Giros B, Wang YM, Suter S, McLeskey SB, Pifl C, Caron MG (1994) Delineation of discreete domains for substrate, cocaine, and tricyclic antidepressant

interactions using chimeric dopamine-norepinephrine transporters. *J Biol Chem*. **269:** 15985-15988.

Giros B, Jaber M, Jones SR, Wightman RM, Caron MG (1996) Hyperlocomotion and indifference to cocaine and amphetamine in mice lacking the dopamine transporter*. Nature* **379:** 606-612.

Glover ED, Rath JM, Sharma E, Glover PN, Laflin M, Tonnesen P, Repsher L, Quiring J (2010) A multicenter phase 3 trial of lobeline sulfate for smoking cessation. *Am J Health Behav*. **34:** 101-109.

Glowinski J and Axelrod J (1966) Effects of drugs on the disposition of H-3-norepinephrine in the rat brain.*Pharmacol Rev.* **18:** 775-775.

Gluck MR, Moy LY, Jayatilleke E, Hogan KA, Manzino L, Sonsalla PK (2001) Parallel increases in lipid and protein oxidative markers in several mouse brain regions after methamphetamine treatment. *J Neurochem* **79:** 152-160.

Gnegy ME (2003) The effect of phosphorylation on amphetamine-mediated outward transport. *Eur J Pharmacol* **479:** 83-91.

Gong W, Neill DB, Justice JB Jr. (1998) GABAergic modulation of ventral pallidal dopamine release studied by in vivo microdialysis in the freely moving rat. *Synapse* **29:** 406-412.

Gonzalez AM, Walther D, Pazos A, Uhl GR (1994) Synaptic vesicular monoamine transporter expression: distribution and pharmacologic profile. *Mol. Brain Res*. **22:** 219-226.

Gonzales R, Mooney L, Rawson RA (2010) The methamphetamine problem in the United States. *Annu Rev Public Health*. **31:** 385-398.

Gossop M, Bradley BP, Brewis RK (1982) Amphetamine withdrawal and sleep disturbance. *Drug Alcohol Depend.* **10:** 177-183.

Grabowski J, Roache JD, Schmitz JM, Rhoades H, Creson D, Korszun A (1997) Replacement medication of cocaine dependence: methylphenidate. *J Clin Pharmacol* **17:** 485-488.

Graham DL, Noailles PA, Cadet JL (2008) Differential neurochemical consequences of an escalating dose-binge regimen followed by single-day multiple-dose methamphetamine challenges. *J Neurochem*. **105:** 1873-1885.

Graves SM and Napier TC (2011) Mirtazapine alters cue-associated methamphetamine seeking in rats. *Biol Psychiatry* **69:** 275-281.

Guan XM and McBride WJ (1989) Serotonin microinfusion into the ventral tegmental area increases accumbens dopamine release. *Brain Res Bull*. **23:** 541-547.

Gu H, Caplan MJ, Rudnick G (1998) Cloned catecholamine transporters expressed in polarized epithelial cells: sorting, drug sensitivity, and ion-coupling stoichiometry. *Adv Pharmacol*. **42:** 175-179.

Guilarte TR, Nihei MK, McGlothan JL, Howard AS (2003) Methamphetamine-induced deficits of brain monoaminergic neuronal markers: distal axotomy or neuronal plasticity. *Neuroscience.* **122:** 499-513.

Guillot TS, Shepherd KR, Richardson JR, Wang MZ, Li Y, Emson PC, Miller GW (2008) Reduced vesicular storage of dopamine exacerbates methamphetamine-induced neurodegeneration and astrogliosis. *J Neurochem*. **160:** 2205-2217.

Hagan MM, Rushing PA, Pritchard LM, Schwartz MW, Strack AM, Van der Ploeg LHT, Woods SC, Seeley RJ (2000) Long-term orexigenic effects of AgRP-(83—132) involve mechanisms other than melanocortin receptor blockade. *Am J Physiol Regul Integr Comp Physiol.* **279:** R47-R52.

Halford JC, Boyland EJ, Lawton CL, Blundell JE, Harrold JA (2011) Serotonergic anti-obesity agents: past experience and future prospects. *Drugs.* **71:** 2247-2255.

Han DD and Gu HH (2006) Comparison of the monoamine transporters from human and mouse in their sensitivities to psychostimulant drugs. *BMC Pharmacol* **6:** 6.

Hanson GR (2002) Methamphetamine abuse and addiction. National Institute on Drug Abuse Research report. NIH Publication number 02-4210:1-8.

Harrod SB, Dwoskin LP, Crooks PA, Klebaur JE, Bardo MT (2001) Lobeline attenuates d-methamphetamine self-administration in rats. *J Pharmacol Exp Ther* **280:** 1432-1444.

Harrod SB, Dwoskin LP, Green TA, Gehrke BJ, Bardo MT (2003) Lobeline does not serve as a reinforcer in rats. *Psychopharmacology (Berl)* **165:** 397-404.

Heinzerling KG, Shoptaw S, Peck JA, Yang X, Liu J, Roll J, Ling W (2006) Randomized, placebo controlled trial of baclofen and gabapentin for the treatment of methamphetamine dependence. *Drug Alcohol Depend*. **85:** 177-184.

Herrold AA, Shen F, Graham MP, Harper LK, Specio SE, Tedford CE, Napier TC (2009) Mirtazapine treatment after conditioning with methamphetamine alters subsequent expression of place preference. *Drug Alcohol Depend.* **99:** 231-239.

Hersch SM, Yi H, Heilman CJ, Edwards RH, Levey AI (1997) Subcellular localization and molecular topology of the dopamine transporter in the striatum and substantia nigra. *J Comp Neurol.* **388:** 211-227.

Higgins ST (2006) Extending contingency management to the treatment of methamphetamine use disorders*. Am J Psychiatry* **163:**1870-1872.

Hikida T, Kaneko S, Isobe T, Kirabatake Y, Watanabe D, Pastan I, Nakanishi S (2001) Increased sensitivity to cocaine by cholinergic cell ablation in nucleus accumbens*. Proc Natl Acad Sci U S A* **98:** 13351-13354.

Hiranita T, Nawata Y, Sakimura K, Anggadiredja K, Yamamoto T (2006) Supression of methamphetamine-seeking behavior by nicotinic agonists*. Proc Natl Acad Sci U S A* **103:** 8523-8527.

Hoffman BJ, Hansson SR, Mezey E, Palkovits M (1998) Localization and dynamic regulation of biogenic amine transporters in the mammalian central nervous system. *Front Neuroendocrinol*. **19:** 187-231.

Hogan KA, Staal RG, Sonsalla PK (2000) Analysis of VMAT2 binding after methamphetamine or MPTP treatment: disparity between homogenates and vesicle preparations. *J Neurochem*. **74:** 2217-2220.

Höltje M, von Jagow B, Pahner I, Lautenschlager M, Hörtnagl H, Nürnberg B, Jahn R, Ahnert-Hilger G (2000) The neuronal monoamine transporter VMAT2 is regulated by the trimeric GTPase Go(2). *J Neurosci*. **20:** 2131-2141.

Homer BD, Solomon TM, Moeller RW, Mascia A, De Raleau L, Halkitis PN (2008) Methampehtamine abuse and impairment of social functioning: a review of the underlying neurophysiologial causes and behavioral implications. *Psychol Bull.* **134:** 301-310.

Horton DB, Siripurapu KB, Norrholm SD, Culver JP, Hojahmat M, Beckmann JS, Harrod SB, Deaciuc AG, Bardo MT, Crooks PA, Dwoskin LP (2011a) meso-Transdiene analogs inhibit vesicular monoamine transporter-2 function and methamphetamine-evoked dopamine release. *J Pharmacol Exp Ther* **336:** 940-51. (Chapter 2)

Horton DB, Siripurapu KB, Zheng G, Crooks PA, Dwoskin LP (2011b) Novel N-1,2-dihydroxypropyl analogs of lobelane inhibit vesicular monoamine transporter-2 function and methamphetamine-evoked dopamine release. *J Pharmacol Exp Ther* **339:** 1-12. (Chapter 3)

Horton DB, Zheng G, Crooks PA, Dwoskin LP (2011c) GZ-793A, a novel vesicular monoamine transporter-2 (VMAT2) inhibitor that probes multiple

sites on VMAT2 as a potential treatment for methamphetamine abuse. *J Neurochem,* submitted. (Chapter 4)

Hotchkiss AJ, Morgan ME, Gibb JW (1979) The long-term effects of multiple doses of methamphetamine on neostriatal tryptophan hydroxylase, tyrosine hydroxylase, choline acetyltransferase and glutamate decarboxylase activities. *Life Sci.* **25:** 1373-1378.

Howell LL, Carroll FI, Votaw JR, Goodman MM, Kimmel HL (2007) Effects of combined dopamine and serotonin transporter inhibitors on cocaine self-administration in rhesus monkeys. *J Pharmacol Exp Ther* **320:** 757-765.

Hua Y, Sinha R, Thiel CS, Schmidt R, Huve J, Martens H, Hell SW, Egner A, Klingauf J (2011) A readily retrievable pool of synaptic vesicles. *Nat Neurosci.* **14:** 833-839.

Hurley MJ and Jenner P (2006) What has been learnt from study of dopamine receptors in Parkinson's disease? *Pharmacol Ther.* **111:** 715-728.

Indarte M, Madura JD, Surratt CK (2008) Dopamine transporter comparative molecular modeling and binding site prediction using the LeuT(Aa) leucine transporter as a template*. Proteins* **70:** 1033-1046.

Ingram SL, Prasad BM, Amara SG (2002) Dopamine transporter-mediated conductances increase excitability of midbrain dopamine neurons. *Nat Neurosci.* **5:** 971-978.

Itzhak Y and Martin JL (2000) Effect of riluzole and gabapentin on cocaine- and methamphetamine-induced behavioral sensitization in mice. *Psychopharmaoclogy (Berl).* **151:** 226-233.

Jacobs BLand Azmitia EC (1992) Structure and function of the brain serotonin system. *Physiol Rev*. **72:** 165-229.

Jardetzky O (1966) Simple allosteric model for membrane pumps. *Nature* **211:** 969-970.

Jayanthi S, Ladenheim B, Cadet JL (1998) Methamphetamine-induced changes in antioxidant enzymes and lipid peroxidation in copper/zinc-superoxide dismutase transgenic mice. *Ann N Y Acad Sci.* **844:** 92-102.

Jayanthi LD, Samuvel DJ, Buck ER, Reith ME and Ramamoorthy S (2007) Regulation of biogenic amine transporters, In: *Handbook of Neurochemistry and Molecular Neurobiology* (Abel L ed) pp 363-386, Springer New York Inc., New York.

Jayaram-Lindstrom N, Wennberg P, Hurd YL, Franck J (2008) Naltrexone for the treatment of amphetamine dependence: a randomized placebo-controlled trial. *J Clin Psychopharmacol.* **24:** 665-669.

Jayaram-Lindstrom N, Hammarberg A, Beck O, Franck J (2008) Naltrexone for the treatment of amphetamine dependence: a randomized placebo-controlled trial. *Am J Psychiatry* **165:** 1442-1448.

Johnson BA, Ait-Daoud N, Elkashef AM, Smith EV, Kahn R, Vocci F, Li SH, Bloch DA; Methamphetamine Study Group (2008) A preliminary randomized, double-blind placebo-controlled study of the safety and efficacy of ondansetron in the treatment of methamphetamine dependence. *Int J Neuropsychopharmacol*. 11: 1-14.

Johnson LA, Furman CA, Zhang M, Guptaroy B, Gnegy ME (2005) Rapid delivery of the dopamine transporter to the plasmalemmal membrane upon amphetamine stimulation. *Neuropharmacology* **49:** 750-758.

Johnson RG (1988) Accumulation of biological amines into chromaffin granules: A model for hormone and neurotransmitter transport. *Physiol Rev.* **68:** 232-307.

Jones R (2007) Double-blind, placebo-controlled, cross-over assessment of intravenous methamphetamine and sublingual lobeline interactions. NCT00439504. Clinical Trials.gov.

Jones SR, Gainetdinov RR, Jaber M, Giros B, Wightman RM, Caron MG (1998a) Profound neuronal plasticity in response to inactivation of the dopamine transporter. *Proc Natl Acad Sci U S A* **95:** 4029-4034.

Jones SR, Gainetdinov RR, Wightman RM, Caron MG (1998b) Mechanisms of amphetamine action revealed in mice lacking the dopamine transporter. *J. Neurosci.* **18:** 1979-1986.

Jones SR, Joseph JD, Barak LS, Caron MG, Wightman RM (1999) Dopamine neuronal transport kinetics and effects of amphetamine. *J. Neurochem*. **73:** 2406-2414.

Kahlig KM, Binda F, Khoshbouei H, Blakely RD, McMahon DG, Javitch JA, Galli A (2005) Amphetamine induces dopamine efflux through a dopamine transporter channel. *Proc Natl Acad Sci USA* **102:** 3495-3500.

Karila L, Weinstein A, Aubin HJ, Benyamina A, Reynaud M, Batki SL (2010) Pharmacological approaches to methamphetamine dependence: a focused review. *Br J Clin Pharmacol* **69:** 578-592.

Kaye S, McKetin R, Duflous J, Darke S (2007) Methamphetamine and cardiovascular pathology: a review of the evidence. *Addiction* **102:** 1204-1211.

Kenakin T. P. (1993) *Pharmacologic Analysis of Drug-Receptor Interaction*. 2nd Edition. Raven Press, New York.

Kenakin TP (2006) A Pharmacology Primer, Second Edition: Theory, Application, Methods. 2nd Edition. Academic Press, San Diego.

Khoshboeui H, Wang H, Lechleiter JD, Javitch JA, Galli A (2003) Ampehtamine-induced dopamine efflux. A voltage sensitive and intracellular Na+-dependent mechanism. *J Biol Chem*. **278:** 12070-12077.

Kilbourn M, Lee L, Borght TV, Jewett D, Frye K (1995) Binding of α-dihydrotetrabenazine to the vesicular monoamine transporter is stereoselective. *Eur J Pharmacol* **278:** 249-252.

King MJ, Hosmer HR, Dresbach M (1928) Physiological reactions induced by alpha-lobelin I. Intravenous injections during anesthesia and certain other forms of depression. *J Pharmacol Exp Ther*. **32:** 241-272.

Kirschner N (1962) Uptake of catecholamines by a particulate fraction of the adrenal medulla. *J Biol Chem.* **237:** 2311-2317.

Kiss JP, Windisch K, De Oliveira K, Hennings EC, Mike A, Szasz BK (2001) Differential effect of nicotinic agonists on the [^{3}H]norepinephrine release from rat hippocampal slices. *Neurochem. Res*. **26:** 943-950.

Kita T, Wagner GC, Philbert MA, King LA, Lowndes HE (1995) Effects of pargyline and pyrogallol on the methamphetamine-induced dopamine depletion. *Mol Chem Neuropathol*. **24**: 31-41.

Knepper SM, Grunewald GL, Rutledge CO (1988) Inhibition of norepinephrine transport into synaptic vesicles by amphetamine analogs. *J Pharmacol Exp Ther*. **247:** 487-494.

Knoth J, Zallakian M, Njus D (1981) Stoichiometry of H+-linked dopamine transport in chromaffin granule ghosts. *Biochemistry* **20:** 6625-6629.

Kogan FJ, Nichols WK, Gibb JW (1976) Influence of methamphetamine on nigral and striatal tyrosine hydroxylase activity and on striatal dopamine levels. *Eur J Pharmacol.* **36:** 363-371.

Kokoshka JM, Vaughan RA, Hanson GR, Fleckenstein AE (1998) Nature of methamphetamine-induced rapid and reversible changes in dopamine transporters. *Eur J Pharmacol*. **361:** 269-275.

Koob GF (1992) Neural mechanisms of drug reinforcement. *Ann N Y Acad Sci.* **654:** 171-191.

Koob GF, Sanna PP, Bloom FE (1998) Neuroscience of addiction. *Neuron* **21:** 467-476.

Krantz DE, Peter D, Liu Y, Edwards RH (1997) Phosphorylation of a vesicular monoamne transporter by casein kinase II. *J Biol Chem***. 272:** 6752-6759.

Krasnova IN and Cadet JL (2009) Methamphetamine toxicity and messengers of death. *Brain Res Rev* **60:** 379-407.

Krochmal A and Krochmal C (1973) *A Guide to the Medicinal Plants of the United States*. Quadrangle/New York Times Book Company, New York.

Krueger BK (1990) Kinetics and block of dopamine uptake in synaptosomes from rat caudate nucleus. *J Neurochem***. 55:** 260-267.

Kuczenski R (1975) Effects of catecholamine releasing agents on synaptosomal dopamine biosynthesis: multiple pools of dopamine or multiple forms of tyrosine hydroxylase. *Neuropharmacology* **14:** 1-10.

Kukkonen A, Perakyla M, Akerman KEO, Nasman J (2004) Muscarinic toxin 7 selectivity is dictated by extracellular receptor loops. *J. Biol. Chem.* **279:** 50923-50929.

Kuribara H (1997) Effects of tetrabenazine on methamphetamine-induced hyperactivity in mice are dependent on order and time-course of administration. *Pharmacol Biochem Behav*. **56:** 9-14.

Kurokawa K, Shibasaki M, Mizuno K, Ohkuma S (2011) Gabapentin blocks methamphetamine-induced sensitization and conditioned place preference via inhibition of α_2/δ-1 subunits of the voltage-gated calcium channels. Neuroscience 176: 328-335.

Lacey MG, Mercuri NB, North RA (1987) Dopamine acts on D2 receptors to increase potassium conductance in neurons of the rat substantia nigra zona compacta. *J Physiol.* **392:** 397-416.

Lee FJ, Liu F, Pristupa ZB, Niznik HB (2001) Direct binding and functional coupling of alpha-synuclein to the dopamine transporters accelerate dopamine-induced apoptosis. *FASEB J*. **15:** 916-926.

Lee FJ, Pei L, Moszczynska A, Vukusic B, Fletcher PJ, Liu F (2007) Dopamine transporter cell surface localization facilitated by a direct interaction with the dopamine D2 receptor. *EMBO J*. **26:** 2127-2136.

Lee M, Gubernator NG, Sulzer D, Sames D (2010) Development of pH-responsive fluorescent false neurotransmitters. *J Am Chem Soc* **132:** 8828-8830.

Lee NK and Rawson RA (2008) A systematic review of cognitive and behavioural therapies for methamphetamine dependence. *Drug Alcohol Rev***. 24:** 309-317.

Lee SH, Kang SS, Son H, Lee YS (1998) The region of dopamine transporter encompassing the 3rd transmembrane domain is crucial for function. *Biochem Biophys Res Commun.* **246:** 347-352.

Lee KH, Kim MY, Kim DH, Lee YS (2004) Syntaxin 1A and receptor for activated C kinase interact with the N-terminal region of human dopamine transporter. *Neurochem Res.* **29:** 1405-1409.

Lehericy S, Brandel JP, Hirsch EC, Anglade P, Villares J, Scherman D, Duyckaerts C, Javoy-Agid F, Agid Y (1994) Monoamine vesicular uptake sites in patients with Parkinson's disease and Alzheimer's disease, as measured by tritiated dihydrotetrabenazine autoradiography. *Brain Res* **659:** 1-9.

Liang NY and Rutledge CO (1982) Evidence for carrier-mediated efflux of dopamine from corpus striatum. *Biochem Pharmacol* **31:** 2479-2484.

Lile JA, Stoops WW, Vansickel AR, Glaser PE, Hays LR, Rush CR (2005) Aripiprazole attenuates the discriminative-stimulus and subject-rated effects of D-amphetamine in humans. *Neuropsychopharmacology* **30:** 2103-2114.

Liu Y and Edwards RH (1997) The role of vesicular transport proteins in synaptic transmission and neural degeneration. *Annu Rev Neurosci* **20:** 125-156.

Liu Y, Peter D, Roghani A, Schuldiner S, Prive GG, Eisenberg D, Brecha N, Edwards RH (1992) cDNA that suppresses MPP+ toxicity encodes a vesicular amine transporter. *Cell* **70:** 539-551.

Ludwig M and Leng G (2006) Dendritic peptide release and peptide-dependent behaviours*. Nat Rev Neurosci.* **7:** 126-136.

Mack F and Bonisch H (1979) Dissociation constants and lipophilicity of catecholamines and related compounds. *Naunyn Schmiedebergs Arch Pharmacol.* **310**: 1-9.

Mantle TJ, Tipton KF, Garrett NJ (1976) Inhibition of monoamine oxidase by amphetamine and related compounds. *Biochem. Pharmacol*. **25:** 2073-2077, 1976.

Marek GJ, Vosmer G, Seiden LS (1990) Dopamine uptake inhibitors block long-term neurotoxic effects of methamphetamine upon dopaminergic neurons. *Brain Res.* **513:** 274-279.

McCann UD and Ricaurte GA (2004) Amphetamine neurotoxicity: accomplishments and remaining challenges. *Neurosci Biobehav Rev*. **27:** 821-826.

McDaid J, Tedford CE, Mackie AR, Dallimore JE, Mickiewicz AL, Shen F, Angle JM, Napier TC (2007) Nullifying drug-induced sensitization: behavioral and electrophysiological evaluations of dopaminergic and serotonergic ligands in methamphetamine-sensitized rats. *Drug Alcohol Depend.* **86:** 55-66.

McGee SM, McGee DN, McGee MB (2004) Spontaneous intracerebral hemorrhage related to methamphetamine abuse: autopsy findings and clinical correlation. *Am J Forensic Med Pathol* **25:** 334-337.

McGregor C, Srisurapanont M, Mitchell A, Wickes W, White JM (2008) Symptoms and sleep patterns durng inpatient treatment of methamphetamine withdrawal: a comparison of mirtazapine and modafinil with treatment as usual. *J Subst Abuse Treat.* **35:** 334-342.

Melega WP, Lacan G, Desalles AA, Phelps ME (2000) Long-term methamphetamine-induced decreases of [(11)C]WIN 35,428 binding in striatum are reduced by GDNF: PET studies in the vervet monkey. *Synapse*. **35:** 243-249.

Mengual E and Pickel VM (2004) Regional and subcellular compartmentatin of the dopamine transporter and tyrosine hydroxylase in the rat ventral pallidum. *J Comp Neurol* **468:** 395-409.

Meredith CW, Jaffe C, Cherrier M, Robinson JP, Malte CA, Yanasek EV, Kennedy A, Ferguson LC, Tapp AM, Saxon AJ (2009) Open trial of

injectable risperidone for methamphetamine dependence. *J Addict Med.* **3:** 55-65.

Meyer AC, Horton DB, Neugebauer NM, Wooters TE, Nickell JR, Dwoksin LP, Bardo MT (2011) Tetrabenazine inhibiton of monoamine uptake and methamphetamine behavioral effects: locomotor activity, drug discrimination and self-administration. Neuropharmacology. 61: 849-856.

Miller DK, Crooks PA, Dwoskin LP (2000) Lobeline inhibits nicotine-evoked [^{3}H]dopamine overflow from rat striatal slices and nicotine-evoked $^{86}Rb^{+}$ efflux from thalamic synaptosomes. *Neuropharmacology* **39:** 2654–2662.

Miller DK, Crooks PA, Teng L, Witkin JM, Munzar P, Goldberg SR, Acri JB, Dwoskin LP (2001) Lobeline inhibits the neurochemical and behavioral effects of amphetamine. *J Pharmacol Exp Ther* **296:** 1023–1034.

Miller DK, Harrod SB, GreenTA, Wong MY, Bardo MT, Dwoskin LP (2003) Lobeline attenuates locomotor stimulation induced by repeated nicotine administration in rats. *Pharmacol Biochem Behav*. **74:** 279-286.

Miller DK, Crooks PA, Zheng G, Grinevich VP, Norrholm SD, Dwoskin LP (2004) Lobeline analogs with enhanced affinity and selectivity for plasmalemma and vesicular monoamine transporters. *J Pharmacol Exp Ther* **310:** 1035-1045.

Millspaugh C (1974) *Lobelia inflata*. In: American Medicinal Plants: An Illustrated and Descriptive Guide to Plants Indigenous to and Naturalized in the United States which are used in Medicine. pp 385-388 New York: Dover.

Miranda M, Dionne KR, Sorkina T, Sorkin A (2007) Three ubiquitin conjugation sites in the amino terminus of the dopamine transporter mediate protein kinase C-dependent endocytosis of the transporter. *Mol. Biol. Cell* **18:** 313-323.

Miranda M and Sorkin A (2007) Regulation of receptors and transporters by ubiquitination: new insights into surprisingly similar mechanisms. *Mol Interv*. **7**: 157-167.

Miwa JM, Freedman R, Lester HA (2011) Neural Systems governed by nicotinic acetylcholine receptors: emerging hypotheses. *Neuron* **70:** 20-33.

Moron JA, Brockington A, Wise RA, Rocha BA, Hope BT (2002) Dopamine uptake through the norepinephrine transporter in brain regions with low levels of the dopamine transporter: evidence from knock-out mouse lines. *J Neurosci*. **22:** 389-395.

Moxzczynska A, Fitzmaurice P, Ang L, Kalasinsky KS, Schmunk GA, Peretti FJ, Aiken SS, Wickham DJ, Kish SJ (2004) Why is parkinsonism not a feature of human methamphetamine users? *Brain* **127:** 363-370.

Mundorf ML, Hochstetler SE, Wightman RM (1999) Amine weak bases disrupt vesicular storage and promote exocytosis in chromaffin cells. *J Neurochem*. **73:** 2397-2405.

Nakanishi N, Onozawa S, Matsumoto R, Kurihara K, Ueha T, Hasegawa H, Minami N (1995) Effects of protein kinase inhibitors and protein phosphatase inhibitors on cyclic AMP-dependent down-regulation of

vesicular monoamine transport in pheochromocytoma PC12 cells. *FEBS Lett.* **368:** 411-414.

Nash JF and Yamamoto BK (1992) Methamphetamine neurotoxicity and striatal glutamate release: comparison to 3,4-methylenedioxymethamphetamine. *Brain Res.* **581:** 237-243.

Near J. A. (1986) [^{3}H]Dihydrotetrabenazine binding to bovine striatal synaptic vesicles. *Mol. Pharmacol.* **30:** 252-257.

Nelson N, Perzov N, Cohen A, Hagai K, Padler V, Nelson H (2000) The cellular biology of proton-motive force generation by V-ATPases. *J Exp Biol*. **203**: 89-95.

Neugebauer NM, Harrod SB, Stairs DJ, Crooks PA, Dwoskin LP, Bardo MT (2007) Lobelane decreases methamphetamine self-administration in rats. *Eur J Pharmacol.* **571:** 33-38.

Newton TF, Roache JD, De La Garza R 2nd, Fong T, Wallace CL, Li SH, Elkashef A, Chiang N, Kahn R (2006) Bupropion reduces methamphetamine-induced subjective effects and cue-induced craving. *Neuropsychopharmacology.* **31:** 1537-1544.

Newton TF, Reid MS, De La Garza R, Mahoney JJ, Abad A, Condos R, Palamar J, Halkitis PN, Mojisak J, Anderson A, Li SH, Elkashef A (2008) Evaluation of subjective effects of aripiprazole and methampehtaine in methamphetamine-dependent volunteers. *Int J Neuropsychopharmacol*. **11:** 1037-1045.

Nickell JR, Krishnamurthy S, Norrholm S, Deaciuc AG, Siripurapu KB, Zheng G, Crooks PA, Dwoskin LP (2010) Lobelane inhibits methamphetamine-evoked dopamine release via inhibition of the vesicular monoamine transporter-2. *J Pharmacol Exp Ther* **332:** 612-21.

Nickell JR, Zheng G, Deaciuc AG, Crooks PA, Dwoskin LP (2010b) Phenyl ring-substituted lobelane analogs: inhibition of [^{3}H]dopamine uptake at the vesicular monoamine transporter-2. *J Pharmacol Exp Ther* **336:** 724-33.

Norrholm SD, Horton DB, Dwoskin LP (2007) The promiscuity of the dopamine transporter: implications for the kinetic analysis of [^{3}H]serotonin uptake in rat hippocampal and striatal synaptosomes. *Neuropharmacology* **53:** 982-989.

Northrop NA, Smith LP, Yamamoto BK, Eyerman DJ (2011) Regulation of glutamate release by α7 nicotinic receptors: differential role in methamphetamine-induced damage to dopaminergic and serotonergic terminals. *J Pharmacol Exp Ther* **336:** 900-907.

Onali P and Olianas MC (1989) Involvement of adenylate cyclase inhibiton in dopamine autoreceptor regulation of tyrosine hydroxylase in rat nucleus accumbens. *Neurosci Lett.* **102:** 91-96.

Onali P, Mosca E, Olianas MC (1992) Presynaptic dopamine autoreceptors and second messengers controlling tyrosine hydroxylase activity in rat brain. *Neurochem Int.* **20** Suppl: 89S-93S.

Owens MJ, Knight DL, Nemeroff CB (2001) Second-generation SSRIs: human monoamine transporter binding profile of escitalopram and R-fluoxetine. *Biol Psychiatry* **50:** 345-350.

Pao SS, Paulsen IT, Saier MH Jr. (1998) Major facilitator superfamily. *Microbiol Mol Biol Rev.* **62:** 1-34.

Parsons SM (2000) Transport mechanisms in acetylcholine and monoamine storage. *FASEB J.* **14:** 2423-2434.

Parsons LH and Justice JB Jr. (1993) Perfusate serotonin increases exracellular dopamine in the nucleus accumbens as measured by in vivo microdialysis. *Brain Res*. **606:** 195-199.

Partilla JS, Dempsey AG, Nagpal AS, Blough BE, Baumann MH, Rothmann RB (1995) Mechanism of the dopamine-releasing actions of amphetamine and cocaine: plasmalemmal dopamine transporter versus vesicular monoamine transporter. *Mol. Pharmacol.* **47:** 368-373.

Paton DM (1973) Mechanism of efflux of noradrenaline from adrenergic nerves in rabbit atria. *Br J Pharmacol*. **49:** 614-627.

Patrick KS, Gonzalez MA, Straughn AB, Markowitz JS (2005) New methylphenidate formulations for the treatment of attention-deficit/hyperactivity disorder. *Expert Opin Drug Deliv*. **2:** 121-143.

Patterson M, Bloom SR, Gardiner JV (2011) Ghrelin and appetite control in humans-potential application in the treatment of obesity. *Peptides.* **32:** 2290-2294.

Peter D, Jimenez J, Liu Y, Kim J, Edwards RH (1994) The chromaffin granule and synaptic vesicle amine transporters differ in substrate recognition and sensitivity to inhibitors. *J Biol Chem*. **269:** 7231-7237.

Peter D, Liu Y, Sternini C, de Giorgio R, Brecha N, Edwards RH (1995) Differential expression of two vesicular monoamine transporters. *J Neurosci.* **15:** 6179-6188.

Peter D, Vu T, Edwards RH (1996) Chimeric vesicular monoamine transporters identify structural domains that influence substrate affinity and sensitivity to tetrabenazine. *J Biol Chem.* **271:** 2979-2986.

Piasecki MP, Steinagel GM, Thienhaus OJ, Kohlenberg BS (2002) An exploratory study: the use of paroxetine for methamphetamine craving. *J Psychoactive Drugs* **34:** 301-304.

Pickel VM, Nirenberg MJ, Milner TA (1996) Ultrastructural view of central catecholaminergic transmission: immunocytochemical localization of synthesizing enzymes, transporters and receptors. *J Neurocytol.* **25:** 843-856.

Pierce RC and Kumaresan V (2006) The mesolimbic dopamine system: the final common pathway for the reinforcing effect of drugs of abuse? *Neurosci Biobehav Rev.* **30:** 215-238.

Pifl C, Drobny H, Reither H, Hornykiewicz O, Singer EA (1995) Mechanism of the dopamine-releasing actions of amphetamine and cocaine: plasmalemmal dopamine transporter versus vesicular monoamine transporter. *Mol Pharmacol* **47:** 368-373.

Pletscher A (1977) Effect of neuroleptics and other drugs on monoamine uptake by membranes of adrenal chromaffin granules. *Br J Pharmacol.* **59:** 419-424.

Prendergast M, Podus D, Finney J, Greenwell L, Roll J (2006) Contingency management for treatment of substance use disorders: a meta-analysis. Addiction 101: 1546-60.

Prisco S, Pagannone S, Esposito E (1994) Serotonin-dopamine interaction in the rat ventral tegmental area: an electrophysiological study in vivo. *J Pharmacol Exp Ther*. **271:** 83-90.

Rawson RA, Gonzales R, Brethen P (2002) Treatment of methamphetamine use disorders: an update. *J Subst Abuse Treat.* **23:** 145-150.

Reith ME, Coffey LL, Xu C, Chen NH (1994) GBR-12909 and 12935 block dopamine uptake into brain synaptic vesicles as well as nerve endings. *Eur J Pharmacol* **253:** 175-178.

Ricaurte GA, Schuster CR, Seiden LS (1980) Long-term effects of repeated methylamphetamine administration on dopamine and serotonin neurons in the rat brain: a regional study. *Brain Res.* **193:** 153-163.

Richmond R and Zwar N (2003) Review of bupropion for smoking cessation. *Drug Alcohol Rev*. **22:** 203-220.

Riddle EL, Topham MK, Haycock JW, Hanson GR, Fleckenstein AE (2002) Differential trafficking of the vesicular monoamine transporter-2 by methamphetamine and cocaine. *Eur. J. Pharmacol*. **449:** 71-74.

Ritz MC, Lamb RJ, Goldberg SR, Kuhar MJ (1987) Cocaine receptors on dopamine transporters are related to self-administration of cocaine. *Science* **237**: 1219-1223.

Roberston GS and Robertson HA (1989) Evidence that L-dopa-induced rotational behavior is dependent on both striatal and nigral mechanisms. *J Neurosci*. **9:** 3326-3331.

Rocha BA, Fumagalli F, Gainetdinov RR, Jones SR, Ator R, Giros B, Miller GW, Caron MG (1998) Cocaine self-administration in dopamine-transporter knockout mice. *Nat Neurosci.* **1:** 132-137.

Roll JM, Petry NM, Stitzer ML, Brecht ML, Peirce JM, McCann MJ, Blaine J, MacDonald M, DiMaria J, Lucero L, Kellogg S (2006) Contingency management for the treatment of methamphetamine use disorders. *Am J Psychiatry* **163:** 1993-1999.

Roll JM (2007) Contingency management: an evidence-based component of methamphetamine use disorder treatments. *Addiction* **102** Suppl 1: 114-120.

Ross SB and Renyi AL (1964) Blocking action of sympathomimetic amines on the uptake of tritiated noradrenaline by mouse cerebral cortex tissues in vitro. *Acta Pharmacol Toxicol (Copenh).* **21:** 226-239.

Ross SB and Renyi AL (1966) In vitro inhibition of noradrenaline-3H uptake by reserpine and tetrabenazine in mouse cerebral cortex tissues. *Acta Pharmacol Toxicol (Copenh).* **24:** 73-88.

Rothman RB and Baumann MH (2003) Monoamine transporters and psychostimulant drugs. *Eur J Pharmacol*. **479:** 23-40.

Rudnick G, Steiner-Mordoch SS, Fishkes H, Stern-Bach Y, Schuldiner S (1990) Energetics of reserpine binding and occlusion by the chromaffin granule biogenic amine transporter. *Biochemistry* **29:** 603-608.

Rudnick G (2006) Structure/function relationships in serotonin transporter: new insights from the structure of a bacterial transporter. *Handb Exp Pharmacol.* **175:** 59-73.

Salminen O, Murphy, KL, McIntosh JM, Drago J, Marks MJ, Collins AC, Grady SR (2004) Subunit composition and pharmacology of two classes of striatal presynaptic nicotinic acetylcholine receptors mediating dopamine release in mice. *Mol Pharmacol*. **65:** 1526-1535.

Salo R, Nordahl TE, Natsuaki Y, Leamon MH, Galloway GP, Waters C, Moore CD, Buonocore MH (2007) Attentional control and brain metabolite levels in methamphetamine abusers. *Biol Psychiatry* **61:** 1272-1280.

Sandoval V, Riddle EL, Hanson GR, Fleckenstein AE (2002) Methylphenidate redistributes vesicular monoamine transporter-2: role of dopamine receptors. *J Neurosci.* **22:** 8705-8710.

Saunders C, Ferrer JV, Shi L, Chen J, Merrill G, Lamb ME, Leeb-Lundberg LM, Carvelli L, Javitch JA, Galli A (2000) Amphetamine-induced loss of human dopamine transporter activity: An internalization-dependent and cocaine-sensitive mechanism. *Proc Natl Acad Sci U S A* **97:** 6850-6855.

Scherman D and Henry JP (1984) Reserpine binding to bovine chromaffin granule membranes. Characterization and comparison with dihyrdrotetrabenazine binding. *Mol Pharmacol*. **25:** 113-122.

Schmitt KC and Reith ME (2010) Regulation of the dopamine transporter: Aspects relevant to psychostimulant drugs of abuse. *Ann N Y Acad Sci*. **1187:** 316-340.

Schneider F and Olsson T (1996) Clinical-experience with lobeline as a smoking cessation agent. *Med Chem Res.* **6:** 562-570.

Schuldiner S (1994) A molecular glimpse of vesicular monoamine transporters. *J Neurochem.* **62:** 2067-2078.

Schuldiner S, Shirvan A, Linial M (1995) Vesicular neurotransmitter transporters: From bacteria to humans. *Physiol Rev.* **75:** 369-392.

Schweri MM, Skolnick P, Rafferty MF, Rice KC, Janowsky AJ, Paul SM (1985) [3H]Threo-(+/-)-methylphenidate binding to 3,4-dihydroxyphenylethylamine uptake sites in corpus striatum: Correlation with the stimulant properties of ritalinic acid esters. *J Neurochem.* **45:** 1062-1070.

Segal DS, Kuczenski R, O'Neil ML, Melega WP, Cho AK (2005) Prolonged exposure of rats to intravenous methamphetamine behavioral and nuerochemical characterization. *Psychopharmacology (Berl).* **180:** 501-512.

Seiden LS, Fischman MW, Schuster CR (1976) Long-term methamphetamine induced changes in brain catecholamines in tolerant rhesus monkeys. *Drug Alcohol Depend.* **1:** 215-219.

Seiden LS, Sabol KE, Ricaurte GA (1993) Amphetamine: Effects on catecholamine systems and behavior. *Annu Rev Pharmacol Toxicol.* **33:** 639-677.

Sekine Y, Iyo M, Ouchi Y, Matsunaga T, Tuskada H, Okada H, Yoshikawa E, Futatsubashi M, Takei N, Mori N (2001) Methamphetamine-related psychiatric symptoms and reduced brain dopamine transporters studied with PET. *Am J Psychiatry* **158:** 1206-1214.

Sekine Y, Minabe Y, Ouchi Y, Takei N, Iyo M, Nakamura K, Suzuki K, Tsukada H, Okada H, Yoshikawa E, Futatsubashi M, Mori N (2003) Association of dopamine transporter loss in the orbitofrontal and dorsolateral prefrontal cortices with methamphetamine-related psychiatric symptoms. *Am J Psychiatry*. **160:** 1699-1701.

Shoptaw S, Klausner JD, Reback CJ, Tierney S, Stansell J, Hare CB, Gibson S, Siever M, King WD, Kao U, Dang J (2006) A public health response to the methamphetamine epidemic: the implementation of contingency management to treat methamphetamine dependence. *BMC Public Health* **6:** 214.

Shoptaw S, Heinzerling KG, Rotheram-Fuller E, Steward T, Wang J, Swanson AN, De La Garza R, Newton T, Ling W (2008) Randomized, placebo-controlled trial of bupropion for the treatment of methamphetamine dependence. *Drug Alcohol Depend.* **96:** 222-232.

Simon H, Scatton B, Moal ML (1980) Dopaminergic A10 neurones are involved in cognitive functions*. Nature* **286:** 150-151.

Simon SL, Domier C, Carnell J, Brethen P, Rawson R, Ling W (2000) Cognitive impairment in individuals currently using methamphetamine. *Am J Addict* **9:** 222-231.

Sonders MS and Amara SG (1996) Channels in transporters. *Curr Opin Neurobiol*. **6:** 294-302.

Sonders MS, Zhu SJ, Zahniser NR, Kavanaugh MP, Amara SG (1997) Multiple ionic conductances of the human dopamine transporter: the actions of dopamine and psychostimulants. *J Neurosci.* **17:** 960-974.

Sora I, Hall FS, Andrews AM, Itokawa M, Li XF, Wei HB, Wichems C, Lesch KP, Murphy DL, Uhl GR (2001) Molecular mechanisms of cocaine reward: combined dopamine and serotonin transporter knockouts eliminate cocaine place preference. *Proc Natl Acad Sci U S A* **98:** 5300-5305.

Sorkina T, Doolen S, Galperin E, Zahniser NR, Sorkin A (2003) Oligomerization of dopamine transporters visualized in living cells by fluorescence resonance energy transfer microscopy. *J Biol Chem*. **278:** 28274-28283.

Sorkina T, Hoover BR, Zahniser NR, Sorkin A (2005) Consitutive and protein kinase c-induced internalization of the dopamine transporter by a clathrin-dependent mechanism. *Traffic* **6:** 157-170.

Sorkina T, Richards TL, Rao A, Zahniser NR, Sorkin A (2009) Negative regulation of dopamine transporter endocytosis by membrane-proximal n-terminal residues. *J Neurosci.* **29:**1361-1374.

Srisurapanont M, Jarusuraisin N, Jittiwutikan J (1999) Amphetamine withdrawal: II. A placebo-controlled, randomized double-blind study of amineptine treatment. *Aust N Z J Psychiatry.* **33:** 94-98.

Stead LF and Hughes JR (2000) Lobeline for smoking cessation (Cochrane Review). In: The Cochrane Library, Issue 2, Chichester, John Wiley and Sons.

Stein WD (1968) The transport of sugars. *Br Med Bull.* **24**: 146-149.

Steinkellner T, Freissmuth M, Sitte HH, Montgomery T (2011) The ugly side of amphetamines: short- and long-term toxicity of 3,4-methylenedioxymethamphetamine (MDMA, 'Ecstasy'), methamphetamine and D-amphetamine. *Biol Chem* **392:** 103-115.

Stephans SE and Yamamoto BK (1994) Methmaphetamine-induced neurotoxicity: roles for glutamate and dopamine efflux. *Synapse* **17**: 203-209.

Stoops WW, Lile JA, Glaser PE, Rush CR (2006) A low dose of aripiprazole attenuates the subject-rated effects of d-amphetamine. *Drug Alcohol Depend*. **84:** 206-209.

Substance Abuse and Mental Health Services Administration, Office of Applied Studies (2008) Results from the 2007 National Survey on Drug Use and Health: National Findings (NSDUH Series H-34, DHHS Publication No. SMA 08-4343). Rockville, MD.

Substance Abuse and Mental Health Services Administration, Office of Applied Studies (2010) Results from the 2009 National Survey on Drug Use and

Health: Volume I. Summary of National Findings (NSDUH Series H-38A, HHS Publication No. SMA 10-4856). Rockville, MD.

Substance Abuse and Mental Health Services Administration, Center for Behavioral Health Statistics and Quality (2010) Treatment Episode Data Set (TEDS): 1998-2008. State Admissions to Substance Abuse Treatment Services, DASIS Series: S-55, HHS Publication No. (SMA) 10-4613, Rockville, MD.

Sudhof TC (2004) The synaptic vesicle cycle. *Annu Rev Neurosci.* **27:** 509-547.

Sulzer D and Rayport S (1990) Amphetamine and other psychostimulants reduce pH gradients in midbrain dopaminergic neurons and chromaffin granules: a mechanism of action. *Neuron* **5:** 797-808.

Sulzer D, Maidment NT, Rayport S (1993) Amphetamine and other weak bases act to promote reverse transport of dopamine in ventral midbrain neurons. *J Neurochem*. **60:** 527-535.

Sulzer D, Chen TK, Lau Y, Kristensen H, Rayport S, Ewing A (1995) Amphetamine redistributes dopamine from synaptic vesicles to the cytosol and promotes reverse transport. *J Neurosci* **15:** 4102–4108.

Sulzer D and Pothos EN (2000) Regulation of quantal size by presynaptic mechanisms. *Rev Neurosci.* **11:** 159-212.

Sulzer D, Sonders MS, Poulsen NW, Galli A (2005) Mechanisms of neurotransmitter release by amphetamines: a review. *Prog Neurobiol.* **75:** 406-433.

Takahashi N, Miner LL, Sora I, Ujike H, Revay RS, Kostic V, Jackson-Lewis V, Prezedborski S, Uhl GR (1997) VMAT2 knockout mice: Heterogyzotes display reduced amphetamine-conditioned reward, enhanced amphetamine locomotion and enhanced MPTP toxicity. *Proc. Natl. Acad. Sci. U S A*. **94:** 9938-9943.

Takamatsu Y, Yamamoto H, Ogai Y, Hagino Y, Markou A, Ikeda K (2006) Fluoxetine as a potential pharmacotherapy for methamphetamine dependence: studies in mice. *Ann NY Acad Sci.* **1074**: 295-302.

Tanda G, Newman AH, Katz JL (2009) Discovery of drugs to treat cocaine dependence: behavioral and neurochemical effects of atypical dopamine transport inhibitors. *Adv Pharmacol* **57**: 253-289.

Teng LH, Crooks PA, Sonsalla PK, Dwoskin LP (1997) Lobeline and nicotine evoke [^{3}H]overflow from rat striatal slices preloaded with [^{3}H]dopamine: differential inhibition of synaptosomal and vesicular [^{3}H]dopamine uptake. *J Pharmacol Exp Ther* **280**: 1432-1444.

Teng LH, Crooks PA, Dwoskin LP (1998) Lobeline displaces [^{3}H]dihydrotetrabenazine binding and releases [^{3}H]dopamine from rat striatal synaptic vesicles: comparison with d-amphetamine. *J Neurochem* **71**: 258-265.

Terry AV Jr., Williamson R, Gattu M, Beach JW, McCurdy CR, Sparks JA, Pauly JR (1998) Lobeline and structurally simplified analogs exhibit differential agonist activity and sensitivity to antagonist blockade when compared to nicotine. *Neuropharmacology* **37:** 93-102.

Thomsen M, Han DD, Gu HH, Caine SB (2009) Lack of cocaine self-administration in mice expressing a cocaine-insensitive dopamine transporter. *J Pharmacol Exp Ther.* **331:** 204-211.

Tiihonen J, Kuoppasalmi K, Fohr J, Tuomola P, Kuikanmaki O, Vorma H, Sokero P, Haukka J, Meririnne E (2007) A comparison of aripiprazole, methylphenidate, and placebo for amphetamine dependence*. Am J Psychiatry*. **164:** 160-162.

Torres GE, Gainetdinov RR, Caron MG (2003) Plasma membrane monoamine transporters: structure, regulation and function. *Nat Rev Neurosci.* **4:** 13-25.

Trujillo KA, Belluzzi JD, Stein L (1991) Naloxone blockade of amphetamine place conditioning. *Psychopharmacology (Berl).* **104:** 265-274.

Tucek S and Proska J (1995) Allosteric modulation of muscarinic acetylcholine receptors. *Trends Pharmacol. Sci.* **16:** 205-212.

United Nations Office on Drugs and Crime (2007) World Drug Report Volume 1. Analysis. United Nations Office on Drugs and Crime, Vienna.

United Nations Office on Drugs and Crime (2011) World Drug Report Volume 1. Analysis. United Nations Office on Drugs and Crime, Vienna.

Vaughan RA and Kuhar MJ (1996) Dopamine transporter ligand binding domains. Structural and functional properties revealed by limited proteolysis. *J Biol Chem*. **271:** 21672-21680.

Vaughan RA, Huff RA, Uhl GR, Kuhar MJ (1997) Protein kinase C-mediated phosphorylation and functional regulation of dopamine transporters in striatal synaptosomes. *J Biol Chem.* **272:** 15541-15546.

Vaughan RA, Agoston GE, Lever JR, Newman AH (1999) Differential binding of tropane-based photoaffinity ligands on the dopamine transporter. *J Neurosci*. **19:** 630-636.

Vocci FJ and Appel NM (2007) Approaches to the development of medications for the treatment of methamphetamine dependence. *Addiction* **102:** 96-106.

Volkow ND, Wang GJ, Fowler JS, Fischman M, Foltin R, Abumrad NN, Gatley SJ, Logan J, Wong C, Gifford A, Ding YS, Hitzemann R, Pappas N (1999) Methylphenidate and cocaine have a similar in vivo potency to block dopamine transporters in the human brain. *Life Sci*. **65:** 7-12.

Volkow ND, Chang L, Wang GJ, Fowler JS, Leonido-Yee M, Franceschi D, Sedler MJ, Gatley SJ, Hitzemann R, Ding YS, Logan J, Wong C, Miller EN (2001) Association of dopamine transporter reduction with psychomotor impairment in methamphetamine abusers. *Am J Psychiatry* **158:** 377-382.

Volz TJ (2008) Neurophamacological mechanisms underlying the neuroprotective effects of methylphenidate. *Curr Neuropharmacol* **6:** 379-385.

Wagner GC, Ricaurte GA, Seiden LS, Schuster CR, Miller RJ, Westley J (1980) Long lasting depletions of striatal dopamine and loss of dopamine uptake

sites following repeated administration of methamphetamine. *Brain Res*. **506:** 236-242.

Wang YM, Gainetdinov RR, Fumagalli F, Xu F, Jones SR, Bock CB, Miller GW, Wightman RM, Caron MG (1997) Knockout of the vesicular monoamine transporter2 gene results in neonatal death and supersensitivity to cocaine and amphetamine. *Neuron* **19:** 1285-1296.

Williams JM and Galli A (2006) The dopamine transporter: a vigilant border control for psychostimulant action. *Handb Exp Pharmacol.* **175:** 215-32.

Wilson JM, Kalasinsky KS, Levey AI, Bergeron C, Reiber G, Anthony RM, Schmunk GA, Shannak K, Haycock JW, Kish SJ (1996) Striatal dopamine nerve terminal markers in human, chronic methamphetamine users. *Nat Med.* **2:** 699-703.

Wimalasena K (2011) Vesicular monoamine transporters: structure-function, pharmacology, and medicinal chemistry. *Med Res Rev*. **31:** 483-519.

Wise RA (1978) Catecholamine theories of reward: a critical review. *Brain Res*. **152:** 215-247.

Wise RA and Bozarth MA (1987) A psychomotor stimulant theory of addiction. *Psychol Rev* **94:** 469-492.

Wise RA (2009) Roles for nigrostriatal-not just mesocorticolimbic-dopamine in reward and addiction. *Trends Neurosci*. **32:** 517-524.

Wooters TE, Smith AM, Pivavarchyk M, Siripurapu KB, McIntosh JM, Zhang Z, Crooks PA, Bardo MT, Dwoskin LP (2011) bPiDI: a novel selective α6β2*

nicotinic receptor antagonist and preclinical candidate treatment for nicotine abuse. *Br. J. Pharmacol.* **163:** 346-357.

Xi ZX, Kleitz HK, Deng X, Ladenheim B, Peng XQ, Li X, Gardner EL, Stein EA, Cadet JL (2009) A single high dose of methamphetamine increases cocaine self-administration by depletion of striatal dopamine in rats. *Neuroscience.* **161**: 392-402.

Yamamoto BK, Moszczynska A, Gudelsky GA (2010) Amphetamine toxicities: classical and emerging mechansims. *Ann N Y Acad Sci.* **1187:** 101-121.

Yano M and Steiner H (2007) Methylphenidate and cocaine: the same effects on gene regulation? *Trends Pharmacol Sci*. **28:** 588-596.

Yao J, Erickson JD, Hersh LB (2004) Protein kinase A affects trafficking of the vesicular monoamine transporters in PC12 cells. *Traffic* **5:** 1006-1016.

Yelin R and Schuldiner S (2000) Vesicular neurotransmitter transporters:Pharmacology, biochemistry, and molecular analysis. In: Neurotransmitter Transporters: Structure, Function, and Regulation (Reith, M. E., ed), pp 313-354 Totowa, NJ: Humana Press.

Zaczek R, Culp S, De Souza EB (1991) Interactions of [^{3}H]amphetamine with rat brain synaptosomes. II. Active transport. *J Pharmacol Exp Ther.* **257:** 830-835.

Zahm DS, Zaborszky L, Alones VE, Heimer L (1985) Evidence for the coexistence of glutamate decarboxylase and Met-enkephalin immunoreactivities in axon terminals of rat ventral pallidum. *Brain Res*. **325:** 317-321.

Zahniser NR and Doolen S (2001) Chronic and acute regulation of Na^+/Cl^- - dependent neurotransmitter transporters: Drugs, substrates, presynaptic receptors, and signaling systems. *Pharmacol Ther.* **92:** 21-55.

Zhang L, Coffey LL, Reith ME (1997) Regulation of the functional activity of the human dopamine transporter by protein kinase C. *Biochem Pharmacol.* **53:**677-688.

Zheng G, Dwoskin LP, Deaciuc AG, Crooks PA (2005a) Defunctionalized lobeline analogues: structure-activity of novel ligands for the vesicular monoamine transporter. *J Med Chem* **48:** 5551-5560.

Zheng G, Dwoskin LP, Deaciuc AG, Zhu J, Jones MD, Crooks PA (2005b) Lobelane analogues as novel ligands for the vesicular monoamine transporter-2. *Bioorg Med Chem* **13:**3899-3909.

Zhou J (2004) Norepinephrine transporter inhibitors and their therapeutic potential. *Drugs Future* **29:** 1235-1244.

Zhu SJ, Kavanaugh MP, Sonders MS, Amara SG, Zahniser NR (1997) Activation of protein kinase C inhibits uptake, currents and binding associated with the human dopamine transporter expressed in Xenopus oocytes. *J Pharmacol Exp Ther.* **282:** 1358-1365.

Zweben JE, Cohen JB, Christian D, Galloway GP, Salinardi M, Parent D, Iguchi M, Methamphetamine Treatment Project. Psychiatric symptoms in methamphetamine users. *Am J Addict*. **13:** 181-190.

VITA

David Bradley Horton

Born

- August 13, 1981 in Lexington, KY

Education

- Transylvania University, Lexington, KY
    - B.A. Biology
- University of Kentucky, Lexington, KY
    - College of Pharmacy, Pharmaceutical Sciences
    - Ph.D. (Successfully defended, November 30, 2011)

Professional Positions

- Lab Assistant - Transylvania University, Lexington, KY
    - Work Study – Biology
    - 1999-2003
- Lab Technician – Martek Biosciences Inc., Winchester, KY
    - Quality Control
    - 2000-2003
- Pre-doctoral Fellowship - National Institute of Drug Abuse, Bethesda, MD
    - Behavioral Neuroscience Branch – Intracranial Injections
    - 2003-2004
- Teaching Assistant – University of Kentucky, Lexington, KY
    - Pharmaceutical Sciences
    - 2004-2005
- Research Assistant – University of Kentucky, Lexington, KY
    - Pharmaceutical Sciences
    - 2005-2011
- Senior Scientist – Pfizer Inc., Groton, CT
    - Global Safety Pharmacology – CNS
    - 2011 - Present

Scholastic and Professional Honors

- Greek and Honor Societies - Transylvania University, Lexington, KY
    - Phi Kappa Tau
        - President (2002-2003)
        - Vice-President (2001-2002
        - Membership Orientation (2000-2001)
    - Order of Omega – Greek Honor Society (2000-2003
    - Phi Delta Epsilon – Pre Medical Fraternity (2001-2003)
    - Beta Beta Beta – Biological Honor Society (2001-2003)
        - Secretary
- NIH Intramural Training Fellowship – National Institute on Drug Abuse, Bethesda, MD
    - Post Baccalaureate (2003-2004)
- Rho Chi – Univeristy of Kentucky, Lexington, KY
    - Pharmacy Honor Society (2006-2011)
- Graduate School Academic Year Fellowship – University of Kentucky, Lexington, KY
    - 2007-2009
- UK College of Pharmacy Helton Travel Award – University of Kentucky, Lexington, KY
    - 2008
- NIDA Training Grant Fellowship NIH T-32, DA016176 – University of Kentucky, Lexington, KY
    - 2008 – 2011
- Outstanding Poster Presenter Award – University of Kentucky, Lexington, KY
    - Bluegrass Society for Neuroscience
    - 2009, 2011

Professional Publications

Zheng G, **Horton DB**, Deaciuc AG, Dwoskin LP, Crooks PA. Des-keto lobeline analogs with increased potency and selectivity at dopamine and serotonin transporters. *Bioorg Med Chem Lett*. 16:5018-5021, 2006.

Norrholm SD, **Horton DB**, Dwoskin LP. The promiscuity of the dopamine transporter: implications for the kinetic analysis of [^{3}H]serotonin uptake in rat hippocampal and striatal synaptosomes. *Neuropharmacology*. 53:982-9, 2007.

Hojahmat M, **Horton DB**, Norrholm SD, Deaciuc AG, Dwoskin LP, Crooks, PA. Lobeline esters as novel ligands for the nicotinic receptors and neurotransmitter transporters. *Bioorg Med Chem*,18:640-649, 2010.

Beckmann J, Siripurapu K, Nickell J, **Horton DB**, Denehy E, Vartak A, Crooks PA, Dwoskin LP, Bardo MT. The pyrrolidine analog of nor-lobelane, cis-

2,5-di-(2-Phenethyl)-pyrrolidine hydrochloride, inhibits VMAT2 function, dopamine release, and methamphetamine self-administration rats. *J Pharm Exp Ther*, 335: 841-851, 2010.

Crooks PA, Zheng G, Vartak A, Culver J, Zheng F, **Horton DB**, Deaciuc AG, Dwoskin LP. Design, synthesis and VMAT2 binding of lobeline analogs as potential therapeutic agents for treating psychostimulant abuse. *Curr Top Med Chem,* 11:1103-1127, 2011.

Horton DB, Siripurapu KB, Norrholm SD, Deaciuc AG, Hojahmat M, Culver JP, Crooks PA, Dwoskin LP. Lobeline and *meso*-transdiene analogs: interaction at neurotransmitter transporters and nicotinic receptors. *J Pharm Exp Ther*, 336:940-951, 2011.

Meyer AC, **Horton DB,** Neugebauer NM, Wooters TE, Nickell JR, , Dwoskin LP, Bardo MT. The effect of tetrabenazine on methamphetamine-induced behaviors and neurochemistry. *Neuropharmacology,* 61: 849-856, 2011.

Horton DB, Zheng G, Siripurapu KB, Deaciuc AG, Crooks PA, Dwoskin LP. N-1,2-Dihydroxylpropyl analogs of lobelane as novel vesicular monoamine transporter (VMAT2) inhibitors and potential treatments for methamphetamine abuse. *J Pharm Exp Ther,* 339: 286-297, 2011.

Horton DB, Zheng G, Crooks PA, Dwoskin LP. GZ-793A interacts with the vesicular monoamine transporter-2 to inhibit the effect of methamphetamine. *J Neurochem,* submitted, 2011.

Smith AM, Meyer AC, Pivavarchyk M, Wooters TE, **Horton DB**, Zheng Z, McIntosh JM, Crooks PA, Bardo MT, Dwoskin LP. The novel nicotinic receptor antagonist r-b3,5L/3PiDDB potently inhibits nicotine-evoked [^{3}H]DA release from rat striatal slices and decreases nicotine self-administration. *J Pharm Exp Ther,* in prep, 2011.

Narayanaswami V, Sen S, **Horton DB**, Cassis LA, Dwoskin LP. Angiotensin AT1 and AT2 receptors modulate the effect of nicotine to evoke [^{3}H]dopamine and [^{3}H]norepinephrine release, from rat sriatal and hypothalamic slices, respectively. *Biochem Pharmacol*, in prep, 2011.

Siripurapu KB, **Horton DB**, Zheng G, Crooks PA, Dwoskin LP, GZ-793A selectively inhibits methamphetamine effects on dopamine release. *Neuropharmacology*, in prep, 2011.

Cao Z, Siripurapu KB, Smith AM, **Horton DB,** Zheng G, Wilmouth CE, Deaciuc AG, Bardo MT, Crooks PA, Dwoskin LP. Acyclic lobelane analogs inhibit vesicular monoamine transporter-2 function and both methamphetamine and nicotine-evoked dopamine release. *J Pharm Exp Ther,* in prep, 2011.

Siripurapu KB, **Horton DB,** (co-first authors) Zheng G, Crooks PA, Dwoskin LP. GZ-793A does not exacerbate methamphetamine-induced dopamine depletions in striatal tissue and striatal vesicles. *Eur J Pharmacol*, in prep, 2011.

Wilmouth CE, Siripurapu KB, **Horton DB**, Zheng G, Crooks PA, Dwoskin LP, Bardo MT. Oral GZ-793A treatment does not exacerbate methamphetamine-induced dopamine depletions in stratal tissue and

striatal vesicles following methamphetamine self-administration. In prep, 2011.

Abstracts

Ikemoto S, **Horton DB**, Macumber IR. Self-administration of nicotine into the ventral tegmental area and adjacent regions. *Society for Neuroscience* Abstract, 2004.

Zheng G, **Horton DB**, Dwoskin LP, Crooks PA. Synthesis and pharmacological studies of mono-hydroxy lobeline analogs to inhibit [^{3}H]dopamine and [^{3}H] 5-hydroxytryptamine uptake into rat striatal and hippocampal synaptosomes. *American Association of Pharmaceutical Sciences* Abstract, 2005.

Horton DB, Hojahmat M, Norrholm SD, Dhawan GK, Crooks PA, Dwoskin LP. Sulfate esters of lobeline: interaction at neurotransmitter transporters and nicotinic receptors. *Society for Neuroscience* Abstract, 227.11 VV80, 2005.

Horton DB, Hojahmat M, Norrholm SD, Dhawan GK, Crooks PA, Dwoskin LP. Sulfate esters of lobeline: interaction at neurotransmitter transporters and nicotinic receptors. *Bluegrass Chapter of Society for Neuroscience* Abstract, 2006.

Horton DB, Hojahmat M, Deaciuc AG, Culver JP, Norrholm SD, Crooks PA, Dwoskin LP. Lobeline and meso-transdiene analogs: interaction at neurotransmitter transporters and nicotinic receptors. *Society for Neuroscience* Abstract, 591.1 PP67, 2006.

Horton DB, Hojahmat M, Deaciuc AG, Culver JP, Norrholm SD, Crooks PA, Dwoskin LP. Lobeline and meso-transdiene analogs: interaction at neurotransmitter transporters and nicotinic receptors. *Bluegrass Chapter of Society for Neuroscience* Abstract, 2007.

Hojahmat M, **Horton DB**, Deaciuc AG, Culver JP, Crooks PA, Dwoskin LP. Synthesis and evaluation of 3,5-disubstituted piperidine analogs related to lobeline as vesicular monoamine transporter ligands. *American Association Pharmaceutical Scientists* Abstract, 2007

Deaciuc AG, **Horton DB**, Hojahmat M, Culver JP, Norrholm SD, Crooks PA, Dwoskin LP. Novel vesicular monoamine transporter (VMAT2) inhibitiors as potential treatments for methamphetamine abuse: 3,5-disubstituted meso-transdiene analogs of lobeline. *Society for Neuroscience* Abstract, 814.5 AA16, 2007.

Horton DB, Zheng G, Deaciuc AG, Crooks PA, Dwoskin LP. Novel vesicular monoamine transporter (VMAT2) inhibitors as potential treatments for methamphetamine abuse: interaction of meso-transdiene and lobelane analogs at neurotransmitter transporters. *Society for Neuroscience* Abstract, 814.5 AA17, 2007.

Horton DB, Zheng G, Deaciuc AG, Crooks PA, Dwoskin LP. Novel vesicular monoamine transporter (VMAT2) inhibitors as potential treatments for methamphetamine abuse: interaction of meso-transdiene and lobelane

analogs at neurotransmitter transporters. *Bluegrass Chapter of Society for Neuroscience* Abstract, 2008.

Zheng G, **Horton DB,** Deaciuc AG, Crooks PA, Dwoskin LP. Synthesis and pharmacological evaluation of N-substituted lobelane analogs at the vesicular monoamine transporter (VMAT2) *American Association Pharmaceutical Scientists* Abstract, 2008.

Horton DB, Zheng G, Siripurapu KB, Deaciuc AG, Crooks PA, Dwoskin LP. Water-soluble analogs of lobelane as novel vesicular monoamine transporter (VMAT2) inhibitors and potential treatments for methamphetamine abuse. *Society for Neuroscience* Abstract, 660.5 GG24, 2008.

Horton DB, Zheng G, Siripurapu KB, Deaciuc AG, Crooks PA, Dwoskin LP. Water-soluble analogs of lobelane as novel vesicular monoamine transporter (VMAT2) inhibitors and potential treatments for methamphetamine abuse. *Bluegrass Chapter of Society for Neuroscience* Abstract, 2009.

Horton DB, Zheng G, Siripurapu KB, Deaciuc AG, Crooks PA, Dwoskin LP. Water-soluble analogs of lobelane as novel vesicular monoamine transporter (VMAT2) inhibitors and potential treatments for methamphetamine abuse. *UK Center for Clinical and Translational Sciences (CCTS) Spring Conference* Abstract, 2009.

Beckmann J, **Horton DB**, Siripurapu KB, Denehy E, Zheng G, Crooks PA, Dwoskin LP, Bardo MT. (R)-cis-N-(2,3-Dihydroxypropyl)-2,6-di-(4-methoxyphenylethyl)piperidine hemisulfate (UK-793A) selectively blocks methamphetamine reinforcement without producing Tolerance in rats. *College on Problems of Drug Dependence* Abstract, 2009.

Zheng G, **Horton DB,** Deaciuc AG, Dwoskin LP, Crooks PA. N-Substituted methamphetamine derivatives as inhibitors of dopamine uptake at the vesicular monoamine transporter (VMAT2). *American Association Pharmaceutical Scientists* Abstract, 2009.

Crooks PA, Dwoskin LP, Zheng G, Deaciuc AG, **Horton DB**. N-Substituted methamphetamine derivatives as inhibitors of dopamine uptake at the vesicular monoamine transporters (VMAT2). *American Association Pharmaceutical Scientists* Abstract, 2009.

Horton DB, Zheng G, Beckmann J, Deaciuc AG, Bardo MT, Crooks PA, Dwoskin LP. *N*-Substituted methamphetamine derivatives as novel vesicular monoamine transporter (VMAT2) inhibitors. *Society for Neuroscience* Abstract, 554.6 AA6, 2009.

Siripurapu KB, **Horton DB**, Zheng G, Crooks PA, Dwoskin LP. GZ-793A selectively inhibits methamphetamine-induced neurochemical effects. *Bluegrass Chapter of Society for Neuroscience* Abstract, 2010.

Sen S, Narayanaswami V, **Horton DB**, Cassis LA, Dwoskin LP. Losartin, an angiotensin II-1 receptor antagonist, inhibits nicotine-evoked [^{3}H]dopamine and [^{3}H]norepinephrine overflow from rat striatum and hypothalamus, respectively. *Bluegrass Chapter of Society for Neuroscience* Abstract, 2010.

Horton DB, Zheng G, Beckmann J, Deaciuc AG, Bardo MT, Crooks PA, Dwoskin LP. *N*-Substituted methamphetamine derivatives as novel vesicular monoamine transporter (VMAT2) inhibitors. *Bluegrass Chapter of Society for Neuroscience* Abstract, 2010.

Beckmann JS, Alvers KM, Denehy ED, Siripurapu KB, Nickell JR, **Horton DB**, Zheng G, Crooks PA, Dwoskin LP, Bardo MT. GZ-793A, a diol analog of *nor*-lobelane, selectively blocks the effects of methamphetamine on dopamine release and specifically blocks methamphetamine self-administration. *Translational Conference in Psychiatry (Innsbruck, Austria*) Abstract, 2010.

Beckmann JS, Alvers KM, Denehy ED, Siripurapu KB, Nickell JR, **Horton DB**, Zheng G, Crooks PA, Dwoskin LP, Bardo MT. GZ-793A, a diol analog of lobelane, inhibits the neurochemical effects of methamphetamine and specifically decreases methamphetamine self-administration and reinstatement. *Translational Research in Methamphetamine Addiction Conference (Pray, Montana*) Abstract, 2010.

Horton DB, Zheng G, Deaciuc AG, Crooks PA, Dwoskin LP. GZ-793A, a novel vesicular monoamine transporter-2 (VMAT2) inhibitor that probes multiple sites on VMAT2 as a potential treatment for methamphetamine abuse. *UK College of Pharmacy Symposium on Drug Discovery and Development* Abstract, 2010

Siripurapu KB, **Horton DB**, Zheng G, Crooks PA, Dwoskin LP. GZ-793A selectively inhibits methamphetamine-induced neurochemical effects. *Society for Neuroscience* Abstract, 669.9 FF2, 2010.

Sen S, Narayanaswami V, **Horton DB**, Cassis LA, Dwoskin LP. Angiotensin AT1 and AT2 receptors modulate the effect of nicotine to evoke neurotransmitter release. *Society for Neuroscience* Abstract, 476.8 NN2, 2010.

Horton DB, Zheng G, Deaciuc AG, Crooks PA, Dwoskin LP. GZ-793A, a novel vesicular monoamine transporter-2 (VMAT2) inhibitor that probes multiple sites on VMAT2 as a potential treatment for methamphetamine abuse. *Society for Neuroscience* Abstract, 669. 669.10 FF3, 2010.

Horton DB, Zheng G, Deaciuc AG, Crooks PA, Dwoskin LP. GZ-793A, a novel vesicular monoamine transporter-2 (VMAT2) inhibitor that probes multiple sites on VMAT2 as a potential treatment for methamphetamine abuse. *Bluegrass Chapter of Society for Neuroscience* Abstract, 2011.

Cao Z, Zheng G, **Horton DB**, Deaciuc AG, Crooks PA, Dwoskin LP. Acyclic lobelane analogs as novel inhibitors of the vesicular monoamine transporter-2. *Bluegrass Chapter of Society for Neuroscience* Abstract, 2011**.**

Horton DB, Zheng G, Deaciuc AG, Crooks PA, Dwoskin LP. GZ-793A, a novel vesicular monoamine transporter-2 (VMAT2) inhibitor that probes multiple sites on VMAT2 as a potential treatment for methamphetamine abuse. *UK Center for Clinical and Translational Sciences (CCTS) Spring Conference* Abstract, 2011

Cao Z, Zheng G, **Horton DB**, Deaciuc AG, Crooks PA, Dwoskin LP. Acyclic lobelane analogs as novel inhibitors of the vesicular monoamine transporter-2. *UK Center for Clinical and Translational Sciences (CCTS) Spring Conference* Abstract, 2011**.**

Dwoskin LP, Beckmann JS, **Horton DB**, Siripurapu KB, Alvers KM, Zheng G, Crooks PA, Bardo, MT. Preclinical evaluation of GZ-793A as a pharmacotherapy for methamphetamine abuse. *College on Problems of Drug Dependence* Abstract 2011.

Horton DB, Beckmann JS, Alvers KM, Siripurapu KB, Zheng G, Crooks PA, Bardo MT, Dwoskin LP. GZ-793A specifically inhibits methamphetamine self-administration and reinstatement through potent and selective inhibition of VMAT2 function. *European Behavioral Pharmacology Society (Amsterdam, Netherlands)* Abstract 2011.

Cao Z, Zheng G, **Horton DB**, Deaciuc AG, Crooks PA, Dwoskin LP. Acyclic lobelane analogs as novel inhibitors of the vesicular monoamine transporter-2. *Society for Neuroscience* Abstract, 2011**.**

Patents

N-2,3-Dihydroxypropyl Analogs of *nor*-Lobelane and Related Compounds for the Treatment of Psychostimulant Abuse and Withdrawal, Eating Disorders, and Central Nervous System Diseases and Pathologies", Peter A. Crooks, Linda P. Dwoskin, Guangrong Zheng, Ashish P. Vartak, and **David B. Horton**, Docket No. PAC-0012, US Provisional Patent Application No., 61,268,472, filed June 12th, 2009**.**

David B. Horton

March 27, 2012